THE APPLICATION OF IMMOBILIZED ENZYMES

IN ANALYTICAL CHEMISTRY

A thesis submitted by

RICHARD KWASI OWUSU B.Sc.

in candidature for the degree

of

Doctor of Philosophy

of the University of London

The Bourne Laboratory,
Royal Holloway and
Bedford Colleges,
(University of London)
Egham TW20 0EX, UK.

DECEMBER 1984

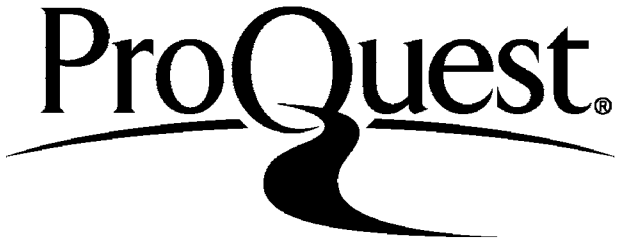

Acknowledgements

I would like to express my gratitude to all the staff at the Bourne Laboratory, (both technical and academic), for their help and co-operation during this work. I am particularly indebted to my Supervisor Dr. Arthur Finch for his patience and support throughout the past three years.

I would also like to thank Dr. Martin J. Trewhella ,(of B.P. Sunbury) for his invaluable help and encouragement especially during my first year. Equally, the regular consultations with Mrs. G. Alliston (of the Laboratory of the Government Chemist) are also acknowledged.

Finally thanks are also due to the S.E.R.C. for the award of a CASE studentship.

Abstract

The use of immobilized enzymes (and cells) in flow analyses and some determinants of the performance of the resulting analytical systems have been examined; the detector used in most cases was the LKB 2017-30 flow microcalorimeter.

The detector time constant and sensitivity, reactor enzyme activity, flow rate and the mode of sample injection were primary determinants of system characteristics such as, sensitivity, minimum detectable concentration, linearity range and speed analysis. These relationships were later applied in the determination of the reaction enthalpy. Glucose, urea, fructose, mannose, glucoseamine, the cofactor ATP, vitamin C and hydrogen peroxide were also determined using the appropriate immobilized enzymes.

The kinetics of the reactions catalysed by immobilized urease, glucose oxidase, acetylcholinesterase or ascorbate oxidase was studied via flow microcalorimetry. Apparent intrinsic kinetic parameters, external and internal substrate moduli, as well as the corresponding effectiveness factors were determined. In all cases, the Michaelis constant (Km) was increased and the observed activity severely limited as a consequence of the slow diffusion of substrate.

Flow analysis using immobilized cells and microcalorimetric monitoring was also examined. This combination is well suited for broad-spectrum analysis. The effects of selected organic solvents (permeablizing agents) on the linearity range (approximately given by the Km) was also of some interest. The specificity (estimated as $(dQ/dt)max/Km^{app}$) for a range of substrate was proposed as a means of differentiating between closely related strains of cells.

Electrochemical monitoring of immobilized enzyme reactions may rival the thermochemical approach in its widespread applicability and simplicity. Both potentiometric and amperometric modes were used; the latter in connection with flow analyses. Two amperometric enzyme reactors and a flow-through enzyme electrode were constructed and successfully used in substrate determinations.

CONTENTS

CHAPTER 1

Introduction

1.1 Calorimetry, Principles and Instrumental Aspects

Calorimetry is the study of chemical and physical processes by the direct measurement of heat taken up or evolved as a consequence of those changes. Although the essential principle dates back to the early eighteenth century, with the work of Lavoisier and de Laplace 1780 (1), it is only recently that it has made any real impact in chemistry. This it would appear was largely due to the unavailability of commercial instrumentation.

The calorimetric approach has notable advantages over some of the relatively more established techniques, e.g., spectrophotometric and electrochemical approaches. These include:

a. a non requirement for optically clear solutions;
b. non-sensitivity to the presence of background electroactive species;
c. often non-destructive and non-evasive nature, and
d. widespread or general applicability, since most processes are accompanied by heat change.

For this latter reason, however, the calorimetric approach is inherently nonspecific. Quantitative applications therefore rely on the process under study being well defined.

1.1.1 Adiabatic and Heat Conducting Calorimeters

The two main principles of calorimeter design have given rise to the adiabatic and heat conducting classes of instrument.

The adiabatic principle is to isolate the calorimeter vessel thermally so that no heat exchange occurs between it and the surroundings. Under those circumstances, the heat change and corresponding temperature change are described by:

$$Q = n\, dH_R \qquad (1.1.1.1)$$

and

$$T = Q/C_p \qquad (1.1.1.2)$$

Where:

Q = heat change

dH_R = reaction enthalpy

C_p = effective heat capacity

n = number of moles

T = temperature (^oC)

From (1.1.1.1) and (1.1.1.2)

$$T = n \times (dH_R/C_p) \qquad (1.1.1.3)$$

The above are the fundamental relations in calorimetric analysis, McGlothlin and Jordan 1975 (2).

In practice, the adiabatic ideal is approximated by instruments fitted with adiabatic shields, i.e., jackets which are heated or cooled in concert with an exothermic or endothermic change within the calorimeter, thus preventing heat exchange with the

surroundings.

The design becomes considerably more simple in the isoperibol or semi-adiabatic calorimeters. This class of calorimeter is thermostated but no attempt is made to eliminate completely heat losses. Instead, where necessary, the extent of heat loss can be estimated and corrections made to quantitative data. An isoperibol calorimeter specifically for use with immobilized enzymes has been patented by Mosbach 1977 (3). It would appear that most calorimeters based on a thermistor/Dewar flask design belong to the isoperibol class.

A further subclass of the general adiabatic instrument is termed ISOTHERMAL. The basic design has been described by Christensen et al. 1968 (4). The instrument operates with no temperature change within the calorimeter cell. Isothermal conditions are maintained by a Peltier unit and a variable input heater which together compensate for exothermic and endothermic changes. Heat effects are measured indirectly as the electrical power exerted in maintaining a constant temperature during a reaction.

The main feature of heat conducting calorimeter design is that there is complete flow of heat from a heat source, the calorimeter vessel, to a (high heat capacity) heat sink across interposed thermocouples. The output from a thermocouple (ie. V, volts) is dependent on the temperature gradient across the cold and hot junctions.

$$V = N \times E \times dT \qquad (1.1.1.4)$$

Where:

N = number of thermopiles in the thermocouple.

E = thermoelectric constant ($V\ ^{o}C^{-1}$)

The temperature gradient (dT) also produces a flow of heat

$$dQ/dt = N \times C \times dT \qquad (1.1.1.5)$$

C is the average thermal conductivity of the thermocouple and has the dimensions - $Js^{-1}\ ^{o}C$

The sensitivity of heat conducting instruments can be defined as the ratio of instrument output to the power developed in the calorimeter vessel; from (1.1.1.4) and (1.1.1.5).

$$S\ (V.\ J\ s^{-1}) = V/(dQ/dt) = \frac{E}{C} \qquad (1.1.1.6)$$

That is, instrument sensitivity, (S), is determined largely by the characteristics of the thermocouples, specifically, the ratio of its thermoelectric constant to the thermal conductivity. Instrument sensitivity can be estimated as $1/E_{ss}$, where E_{ss} is the steady state calibration constant with the dimensions of

$$J\ s^{-1}\ V^{-1}$$

Heat conducting calorimeters have been designated as either batch

or flow. Commercially available* and hence widely used examples of the two types are:

a. the Prosen-Berger Microbiocalorimeter, also called the National Bureau of Standards (NBS) batch calorimeter, Prosen 1973 (5) (Thermometrics Corp. San Diego USA), and

b. the LKB 2017-30 sorption microcalorimeter (LKB Producter A.B. Bromma Sweden).

The latter instrument can be used in a batch as well as in a flow mode.

1.1.2 The LKB 2017-30 Sorption Calorimeter - output-time relations and calibration

The commercial instrument is closely based on a heat conducting instrument described by Wadso 1968 (6). In essence it is a twin cell calorimeter; the two cell compartments each lie within a separate calorimetric unit. One is designed for batch and the other for flow-through modes of operation. A pair of thermocouples from each unit are connected in opposition, in a differential arrangement, such that spurious heats common to both units cancel. The calorimeter is housed in a $50dm^3$ air bath fitted with an LKB proportional controller and a thermistor sensor. For operation, the whole instrument is further placed in a constant temperature room at $20^{o}C$ ($\pm$ $0.5^{o}C$ per day).

* footnote: a new instrument, the BIO - DSC batch and flow microcalorimeter, is being marketed by SETARAM (Caluire, France)

Two basic forms of instrument output are illustrated, Figure (1.1.2.1)

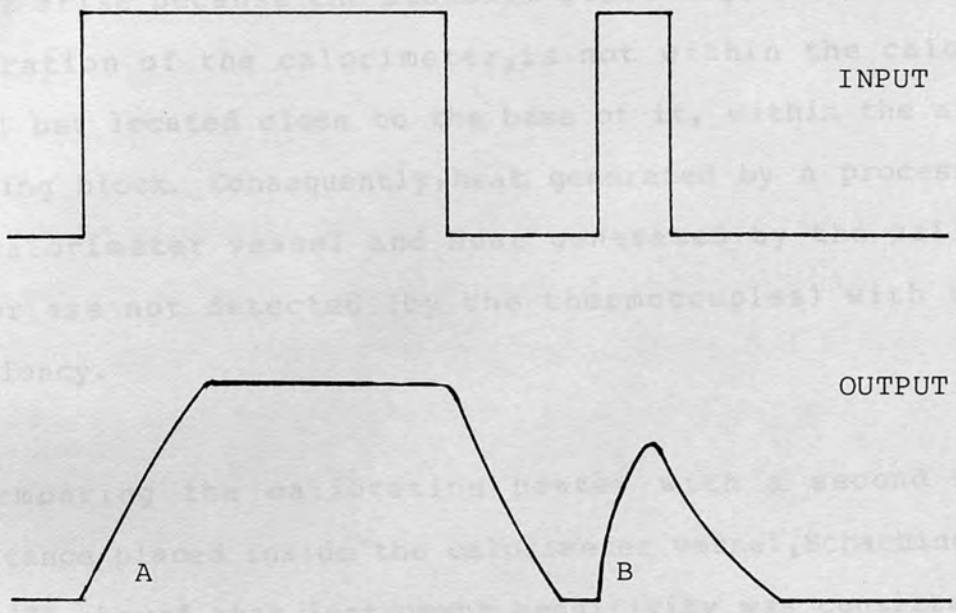

Figure (1.1.2.1) - Steady State (A) and Transient (B) output from the LKB 2017-30 Sorption Microcalorimeter.

There is some indication in the literature, and from simulation studies presented later (s 3.1) that these output - time relationships are well approximated by the standard exponential forms:

$$\theta(t) = \theta max\ [1 - exp\ (t/T_1)] \qquad (1.1.2.7)$$

and

$$\theta(t) = \theta max\ [1-exp(-t/T1)] * exp\ (-t/T_1 - t/2) \qquad (1.1.2.8)$$

for the steady state (A) and transient (B) response respectively.

$\theta(t)$ = output as a function of time, t

T = time constants for transient processes in the calorimeter (s 3.1)

Two reports have recently drawn attention to sources of systematic error associated with the present instrument. The errors arise because the standard resistor,used for electrical calibration of the calorimeter,is not within the calorimeter vessel but located close to the base of it, within the aluminium mounting block. Consequently,heat generated by a process within the calorimeter vessel and heat generated by the calibration heater are not detected (by the thermocouples) with the same efficiency.

By comparing the calibration heater with a second standard resistance placed inside the calorimeter vessel,Schachinger et al. 1983 (7) showed that instrument sensitivity was consistently 11% less in the latter case. That is, heat generated by the calibration heater was relatively better detected. This was attributed to incomplete heat flow from the calorimeter vessel to the heat sink; thus the flow cell for this instrument does not remain completely isothermal during use. It was recommended that sensitivity measurements should be multiplied by a correction factor of 0.89.

Poore and Beezer 1983 (8) have also reported on systematic errors originating from the same design feature discussed above. The gist of their initial thesis and findings are summarized as:

a. Not all the heat generated in a calibration experiment is detected. This is due to heat loss which increased with flow rate, (heat loss was measured as a decrease in the

calibration constant, E_{ss})

b. Since the calibration heater and calorimetric vessel have a different geometrical relationship to the thermocouples, their heat loss dependence on flow rate would also be different.

Under those circumstances the usual practice, of calibrating under the same conditions as used in an experiment, would not adequately compensate for heat losses. Poore and Beezer suggested that calibrations might be done at zero flow rate to obtain a true value for E_{ss}, and then the effects of a heat loss in experiments corrected for by the addition of heat loss factor.

1.1.3 Applications of Calorimetry in the Lifesciences

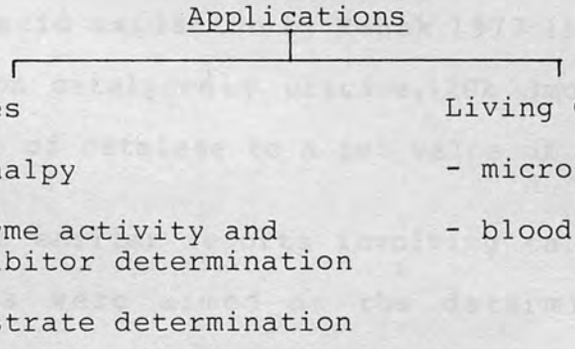

Figure (1.1.3.1) - Applications of calorimetry in the lifesciences

The application of calorimetry in the study of biological systems resolves into two broad areas as indicated above. Studies involving enzymes may emphasise fundamental, i.e.,

thermodynamic/kinetic study, or else are more pragmatic, eg., deal with substrate determination. There is considerable overlap.

The enthalpies of reactions which are useful in clinical analysis are important because dH_R can be considered a sensitivity parameter in calorimetric analysis. There is some interest in the values of dH_R for reactions catalysed by oxidases. Poe 1970 (9) has, for instance, determined the enthalpy for oxidation of reduced nicotinamide dinucleotide (NADH) by dissolved oxygen to be 258 kJ mol^{-1}. This reaction is important in two respects. First, it could be used to increase the sensitivity of analysis involving dehydrogenation reactions which in themselves are not stongly exothermic. Secondly, oxidation leads to the regeneration of the cofactor NAD at the expense of oxygen.

The principle of heat amplification is again apparent in the study of uric acid oxidation by Rehak 1977 (10). The dH_R for the initial reaction catalysed by uricase, (20k $Jmol^{-1}$) was increased in the presence of catalase to a net value of 153 kJ mol^{-1}.

The majority of earlier reports involving calorimetric study of enzyme systems were aimed at the determination of enzyme concentration using saturating concentrations of substrate. For instance, Monk and Wadso 1969 (11) have determined the concentrations of soluble cholinesterase, alkaline phosphatase, lactate dehydrogenase and ATP-ase using the heat effect with saturating concentration of the appropriate substrate. Beezer et al. 1973 (12), also using the LKB 2017-30 sorbtion microcalorimeter, have determined the kinetic parameters for

soluble jack bean urease. Other important examples of the use of calorimetry in enzyme kinetics include studies of ribonuclease or chymotrypsin, ribonuclease and trypsin by Tribout et al. 1976 (13) or Eftink et al. 1981 (14). The determination of residual enzyme activity, during or after exposure to inhibitors, was the basis for the calorimetric analysis of organophosphorous compounds using soluble cholinesterase, Konickova and Wadso 1971 (15), Beezer and Stubbs 1973 (16).

The number of reports devoted to substrate determination using soluble or immobilized enzymes and calorimetry is now reasonably large. Examples using soluble enzymes include the determination of glucose, Goldberg et al. 1975 (17), McGlothlin and Jordan 1975 (18). Immobilized enzymes have been used in the calorimetric analysis of penicillin, Johansson et al. 1973 (19), glucose, Schmidt et al. 1976 (20) and urea, Danielsson et al. 1976 (21).

Microbiological calorimetry is an important growth area. The heat output profile (thermogram) from a micro-organism can yield information about metabolism and growth. The fine structure of the thermogram may be characteristic of the organism, hence there is a possibility of a future use of calorimetry in taxonomy. Examples of the use of micro-organisms for calorimetric quantitation of antibiotics and poisons have been reported by Beezer et al, 1977 (22) and Mattiasson et al. 1977 (23) respectively. The current scope of the application of calorimetry to micro-biological systems has been appraised in a monograph

edited by Beezer 1980 (24). The calorimetric study of blood cells may eventually produce a new approach of diagnosing blood disorders, Cerny et al. 1974 (25). For further information reference should be made to the reviews by Spink and Wadso 1976 (26), Martin and Mirini 1979 (27) and Spink 1980 (28).

1.2 Chemical and Enzyme Kinetic Considerations

1.2.1 Basic Kinetic Concepts

A main concern in chemical kinetics is the study of the dependance of reaction rate on such factors as the concentration of reactants and temperature. Only concentration dependence of rate is of interest in the following discussion.

Rate - concentration relationships are usually summarized in terms of reaction order.

$$A + B \dashrightarrow C + D \qquad (1.2.1.1)$$

For instance, from empirical observation, the rate of the above process might be found to be dependent on the concentration of both reactants according to the relation:

$$\text{rate} = k * A^{x} * B^{y} \quad : x + y = n;$$

where, k is a proportionality constant, the nth order rate constant and $x, y \geq 0$.

The above reaction would then be said to be xth and yth order with respect to A and B, and nth order overall. The order of a reaction in physical terms is a good indication of the number(s) of reactant molecules involved in the formation of a transition state.

Enzyme kinetics is concerned largely with cases where $n \leqslant 1.0$. As a rule enzyme catalysed reactions involve two or more reactants (hereafter called substrates) but the above condition is enforced by having all but one of the substrates in a large excess.

1.2.2 Initial rate Michealis - Menten and Langmuir kinetics

The rate of an enzyme - catalysed reaction follows first order kinetics at a low concentration of the limiting substrate. Unlike the analogous, purely chemical system, however, this relation breaks down at higher concentrations of substrate. Eventually the reaction enters a zero-order phase where no increase in rate is observed with increasing concentration of substrate. This saturation is due to a 1:1 complex being formed between enzyme and substrate, with recycling of the enzyme, Brown 1902 (30). The hyperbolic rate - concentration dependence seen in enzyme catalysed reactions is summarized in the Michaelis - Menten equation, Michaelis and Menten 1913 (31); Table (1.2.2.1).

The Michaelis - Menten description of enzyme steady state kinetics is mathematically analogous to the Langmuir model for the adsorption and desorption of gases from the general solid phase or a heterogenous catalyst. Some key elements of the model are summarized below (a - d) (32):

a. a solid surface with a large number of active sites;

b. adsorption on adjacent sites are independent events;

c. the fraction of occupied sites is ϕ; the fraction of free sites is $(1 - \phi)$;

d. the rate of adsorption is proportional to the pressure or concentration of gas, G.

From these considerations the respective rate of adsorption and desorption are described by (1.2.2.1) and (1.2.2.2).

$$R_a = k_1 G (1 - \acute{\phi}) \qquad (1.2.2.1)$$

$$R_d = k_2 G (1 - \acute{\phi}) \qquad (1.2.2.2)$$

At equilibrium the adsorption and desorption rates are equal, hence:

$$\acute{\phi} = G/(Km + G)$$

where Km is the dissociation constant k_2/k_1; the ammount of gas adsorbed, A, is proportional to the fraction of sites occupied, $\acute{\phi}$, therefore

$$A = \frac{[a]\ G}{Km + G} \qquad (1.2.2.3)$$

The nature of the constants [a] and Km is readily seen by considering two limiting gas concentrations

a. $G >> Km$

$A = [a]$, i.e., $[a]$ is the maximum loading capacity of the solid

b. $G << Km$

$A = \frac{[a]}{Km} G = kG$, i.e., the ammount of gas adsorbed is directly proportional to the concentration of gas.

Finally, when

$A = 1/2\ [a]$, $Km = G$

The above method is essentially applicable to the steady state kinetics of enzyme free in solution or to immobilized enzyme kinetics in the absence of diffusion control (s 1.4). The

essential character of the Michaelis - Menten equation may be understood through a one-to-one comparison of terms with those appearing in (1.2.2.3).

In the Michaelis-Menten model for enzyme-substrate interaction, it is assumed that:

a. the concentration of enzyme is very small relative to the concentration of substrate;
b. product concentration is initially zero and does not rise significantly during reaction rate measurements, and
c. the release of product molecules from the enzyme is slow so that the free enzyme rapidly reaches an equilibrium with the enzyme-substrate complex.

Enzyme-substrate systems accurately described by the above model have one chief characteristic. They give a hyperbolic velocity versus substrate concentration curve ; all linear transformations of the steady state kinetic data from such a Michaelis-Menten enzyme, Table (1.2.2.1), are expected to lead to a linear graph.

The Michaelis constant (Km) and the maximal velocity (Vmax) may be determined from a progress curve observed at a single initial substrate concentration (S), Table (1.2.1.1.2). For instance, a plot of P versus -ln (S/(S-P))will be linear with a slope of Km and an intercept value equal to Vmax. There are, however, difficulties associated with the use of the reaction progress curve in the way described. During the time-course of an enzyme catalysed reaction, at a single substrate concentration, there may be:

a. changes in enzyme concentration, e.g., by gradual inactivation

b. nonenzyme catalysed product formation

c. changes in reaction conditions, e.g., pH., and

d. substrate depletion and product buildup.

Traditionally these problems are circumvented by the adoption of the initial rate assay protocol.

The initial rate principle involves the use of the initial slope of a progress curve, Table (1.2.2.1.2) $Lm_{t \rightarrow 0}$) as a measure of reaction rate. The duration of the assay is such that $P < 0.05\ S$. Characteristically several such rate measurements are made, at a range of S, and the kinetic parameters Km and Vmax determined using one of the linear transformations of the Michaelis - Menten equation.

Table (1.2.2.1) Some Important Kinetic Relations

1. General First Order Kinetics

rate equation: $v = -dA/dt = kA$

integrated form: $\ln(A/A_t) = kt$

exponential form: $A_t = A \exp(-kt)$

2. Initial rate Michaelis - Menten Kinetics

rate equation $= v = dp/dt = Vmax\ S/(Km + S)$

integrated form: $P = Vmax\ t - Km * \ln(S/(S-P))$

exponential form: $S_t = S \exp[-(Vmax\ t-P)/Km]$

progress curve: $P_t = S - S_t$

$= S[1 - EXP[-Vmax\ t-P)/Km]]$

3. Linear Transformations of the Michaelis - Menten Equation

Lineweaver - Burk : $1/v = (1/S)\ Km/Vmax + 1/Vmax$

Eadie: $v = Vmax - (V/S)Km$

Hanes: $S/v = Km/Vmax + S/Vmax$

Integrated Michaelis - Menten

$$P/t = Vmax - 1/t * Km * \ln (S/(S-P))$$

1.2.3 Non-Initial Rate Kinetics

Initial rate conditions may not be readily enforced in several important cases. First, there may be limits to the decrement in assay time or dilution of enzyme sample possible (a low enzyme concentration ie. low Vmax, increases the period during which there is a linear relationship between P_t and t.) Secondly, it is particularly difficult to control reaction time in a flow system. The sorts of deviations from Michaelis - Menten kinetics in flow systems have recently been reviewed by Eftink et al. 1981 (35). Errors may arise, in the determination of Km and Vmax estimates using linear transformations of the Michaelis-Menten equation, as a result of substrate depletion, product inhibition and reaction reversal. The determination of Km and Vmax under non-initial rate assay conditions, Table (1.2.3.1), is considered in chapter 4.

Another source of deviation from Michaelis-Menten kinetics is high enzyme concentration. As discussed above, the condition of excess substrate concentration was assumed in the rapid equilibrium model. The use of very dilute enzyme concentration is conventional in the study of soluble enzyme kinetics. Naturally

and artificially immobilized enzyme systems, (most enzymes may be temporarily or permanently immobilized inside cells) are, however, characterised by relatively higher enzyme concentrations.

In a theoretical study, Cha 1970 (36) predicted 50 - 200 % error in Km estimates in situations where the enzyme concentration is of a similar mangitude to Km. The level of error could however be reduced, to 50% or less, by the use of several proposed alternatives to the Lineweaver-Burk plot. However, according to Engasser and Horvarth 1973 (37), a distinction is necessary in the consideration of the effect of high enzyme concentration on Michaelis - Menten kinetics between closed and open enzyme systems.

The Cha description is accurate only where the enzyme assay is under closed system conditions; i.e., the reaction vessel exchanges energy but not matter with the surroundings. Examples of closed system enzyme assays include reactions run in test-tubes, beakers or batch reactors. Biological systems and flow-through immobilized enzyme reactors are open systems; they exchange both energy and matter with the surroundings. Under those conditions the kinetics of an enzyme (in the absence of diffusion effects) is Michaelis-Menten irrespective of enzyme concentration.

Table (1.2.3.1) A Non-initial rate kinetics (34,35)

1. Competitive Product Inhibition

rate equation: $v = Vmax\ S/[Km(1+P/K_p) + S]$

integrated form: $P/t = Vmax/(1-Km/Kp) - (1/t) * Km * In\ (S/(S-P) * (1+S/Kp)/(1 - Km/Kp)$.

P/t is plotted against - (1/t) (1 + S/Kp) * Ln (S/(S-P)

slope (m) = Km/1-Km/Kp) ; Km =mKp/(m+Kp)

intercept (c) = Vmax/(1 - Km/Kp); Vmax = c(1-Km/Kp)

2.Non-competive Product Inhibition

rate equation: Vmax S/(1+P/Kp) (Km +S)

integrated form: P/t(1-P/(2Km - 2Kp)) =

Vmax/(1-Km/Kp - ((1 + S/Kp)/(1 - Km/Kp))*(1/t) * Km ln(S/(S-P).

assuming Km << Kp, p/t (1 +P/2Kp) is

plotted against -(1/t) (1 + s/Kp) ln (S/(S-P)).

slope, intercept, Km and Vmax are the same as above.

3. Substrate Inhibition

rate equation: $v= Vmax\ S/(S +KM + S^2/Ks)$

integrated form: P(2S - P + 2KS) / (2t Ks)

Vmax - (1/t) Km in (S/(S-P).

P(2S - P + 2Ks)/(2t Ks) is plotted against -(1/t)

In (S/(S - P)

slope = KM

intercept = Vmax

a. for immobilized enzyme reactors $t = \varepsilon\tau$; ε is the ratio of support to reactor volume and τ is the column space-time (sl.3)

1.3 Flow Injection Analysis with Immobilized Enzyme Reactors

Analytical methods involving liquid flow systems can be designated as Continuous Flow Analysis (CFA), Skeggs 1957 (38) or Flow Injection Analysis (FIA), Ruzicka 1975 (39). Some features common to both CFA and FIA include :

a. the injection of sample into a reactant or carrier stream and the flow of the combined stream through a delay or equilibrium coil to a detector, and

b. the addition of sample in the form of a narrow pulse (pulsed injection) or as a broad slug (continuous injection). The detector output as a function of time, in these two cases are described as transient and steady state respectively, Fig. (1.1.2.1).

The basic difference between CFA and FIA would appear to be the introduction of air bubbles into the flow stream in the former case. Stream segmentation apparently reduces the longitudinal spread of sample, thus improving the dynamic characteristics of CFA systems. The two forms of flow analysis do not appear differentiated by the mode of sample injection or by instrument requirements. The typical CFA set-up may however be slightly more complicated because of the additional equipment for adding and removing air bubbles to and from the flow stream. The CFA approach is widely adopted in current commercial instrumentation for automated flow analysis, Saltpeter and Leperch 1981 (40). The general area of flow analysis has recently been reviewed by Ruzicka and Hansen 1978 (41), 1980 (42), 1981 (43) and Snyder 1980 (44); a monograph has also been produced by Ruzicka and Hansen (1981)(45).

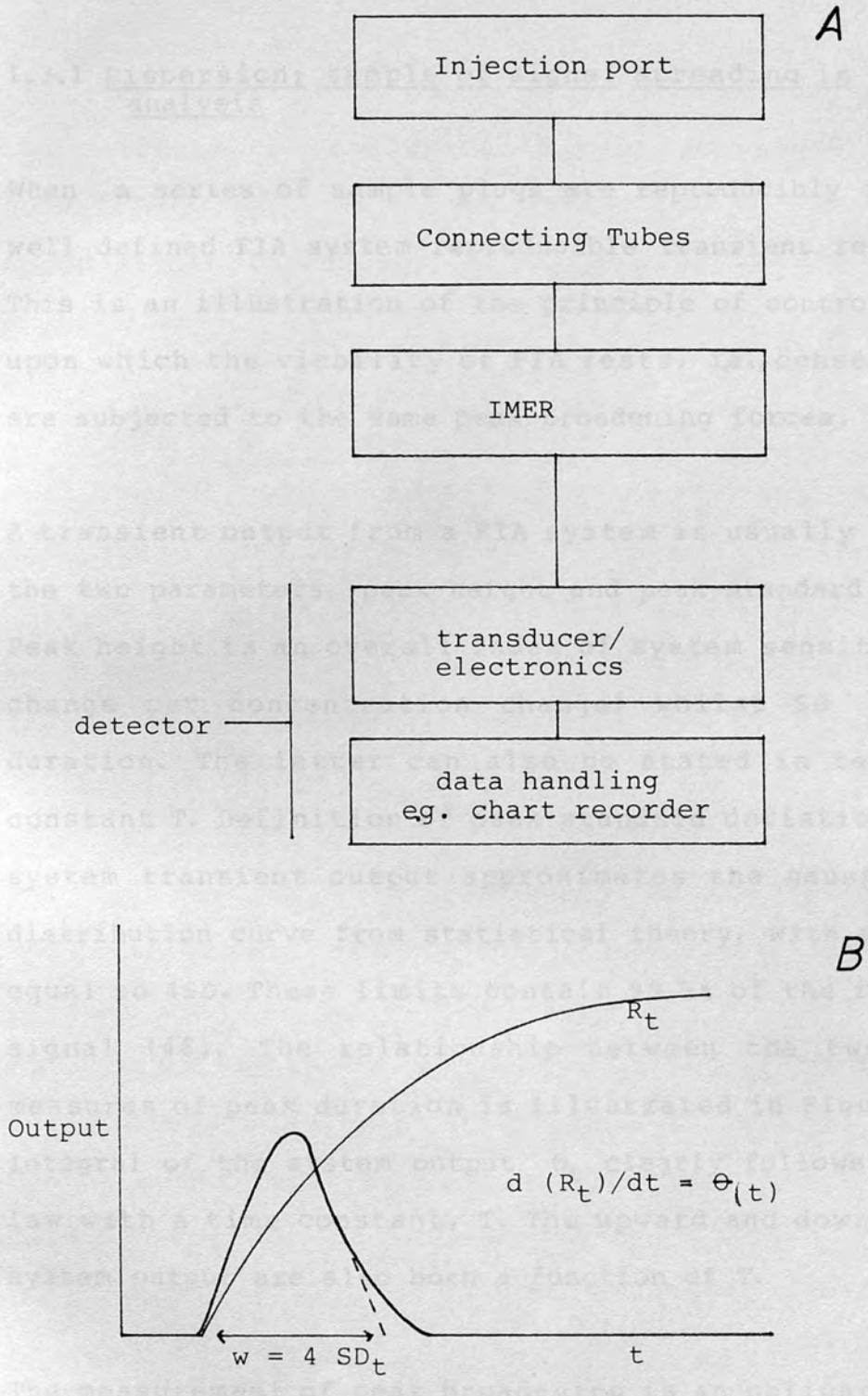

Figure (1.3.1) The subsystems comprising the FIA system of Interest (A). The relation between T and SD (B) (cf. text).

1.3.1 Dispersion; sample of signal spreading in flow injection analysis

When a series of sample plugs are reproducibly injected into a well defined FIA system reproducible transient responses emerge. This is an illustration of the principle of controlled dispersion upon which the viability of FIA rests, i.e., consecutive samples are subjected to the same peak-broadening forces.

A transient output from a FIA system is usually represented by the two parameters, peak height and peak standard deviation (SD). Peak height is an overall index of system sensitivity, (signal change per concentration change) whilst SD measures peak duration. The latter can also be stated in terms of a time constant T. Definition of peak standard deviation assumes that system transient output approximates the gaussion or normal distribution curve from statistical theory, with a base width (W) equal to 4SD. These limits contain 99.5% of the ideal transient signal (46). The relationship between the two most common measures of peak duration is illustrated in Figure (1.3.1). The integral of the system output Θ_t clearly follows an exponential law with a time constant, T. The upward and downward phases of system output are also both a function of T.

The measurement of peak broadening is an obligatory first step towards a clear description and the subsequent adoption of an effective opimization procedure for a given FIA system. For instance, it has been suggested that to avoid significant merger of adjacent peaks, samples should be separated by at least 4SD

intervals, Snyder 1972 (47); this corresponds to a chromatographic resolution (R_s) of unity, (R_s = W/distance between adjacent peak maxima). Under such circumstances analysis speed or sample throughput can be estimated according to the expression:

$$f(h^{-1}) = 1/(4SD) \qquad (1.3.1.1)$$

Peak duration can be affected by the dynamic behaviour of the subsystems comprising the FIA system (Fig. 1.3.1). For instance slow sample injection relative to carrier flow rate would result in a more squat and broad peak. This idea by analogy to the additivity of variances is usually stated as:

$$\Sigma SD = SD_{ip} + SD_{ct} + SD_r + SD_D \qquad (1.3.1.2)$$

That is, the total peak broadening in a FIA system is the sum of the contributions from the component subsystems. These are in the present system, injection port (ip), connecting tube (ct), immobilized enzyme reactor (r), and detector (D). Some implications of (1.3.1.2) are as follows. Firstly, each subsystem can be considered separately with respect to its contribution to peak broadening. Secondly, where an individual contribution is disproportionately large, optimization efforts directed at components beside this limiting subsystem will prove unproductive. Further, under such circumstances, the expected sample throughput rate for the whole FIA system is immediately estimable, using the SD value for the limiting subsystem, from (1.3.1.1)

A third feature of FIA systems discussed in terms of SD is detector fidelity. A detector will not accurately reproduce a transient process which is sufficiently fast. For good fidelity it has been suggested that $SD_D \leqslant 0.3\ SD_x$, where SD_x is a measure of the duration of the transient process.

In accord with the above discussion, it is important to consider more closely individual peak broadening contributions from components of the present FIA system, Fig. (1.3.1). Towards this aim it is intended to outline some mechanisms of and factors affecting dispersion in the four subsystems above.

1. Injection Port - as discussed above, slow sample injection relative to carrier flow rate can lead to peak spreading. However, FIA systems are usually fitted with injection valves/sample loops designed to enable rapid injection. The signal width increase contribution from this source is therefore likely to be relatively small.

2. Connecting Tubes - friction between a tube wall and fluid flowing through it results in a parabolic velocity profile in the fluid. This laminar flow pattern causes spreading of sample along longer sections of tubing. Spreading in open tubes also occurs by diffusion at the sample plug-solvent boundary. The dependence of the dispersion on factors like tube radius (R), tube length (L), sample flow rate (F) and sample residence time (t), is summarized by the relations (1.3.1.3) and (1.3.1.4), Taylor 1953 (48).

$$SD_t^2 = \frac{2Dlt^2}{F} + \frac{\pi R^4 l}{24DF} \qquad (1.3.1.3)$$

$$SD_v^2 = 2DFlt^2 + \frac{\pi R^4 lF}{24D} \qquad (1.3.1.4)$$

Where SD_t^2 or SD_v^2 is the peak variance with the dimensions of time or volume, respectively; D is the diffusion coefficient ($cm^2\ s^{-1}$) of sample molecules. It is difficult to assess the importance to peak spreading of contributions from this source. The relations (1.3.1.3) and (1.3.1.4) give considerable over-estimates of the observed sample dispersion, especially it would seem, when the connecting tube is coiled. Schifreen et al. 1977 (49) considered the dispersion in connecting tubes to be predominant in their evaluation of a thermistor-based thermochemical FIA system.

3. Immobilized Enzyme Reactor (IMER) - concentration - time relationships, i.e., the way in which the concentrations of substrate and product change with time, in any real IMER, fall within limits set by the concentration-time relationships of two idealized theoretical reactor models. These are the Plug Flow Reactor (PFR) and Continuously Stirred Tank Reactor (CSTR) models. It simplifies matters considerably if there is 100% reaction or no reaction at all within the reactor. This and other assumptions made in the PFR and CSTR models are discussed by Vierth et al. 1976 (33).

A square sample plug injected as a pulse or continuously into the theoretical PFR travels with infinitely sharp boundaries as there is no mixing or diffusion at sample/solvent interphase.

Each sample molecule is resident within the reactor for an average of time directly and inversely proportional to the reactor volume (V) and sample flow rate (F) respectively.

$$T^* = V/F \qquad (1.3.1.5)$$

Because there is no sample dilution in the theoretical PFR, the peak height value and contribution to analysis time are the optimum (i.e., highest and lowest respectively) possible for any real IMER. The PFR ideal is far removed from the behaviour of the typical IMER; in this respect it is less useful than the CSTR model discussed below.

The CSTR or the perfectly mixed reactor theoretical model represents the lower limit or "worst-case" of real IMER performance. A CSTR is perhaps most summarily described as an exponential diluter. When initially filled with sample, the concentration-time relation follows first order kinetics with a dilution constant, k;

$$k = F/V = 1/T \qquad (1.3.1.6)$$

T does not represent a real residence time in an exponential diluter because sample molecules will in theory be present at infinite time. The ratio V/F is called the reactor "space-time", or time constant, to distinguish it from T^*, the residence time in the PFR model. Concentration-time relationships in an exponential diluter with continuous or pulsed sample injection are described by (1.3.1.7) and (1.3.1.8)

$$S = S\,[1 - \exp(-t/T)] \qquad (1.3.1.7)$$

and

$$S = S\,[1 - \exp(-t/T)]\exp(-t/T) \qquad (1.3.1.8)$$

These relations have the same form as (1.1.2.7) and (1.1.2.8). The above is a review of the limiting cases for IMER performance in terms of concepts traditionally borrowed from process engineering. The performances or real IMER, i.e., intermediate between the PFR and CTSR models, have on the other hand been discussed in terms of models and concepts from Chromatography.

In the plate model, Martin and Synge 1941 (50), column chromatographic separation is seen as the result of multiple partitioning processes taking place within successive theoretical volume elememnts or plates. In the performance of two 'similar' columns, that column having the greater number of plates (N) would give better separation. The multiple partitioning process is mathematically described by the Poisson distribution and for a large number of plates the final sample elution profile follows the gaussian or standard normal probability curve, (1.3.1.9).

$$P(x) = 1/(SD\ 2\sqrt{\pi})\ \ ep[-(x-\bar{x})^2/2SD^2] \qquad (1.3.1.9)$$

$P(x)$ = probability of the statistic x

$\bar{x}$ = mean of the normal distribution

SD^2 = population variance

The corresponding sample elution profile can then be written, by a one to one translation of terms, as:

$$\frac{\theta(t)}{\theta} = 1/(SD^2 2\sqrt{\pi}) \exp[-(t - t^*)^2 / 2SD^2] \qquad (1.3.1.10)$$

Where $\theta(t)$ = sample elution as a function of time

θ = concentration injected

t^* = time from injection to peak maximum (retention time)

SD^2 = variance measured in time units

The elution profile (1.3.1.10) is related to the number of column theoretical plates by defining the number of plates as

$$N = (t^*/SD)^2 \qquad (1.3.1.11)$$

The peak maximum of the sample elution profile is a function of N.

$$\theta(max) = \frac{\theta}{t^*} \sqrt{\frac{N}{2\pi}} \qquad (1.3.1.12)$$

θ(max) is the concentration of solute at the peak maxima. For a series of bell-shaped curves(1.3.1.10), an increase in the value of N results in sharper, less broad peaks and also an increase in peak height.

Developments in the theory of liquid chromatography, since the initial report by Martin and Synge discussed above, have largely been towards understanding how N is affected by experimental parameters. An initial assessment by Martin and Synge is that:

a. N & F , because a low flow rate would allow greater time for interplate diffusion of solute molecules, and

b. N & I/d^2 (where d is the diameter of column support), since total column support surface area decreases in direct proportion to d^2.

A more detailed analysis of the dependence of N on column characteristics and processes has been presented in the random walk model of Giddings 1970 (51).

$$HETP = L/N = a + b + cm + cs + x \qquad (1.3.1.13)$$

Five processes are identified as affecting the number of theoretical plates. The above expression , called the Van Deemter equation, summarises these. The terms in (1.3.1.13) are listed below with a brief description of the cause of spreading in each case.

a - (Eddy diffusion) - some solute molecules follow longer flow paths around support particles.

b - (Axial dispersion) - diffusion at sample plug solvent boundary.

cm - (Resistance to mass transfer in the mobile phase) - flow inequalities analagous to laminar flow in open tubes, and diffusion of solute between adjacent flow lines;

cs - (Resistance to mass transfer in the stationary phase) - a solute molecule diffusing into the stationary phase is left behind by solvent flow.

x - (Stagnant mobile phase) - solute molecules enter into dead

end flow paths.

The conclusions of Martin and Synge as regard the dependence of N on support diameter are substantiated by later treatments; the dependence of N on flow rate is however more complex. The number of plates initially increases with flow rate but passes through a maximum then decreases, Synder 1969 (52).

These considerations are important because the chromatographic processes discussed above, have direct analogy in an IMER. Band spreading theories in chromatography have been reviewed by Grushka 1975 (53).

4. Detector - the time-response characteristics of electronic components can be described in terms of first order kinetics, Table(1.2.2.1).The transducer (thermocouples), amplifier, and data handling sytem can all therefore be lumped together into a single electronic unit - the detector. The dynamic characteristics of the detector can then be described by reference to a single time constant, Poppe 1980 (54). As discussed above, the dynamic characteristics of a detector can become limiting for fast transient processes. This contribution to peak broadening is particularly important in the present F.I.A. system (s 3.1).

1.3.2 Immobilized Enzyme Reactors in FIA

The main classes of enzyme reactors have been described by Vierth et al 1976 (33). These include batch reactors, continuously

stirred tank reactors, fluidized bed reactors, packed bed reactors and tubular reactors. Only the last two categories have found widespread use in analytical chemistry. The level of dispersion seen with the other reactor types makes them less suitable.

The earliest mention of a packed bed reactor is probably in the report by Reisel and Katchalski 1964 (55). A packed bed reactor consists of a column containing a compact bed of (immobilized enzyme) particles. Packed bed reactors have been interphased with a large variety of detectors for analytical applications, eg., uV absorbance, Ikeda et al. 1974 (56), colorimetry, Hicks and Updike 1966 (57), ion selective electrode potentiometry, Johansson et al. 1976 (58), amperometry, Updike and Hicks 1967 (59), thermometry (21) and chemiluminescence, Auses et al. 1975 (60). Some important characteristics of packed bed reactors include:

a. A high surface area per unit reactor volume, particularly when loaded with porous support, and

b. a large pressure drop across the reactor compared to other types of enzyme reactor discussed below.

A tubular reactor is generally an open tube to the inside walls of which enzymes are attached. The early forms described by Campbell et al. 1975 (61) were nylon or polyamide tubes. An advantage of a tubular over a packed bed reactor is that there is a low pressure drop across the open tube. The former, however, generally present about an order of magnitude drop in surface

area per unit volume. More recently, enzymes have been attached to the walls of capillaries after etching with acid to increase the surface area, Iob and Mottola 1981 (62). An alternative approach involves coating the inside of the glass tubing with a porous or gel layer, Horvarth and Solomon 1972 (63). Tubular reactors have, like packed bed reactors, also found widespread use in analytical chemistry particularly in CFA. However, it seems that without air segmentation, at the flow rates required for adequate sensitivity (see below), dispersion is a major problem in FIA applications.

A new form of tubular reactor, the Single-String-Bead Reactor (SSBR) has recently been applied to enzymic analysis, Ramaswamy and Mottola 1982 (64). Additional surface area for enzyme immobilization is provided by a single string of glass beads in the lumen of the tube. The presence of the glass beads also improves the dispersion in the reactor relative to the open-tube arrangement.

The last category to be described may not qualify as an IMER. A typical example is a closed loop flow through system consisting of a stirred reservoir, (with a high concentration of soluble enzyme) reaction or delay coils, a detector, pump and a sample injection valve connected in a closed loop, Woolf and Mottola 1978 (65). The above arrangement enabled repeated sample analysis with recycle and re-use of enzyme. There was however no separation of the enzyme from substrate or products (s 2.1).

The use of immobilized enzyme in analytical chemistry has been reviewed by, eg., Johansson 1982 (66), 1983 (67), Johnasson et al. 1984 (69), Mottola 1983 (70) and in the monograph by Carr and Bowers 1980 (68).

1.3.3 Reactor Kinetics and Applications in FIA

As described by Lilly et al. 1966 (71), the kinetics of a reaction occuring in an IMER, through which there occurs 'piston' or plug flow, can be described by the intergrated Michaelis-Mentin equation, Table (1.2.2.1). Owing to the absence of sample dispersion the kinetics shown in a PFR is expected to be identical to that observed in a batch reactor of equivalent volume. The reaction time (t) is given by a product of the sample residence time and the fraction of the packed bed occupied by fluid (ϵ).

$$t = \epsilon V/F \qquad (1.3.3.1)$$

The kinetic constants Vmax and $Km^{app.}$ may be determined from a plot of P/t against (1/t) ln (S/(S-P)); the slope and intercept values are equal to $Km^{app.}$ and Vmax respectively (Chapter 4).

The first-order phase of the Michaelis-Mentin equation (S << Km) is important in the analytical application of enzymes. In the first order phase (S $\sim$ 0.01Km) there is direct proportionality between the reaction rate (v) and S. In applications involving immobilized enzymes, diffusion and non-initial rate effects may result in one to two orders of magnitude increase in Km: (i.e.,

$Km^{app.} \sim 10 - 100$ Km); consequently a linear relationship between reaction rate and S may be seen at substrate concentration values equal or greater than the intrinsic Michaelis constant (Km). The Km of an enzyme may be taken as an indication of the limit of linearity in analysis employing the enzyme in immobilized form.

Integration of the Michealis-Mentin equation (S << Km) yields

$$\text{In } (S/(S-P)) = k^{app}t \qquad (1.3.3.2)$$

where ^{app} is the first order rate constant ($Vmax/Km^{app}$) for a reaction catalysed by an immobilized enzyme. Hence:

$$\text{In } (1 - X) = -k^{app}t \qquad (1.3.3.3)$$

$$X = 1 - \exp(-k^{app}t) \qquad (1.3.3.4)$$

X is the fractional conversion of substrate, S/P. The dependence of X on IMER characteristics e.g. enzyme loading (Vmax), mass transfer effects (s 1.4) and the column dimension may be inferred from (1.3.3.4). For instance sample residence time at any flow rate is dependent on the column dimensions; from (1.3.3.1)

$$t = (\varepsilon \pi R^2 \, l \,)/F \qquad (1.3.3.5)$$

Reactor performance in general can be predicted and optimized using the above quantitative relations. The results of a theoretical optimization excercise by Johansson et al. (67) are interesting. For a large number of enzymes, packed bed reactors

with a volume of a few microlitres and a residence time of a few seconds are feasible.

1.4 Kinetics of Reactions Catalysed by Immobilized Enzymes

1.4.1 Factors affecting immobilized enzymes

There is increasing interest in artifically immobilized enzymes and cells as possible new-generation biocatalysts for industrial and medical applications. Immobilized enzymes can also serve as models for enzyme system *in vivo*; a large number of enzymes occur naturally immobilized in nature. Increased understanding of immobilized enzymes is thus perhaps a prerequisite for their more efficient and novel applications. The characteristics of an immobilized enzyme may differ from those of the corresponding native enzyme because of four main factors.

These are:

a. enzyme conformational change as a result of immobilization;
b. steric interactions of enzyme substrate with the enzyme support matrix;
c. electrostatic effects, and
d. mass transfer limitations.

In the presence of one or a combination of these effects, the prefixes - "intrinsic", "inherent", "apparent", or "effective", are used to describe such properties as stability or kinetics,

FIG(1·4·1·1)-Factors affecting immobilized enzymes and some prefixes commonly used in describing their properties

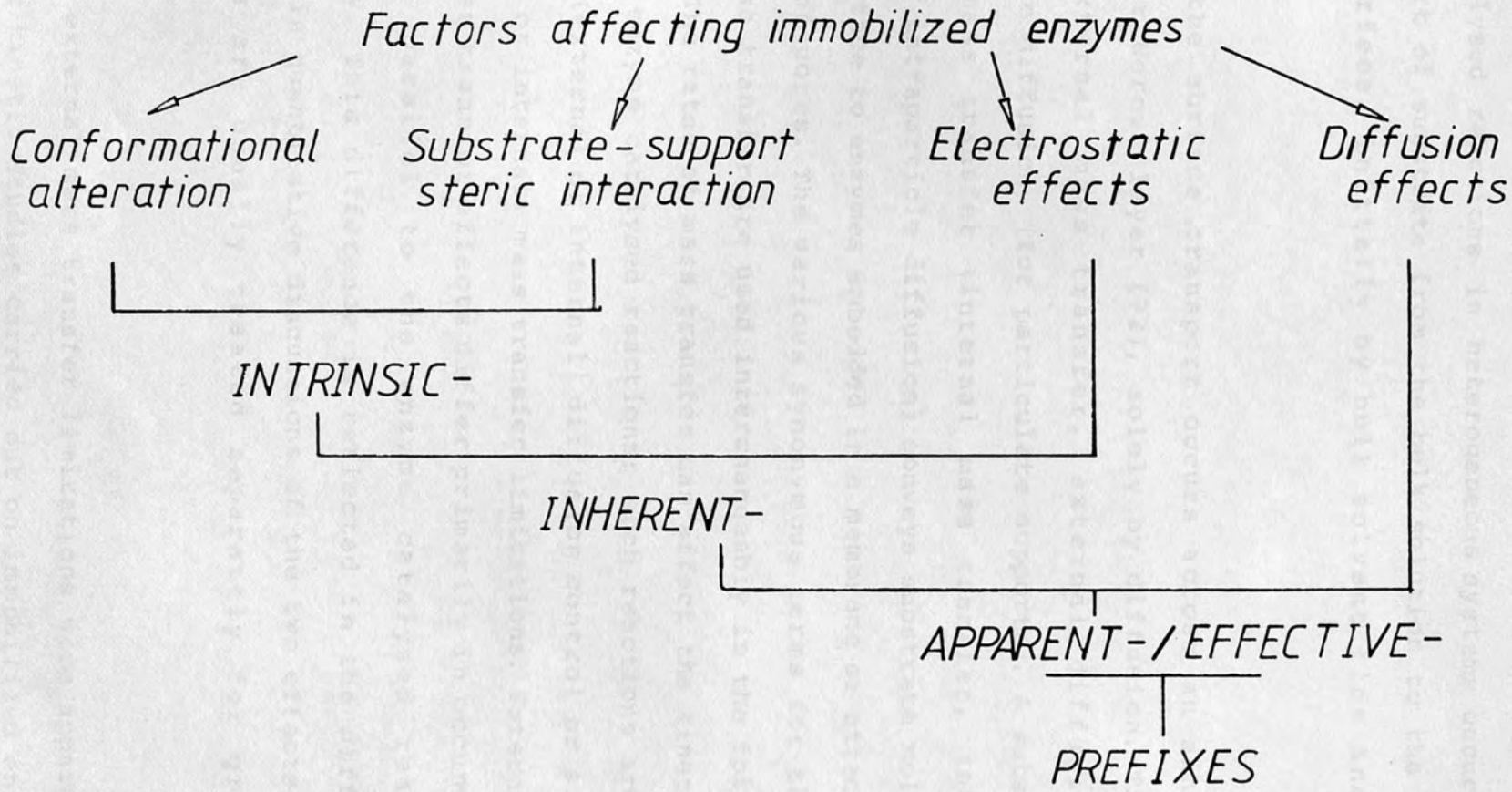

Enzyme catalysed reactions in heterogeneous systems occur after the transport of substrate from the bulk solution to the enzyme support surface, initially by bulk solvent flow and then diffusion.

Very near the surface ,transport occurs across an adhering, unstirred or Nernst layer (72), solely by diffusion. This is termed external mass transfer, external diffusion or interparticle diffusion, (for particulate supports). A subsequent diffusive mass transfer (internal mass transfer, internal diffusion or intraparticle diffusion) conveys substrate molecules from the surface to enzymes embedded in a membrane or attached to the inside of pores. The various synonymous terms for the two forms of mass transfer are used interchangeably in the following discussion. The rates of mass transfer can affect the kinetics of immobilized enzyme catalysed reactions; such reactions are said to be under (external or internal) diffusion control or subject to (external or internal) mass transfer limitations. External and internal mass transfer effects differ primarily in occurring in series and parallel to the enzyme catalysed reaction respectively. This difference is reflected in the different models used in quantitative discussions of the two effects; such discussions are usually treated separately for greater simplicity.

Evidence for external mass transfer limitations were apparent in the earliest kinetic studies carried out on immobilized enzymes. The Michaelis constant of a carboxymethyl cellulose bound

protease, ficin, was found to be dependent on flow rate. The Km value (with N. Benzoylarginine ethyl ester, (BAEE) as substrate) was 15.9mM, 4.9mM and 3.5mM with flow rates of $30cm^3\ h^{-1}$, $140cm^3\ h^{-1}$ and "very fast" respectively, Lilly et al 1966 (71). The above results were later extrapolated to yield a value of Km unaffected by external diffusion effects (i.e., at infinite flow rate), of 1.8mM, Lee and Ryu 1979 (73). The Km of soluble ficin is 20mM. A similar dependence of Km on flow rate has been reported for enzymes entrapped in artificial membranes, Goldman et al. 1971 (74), covalently attached to the inside of nylon tubing, Onyezili and Onitiri 1981 (75) and for glucose transport systems in the intestine, Dugus et al. (76). In all cases the dependence of Km on sample flow rate was taken as indicating the presence of an unstirred layer.

Internal mass transfer is not sensitive to flow or stirring rate because, the distances over which diffusion occurs are in this case (inside pores, gels or membranes) not affected by flow. The Km of an alkaline phosphatase layer adsorbed on a collodion (nitrocellulose) membrane, ranged from 0.85 - 12mM for a layer thickness of 1.6-8.8 μm. The experimental design adopted by Goldman et al. (74) however did not enable separation of the effects of layer thickness from increased enzyme concentration; this changed by a factor 8-fold over the range of results cited above. The observed activity of the enzymne layers, relative to the quantity of enzyme immobilized, (e.g. removed from solution) decreased with increasing immobilized enzyme concentration and

layer thickness. A further consequence of diffusion effects was that the kinetics of the reaction catalysed by membrane alkaline phosphatase was no longer Michaelis-Menten. In spite of this, a velocity against substrate concentration plot was still hyperbolic.

A dependence of the Michaelis constant on membrane enzyme loading has been reported for polyacrylamide gel entrapped B-galactosidase by Bunting and Laidler 1972 (77). The Km value for the substrate, o-nitrophenyl- β-D-galactopyronoside, decreased from 8.6×10^{-4}M to 1×10^{-4}M with a 30 fold decrease in membrane enzyme concentration. The apparent per cent recovered activity, after immobilization, appeared to increase with lower enzyme loading. The Lineweaver-Burk plot, Table (1.2.2.1.3) was shown to increase in slope as a function of increased membrane thickness or increased enzyme loading. Finally, Vmax was found to be proportional to the square root of enzyme concentration, in contrast to the direct proportionality seen in free solution. Further practical confirmation, and general support for the concept of internal mass transfer limitations, has been provided in the recent study of sepharose-bound alkaline phosphatase by Mueller and Zwing 1982 (78).

Electrostatic effects are likely, in low ionic strength media, if the enzyme support is charged. Trypsin covalently immobilized on a maleic anhydride - ethylene copolymer (an anionic support at neutral pH) had a Km^{app} of 0.2mM, in low ionic strength buffer, for the basic substrate benzoyl arginine amide (BAA), Goldstein

et al. 1964 (79). The pH-activity profile maxima, for the immobilized enzyme, occurred in a more alkaline region (2.5 pH units). In high ionic strength buffer the Km^{app} increased to 5.2 mM, a value more comparable to the Km of soluble Trypsin (6.8mM). The pH-activity profile maxima shift, relative to the soluble enzyme profile, was also absent. The altered characteristics of immobilized trypsin in low ionic strength media were attributed to an unequal partitioning of positively charged species (BAA, H^+) between the bulk and negatively charged matrix phases, as a result of electrostatic interaction. Goldstein et al, (79), have provided a quantitative treatment of the partitioning of species under such coulombic forces. The unequal distribution between solution and a charged support can be described by:

$$Q = \frac{a'}{a} = \exp - [z \psi e/(K_B T)] \qquad (1.4.1.1)$$

Q = partition coefficient, the ratio of the activity of the species in a matrix (a′) to the activity m the bulk phase (a)

z, ψ and e = number of charges on the species, membrane charge (mV) and electron charge (coulomb) respectively.

Electrostatic effects in immobilized enzyme systems have also been reported by Levin et al. 1964 (80) Hornby et al. 1966 (81), Lilly et al. 1966 (71), Goldmain et al 1971 (74) Bunting and Laidler 1972 (77) and Remy et al. 1978 (82).

Steric interactions between high molecular weight substrate or inhibitors and the enzyme support have been invoked by Levin et al. 1964 (80) to account partly for :

a. the apparently decreased activity of immobilized trypsin when measured using a high molecular weight substrate (e.g. denatured casein) relative to the activity observed with a low molecular weight substrate 'benzoyl arginine ethyl ester - BAEE), and

b. a decreased sensitivity of immobilized trypsin to inhibition by high molecular weight inhibitors.

Similar results, again from a study of the inhibition of trypsin, have been reported by Duggal and Buccholtz 1982 (83).

There is relatively little information about possible enzyme conformation or tertiary (3^{o}) structure changes as a consequence of immobilization. This may, in part, be because there are few direct methods for assessing such changes. Determination of intrinsic kinetics may be one such approach however, the techniques available are posibly insufficiently refined at the present stage of development (see below). Differential Scanning Calorimetry, (DSC) may have considerable promise as a direct method for probing immobilized enzyme 3^{o} structure. In a DSC study of the thermal denaturation of nicotinamide adenine dinucleotide (NAD(H)) dependent dehydrogenases (e.g. lactate dehydrogenose, (LDH)) by Koch-Schmidt and Mosbach 1977 (84), the

presence of the cofactor NADH resulted in a 12°C increase in the transition temperature of both native and sepharose bound LDH. In a subsequent study by Koch-Schmidt and Mosbach 1977 (85) ribonuclease - A (R NAase) was bound to sepharose by a controlled number of (one to eight) covalent linkages. Thermal denaturation studies by DSC were then carried out in conjunction with specific activity measurements on the immobilized RNAase preparations. The increase in the points of attachment between enzyme and support was found to correlate with:

a. increases in transition temperature (6°C for the maximum number of eight bonds);
b. decreases in the enthalpy of transition (by 30% for eight bonds);
c. decreases in specific activity (eg. 41% - 86% for the range of one to eight bonds), and
d. a decrease in the reversibility of thermal denaturation.

It seems that the covalent immobilization of RNAase to a sepharose support is accompanied by an alteration, a partial unfolding, of the native enzyme 3° structure; (interestingly the first few attachments seem to have a disproportionately great impact). An increase in the number of covalent bonds also appeared to lend some rigidity to the remaining 3° structure; the transition temperature is increased and reversible thermal denaturation of immobilized RNAase is inhibited.

1.4.2 Quantitative Aspects of External and Internal Mass Transfer Effects

Historically the importance of diffusion in biological systems may first have been noted by physiologists like Warburg 1923 (86). The concept of diffusion effects was later extended to Michaelis-Menten kinetics by Blum 1956 (87). The original idea of a non-stirred or diffusion layer, is however, attributed to Nernst 1904(72).

The presence of an unstirred or Nernst layer adjacent to a catalytic surface results in a concentration gradient of substrate from the bulk solution to the surface. The flux of substrate (J', mol cm^{-2} s^{-1}) to the surface is described by Fick's law:

$$J' = D/d\ ([S]_B - [S_s]) \qquad (1.4.2.1)$$

where the subscripts B and s denote bulk and surface respectively. The ratio of the substrate diffusion coefficient (D, cm^2 s^{-1}) to the Nernst layer (d, cm) defines an external mass transfer coefficient, h_s, (cm s^{-1}). Under steady state conditions, the rate of external mass transfer and the immobilized enzyme catalysed reactions are equal, hence

$$[B]_B - [B]_S = Z^* [B]_S/(1+[B]_S) \qquad (1.4.2.2)$$

$(B = S/Km;\quad Z^* = Vmax"/hs\ Km)$

The maximum rate of reaction in the above expression, Vmax", is measured with reference to the geometric surface area per unit

volume of support A (cm^{-1}), where A = $\epsilon 3/R$. Thus Vmax" has the dimensions of mol cm^{-2} s^{-1} rather than mol cm^{-3} s^{-1} for (Vmax) enzymes in free solution (Vmax" = Vmax/A). The term Z* is a dimensionless number, called the external substrate modulus or Damkohler number. It is the ratio of the intrinsic first order rate constant for the immobilized enzyme (Vmax" /Km) to rate constant for substrate diffusion, h_s (1.4.2.2). Thus the condition for significant and insignificant external diffusion effects are Z* >> 1.0 and Z* <0.1 respectively. Winne 1973 (88) has rearranged a version of the relation (1.4.2.2) to give a quadratic in terms of the surface concentration. The solution of this equation is shown (1.4.2.3); it is useful because it expresses the observed rate of reaction, in the presence of external diffusion effects, in terms of experimentally measurable quantities.

$$J = 0.5h_s [(Km + S + Vmax"/hs) \pm ((Km + S + Vmax"/hs)^2 + 4 S Km)^{1/2}) \qquad (1.4.2.3)$$

Where substrate transfer occurs through a diffusion barrier comprising a membrane as well as a Nernst layer, the external substrate modulus takes the form (1.4.2.4), Kashe 1983 (89);

$$z^* = (Vmax"/Km) (P + hs)/P\ hs \qquad (1.4.2.4)$$

where P is the membrane permeability coefficient. The mass transfer coefficient hs is sensitive to the degree of fluid agitation in a system (i.e. flow or stirring rate). For a spherical support geometry,

$$hs = Sh \cdot D / 2d \qquad (1.4.2.5)$$

Sh called the Shirwood number has a value of two under quiescent conditions and increases with the degree of agitation to a maximum value of about 20.

The coupling of diffusion and an immobilized enzyme catalyzed reaction in parallel is described by the differential equation (1.4.2.6) for a spherical support.

$$\frac{dB}{dq2} + \frac{2dB}{qdq} = \frac{9}{1} \frac{\phi}{+} \frac{Bs}{B_s} \qquad (1.4.2.6)$$

($\phi = r/3\ (Vmax"/Km^{1}\ D_{eff})^{1/2}$; $B = S/Km$)

(q = normalized radial coordinate (r/R))

The dimensionless number, ϕ, is the internal substrate modulus or Thiele modulus, Thiele 1939 (90). The magnitude of the Thiele modulus is indicative of the importance of internal diffusion effects. For instance the conditions $\phi > 0.1$ and $\phi << 0.1$ indicate strong and insignificant diffusion effects respectively. The boundary conditions for the solution of (1.4.2.6) are that:

a. There is no external diffusion control and,

b. there is no change in substrate concentration, as a function of distance, at the centre of the support;

Formally:

$[B] = [B]_S$ at $q = 1$

$d[B]/dq = 0$ at $q = 0$

The solution of (1.4.2.6) *e.g.* by numerical methods gives the radial concentration profile within the spherical particle.

Effectiveness Factor

The activity expressed by immobilized enzyme preparations may be less than expected from the quantity of enzyme present due to diffusion effects. The extent to which the intrinsic activity is affected, is discussed in terms of the chemical engineering concept, effectiveness factor (E), Moo - Young and Kabayashi 1972 (91)

$$E = \frac{\text{observed activity}}{\text{activity with no diffusion control}} \qquad (1.4.2.7)$$

The definitions of other forms of effectiveness factor frequently found in the literature are summarized below (a-d):

a. The first and zero order effectiveness factor (E_1 and E_o) are defined by the ratio of rates made in the first and zero order limiting cases, in the Michaelis-Menten formulation, respectively.

b. The operational effectiveness factor (E_{op}) is defined as the ratio of times required for a specified fractional conversion.

c. The stationary effectiveness factory (E) is defined by the relation (1.4.2.7)

d. the external and internal effectiveness factors (E_e and E_i) - the effects of external and internal are separated in

these two terms, the essential definition is otherwise unchanged, ($E = E_e \times E_i$)

The effectiveness factor is a function of the external substrate modulus, Z^* and the normalised substrate concentration, B.

Table (1.4.2.1) Some Relations Between the external Effectiveness factor and Z*, B

$$E_e(B, Z^*) = \frac{1 + B}{(Z^* + 1) + B}$$

$$\lim_{B \longrightarrow 0} E_e (B_1 Z^*) = 1.0$$

$$\lim_{B \longrightarrow 0} E_e (B, Z^*) = \frac{1}{Z^* + 1}$$

$$\lim_{Z^* \longrightarrow 0} E_e (Bm\ Z^*) = 1.0$$

The internal effectiveness factor is also a function of the (internal) substrate modulus ($\emptyset$) and the normalised substrate concentration , B. It is in addition sensitive to support geometry. The discussion below will be limited to a brief outline of some useful relations for the case of a spherical support. Expressions for planar supports, eg. membranes, are discussed by Moo-Young and Kobayshi (91).

$$\lim_{\emptyset \longrightarrow 0} E_i (B,\emptyset) = 1.0 \qquad (1.4.2.8)$$

$$\lim_{B \longrightarrow 0} E_i (B_1\ \emptyset) = 1/\emptyset\ [1/\tanh(3\emptyset) - 1/3\emptyset] \qquad (1.4.2.9)$$

$$\lim_{B \longrightarrow 0} E_i (B,\emptyset) = 1/\emptyset \qquad (1.4.2.10)$$

$\emptyset > 10$

Finally the effectiveness factor and substrate modulus are

related to the apparent and intrinsic Michaelis constants according to (1.4.2.11) and (1.4.2.12).

$$Km = \emptyset \times Km^{app} \qquad (1.4.2.11)$$

$$Km = (1 + Z^*)Km^{app} \qquad (1.4.2.12)$$

for internal and external diffusion effects respectively. The theoretical literature on diffusion effects in immobilized enzyme systems is quite extensive. The reviews by Engasser and Horvarth 1973 (92), 1976 (93), Hamilton et al. 1974 (94), Lee and Tsae 1974 (95), Pitcher 1978 (96) and Vincent and Thellier 1983 (97) were useful sources for the outline presented above.

1.4.3 Diagnosis of Diffusion Effects and Determination of Intrinsic Kinetic Constants.

Mass transfer limitations of immobilized enzyme catalysed reactions are associated with certain invariable kinetic features which have therefore come to be seen as diagnostic of diffusion control. Some of these features include:

a. sensitivity of kinetic constants to flow or stirring rate
b. non-Michaelis-Menten kinetics e.g. seen as characteristic irregularities in the clasical linearization plots, Table (1.2.1.1)
c. decreased reaction activation energy at elevated temperatures
d. decreased sensitivity to inhibition.

The sensitivity of the Michaelis constant to flow or stirring rate is usually an indication of the presence of external diffusion effects. Increased flow rate is expected to result in a reduced Nernst layer thickness and hence an increase in the

external mass transfer coefficient, (1.4.2.1) and (1.4.2.5). The result is to reduce Km^{app} to a value more approaching that of the intrinsic Km.

In the presence of either external or internal diffusion control, the kinetics of immobilized enzymes is non-Michaelis-Menten. For instance , the slope of the Lineweaver-Burk plot is generally increased relative to the plot for the native enzyme. There is also a curvature at the low substrate concentration part of the plot, Vincent and Thellier 1983 (97), Hamilton et al. 1974 (98). Engasser and Horvarth 1974 (99) have made a theoretical assessment of the effects of both external and internal diffusion effects on the Eadie plot. Characteristic irregularities appear which may be used to distinguish the two forms of diffusion control. However, the presence of, e.g., product inhibition (in the absence of diffusion effects) can lead to similar results, thus complicating data interpretation (Chapter 4). Similar difficulties result from the effect of external diffusion effects on the Eadie plot for single and two transport systems, Preston 1982 (100).

The activation energy (E_{act}) for mass transfer is generally lower than the average value for enzyme catalysed reactions. An Arrhenius plot, of log. rate against inverse temperature, therefore shows a decreased slope in the presence of diffusion control. Such changes in E_{act} have for example been observed for polyacrylamide gel entrapped acetylcholinesterase by Ngo and Laidler 1978 (101). With a high substrate concentration and over

low temperatures E_{act} was found to be, 37.9 kJ mol^{-1}, nearly identical to the value for the soluble enzyme (41.3 $kJmol^{-1}$). However, at a low substrate concentration and/or over high temperatures E_{act} decreased to a value of 23.8 kJ mol^{-1}.

The fourth possible indication of diffusion control, is a decrease in the sensitivity to inhibition. The mechanism does not depend on steric interaction between inhibitor and enzyme support as discussed for trypsin, Levin et al. 1964 (80). Briefly, it would appear that the effects of an inhibitor, on the rate of a reaction catalysed by an immobilized enzyme, will not be seen if the residual activity is greater than the maximum rate of substrate diffusion. Further, inhibition may improve the effectiveness factor of an immobilized enzyme. These considerations apply to all forms of inhibition (including denaturation which is considered as a form of irreversible inhibition) with the exception of substrate inhibition, Engasser and Horvarth 1974 (102).

The practical determination of the intrinsic kinetics of immobilized enzymes requires the removal of diffusion effects. The conditions necessary are however often difficult to achieve experimentally. For instance, Vmax can in theory be directly determined (at $S \sim 100\ Km^{app}$) if a substrate is sufficiently soluble and the enzyme in question is not subject to substrate or product inhibition. The direct determination of intrinsic Michaelis constant (Km´) requires the removal of external

diffusion effects, e.g., by the use of a high flow rate. The results of the analysis of the data of Lilly et al. 1966, (71), by Lee and Ryu 1979 (73), illustrate the uncertainty of this direct approach. Secondly, internal diffusion effects also need to be removed, eg., by decreasing support thickness or radius. The support dimensions at which there is insignificant diffusion effects (as with flow rate) can only be found empirically.

IF the effectivness factor is known, it immediately enables the determination of intrinsic kinetic constants. Mueller and Zwing 1982 (78), determined the internal effectiveness factor from first principles. The approach involved the comparison of the activity in the presence of diffusion effects, of sepharose bound alkaline phosphatase, with the amount of enzyme protein removed from solution during the immobilization process. The essential step in this approach, i.e. confirmation of the assumption that the specific activity of alkaline phosphatase is unchanged as a result of the immobilization procedure per se, was possible after resolubilization of the immobilized enzyme with dextranase. Without this independent assessment of specific activity of the immobilized enzyme, the amount of protein bound cannot be taken as indication of the immobilized enzyme activity in the absence of diffusion. Where an inorganic support is involved the resolubilization step in the above technique will pose some difficulties.

Intrinsic kinetics may also be determined from theoretical correlations between modified substrate moduli and the respective

effectiveness factors. The modified substrate moduli are distinguished from Z* and $\emptyset$ in being defined in terms of practically determined quantities only. For example Kobayashi and Laidler 1973 (103) have produced a graph of a modified internal substrate modulus, h ($h = R^2 Vmax/(2D_{eff} Km^{app})$) against the ratio Km'/Km^{app}. As h can be calculated from experimental values of Vmax and Km^{app}, together with an appropriate D_{eff} value , Km' can be determined. Engasser 1978 (104) has also produced a theoretical relationship between the external and internal effectiveness factor and the appropriate modified substrate moduli. This work is explored further in Chapter 4.

The final approach to be considered, for the determination of the intrinsic kinetic constants of immobilized enzymes, involves the study of the effects of altering transport characteristics on the apparent kinetics. An example based on the determination of Km^{app} and Vmax on two or more support dimensions has been described by Engasser and Horvarth (92). This is considered in greater detail in Chapter 4. Finally, as discussed above, Lee and Ryu extrapolated the Km^{app} value of caroboxymethyl cellulose bound ficin, at various sample flow rates to give a Km estimate unaffected by diffusion.

1.5 Scope of the Present Work

The area of research presented in this thesis is concerned with the application of immobilized enzymes (including living cells) in analytical chemistry. The majority of the work involves flow

microcalorimetric monitoring, although Chapter 6 describes work carried out using potentiometric and amperometric detectors.

The non-specific calorimetric principle (i.e. enthalpy change) combined with immobilized enzymes has been successfully applied to the highly selective identification and quantification of a large number of compounds. However, little detailed examination of the factors affecting system performance characteristics, e.g. sensitivity, speed and linear range of analysis, has been done. In Chapter 3,the effects of such factors as detector response time, immobilized enzyme apparent kinetics (see below), sample flow rate and sample dispersion are examined. Such work is expected to be relevant to the area of flow analysis in general. Two characteristics of immobilized enzymes, specifically,the affinity for the analyte ($\sim 1/Km^{app}$) and the maximal rate of the catalysed reaction, (mol (analyte) dm^{-3} min^{-1} mg^{-1} (enzyme-support)) are of immediate interest in analytical applications. However, the use of the flow analysis format prevents the determination of Km^{app} and Vmax using the methods of classical steady state enzyme kinetics,i.e.,the initial rate approach (s 1.2). Beyond this, the study of immobilized enzymes in general is dominated by the concept of diffusion control (s. 1.4). The ubiquity of enthalpy changes and the capacity for direct power (i.e. rate) measurement afforded by the heat-leak design principle would be expected to make flow microcalorimetric monitoring particularly useful in these areas.

Chapter 4 describes the application of flow microcalorimetric

monitoring to the study of the kinetics of reactions catalysed by immobilized enzymes. Although others have studied soluble enzyme systems (s. 1.1.3) there would not appear to be reports of a similar study of immobilized enzymes. This theme is extended to the characterization of immobilized living (yeast) cells in Chapter 5.

Finally, Chapter 6 describes work concerned with the use of immobilized enzymes in electrochemical analysis. The analysis of several analytes using the enzyme electrode and the IMER formats are examined.

CHAPTER 2

Methods and Procedures

2.1 Immobilization of Enzymes and Cells

2.1.1 Enzyme Immobilization

Enzyme immobilization may be defined as any process which enables simple physical separation of enzyme from reactants and products for re-use. This often involves the attachment of an enzyme to an insoluble support. Glucose oxidase was retained in a semi-permeable membrane in the fabrication of an early enzyme electrode (s 6.);therefore,insolubilization would not appear to be essential in the above definition. On the other hand,a high concentration of enzyme within a closed system may be reused but without separation and is therefore excluded.

The field of enzyme immobilization probably began with the adsorption of invertase and other proteins on, e.g., charcoal, alumina, koalineite and glass beads; Nelson and Griffin 1916 (105), Nelson and Hitchcocks 1921 (106) Langmuir and Shaefer 1938 (107). These early examples of immobilization generally produced unstable systems due to the tendency for adsorbed proteins to become desorbed. The covalent binding of enzymes to support was not frequently applied before 1945. During the immediate post-war period,the range of commercially available supports would appear to have been limited to derivatives of polystyrene and cellulose. Thus Grubhofer and Schleith 1953 (108) immobilized carboxypeptidase and amylase on diazotized poly (p-aminostyrene).

Other workers, Manecke and Gilber 1955 (109), Bradenberger 1956 (110), Manecke and Singer 1960 (111), used the same support as above or poly (isocyanatostyrene). Mitz and Summaria 1961 (112) used carboxymethyl cellulose hydrazide as support. There was a relatively rapid increase in the number of supports available after 1960; this is illustrated by the appearance of ethylene-maleic anhydride polymer, Levin et al. 1964 (80), Carboxymethyl cellulose, Weetall and Weliky 1964 (114), polyacrylamide gel, Mosbach 1966 (115), cyanogen bromide activated sephadex, Axen et al. 1967 (116), derivatized glass, Weetall 1969 (117) and nylon, Hornby and Filuppuson 1970 (118) between 1960 and 1970. The use of radiation graft polymers, Cornet 1979 (119), aqueous-non aqueous phases, Mattiasson 1982 (120), and glycoprotein/lectin interactions, Matiasson 1982 (121), for enzyme immobilization represent some more recent developments in techniques for enzyme immobilization.

Immobilization methods can be placed in four categories. These are:

a. adsorption
b. entrapment (including microencapsulation)
c. cross linking and
d. covalent binding.

Some important features of each method are now discussed below:

Adsorption; enzyme binding to the support involves H-bonding, electrostatic and van der Waals' forces. This method has the advantages of relatively low cost (since a minimum of support

preparation is required), simplicity and a small degree of enzyme inactivation (because of the non-involvement of covalent bond formation). The chief disadvantage of the adsorption method is that the resulting immobilized enzyme has a tendency to desorb from the support as a result of changes in e.g. ionic strength, pH and temperature.

Entrapment; this involves the physical containment of the enzyme within the pores of a gel support. As with adsorption, entrapment also results in a high recovery of enzyme activity. The entrapment method is widely used for cell immobilization (Chapter 5). There is a wide distribution of pores within most gels and therefore a likelihood of enzyme loss by leaching. Entrapment is only suitable as a means of immobilization where small molecular weight substrates are involved. Even in such systems mass transfer effects will still be relatively greater with entrapment compared to the other immobilization methods. A further criticism, discussed in more detail below, is that most supports used for entrapment are organic.

Cross-Linking; With this method, the enzyme molecule is immobilized by treatment with a bifunctional reagent,e.g., glutaraldehyde. This approach is particularly suitable when thin membranes or layers of immobilized enzyme,e.g. as is used in enzyme electrode preparation (s. 2.1.3), are required. Immobilization by cross-linking is generally considered inefficient as part of the enzyme molecule must act as a support.

Covalent Binding; employs an activated group on a support or a

bifunctional reagent to attach the enzyme covalently. The covalent bond may be formed with a terminal NH_2, E-NH_2 (of lysine), -OH (of tyrosine serine or threonine) -SH (of cysteine) or the nitrogen (of imidazole in histidine) grouping on the protein. This method was widely used (Chapter 3, Chapter 4) and is therefore considered in some detail below.

The choice of support for covalent immobilization extends in principle to all materials with surface oxide, OH, NH_2 or alkene functional groups. These supports have recently been categorised as porous or non-porous, Messing 1975 (122). Porous supports present a larger surface area for immobilization. Much of this surface area is internal and therefore the immobilized enzyme is protected from turbulence as well as liquid shear forces. In situations where the pore diameter is less than about 1000Å there is also protection from direct attack from bacteria. On the other hand, porous supports may exclude large molecular weight substrates; there are frequently internal mass transfer effects.

Non-porous supports characteristically have a low surface area. This may be an advantage for applications involving contact of the support with blood. A small contact area then reduces possible immune responses to the support. Finally, internal diffusion effects are absent in immobilized enzyme systems employing non-porous supports. The major disadvantage of using a non-porous support is that there is a relatively low support specific surface area for enzyme immobilization.

Other characteristics are also important in support choice. Thus the ideal support is chemically inert (although allowing surface modification), not subject to microbial degradation and has high mechanical strength. These features are most frequently found with inorganic supports.

Controlled Porosity Glass

The inorganic support controlled porosity glass (CPG) is used extensively in work reported later (Chapter 3, Chapter 4). Some characteristics of this support are now discussed.

Chemically CPG is almost pure, fused, silica; Haller 1965 (123). The preparation of CPG may be summarized as follows:

a. Homogenous borosilicate glass is heated and allowed to cool over about 100h. This treatment results in a separation of the glass into interconnected borate-rich pockets dispersed in a silica phase. The mean diameter of the pockets of the borate-rich areas depends on the cooling-curve of the glass.

b. The heat-treated glass is crushed and sieved to give a required range of particle diameters.

c. The glass beads are treated with acid (3N HCL, 50^{o}C, 6h) and then alkali (0.5N Na OH, 25^{o}C, 5 h). This is to remove the acid-soluble, borate-rich areas, and a precipitate of silicate left behind (by the acid treatment) respectively. The latter process also results in some widening of the pores created inside the glass.

A given batch of CPG support can be distinguished by three characteristics. These are pore diameter, specific surface area ($m^2\ g^{-1}$) and particle diameter. The pore diameter, determined by high pressure mercury porosimetry, is controlled during manufacture of the support to a distribution of $\pm$ 10%. Unlike the normal statistical distribution the limit $x \pm SD_{n-1}$ (ie. mean pore diameter $\pm$ one standard deviation) by convention contains 80% and not 68.3% of pore diameter values. The surface area of CPG is determined by the BET-nitrogen adsorption technique. There is an inverse relationship between the mean pore diameter and support surface area, Table (2.1.1.1). Particle diameter is determined by the mesh size (ie. number of strands of material per unit area) used in the separation of the crushed CPG. The particle diameter range is frequently given as two numbers reflecting the mesh size range used in isolating a particular range of sizes of support, Table (2.1.1.1).

Controlled porosity glass is also sometimes described with the abbreviation 'CPG' qualified with an integer eg. CPG-100, CPG-200. The origin of the qualifying number appears to differ with different suppliers of CPG. For instance, the number may simply state the mean pore diameter, Pierce catalogue 1982 - 83 (124), or reflect the water regain of the support i.e. g (water absorbed)g^{-1} dry weight of CPG, Pharmacia 1983 (125) .

The general areas of enzyme immobilization methods, the chemistry of immobilization and support choice have been reviewed, eg. by, Weetall 1973 (126), Filbert 1975 (127), Goldstein and Manecke

Table (2.1.1.1)* Some Characteristics of Controlled Porosity Glass:

a. Mesh size designation of particle diameter

b. Approximate pore diameter/specific surface area (SSA) relations

Mesh Size	Particle Diameter (μm)[a]
20/80	180 - 840
40/60	~ 200
80/120	125 - 177
120/200	74 - 125
200/400	37 - 74

Pore Diameter (Å)	SSA (m^2g^{-1})[b]
75	185
240	100
350	75
700	37
1000	26
2000	13

* compiled from references (124, 127, 130)

1976 (128) or Kilara and Shahani 1979 (129). The characteristics of CPG have been reviewed by Haller 1983 (130). The monographs edited by Messing 1975 (131), Weetall 1975 (132), Mosbach 1976 (133) or Ghose et al. 1978 (134) are also important sources.

2.1.2 Covalent Immobilization of Enzymes to Controlled Porosity Glass

Some important characteristics of CPG were discussed above. This material was chosen because of its rigidity. This is important since flow rate through a rigid packed bed of support is directly related to the applied pressure. CPG is resistant to most acids, (except hydrofluoric and strong phosphoric acid) organic solvents and microbial degradation. CPG is apparently soluble at pH > 9.

A large number of enzymes have been immobilized on CPG. Examples include alcohol dehydrogenase, alkaline phosphatase, chymotrypsin glucoamylase, invertase, papain and trypsin and penicillinase. Reports of glucose oxidase, urease, and acetylcholinesterase immobilized on CPG are cited in Chapter 4.

Glutaraldehyde (25% w/v) and 3-aminopropyltriethoxysilane (APTES) were supplied by Sigma UK. Controlled porosity glass (200/400 mesh 55μ mean particle diameter, 126Å $\pm$ 7% pore diameter, 187.1m^2 g^{-1}) and all other reagants were obtained from the British Drug House (BDH) Ltd. Poole, England.

The alkylamine/glutaraldehyde approach used for enzyme immobilization to CPG was based on a modification by Robinson et

al. 1971 (135) of the original method described by Weetall 1969 (117). The modified approach may result in an increase in the coverage of NH_2 groups from 30 - 35 to 80 - 90 moles per gram support.

Controlled porosity glass was washed in hot dilute nitric acid, (30% v/v, 80°C; 1 h) placed in a sintered glass funnel and rinsed with de-ionized water until neutral. The support was placed in a 1% solution of APTES in acetone. After evaporating to dryness at room temperature the support was baked at 115°C for 12h. With such treatment the slightly anionic CPG surface is replaced by a slightly cationic alkylamine-CPG surface, Messing et al. 1969 (136). The modified CPG was stored at room temperature for future use.

To activate, the alkylamine-CPG was suspended in 1% glutaraldehyde in phosphate buffer (0.2M, pH 7.0) at room temperature for 1 h. As discussed by Ford and Pesce 1981 (137) the mechanism of glutaraldehyde interaction with amine groups is uncertain because the former exists in several forms in solution. As a result of the exposure to glutaraldehyde, however, the alkylamine CPG changes colour from white or pale yellow to deep orange or tan and gains the capacity of forming covalent bonds with added protein. To immobilize a given enzyme the activated support was exhaustively washed to remove free glutataldehyde, and then exposed to a 1 -2 mg cm^{-3} solution of the protein in phosphate buffer. Immobilization was allowed to occur at 0 - 5°C

for 8 - 12 h and the CPG enzyme then washed with 0.5M potassium chloride to remove non-covalently bound enzyme. Finally the CPG-enzyme was then exposed to trishydroxymethylaminomethane (THAM) buffer. The THAM reacts with and blocks any unreacted aldehyde functions.

2.1.3 Non-Covalent Immobilization of Enzymes and Cells

Entrapment of yeast (Saccharomces cerevisiae) cells in calcium alginate gel.

Alginic acid is a polysaccharide containing α(1 - 4) - linked L-guluronic acid residues and β(1 - 4) - liked D-mannuronic acid residues. The naturally occurring polymer isolated from kelp, has regions rich in one or the other of the above subunits interspersed with more mixed regions. These regions are hydrolysed and separated to produce variants on the basic polymer. Alginic acid is insoluble. The sodium salt is soluble but gives rise to an insoluble gel in the presence of calcium and other divalent metal ions.

Some physical characteristics of alginate gels relevant to their use for immobilization were studied recently by Kierstan et al. 1982 (138). The approach adopted was to monitor the release of, e.g., nicotinamide adenine dinucleotide (NAD) from alginate gels as a function of the concentration of gelation agent ($CaCl_2$), or alginate. It was found that the retention of NAD by a gel was unaffected by:

a. the concentration of calcium chloride between 0.125 - 0.5M

b. alginate concentration between one and four percent and,

c. the use of barium rather than calcium ions for gelation.

Increasing the alginate gel fibre diameter however increased the retention of entrapped NAD. Examples of the use of calcium alginate gel for the entrapment of enzymes and cells include the studies by Kierstan and Bucke 1977 (139), Larsson and Mosbach 1979 (140) Krouwel 1979 (141) or Svensson and Ottesen 1981 (142).

Alginic acid (sodium salt, Type IV practical grade form Macrocystis pyrifera (kelp) and Saccharomyces cerevisiae, (Type 11 bakers' yeast, fast-dried to yield 90% active viable cells) were commercial samples. Sigma UK. Laboratory grade calcium chloride was supplied by BDH Ltd.

Yeast cells were entrapped in calcium alginate using a previously described method (e.g. cf 140, 142). Freeze-dried yeast (2.5 - 5g.) was reconstituted in (distilled) water and added to a sodium alginate solution in water (4% w/v;20g). The resulting mixture was loaded into a $30cm^3$ syringe and extruded into a stirred solution of calcium chloride (0.3M; pH 6.0 - 6.5). The strings of calcium alginate yeast formed were stored in a fresh change of calcium chloride at 0 - $4^{o}C$.

Cross-Linking of Glucose Oxidase and Bovine Serium Albumin with Glutaraldehyde

Glucose Oxidase (β - D - Glucose : Oxygen 1- oxidoreducatse, EC 1.1.34, Type X from Aspergillus niger, 100,000 - 150,000 units per gram solid (0.75g protein)), bovine serum albumin and glutaraldehyude (Grade II, 25% aqueous solution) were commercial samples. All other compounds were supplied by BDH Ltd.

The method used for preparing glutaraldehyde cross-linked glucose oxidase was essentially that described by Tran-Minh and Broun 1975 (143). In this instance glucose oxidase powder (2mg) was dispersed in 200mg of bovine serum albumin and 1 cm^3 of glutaraldehyde (0.8% v/v; in 0.2M phosphate buffer, pH 7.0) added. After stirring vigorously for about thirty seconds the protein emulsion was deposited on to a glass or platinum electrode as a thin membrane layer. The cross-linked enzyme preparation was first allowed to dry at room temperature and then immersed in buffer to remove excess glutaraldehyde. The use of the cross-linked enzyme in enzyme electrode preparation is described in the next section.

2.2 The Preparation of Enzyme Electrodes and Other Devices of Electro-Chemical Analysis

2.2.1 Preparation of a 'Type-3' Potentiometric Electrode Sensitive to Glucose

The potentiometric base sensor was a hydrogen ion selective electrode (Orion model 90 - 01 Orion U.S.A.) in combination with

a double junction reference electrode (Orion model 90 - 02) obtained from the same supplier. Glucose oxidase (is described in detail above; s.2.1.2) and dialysis membrane were from Sigma-UK.

The designation 'Type-3' refers to an enzyme electrode constructed from a dialysis or cellophane membrane entrapped enzyme, Guilbault and Lubrano 1973 (144). As described by Nilsson et al. 1973 (145) a fine paste of glucose oxidase was placed between two layers of dialysis membrane. The whole was then applied to the base sensor and secured in place with an 0-ring. The finished Type-3 electrode was allowed to equilibrate with buffer before use.

2.2.2 Preparation of a 'Type-1' Amperometric Enzyme Electrode

The amperometric base sensor was a twin-platinum micro electrode (Metrohm Herisau-Switz); this was used in combination with a standard mercuric sulphate electrode (SMSE) from the same supplier.

The 'Type-1' designation describes an enzyme electrode constructed from a chemically modified immobilized enzyme layer. A Type-1 electrode sensitive to glucose was constructed from glucose oxidase cross-linked to bovine serum albumin. The twin-platinum electrode was first cleaned by heating in hot dilute nitric acid (30%, 80^{o}C) for 1 h. After drying, the platinum surface was dipped into a bovine serum albumin/glucose oxidase/glutaraldehyde emulsion (s 2.1.3). A thin coating of protein placed on the platinum surface was allowed to dry at room

temperature. Finally, a nylon mesh was placed over the enzyme layer and secured with an O-ring, Fig. (2.2.4.1). This was necessary because of the poor adhesion of the enzyme layer to the platinum surface. The electrode was allowed to equilibrate with buffer overnight before use.

2.2.3 Design and Building of a Device for Measuring Small Electrical Currents

Standard methods and instrumentation for measuring small electrical currents have been outlined by Lingane 1958 (146). Two methods in particular allow automatic recording of electric currents in amperometry. These involve:

a. a three-electrode arrangement where the potential of a working electrode is measured against a standard reference electrode and,

b. the measurement of the potential (drop across a known standard resistor placed in series with the electrolytic cell).

A device based on the second principles was made for current measurements. The detailed circuitry is shown in Figure (2.2.3.1); two FET - Input amplifiers and a 1V standing offset have been added to the standard resistor, (R = 1.5kΩ). The offset was required because the expected potential drop across the standard resistor is one to two orders of magnitude smaller than the applied potential difference across the electrolytic cell.

FIG(2·2·3·1)- Circuit diagram of a device for measuring small electrical currents across a standard resistance

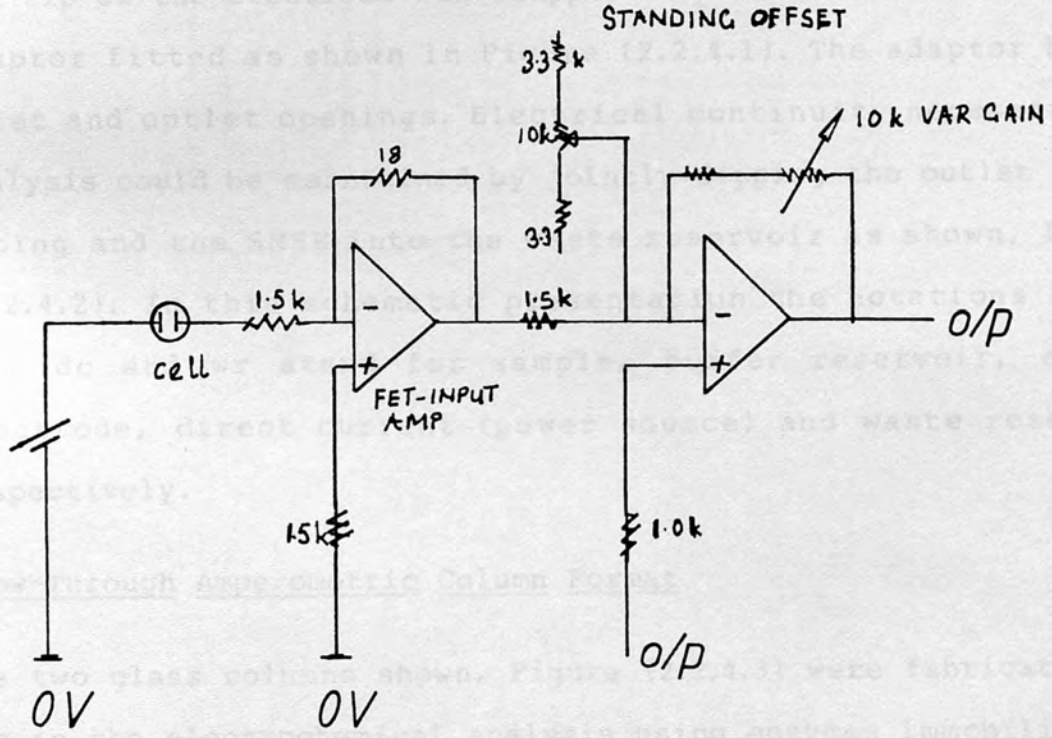

2.2.4 Flow Amperometric Systems for the Analysis of Enzyme Substrates

Two formats for adapting the key elements for enzyme-based electrochemical analysis (s 2.2.2, 2.2.3) to flow analysis are now described.

Flow-Through Enzyme Electrode Format

The Type-1 enzyme electrode (s 2.2.2) was modified as follows: the tip of the electrode was wrapped in parafilm and an air-tight adaptor fitted as shown in Figure (2.2.4.1). The adaptor had inlet and outlet openings. Electrical continuity necessary for analysis could be maintained by jointly dipping the outlet teflon tubing and the SMSE into the waste reservoir as shown, Figure (2.2.4.2). In this schematic presentation the notations s, br, e.e, dc and wr stand for sample, buffer reservoir, enzyme electrode, direct current (power source) and waste reservoir respectively.

Flow-Through Amperometric Column Format

The two glass columns shown, Figure (2.2.4.3) were fabricated for use in the electrochemical analysis using enzymes immobilized on CPG. The versions (A) and (B) are for use in platinum electrode versus SMSE and platinum versus platinum electrode amperometry respectively. Each column has a water jacket for temperature control. Electrical contact with the platinum electrode(s) was achieved using mercury. The set up of a column based flow system is readily seen when e.e. is replaced by one of the columns described above.

FIG(2·2·4·1)

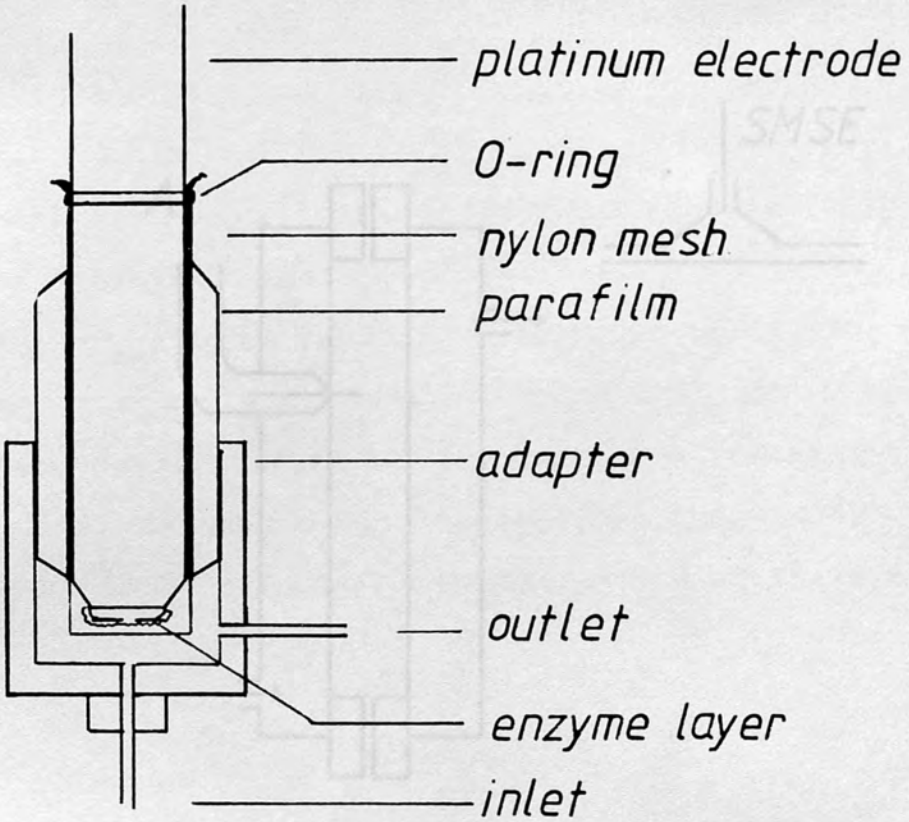

FIG(2·2·4·2)

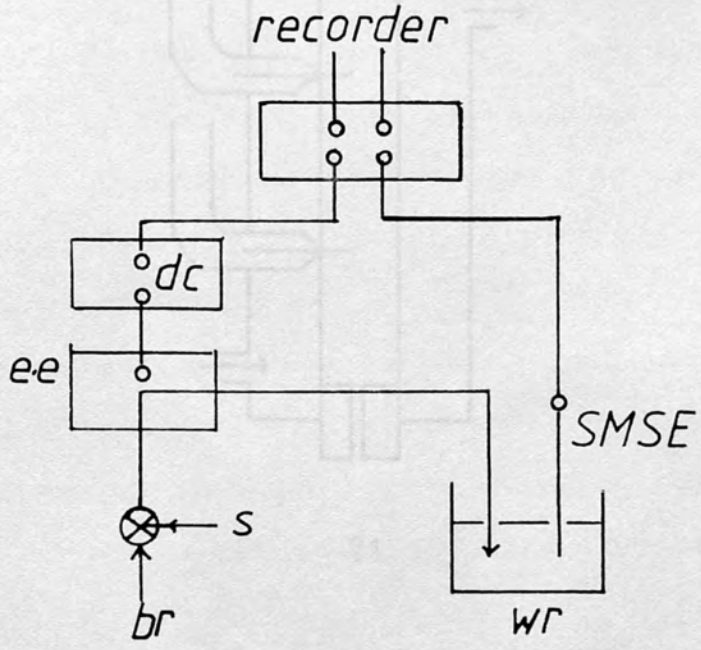

FIG(2·2·4·3)

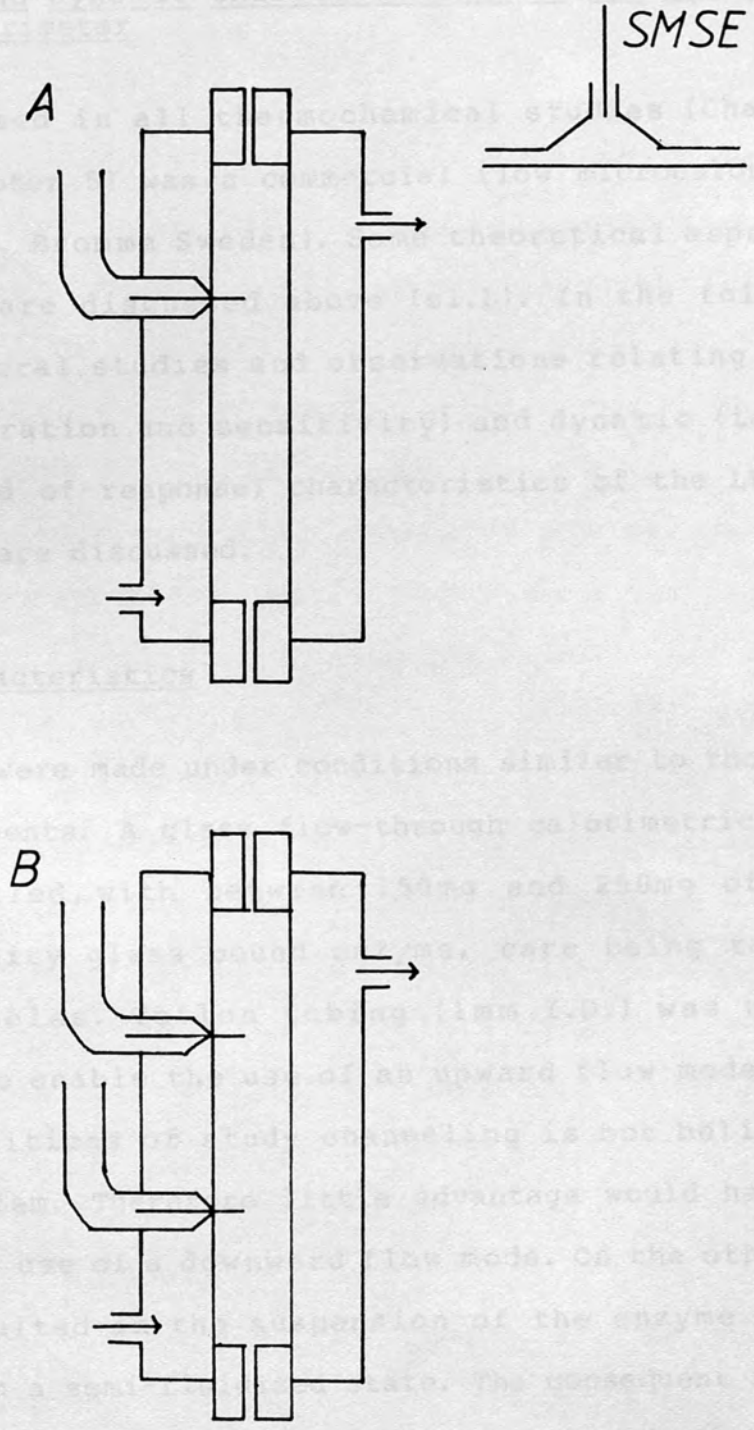

CHAPTER 3

Flow Injection Analysis with Immobilized Enzymes and Flow Microcalorimetric Monitoring

3.1 Static and Dynamic Characteristics of the LKB 2017-30 Microcalorimeter

The instrument used in all thermochemical studies (Chapter3, Chapter 4 and Chapter 5) was a commercial flow microcalorimeter (LKB 2017-30, LKB Bromma Sweden). Some theoretical aspects of this instrument are discussed above (s1.1). In the following section some general studies and observations relating to the static (i.e. calibration and sensitivity) and dynamic (i.e. time constant and speed of response) characteristics of the LKB flow microcalorimeter are discussed.

3.1.1 Static Characteristics

Calibration runs were made under conditions similar to those used in actual experiments. A glass flow-through calorimetric vessel ($0.5cm^3$) was filled, with between 150mg and 250mg of moist controlled porosity glass bound enzyme, care being taken to exclude air bubbles. Teflon tubing (1mm I.D.) was used in plumbing so as to enable the use of an upward flow mode. Under the present conditions of study channeling is not believed to have been a problem. Therefore little advantage would have been derived from the use of a downward flow mode. On the other hand, upward flow resulted in the suspension of the enzyme support which was thus in a semi-fluidized state. The consequent increase in mixing of the support would be expected to increase contact of immobilized enzyme with substrate. Reference buffer was pumped

though the flow system using a peristaltic pump (LKB 10,700) at a flow rate of 14.8 $cm^3\ h^{-1}$. In order to avoid possible leaking at ill-fitting connections, flow was effected via negative pressure by placing the pump at the flow outlet.

The facility for electrical calibration is inbuilt into the commercial microcalorimeter. All the required functions involved with current selection and timing are incorporated into an instrument control unit or panel. The steady state calibration constant E_{ss} was determined by passing known currents through a standard resistor (R= 49.76 ohm) for between 600s and 1000s. The resulting steady state potential (Volt, V) was measured on a Philips chart recorder after amplification by a Keithley 150B microvoltmeter; E_{ss} is calculated using the expression:

$$E_{ss} = I^2R/V \qquad (3.1.1.1)$$

As discussed above, E_{ss} has the dimensions of $Js^{-1}V^{-1}$ or watt V^{-1}. Transient calibrations were carried out in a similar manner. The transient type response (s.1) is however obtained by applying current to the standard resistor for a shorter duration than is the practice during steady state calibration. The transient calibration constant is the ratio of the heat output from the standard resistor (I^2Rt) to the peak area (cm^2).

$$E_{tr} = I^2Rt/\text{pk. area } (J\ cm^{-2}) \qquad (3.1.1.2)$$

Over the power input range:

0.2mJ s^{-1} to 5.42 mJ s^{-1} (3.7 μV to 100 μV instrument response) E_{ss} had a value of 52 $\pm$ 1.02 J s^{-1} V^{-1}. On the other hand, with a stopped buffer flow, E_{ss} was 53.8 $\pm$ 0.45 J s^{-1} V^{-1}. The corresponding detector sensitivities (I/E) are:

1.92×10^{-2} V s J^{-1} and 1.86×10^{-2} V s J^{-1} respectively.

The transient calibration constant, E_{tr}, is dependent on the chart speed. At higher chart speeds, peak area increases for any level of heat output and therefore E_{tr} is correspondingly smaller. The value of E_{tr} is also dependent on the level of signal amplification set on the Keithley amplifier. For instance, using a chart speed of 2.5mm min^{-1} and an amplification setting of 300μV, 100 μV or 30 μV full scale deflection (FSD) resulted in E_{tr} values of 6.90×10^{-2} J cm^{-2}, 2.34×10^{-2} J cm^{-2} and 6.8×10^{-3} J cm^{-2} respectively. It is therefore important that transient calibrations are carried out with the same chart speed and signal amplification setting as used in experimental runs.

3.1.2 Dynamic Characters

The expression describing the typical steady state detection response was given earlier (s.1.1). The more general form below (3.1.2.1) was used in the determination of the detector time constant, T_d.

$$Y = A - B \exp(-t/T_d) \qquad (3.1.2.1)$$

where Y is the instantaneous instrument output, A is an approximate steady state response and B is the 'calculated' steady state response. Consequently the detector time constant was determined from a plot of ln (A-Y) against t, Table (3.1.2.1), Figure (3.1.2.1).

Table (3.1.2.1) - Determination of the detector time constant, T_d, associated with the upward phase of a steady state response.

a Instantaneous Response, Y (μV)	t(s)	b (A - Y)	c In (A - Y)
0	0	14	2.6393
2.25	30	11.75	2.4648
6.75	90	7.25	1.9810
9.75	150	4.25	1.4469
11.25	210	2.75	1.0116
12.15	270	1.85	0.6152
12.75	330	1.25	0.2231
13.28	390	0.72	-0.3285
13.42	450	0.57	-0.5534
13.95	750	0.05	-2.2950

a. Instrument response as function of time (t,s) from the initiation of a calibration run.

b. A is the observed steady state response an approximation of the asymptote B in expression (3.1.2.1); it has a value of 14 μV

c. from Figure (3.1.2.1), B = 14.006 μV, and r = - 0.9991

The slope and intercept of this plot is $1/T_d$ and ln B respectively. The instrument time constant, estimated from the data presented (Table (3.1.2.1), Figure (3.1.2.1) is 134.23s.

The decay phases of the steady state and transient responses are described by the same expression, ie. $Y = \exp(-t/T_d)$, therefore a plot of ln Y against t, Table (3.1.2.2), Figure (3.1.2.1) enabled the determination of the associated time constant.

Table (3.1.2.2) Determination of the Detector Time Constant, d' associated with the decay phase of a steady state response.

Instantaneous	t (s)	ln Y
32.00	0	3.4657
26.00	30	3.2581
19.50	60	2.9704
16.50	90	2.8034
12.45	120	2.5217
10.00	150	2.3026
7.95	180	2.0732
6.50	210	1.8718
5.00	240	1.6094
4.00	270	1.3863

$r = 0.9996$; $T_d = 129.72$ s

The time constants cited above are single estimates. The results from a set of four steady state calibration runs covering 0.2mJ s^{-1} to 5.42mJ s^{-1} heat effect, with and without buffer flow, is reported below Table (3.1.2.3)

FIG(3·1·2·1)-Determination of instrument time constant (Table(3·1·2·1); Table(3·1·2·2))

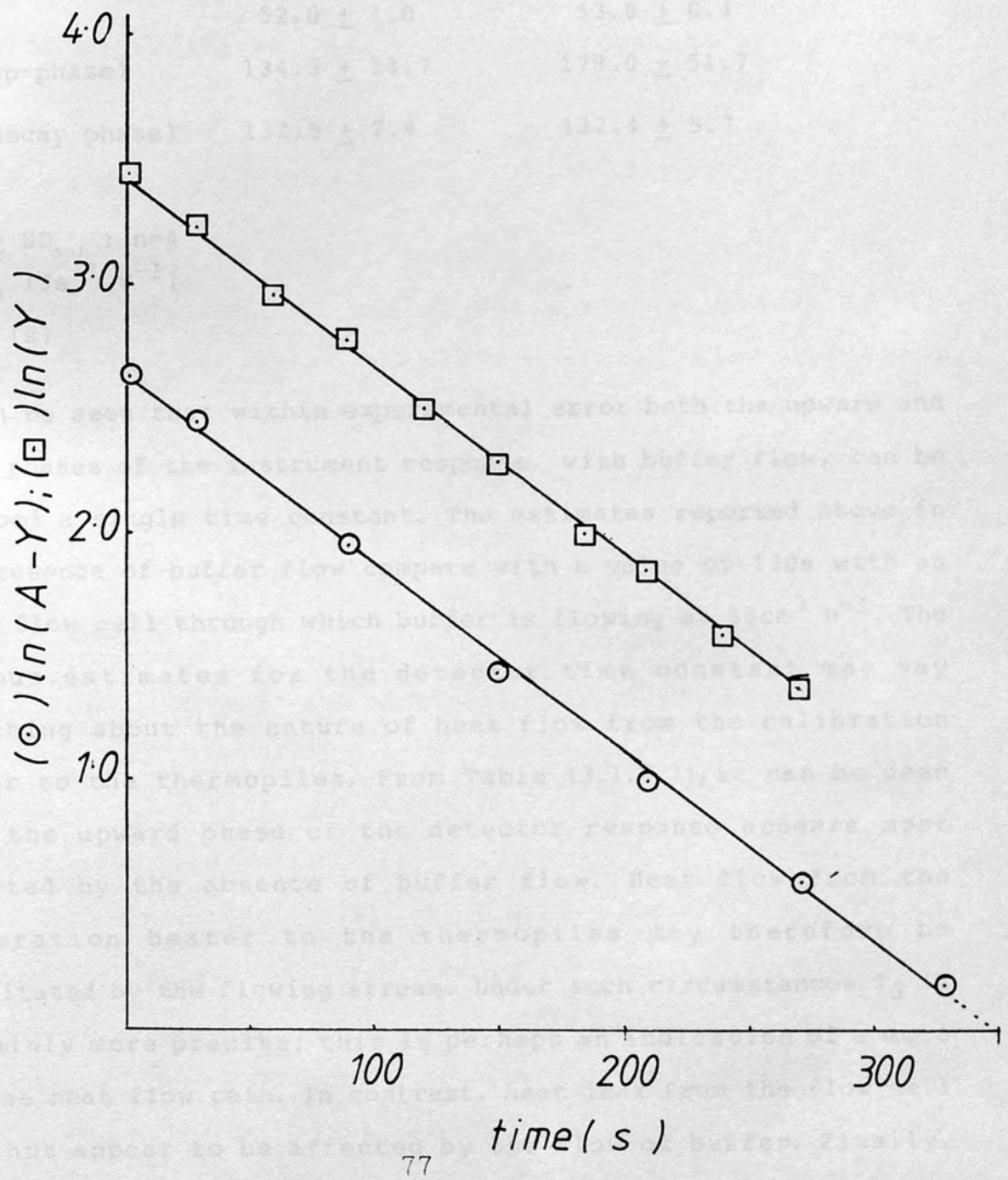

Table (3.1.2.3) - Some Static and Dynamic Characteristics of the 2KB 2017-30 Micro-Calorimeter

[a] Parameter	+ Flow	- Flow
[b] E_{ss}	52.0 ± 1.0	53.8 ± 0.4
[c] T_d (up-phase)	134.3 ± 14.7	179.0 ± 51.7
[c] T_d (decay phase)	132.5 ± 7.4	132.4 ± 5.7

a. $\bar{x} \pm SD_{n-1}$; n=4
b. E_{ss} ($Js^{-1}\ V^{-1}$)
c. T_d (s)

It can be seen that within experimental error both the upward and decay phases of the instrument response, with buffer flow, can be ascribed a single time constant. The estimates reported above in the presence of buffer flow compare with a value of 130s with an empty flow cell through which buffer is flowing at $15cm^3\ h^{-1}$. The various estimates for the detector time constant may say something about the nature of heat flow from the calibration heater to the thermopiles. From Table (3.1.2.3), it can be seen that the upward phase of the detector response appears most affected by the absence of buffer flow. Heat flow from the calibration heater to the thermopiles may therefore be facilitated by the flowing stream. Under such circumstances T_d is certainly more precise; this is perhaps an indication of a more precise heat flow path. In contrast, heat leak from the flow cell does not appear to be affected by the flow of buffer. Finally,

detector sensitivity (I/E_{ss}) may be slightly improved by the flow of buffer.

3.1.3 Simulation Studies

From the previous expression given for the upward and decay phases of the steady state response, the transient response should be approximately described by a function of the form,

$$Y = [\ 1 - \exp(-t/T_d)]\ \exp(t/T_d)$$

or $$Y = \exp(-t/T_d) - \exp(-2t/T_d) \qquad (3.1.3.1)$$

Beezer and Tyrrell 1972 (147), Randzio and Suurkuurk 1980 (148). This is a combination of the upward and decay phases of the detector response. Under the influence of other transient processes such as those associated with sample flow rate, sample plug dispersion, and enzyme reaction, the actual instrument transient response can be represented by the more general equation:

$$Y = \exp(-t/T_d) - \sum_{i}^{n} \exp(-t/T_i) \qquad (3.1.3.2)$$

where T_i ..... T_n are various time constants all expressible in terms of T_d.

The following relation:

$$Y = [\ 1 - \exp(-t/T_d)\ \exp(-t/T_d - t/T_x)$$

was used to simulate a transient peak, and examine the effects of altering one time constant on the response. The necessary calculations were done using a programmable calculator (CASIO FX - 702P). For simplicity only two time constants were considered;

T_d was given a value of 130s and T_x (a second unidentified time constant) varied from 15s to 6 x 10^3s. The above range of T_x values is intended to reflect fast to extremely slow transient processes. The results are presented in Table (3.1.3.1), Figure (3.1.3.1)

Table (3.1.3.1) Dependence of Simulated Transient Peak Characteristics on the Secondary Time Constant T_x

T_x (S)	rel. pk. hght.	rel. pk. area*
12	0.0296	0.0179
30	0.0631	0.0820
100	0.1270	0.3112
150	0.1562	0.5779
300	0.1900	0.7980
600	0.2460	1.1810
6000	0.2500	1.2250

* pk. area is estimated as W (at 0.5 pk. ht) x pk. ht.

It can be seen that both peak height and peak area become smaller in response to a smaller value of T_x ie. a fast secondary transient process. It is reasonable to suppose that if sample flow rate through a flow-through detector is too great, then the full signal will not be registered. This follows from the above results if $T_x = V_R/F$. The flow rate used in practical studies normally ranged from 10.2 - 50 cm^3 h^{-1}; thus T_x had values between 176.5s and 36s in experiments.

The above ideas were tested in a flow system using a spectrophotometric (Pye Unicam 1800) detector, teflon tubing, a

FIG(3·1·3·1)- Simulated transient responses of the LKB 2013-70 flow microcalorimeter (Table(3·1·3·1))

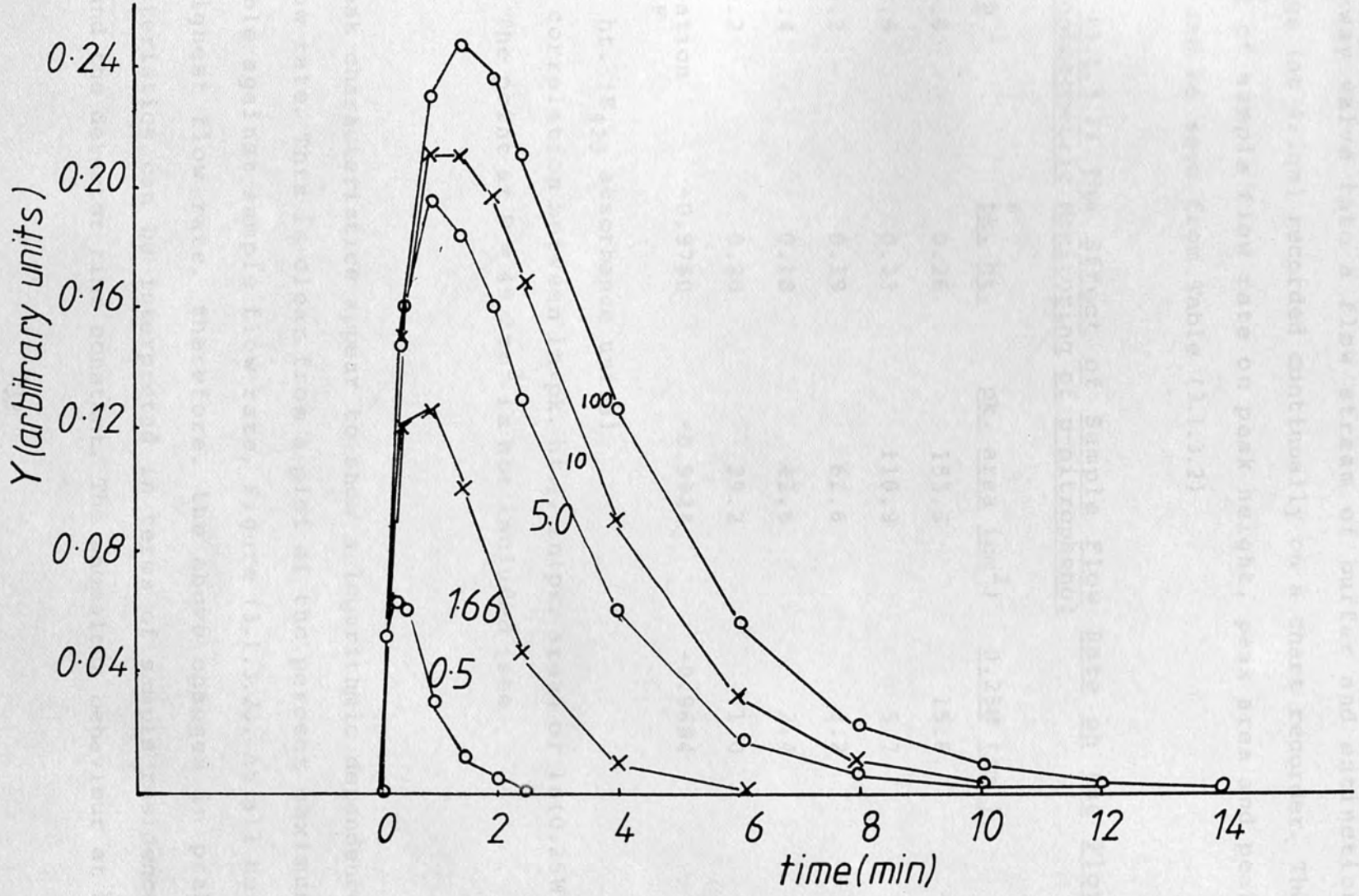

flow-through cell, and a syringe pump (Razel). Solutions of p-nitrophenol (29.3 x 10^{-6}M; 0.5cm^3) were then injected via a three-way valve into a flow stream of buffer and extinction readings (at 420nm) recorded continually on a chart recorder. The effect of sample flow rate on peak height, peak area and peak width can be seen from Table (3.1.3.2)

Table (3.1.3.2) The Effect of Sample Flow Rate on the Flow Spectrophotometric Monitoring of p-nitrophenol

F(cm^3 h^{-1}	pk. ht.[a]	pk. area (cm^2)	0.25W (cm.)
6.6	0.26	153.5	15.6
12.6	0.23	110.9	5.7
25.2	0.19	62.6	3.2
35.4	0.18	42.6	2.4
49.2	0.20	29.2	1.0
[b]Correlation with F	-0.9760	-0.9924	-0.9684

a. pk. ht. (E_{420} absorbance units)

b. ie. correlation between ln(pk. ht.), ln(pk. area) or ln(0.25W) and F. The point at F = 49.2cm^3 is not included (see text).

All peak characteristics appear to show a logarithmic dependence on flow rate. This is clear from a plot of the percent maximum variable against sample flow rate, Figure (3.1.3.2). At all but the highest flow rate, therefore, the above changes in peak characteristics can be interpreted in terms of sample residence time and the detector time constant. The anomalous behaviour at a

FIG(3·1·3·2)-Effect of sample flow rate on pk.ht(*), pk.area(○) and 0·25W(□)(Table(3·1·3·2)).

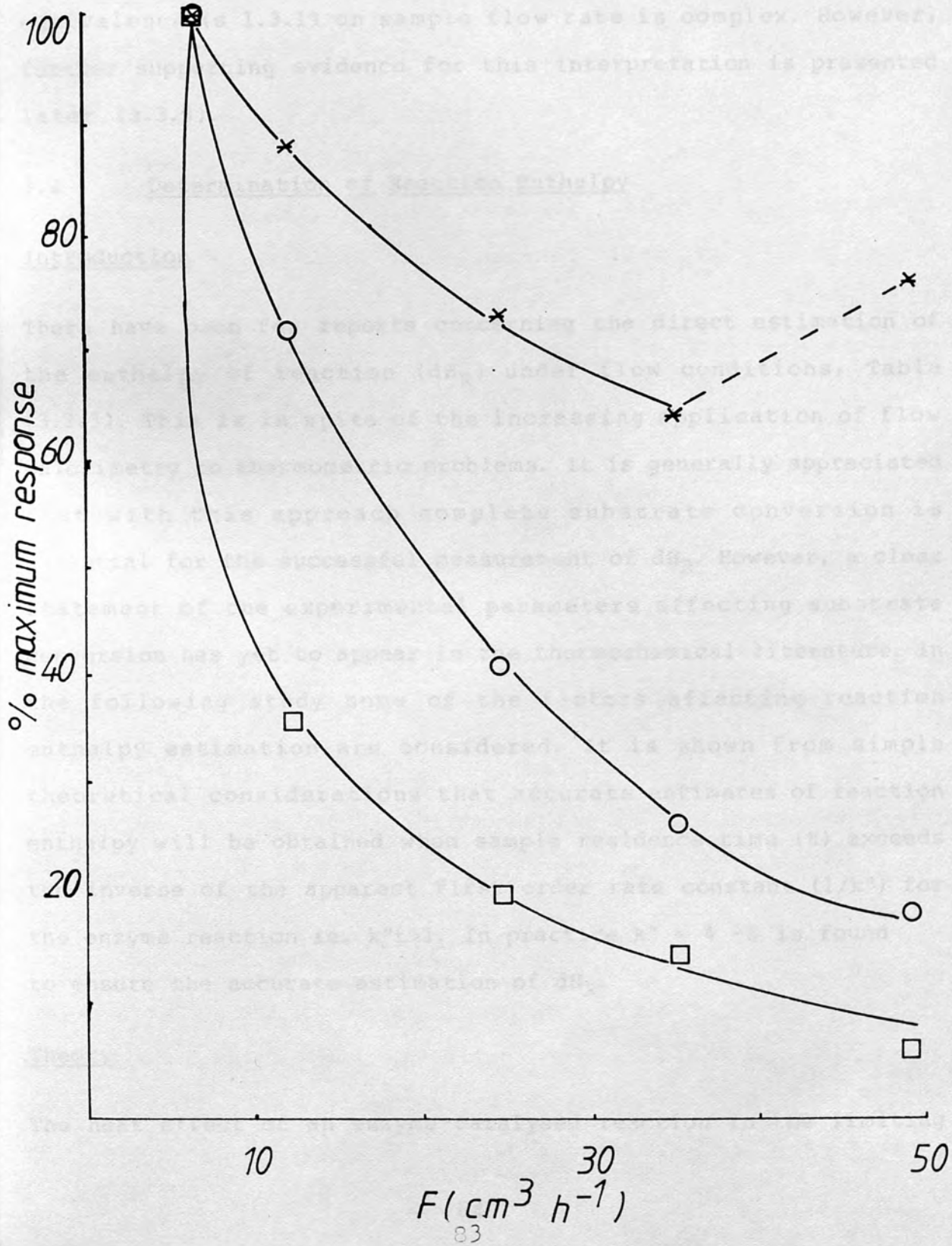

sample flow rate of 49.2cm^3 h^{-1} is perhaps most readily explained as due to decreased sample dispersion at high sample flow rate. As discussed previously the dependence of the height theoretical equivalence (s 1.3.1) on sample flow rate is complex. However, further supporting evidence for this interpretation is presented later (s.3.3).

3.2 Determination of Reaction Enthalpy

Introduction

There have been few reports concerning the direct estimation of the enthalpy of reaction (dH_R) under flow conditions, Table (3.2.3). This is in spite of the increasing application of flow calorimetry to thermometric problems. It is generally appreciated that with this approach complete substrate conversion is essential for the successful measurement of dH_R. However, a clear statement of the experimental parameters affecting substrate conversion has yet to appear in the thermochemical literature. In the following study some of the factors affecting reaction enthalpy estimation are considered. It is shown from simple theoretical considerations that accurate estimates of reaction enthalpy will be obtained when sample residence time (t) exceeds the inverse of the apparent first order rate constant (1/k") for the enzyme reaction ie. k"t>1. In practice k" = 4 -5 is found to ensure the accurate estimation of dH_R.

Theory

The heat effect of an enzyme-catalysed reaction in the limiting

first and zero order phase of the Michaelis-Menten equation has been discussed by Beezer 1973, (149). For a flow calorimeter containing immobilized enzymes the steady state heat effect is:

$$dQ/dt = k'' \cdot S. V_R \, dH_R \qquad (3.2.1)$$

$$dQ/dt = k_o' \cdot V_R \cdot dH_R \qquad (3.2.2)$$

in the first and zero-order phases (ie. $S << Km^{app}$ and $S >> Km^{app}$) respectively. The various terms have the following meaning; k" is the apparent first-order rate constant ($Vmax'/Km^{app}$), k_o is the zero-order rate constant (Vmax') and S is substrate concentration. The relation (3.2.3) is a dimensionally equivalent, working version of (3.2.1):

$$dQ/dt = dH_R'. S. F \qquad (3.2.3)$$

a plot of heat effect against the product of the substrate concentration and flow rate (ie. S.F) will therefore be expected to be linear with a slope equal to an apparent enthalpy of reaction (dH'_R). The latter will be an accurate estimate of dH_R only when there is complete conversion during a single pass of substrate through an IMER.

The condition for complete conversion is simply derived. For example, letting $dH_R' = dH_R$, then from (3.2.1) and (3.2.3)

$$F = k'' V_R \quad \text{or} \quad k''t = 1 \qquad (3.2.4)$$

where t is a nominal sample residence time. The condition for complete reaction and hence accurate estimation of dH_R is now readily stated as $k''t > 1$. It can be seen that this condition will be more nearly met by using high enzyme activity (Vmax)'

and low sample flow rate.

An alternative treatment is possible based on the IMER kinetics (s 1.4.3). As discussed above, the fractional conversion in an enzyme reactor under first-order conditions can be expressed as:

$$X = 1 - \exp(-kt) \qquad (3.2.5)$$

The above expression predicts near complete fractional conversion (X = 0.996) when the product Kt is 5.

Materials and Methods

Glucose oxidase (β - D - Glucose: oxygen 1- oxidoreductase, EC 1.1.3.4; Type X from Aspergillus niger, 100 - 150 units per mg. solid) Catalase, (H_2O_2: H_2O_2 oxidoreductase, EC 1.11.1.6, from bovine liver; 2000 - 5000 units per mg. protein.) urease, (EC. 3.5.1.5, Type VII from Jack bean; 40 - 100 units per mg.) glucose and urea were all commercial samples from Sigma UK. All other reagents were of analytical grade from the British Drug House (BDH). The enzyme immobilization procedure was as described in detail above (Chapter 2).

The LKB 2017-30 sorption microcalorimeter used in these studies has been described in Chapter 1. The immobilized enzyme was retained within the instrument flow cell with teflon filters. A similar experimental set-up has been described by Johansson et al. 1973 (19) and Schmidt et al. 1976 (20). A peristaltic pump (LKB 10,700) and a syringe pump (Razel) were used to pump samples in the range 10.2 cm^3h^{-1} to 50 cm^3h^{-1}.

Results

Estimates of reaction enthalpy for urea hydrolysis in phosphate and THAM-HCl buffers, as a function of column enzyme activiity, (Vmax′) and nominal sample residence time (t) are listed in Table (3.2.1) and Table (3.2.2)

Table (3.2.1) Estimates of dH_R for Urea Hydrolysis in Phosphate Buffer (0.2M, pH 7.0; 10^{-3}M EDTA) as a function of column enzyme activity (Vmax′) and nominal sample residence time (t)

[a] V_{max}'	[b] $t_{(s)}$	[c] k''	[d] X	[e] dH_R'	[e] dH_R''
1.48	177.0	22.3	0.9824	60	61
1.48	79.2	22.3	0.8361	52	62
1.00	49.2	21.7	0.6552	32	49
0.08	159.0	2.7	0.3382	16	47

a. Vmax′(mMs^{-1})

b. t = V/F

c. k"(s^{-1}) x 10^3 = $Vmax'/Km^{app}$; enzyme kinetic constants were determined using a Lineweaver-Burk Plot (Chapter 4).

d. fractional conversion (X) was calculated from (3.2.5)

e. dH_R ($kJ\ mol^{-1}$)

Table (3.2.2)[a] Estimates of dH_R for Urea Hydrolosis in THAM buffer (0.2M, pH 7.0; 10^{-3}M EDTA) as a function of column enzyme activity (Vmax′) and nominal sample residence time (t)

Vmax′	t(s)	k"	X	dH_R'	dH_R''
0.40	157.8	12.62	0.8633	17	20
0.40	97.8	12.62	0.6317	10	16
0.32	97.8	7.21	0.5034	9	18
0.20	97.9	2.73	0.2343	3	13

a. see legend to Table (3.2.1)

The dependence of the apparent reaction enthalpy on the above parameters is generally as predicted by theory. The last columns in Table (3.2.1) and Table (3.2.2) contain apparent enthalpy values extrapolated to 100% sample conversion (dH_R"). The final dH_R values are compared with some published values in Table (3.2.3). The enthalpies of urea hydrolysis are estimated in this work as 60 $\pm$ 3.0 kJ mol^{-1} and 17 $\pm$ 1.0 kJ mol^{-1} in phosphate and THAM buffers respectively.

The value of dH_R for glucose oxidation by buffer dissolved oxygen, catalysed by glucose oxidase and catalase co-immobilized on CPG, was also estimated as 261 $\pm$ 9.0 kJ mol^{-1}. This value compares with a value of 207.11 kJ^{-1} reported by Schmidt et al. 1976 (20) under experimental conditions similar to those employed in this study. It is also possible to arrive at an estimate of about 258 kJ mol^{-1} from data presented by Johanasson 1973 (155). All the dH_R values cited for the oxidation of glucose were

Table (3.2.3) Some Published Value for dH_R kJ mol^{-1} of Urea Hydrolosis

dH_R (THAM)	dH_R (phosphate)	Reference
18.70 ± 0.63	61.23 ± 0.79	Jesperson 1975 (150)[a]
19.80	57.1 ± 1.0	Trewhella 1981 (151)[c]
-	33	Beezer 1973 (152)[b]
6.57	-	Brown 1968 (153)[a]
7.12	-	Schmidt et al. 1976 (20)[c]
-	56.6	Bauer and Gemmil 1952 (154)[a]
17 ± 1.0	60 ± 3.0	This work[c]

a - batch calorimeter

b - flow microcalorimeter with soluble enzyme

c - flow microcalorimeter with immobilized enzyme

determined using the co-immobilized glucose oxidase-catalase system in combination with the LKB flow microcalorimeter. In previous studies the possible effect of α- β mutarotation of glucose on the value of dH_R was not considered. Assuming that there is only slight conversion of α- glucose to β- glucose during the sample residence time (Chapter 4.2) and from the 0.629 proportion of β -glucose at mutatoratory equilibrium, the `true´ dH_R value for glucose oxidation is of the order of 415 kJ mol^{-1}.

3.3 Steady State and Transient Analysis of Glucose and Urea

Introduction

The combination of thermochemical monitoring with immobilized enzymes has been widely exploited in the development of flow analyses sytems for such analytes as glucose, penicillin, urea and phenol, (s.1.1.3). Reports involving the specific use of the LKB flow microcalorimeter include those by Johansson 1973 (155), Johansson et al. 1973 (19) and Schmidt et al. 1976 (20).

Sample injection in flow analysis may be pulsed or continuous (s 1.3) . The resulting forms of analysis are termed transient or steady state respectively. System characteristics, linearity range, minimal detectable concentration, and sample throughput rate may depend on the sample injection regime adopted. In the following study a careful comparison is made between the two modes of sample injection.

Materials and Method

The materials and methods used are the same as described previously (s.3.1). Sample volume for transient and steady state analysis were $0.5cm^3$ and $8cm^3$ respectively. For glucose analysis, standards were prepared 8 - 12 hours before use to allow complete α - β muturotation. The abbreviations CPG-GLO/CAT or CPG-urease are used to describe glucose oxidase/catalase or urease immobilized on CPG.

Results

Several aspects of a transient analytical signal may be used as an index for analysis. For instance peak height, initial slope and peak area all appear to be useful indices Table (3.3.1). The precision of glucose analysis (measured as mean coefficient of variations, CV = (SD/x * 100)/n)) based on these indices was estimated at 7.71%, 9.72% and 4% for peak height, initial slope and peak-area data respectively. The precision of peak-height data appears to improve significantly with an increase in the magnitude of the heat signal being measured; in urea analysis, the precision for the peak-height data, Table (3.3.2), is only 1.33%. The precision for the corresponding peak-area data is initially 6.98%. This figure, however, includes a 3% contribution from a planimeter used in peak area measurements. The above indices are compared over the linear range for glucose analysis in Figure (3.3.1).

Table (3.3.1) Transient analysis of glucose using CPG - GLO/CAT

(0.2M phosphate buffer, pH 7.0; 10^{-3}M EDTA)

[Glucose]; x 10^{-3}M	Pk. ht. $\bar{X} \pm SD$ (μV)	Pk. area (cm^2)	Integral heat (mJ)	Initial slope
20.0	31.8 $\pm$ 0.35	16.4 $\pm$ 0.28	191.5	8.7 $\pm$ 0.93
10.0	33.0 $\pm$ 1.41	14.1 $\pm$ 0.17	164.6	9.1 $\pm$ 0.10
5.0	31.1 $\pm$ 2.0	13.1 $\pm$ 0.24	152.4	7.9 $\pm$ 0.42
2.0	26.5	9.1 $\pm$ 0.84	101.6	6.2 $\pm$ 0.22
1.0	17.5	5.5 $\pm$ 0.12	63.8	6.0 $\pm$ 1.41
0.5	11.1 $\pm$ 3.0	2.7 $\pm$ 0.22	32.1	2.8 $\pm$ 0.56
0.2	5.6 $\pm$ 0.9	2.1 $\pm$ 0.1	24.5	1.2 $\pm$ 0.56
0.1	2.5	1.0	12.1	-

E_{tr} transient steady state constant = 11.67 mJ cm^{-2}; F = 18 cm^3 h^{-1}

Table (3.3.2) Transient analysis of urea using CPG Urea

(0.2 phosphate buffer, pH 7.0; 10^{-3}M EDTA)

[Urea] x 10^{-3} M	Pk.Ht. $\bar{x} \pm$ SD(μV)	Pk.area (cm^2)	Integral heat (mJ)
200	472.5 $\pm$ 9.22	192.1 $\pm$ 8.60	4485.7
100	308.2 $\pm$ 3.46	106.0 $\pm$ 4.26	2473.0
50	179.8 $\pm$ 4.58	61.7 $\pm$ 8.63	1406.0
30	105.3 $\pm$ 0.94	31.0 $\pm$ 0.98	717.3
20	76.0 $\pm$ 1.15	23.0 $\pm$ 3.20	458.1
10	42.5	11.5 $\pm$ 0.27	268.7

E_{tr} = 23.34 mJ cm^{-2}; F = 18cm^3h^{-1}

FIG(3·3·1) - Transient analysis of glucose. Plot of peak height(*), peak initial slope(⊙) and peak area(⊡) against concentration of glucose(⩽ 2 mM; 0·5 cm^3 pulse)

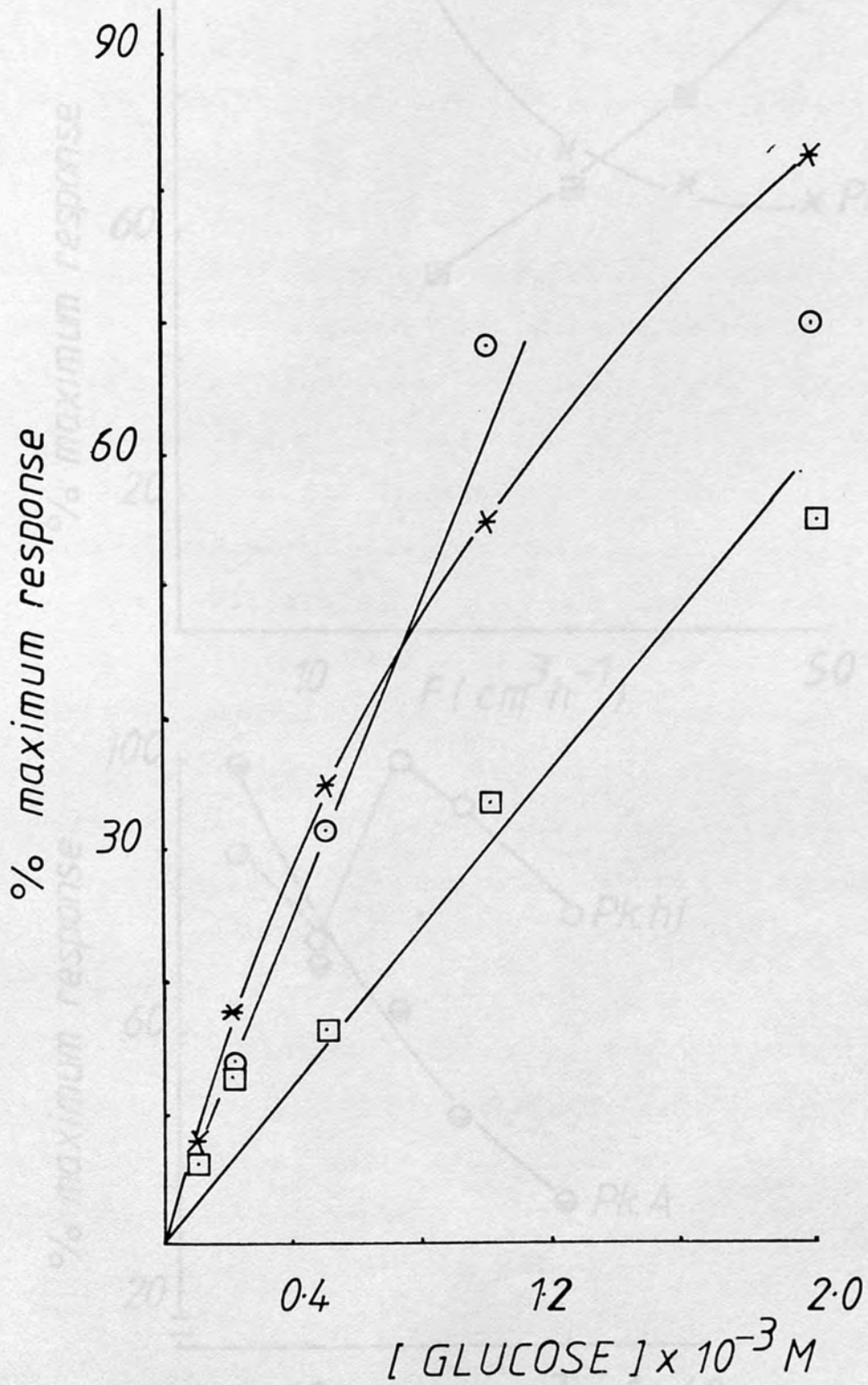

FIG(3·3·2)- Effect of flow rate on transient output for glucose(*,⊠) and urea(○,◒) analysis

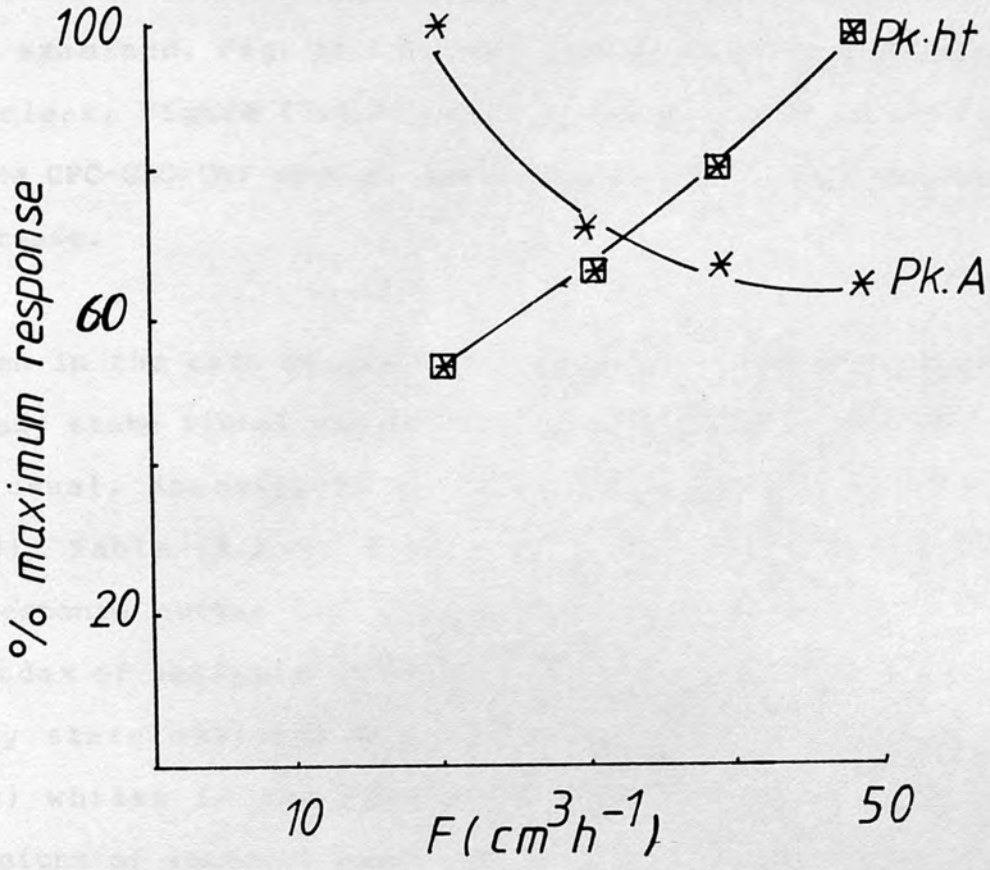

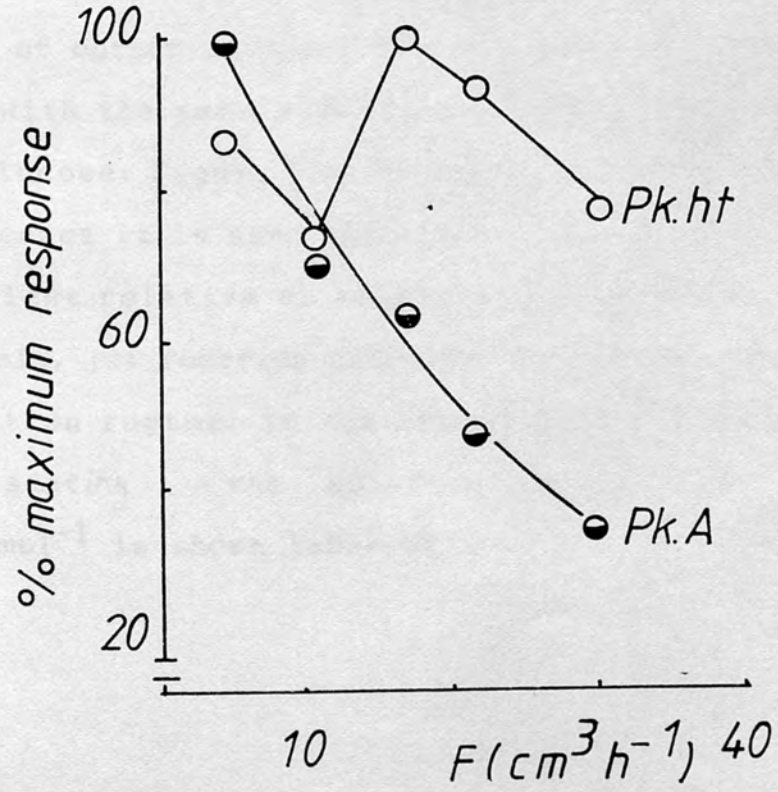

The theoretical dependence of a transient response on sample flow rate was discussed above (s.3.1). The experimentally observed peak area decreases with increasing flow rate over the whole range examined, Fig. (3.3.2). The situation with peak height is less clear, Figure (3.3.2) there is an increase in peak height for the CPC-GLO/CAT system, but this pattern is not observed with CPG-urease.

As seen in the case of transient signals, a number of aspects of a steady state signal can be used as an index for analysis. It is most usual, however, to use the steady state response. Table (3.3.3), Table (3.3.4); Figure (3.3.3) and Figure (3.3.4) show the response curves for glucose and urea analysis respectively. The index of analysis (Y-axis, Figure (3.3.3), Figure (3.3.4) in steady state analysis has the dimensions of power (J s^{-1} or watts) whilst in the case of Transient analysis it has the dimensions of integral power (J). A direct comparison of the two kinds of output is therefore only possible after conversion into data with the same dimensions. Such a comparison has been made for glucose, Figure (3.3.5) and urea, Figure (3.3.6) analysis. In both cases it is seen that the linearity range is extended with transient relative to steady-state analysis. The sensitivty of analysis, (cf reaction enthalpy) is however independent of sample injection regime. In the urease study, Figure (3.3.6) the line representing the optimum sensitivity, with a slope of 60kJ mol^{-1} is shown labelled (A).

Under ideal conditions it is possible to measure a system output of about 25mJ with good precision. The lowest detectable concentration for glucose (G) and urea (U) analysis, Table (3.3.5), was calculated from this figure and data presented in Table (3.3.1) - Table (3.3.4).

Table (3.3.5) Lowest detectable Concentration and Upper Limit of Linearity (linearity range) for transient and steady state analysis of glucose and urea under ideal conditions

	Pulsed Injection	Continuous Injection
G x 10^{-3}M	0.2 - 1.0	0.04 - 0.5
G x 10^{-7}mol	1.0 - 5.0	0.21 - 2.5
(r)	0.9803	0.9845
U x 10^{-3}M	0.91 - 200	0.14 - 30
U x 10^{-6} mol	0.46 - 100	0.07 - 15.0
(r)	0.9972	0.9935

With both glucose and urea analysis, lowest detectable concentration is improved (i.e. is lower) for steady state analysis (continuos sample injection) compared with transient analysis (pulsed sample injection). The sample throughput for pulsed and continuous injection, under the present condition of near optimum sensitivity, was four samples per hour and one sample per hour respectively.

Table (3.3.3) steady-state analysis of glucose using CPG-GLO/CAT

(0.2M phosphate buffer, pH 7.0; 10^{-3}M EDTA

[Glucose] x 10^{-3}M	ss-disp (μV)	Heat effect (mJ s^{-1})	Integral heat (mJ)
20.0	28.5	0.5070	50.70
10.0	28.0	0.4981	49.81
5.0	29.5	0.5248	52.48
2.0	29.5	0.5248	52.48
1.0	28.2	0.5026	50.26
0.5	21.5	0.3825	38.25
0.2	12.0	0.2135	21.35
0.1	6.0	0.1067	10.67

E_{ss} = 17.80 $Js^{-1}V^{-1}$; F = 18cm^3 h^{-1}

FIG(3·3·3)- Steady state analysis of glucose· Plot of steady state heat effect against concentration of glucose (⩽ 2 mM ; Table(3·3·3))

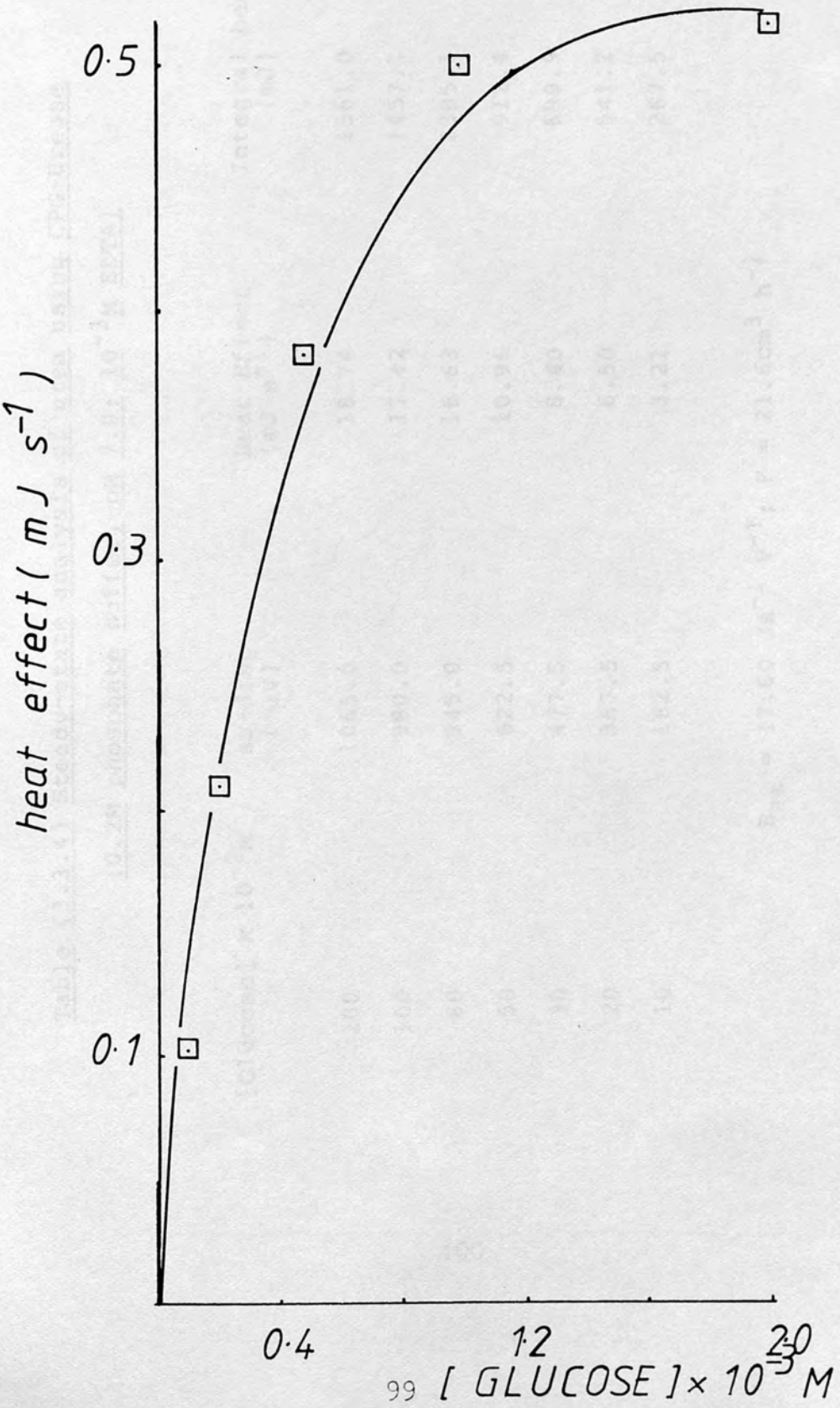

Table (3.3.4) Steady-state analysis of urea using CPG-Urease

(0.2M phosphate buffer, pH 7.0; 10^{-3}M EDTA)

[Glucose] x 10^{-3}M	ss-disp (μV)	Heat Effect (mJ s^{-1})	Integral heat (mJ)
200	1065.0	18.74	1561.0
100	990.0	17.42	1457.1
80	945.0	16.63	1385.1
50	622.5	10.96	912.4
30	477.5	8.40	699.9
20	367.5	6.50	541.2
10	182.5	3.21	267.5

E_{ss} = 17.60 Js^{-1} V^{-1}; F = 21.6cm^3 h^{-1}

FIG(3·3·4)-Steady state analysis of urea· Plot of steady state heat effect against concentration of urea(Table(3·3·4))

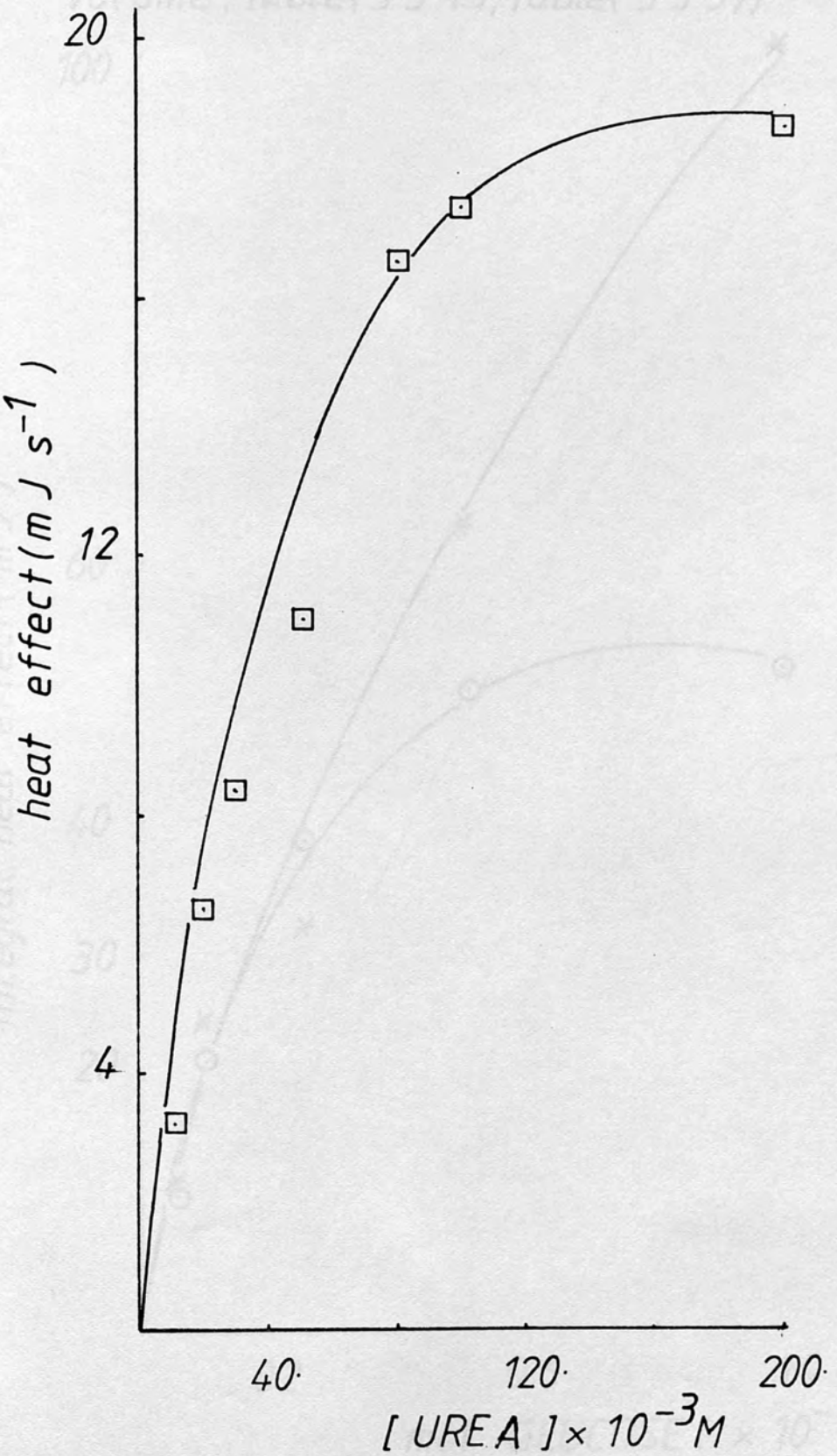

FIG(3·3·5)–Comparison of transient (*) and steady state (○) response curves for glucose · ($\leqslant 1 \times 10^{-6}$ mol, 0·5 cm^{-3} sample volume ; Table(3·3·1), Table(3·3·3))

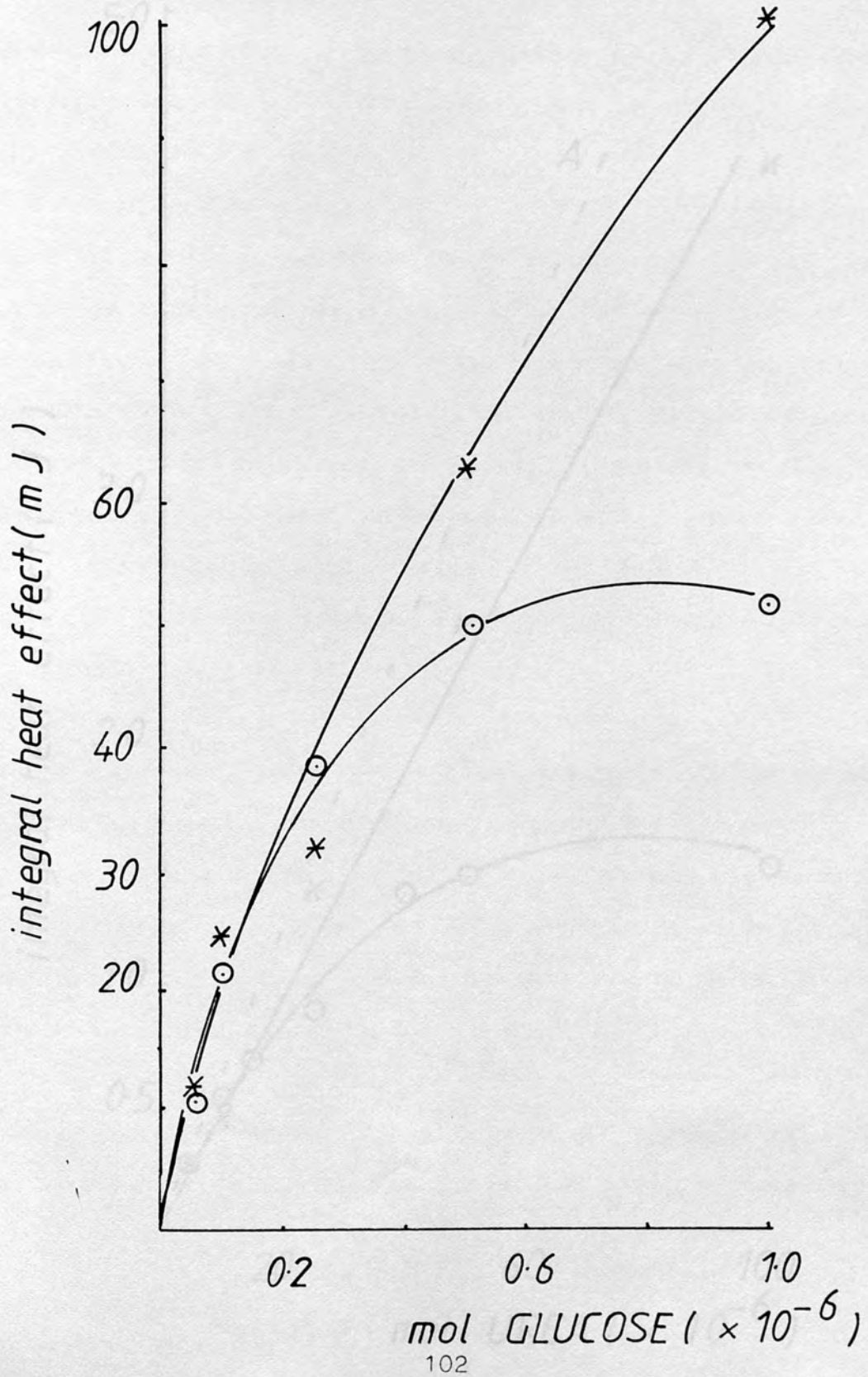

FIG(3·3·6)-Comparison of transient(*) and steady state(⊙) response curves for urea ($\leqslant 100 \times 10^{-6}$ mol, 0·5 cm^{-3} sample volume; Table(3·3·2), Table(3·3·4))

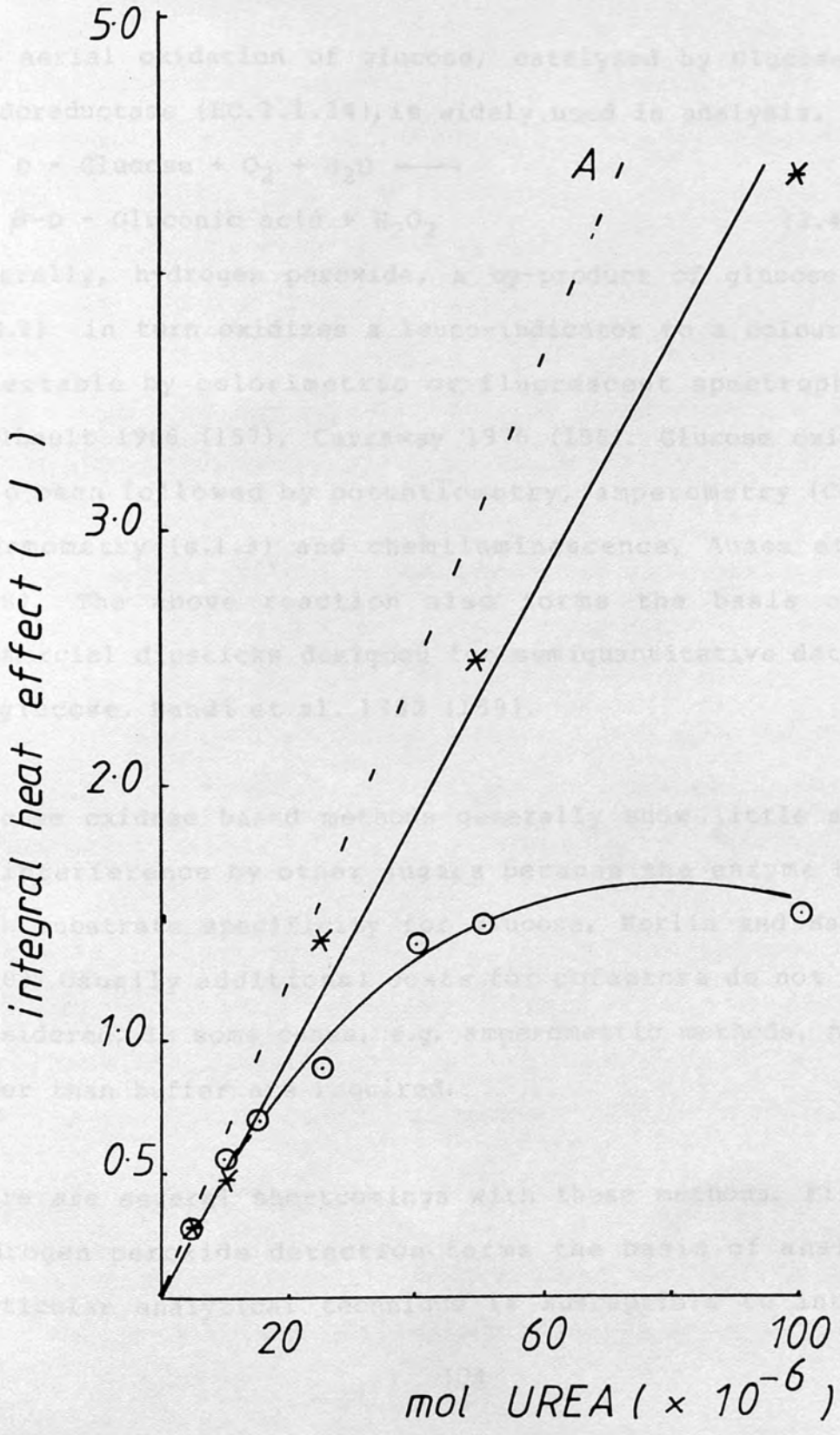

3.4 Determination of Glucose in the Presence of Artificial Electron Acceptors

Introduction

The aerial oxidation of glucose, catalysed by Glucose;Oxygen-1-oxidoreductase (EC.1.1.34), is widely used in analysis.

$$\beta\text{- D - Glucose} + O_2 + H_2O \longrightarrow \beta\text{-D - Gluconic acid} + H_2O_2 \qquad (3.4.1)$$

Generally, hydrogen peroxide, a by-product of glucose oxidation (3.4.1) in turn oxidizes a leuco-indicator to a coloured species detectable by colorimetric or fluorescent spectrophotometry, Guilbault 1966 (157), Carraway 1976 (156). Glucose oxidation has also been followed by potentiometry, amperometry (Chapter 6), thermometry (s.1.3) and chemiluminescence, Auses et al. 1975 (158). The above reaction also forms the basis of several commercial dipsticks designed for semiquantitative determination of glucose, Bandi et al. 1982 (159).

Glucose oxidase based methods generally show little sensitivity to interference by other sugars because the enzyme has a very high substrate specificity for glucose, Kerlin and Hartree 1948 (160). Usually additional costs for cofactors do not need to be considered. In some cases, e.g. amperometric methods, no reagents other than buffer are required.

There are several shortcomings with these methods. First, where hydrogen peroxide detection forms the basis of analysis, the particular analytical technique is susceptible to interferences

by reducing compounds naturally present in samples. Examples of compounds common in samples of biological origin include ascorbic acid, White-Stevens 1982 (161), uric acid and the drug paracetamol, Roddis 1981 (162). Second, glucose oxidase is believed to be inactivated by hydrogen peroxide (Chapter 4); such enzyme activity loss will reduce the useful life of an IMER. Third, the upper end of the linear range is limited by the low dissolved oxygen concentration in buffer under normal laboratory conditions (Chapter 4).

It is known from the early studies of glucose oxidase that oxygen can be replaced by other electron acceptors, Frank and Lorenz 1939 (163). More recently Williams et al. 1970 (164) successfully replaced oxygen with 1,4-benzoquinone, in the electrochemical analysis of glucose, and thereby extended the upper limit of linearity by about 20-fold. Further possible advantages of using artificial electron acceptors include a possible reduction in the susceptibility to interferences and an increase in the stability of glucose oxidase.

In the following thermochemical study, 1,4-benzoquinone, 2,6-dichlorophenol-indophenol (DCPIP), ferrocene, ferricyanide, methylene blue, and toluidine blue were studied as prospective replacements for oxygen in the glucose oxidase reaction.

Materials and Methods

1,4-benzoquinone, ferricyanide methylene blue and toluidine blue were supplied by BDH. All other reagents were purchased from

Sigma UK.

Much of the detail concerning the methods, e.g. of preparation and use of CPG-GLO/CAT, are as described in previous sections. Glucose samples in this study were however made up in buffer solutions of individual test compounds; the latter also served as reference buffer or carrier medium. As the compounds under study differed greatly in their solubiity in aqueous solutions the concentrations used was different in each case.

Results

The response curve for the transient analysis of glucose, in the presence of oxygen and the more effective artificial electron acceptors, is illustrated Figure (3.4.1). The corresponding numerical data, except for the control (ie. dissolved oxygen) study, appear in Table (3.4.1) and Table (3.4.2). From Figure (3.4.1) there is clearly a progressive increase in linearity range on passing from oxygen to methylene blue and finally to 1,4-benzoquinone. The other compounds tested were less successful and did not produce observable differences from the control.

The apparent Michaelis constant was determined for CPG-GLO/CAT in each case; Km^{app} agrees very closely with the upper limit of linearity for both transient and steady state analysis. This was however not the case in the presence of methylene blue and 1,4-benzoquinone.

Table (3.4.1) Transient Analysis of Glucose using CPG-GLO/CAT (0.2M phosphate buffer, pH 7.0; 10^{-3}M EDTA) in the Presence of Methylene Blue (50 x 10^{-3}M)

[Glucose] x 10^{-3}M	Peak Area (cm^2)
30.0	29.21
30.0	26.43
20.0	28.38
20.0	28.00
10.0	25.30
10.0	23.95
5.0	16.40
5.0	16.70
2.0	8.70
1.0	5.00
1.0	5.23
0.0	0.00

$r = 0.9878$; $0.0 \leqslant x \leqslant 5 \times 10^{-3}$M,

x is the analytically useful range

$r = 0.9798$; $0.0 \leqslant x \leqslant 10 \times 10^{-3}$M

Table (3.4.2) Transient Analysis of Glucose using CPG-GLO/CAT 10.2M phosphate buffer, pH 7.0; 10^{-3}M EDTA in the Presence of 1,4-benzoquinone

[Glucose] x 10^{-3}M	Peak Area (cm^2)
70.0	69.56
70.0	69.26
60.0	70.74
60.0	70.35
50.0	65.62
40.0	57.27
30.0	44.84
20.0	31.10
10.0	15.40
10.0	15.50
5.0	7.80
5.0	7.80
5.0	7.60
0.0	0.0

$r = 0.9910$; $0.0 \leqslant x \leqslant 60 \times 10^{-3}$M

$r = 0.9975$; $0.0 \leqslant x \leqslant 50 \times 10^{-3}$M

FIG(3·4·1)-Transient analysis of glucose in the presence of benzoquinone(⊡), methylene blue(⊙) and oxygen(*)as electron acceptors (Table(3·4·2), Table(3·4·1) and Table(3·3·1))

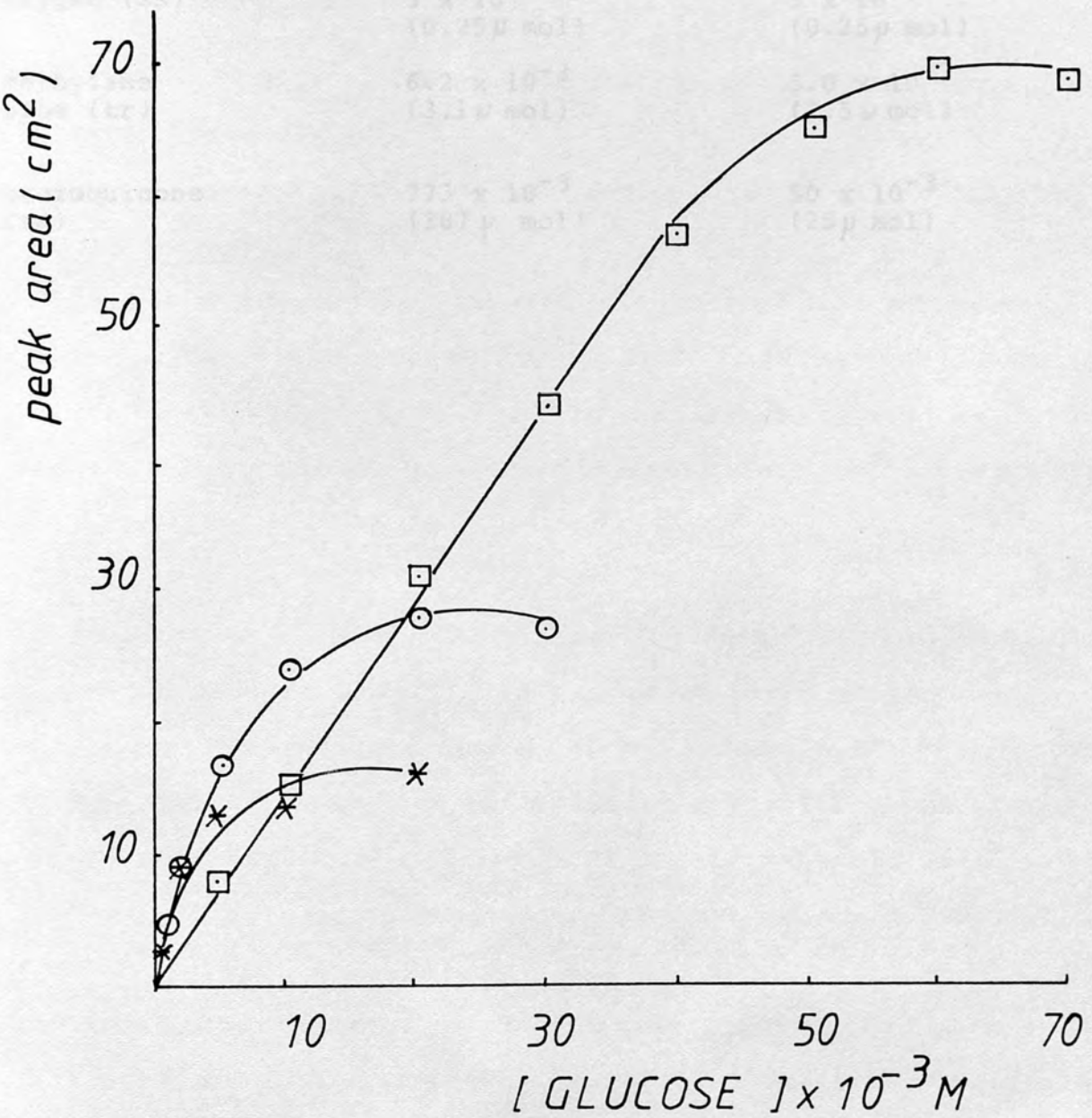

Table (3.4.3) - The apparent Michaelis Constant (Km^{app}) and Observed Upper Limit of Linearity in Glucose Analysis. (tr) and (ss) denote transient and steady-state analysis.

System	Km^{app} (M)	Upper Limit of Linearity (M)
oxygen (tr)	1.29×10^{-3} (0.64 μ mol)	1×10^{-3} (0.5 μ mol)
oxygen (ss)	5×10^{-4} (0.25 μ mol)	5×10^{-4} (0.25 μ mol)
methylene blue (tr)	6.2×10^{-3} (3.1 μ mol)	5.0×10^{-3} (2.5 μ mol)
benzoquinone (tr)	773×10^{-3} (387 μ mol)	50×10^{-3} (25 μ mol)

3.5 Determination of Selected Substrate Using the Appropriate Immobilized Enzyme and the LKB 2017-30 Microcalorimeter

3.5.1 Determination of Glucose, Fructose, Mannose, Glucosamine and Adenosine-5'-trihosphate using hexokinase immobilized on Controlled Porosity Glass

Introduction

Hexokinase catalyses the phosphorylation of D-hexoses according to the scheme.

$$D.Hex.eq + \Sigma ATP \longleftrightarrow eq.D.Hex.6p + ADP + H^{+} \quad (3.5.1.1)$$

Where Σ ATP denotes all possible ionic forms of adnosine-5'-triphosphate (ATP), such as ATP^{4-}, $HATP^{3-}$ and $Mg^{2+}ATP^{2-}$.D.Hex.eq refers to all mutarotatory forms of the hexose, as well as in the case of fructose, the pyranose/furanose forms, Goldberg 1975 (165).

In combination with glucose-6-phosphate adehydrogenase (G-6 P.D. H), hexokinase is widely used in the analysis of glucose. The spectrophotmetric method depends on the reduction of the cofactor NADP by G-6-P. The method has absolute specificity for glucose and is not susceptible to interference by ascorbic acid, uric acid and other reducing compounds, Peterson and Young 1968 (166).

The thermochemistry of the hexokinase reaction has been well characterised, for example by Goldberg, 1975, (165); Goldberg 1976 (167) and by McGlothlin and Jordan 1975 (2). The enthalpy of

phosphorylation of fructose, mannose and glucose (THAM-HCl buffer pH 8.7) is about 62.0 kJ mol^{-1}, 69 kJ mol^{-1} and 71.0 kJ mol^{-1} respectively. Typically about 47.5 kJ mol^{-1} of the total enthalpy change derives from the enthalpy of buffer protonation.

Hexokinase has low substrate specificity. Even so, the combination with thermochemical monitoring has some advantages. First, clinical and other non-homogeneous samples do not require deprotinization or similar pretreatment. Second, there is no requirement for a coupling reaction, hence there is reduced enzyme and cofactor requirement. Finally, low substrate specificity leads to a method sensitive to a wide range of hexose sugars. This last characteristic may be of some importance where a more general index of sugar content rather than the specific identification of hexoses is required. Soluble hexokinase has a bench life at room temperature of about 5 h , Carraway 1976 (156). It is also a fairly expensive enzyme in relation to the quantities used, (Sigma Uk Type C300 enzyme costs £2.14 for 200 units in 1983). Hexokinase is thus a good candidate for immobilization. In spite of these considerations, there have been few reports of the use of immobilized hexokinase in thermochemical analysis. The use of controlled porosity glass bound hexokinase for the determination of the hexoses, glucose, fructose, mannose, glucosamine and the cofactor ATP is reported below.

Materials and Methods

Hexokinase, (E.C. 2.7.1.1; Type C-300 from yeast) disodium adenosine-5'-triphosphate and all D-hexoses were commercial, Sigma UK. All other materials and sources were as described previously. The method of enzyme immobilization and use has been described in preceding sections.

The dependence of heat output on buffer concentration and magnesium ion concentration is of some interest. The effect of THAM-HCl buffer concentration was examined as follows. Quantities of a stock glucose-buffer solution (0.4M THAM-HCl, pH 8.0; 6.mM $MgCl_2$, 8mM glucose) and a stock diluent (pH 8.0, 6mM Mg Cl_2, 8mM glucose) were mixed to give a range of concentrations of THAM. These diluted buffer solutions were each then used as a reference medium. The heat effect at a particular buffer concentration was subsequently measured using as a sample a small portion of the reference buffer made 1.5×10^{-3}M with respect to the cofactor ATP. The same principle was applied in the study of the dependence of heat output on Mg^{2+} concentration. Again the initial stock solution and the diluent differed only as regards one variable which in the present case was the magnesium ion concentration.

Stock solutions of glucose and other hexoses (8×10^{-3}M) were left overnight at 4°C to allow complete mutarotation of α and β forms to equilibrium proportions. A range of concentrations of a particular hexose was prepared by adding ATP ($2cm^3$, 6×10^{-3}M to

a volume of hexose not exceeding $2cm^3$ and making up to a final volume of 5ml with buffer. Sample pulses (0.5 cm^3) were injected via an Altex sample loop. Analysis was carried out in THAM-HCl buffer (0.2M, pH 8.0; 6mM $MgCl_2$).

Results

In accord with the importance of buffer protonation in the overall thermochemistry of the hexokinase reaction, peak height was observed to increase as a function of THAM buffer concentration ($10^{-5}M$ - 2 x $10^{-1}M$).

Hexokinase is activated by magnesium ions. The optimum concentration was found to be between $10^{-3}M$ and $10^{-4}M$ ($3 < pMg^{2+} < 4$) . This compares with pMg^{2+} values of between 3 and 3.5 for the soluble enzyme, Goldberg 1976 (167).

The requirement for added cofactor (ATP) distinguishes the hexokinose system from any other studied. There was a constant background heat effect associated with samples containing no hexose. First, such background heats were quite large, typically between 20% and 25% of the maximum response for each hexose. Second, these background effects were not seen when ATP was injected into a column containing just controlled porosity glass. It is therefore unlikely that such heat derives from the heat of dilution of samples. Following the usual practice under such circumstances the constant background value has been substracted from the data presented below Table (3.5.1.1) - Table (3.5.1.5).

The CPG-hexokinase system showed sensitivity to all the hexoses tested, Figure (3.5.1.1) and Figure (3.5.1.2). Thus glucose, fructose, mannose, and glucosamine were all successfully determined with the above system. Finally, by making the ATP concentration limiting, the hexokinase system could also be used to determine ATP, Figure (3.5.1.3)

Table (3.5.1.1) Transient analysis of glucose and mannose using CPG- hexokinase

(0.2M THAM buffer, pHo 8.0; 6mM $MgCl_2$)

[Glucose] x 10^{-3}M	Pk. Ht. (μV)	[Mannose] x 10^{-3}M	Pk. Ht. (μV)
3.05	6.2	3.33	6.4
2.24	4.5	2.25	4.1
2.04	3.8	1.66	3.1
1.63	3.1	1.11	2.4
1.43	2.9	0.83	1.4
1.22	2.4	0.67	1.0
1.02	2.0	0.48	0.8
0.82	1.6	0.00	0.00
0.61	1.3		
0.51	1.0		
0.31	0.6		
0.00	0.0		

$3.1 \times 10^{-4}M < G < 3.05 \times 10^{-3}M$, $r = 0.9979$

$4.8 \times 10^{-4}M < M < 3.33 \times 10^{-3}M$, $r = 0.9954$

FIG(3·5·1·1)-Transient analysis of glucose and mannose. Plot of peak height against concentration of glucose(⊙) and mannose(⊡) (⩽3·5 mM; Table(3·5·1·1))

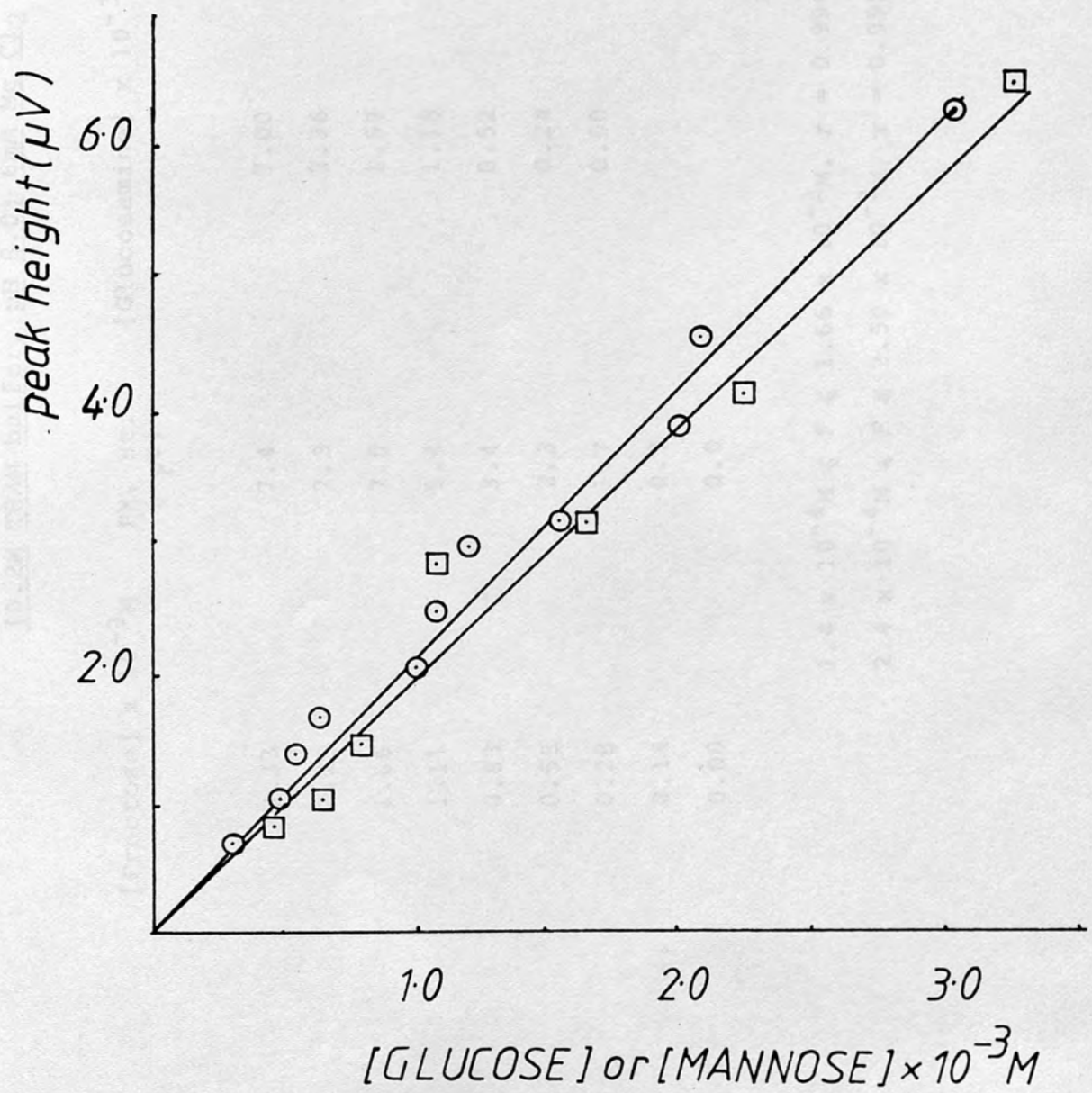

Table (3.5.1.2) Transient analysis of fructose and glucosamine using CPG-hexokinase

(0.2M THAM buffer, pH 8.0; 6mM Mg Cl_2

[Fructose] x 10^{-3}M	Pk. Ht. (μV)	[Glucosamine] x 10^{-3}M	Pk. Ht. (μV)
3.33	7.4	3.00	4.4
2.25	7.3	2.36	4.4
1.66	7.0	1.57	3.1
1.11	5.4	1.18	2.0
0.83	3.4	0.52	1.2
0.55	2.3	0.24	0.3
0.28	1.7	0.00	0.0
0.14	0.7		
0.00	0.0		

$1.4 \times 10^{-4}M \leqslant F \leqslant 1.66 \times 10^{-3}M$, r = 0.9902

$2.4 \times 10^{-4}M \leqslant F \leqslant 2.50 \times 10^{-3}M$, r = 0.9950

FIG(3·5·1·2)- Transient analysis of fructose and glucosamine. Plot of peak height against concentration of fructose(⊙) and glucosamine(⊡). (⩽2·5 mM; Table(3·5·1·2))

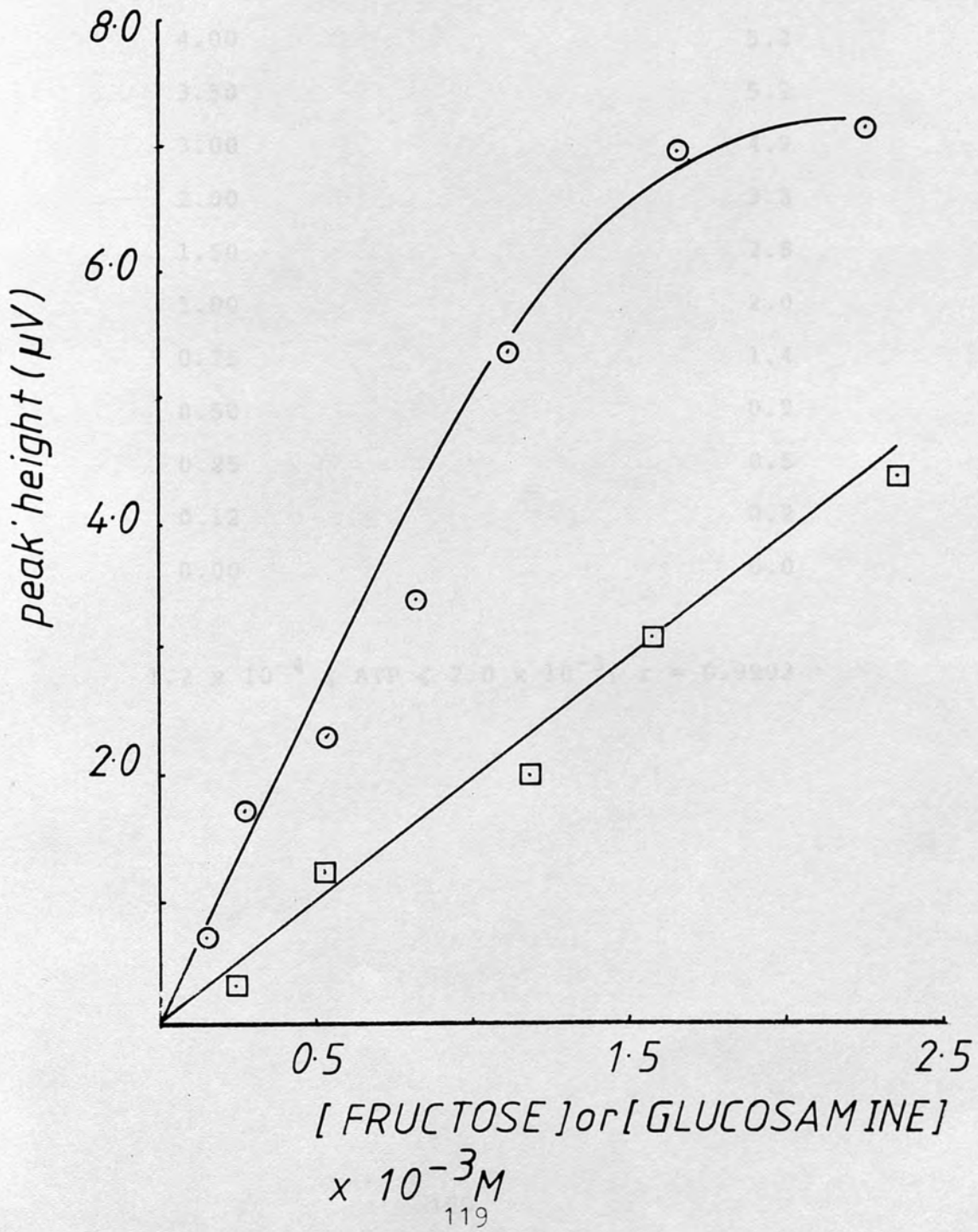

Table (3.5.1.3) Transient Analysis of Adenosine-5′-triphosphate (ATP) using CPG-hexokinase, (0.2M THAM buffer, pH 8.0; 6mM $MgCl_2$)

[ATP] $x10^{-3}$M	Pk Ht. (μV)
4.00	5.2
3.50	5.2
3.00	4.9
2.00	3.8
1.50	2.8
1.00	2.0
0.75	1.4
0.50	0.9
0.25	0.5
0.12	0.2
0.00	0.0

$1.2 \times 10^{-4} \leqslant ATP \leqslant 2.0 \times 10^{-3}$, r = 0.9993

FIG(3·5·1·3)–Transient analysis of ATP·
Plot of peak height against concentration
of ATP·(≤ 3 mM; Table(3·5·1·3))

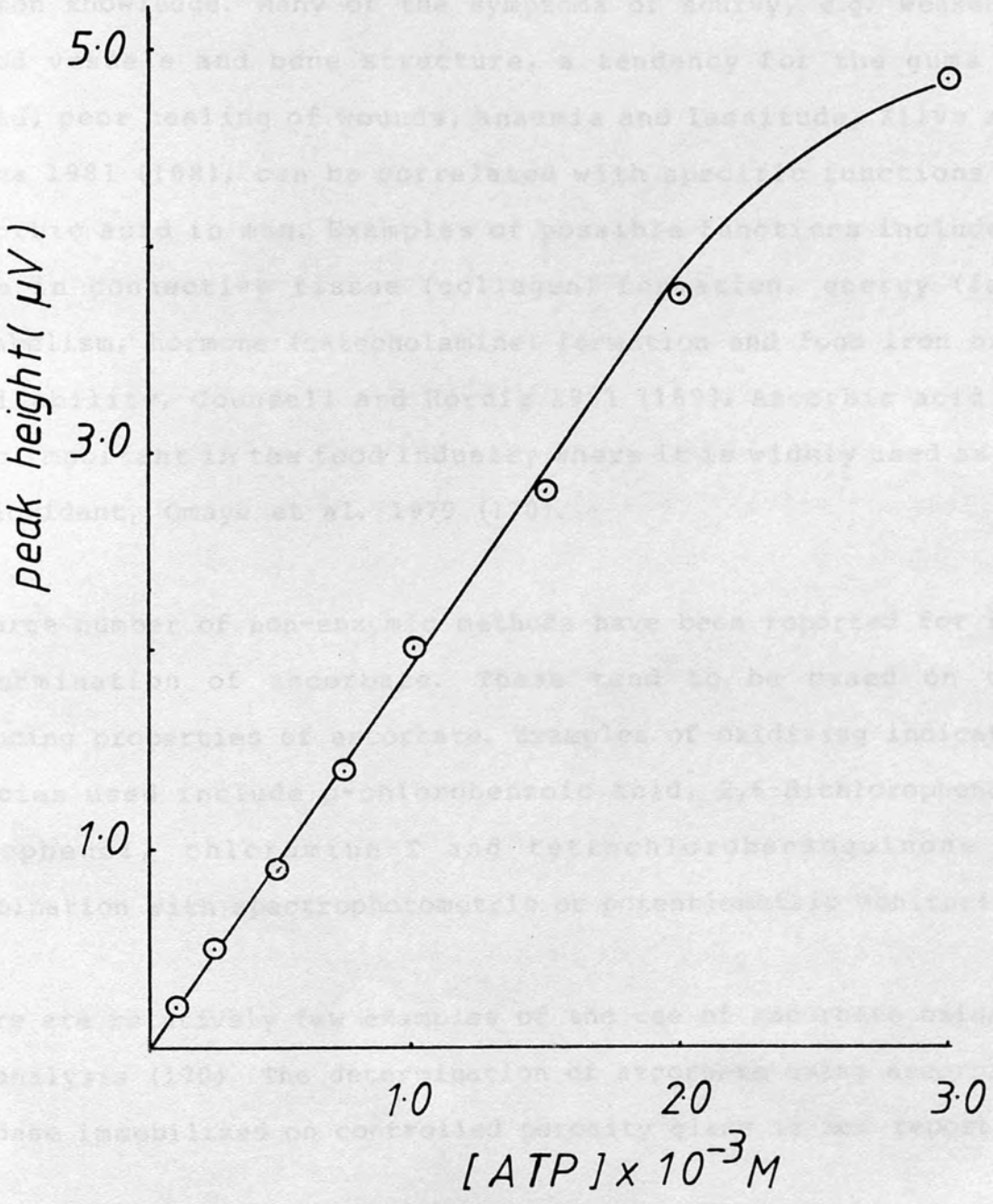

3.5.2 Determination of Ascorbate (Vitamin C) using Ascorbate Oxidase and Catalase co-immobilized on controlled Porosity Glass

Introduction

The connection between ascorbate deficiency and scurvy in man is common knowledge. Many of the symptoms of scurvy, e.g. weakened blood vessels and bone structure, a tendency for the gums to bleed, poor healing of wounds, anaemia and lassitude, Zilva and Panna 1981 (168), can be correlated with specific functions of ascorbic acid in man. Examples of possible functions include a role in connective tissue (collagen) formation, energy (fat) metabolism, hormone (catecholamine) formation and food iron bio-availability, Counsell and Hornig 1981 (169). Ascorbic acid is also important in the food industry where it is widely used as an antioxidant, Omaye et al. 1979 (170).

A large number of non-enzymic methods have been reported for the determination of ascorbate. These tend to be based on the reducing properties of ascorbate. Examples of oxidizing indicator species used include p-chlorobenzoic acid, 2,6-dichlorophenol-indophenol, chloramine-T and tetrachlorobenzoquinone in combination with spectrophotometric or potentiometric monitoring.

There are relatively few examples of the use of ascorbate oxidase in analysis (170). The determination of ascorbate using ascorbate oxidase immobilized on controlled porosity glass is now reported.

Materials and Methods

Ascorbate oxidase or L-Ascorbate:O_2 oxidoreductase (EC 1.10.3.3) Type A2769 from curcubita species, (121 units per mg. protein) catalase (H_2O_2:H_2O_2 oxidoreductase; EC 1.11.1.6), Type C - 10 from bovine liver, and L-Ascorbic acid were commercial, Sigma UK. Analytical grade disodium monohydrogen phosphate, sodium dihydrogen phospate and ethelenediamine tetracetic acid (EDTA) were supplied by BDH, Poole, England.

The method of immobilization and use of ascorbate oxidase for analysis was similar to that described for urease and glucose oxidase (s 3.3). Analysis was performed in phosphate buffer (0.2M pH 7.0) in the presence of EDTA (10^{-3}M) to prevent non-enzyme catalysed oxidation of ascorbate by metal ions. In the absence of EDTA reproducible peaks were not obtained. Instead successive injection of a fixed concentration ascorbate gave progressively larger peaks.

Results

The results of the transient analysis of ascorbate (0.5 cm^3 samples) is shown as a plot of instrument response (peak height) against ascorbate concentration over the range of 1×10^{-4}M to 3×10^{-3}M, Figure (3.5.2.1)

Table (3.5.2.1) Transient Analysis of Ascorbate (Vit. C) CPG-AAO/CAT (0.2M Phosphate Buffer, pH 7.0; 10^{-3}M EDTA

[Ascorbate] x 10^{-3}M	Pk. Ht. (μV)
3.00	9.6
2.00	8.3
1.60	7.1
1.20	5.6
0.80	4.2
0.50	3.3
0.40	2.5
0.30	2.2
0.20	1.4
0.10	0.70
0.00	0.0

$r = 0.9955$; $1 \times 10^{-4} \leqslant x \leqslant 5 \times 10^{-4}$M

x is the analytically useful range of ascorbate.

The effects of bubbling oxygen through the reference buffer and samples just prior to injection is shown. In Figure (3.5.2.2) the response curves from transient and steady state analysis are compared.

FIG(3·5·2·1)-Transient analysis of ascorbate (Vit·C)· Plot of peak height against concentration of ascorbate (⊙); effect of oxygen saturation(⊡)·(Table(3·5·2·1))

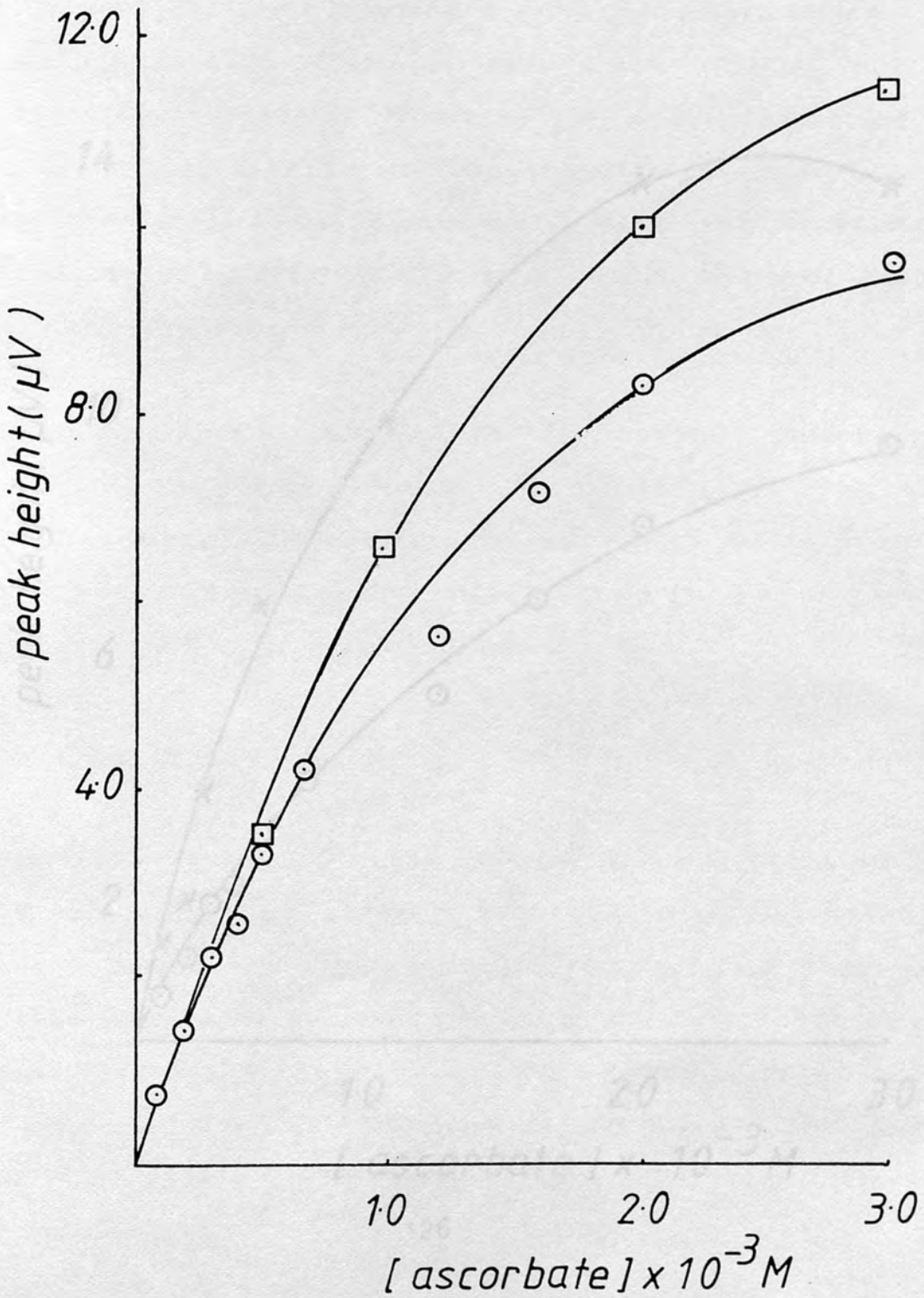

FIG(3·5·2·2)-Analysis of ascorbate· Comparison of transient(⊙) and steady state(*)instrument output(cf. FIG(3·3·5); FIG(3·3·6))

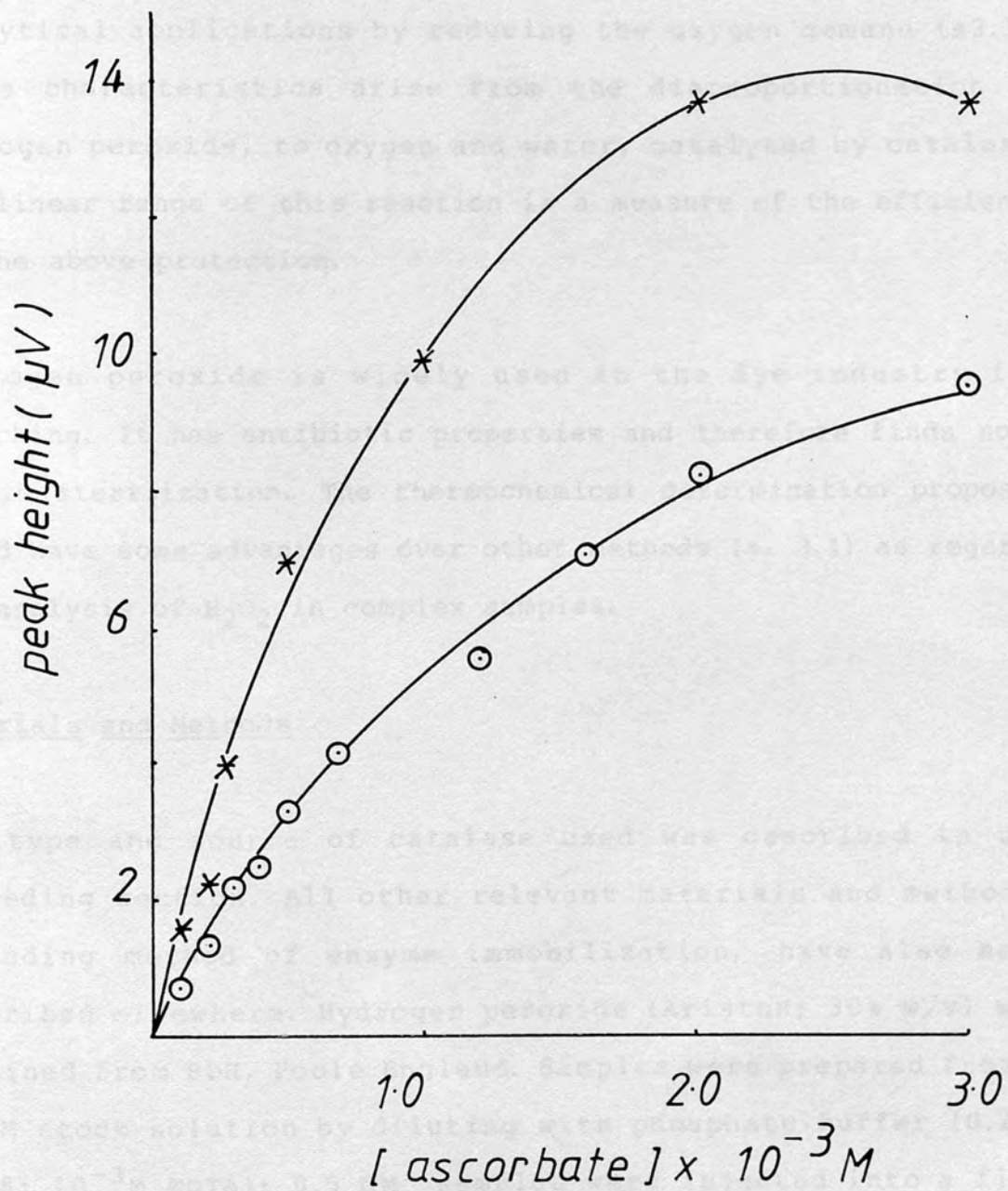

3.5.3 Determination of Hydrogen Peroxide Using Catalase Immobilized on Controlled Porosity Glass

Introduction

Catalase may protect immobilized oxidase systems from inactivation by hydrogen peroxide (s 4.2); co-immobilization with the flavin oxidases in particular improves the linearity range in analytical applications by reducing the oxygen demand (s3.3). These characteristics arise from the disproportionation of hydrogen peroxide, to oxygen and water, catalysed by catalase. The linear range of this reaction is a measure of the efficiency of the above protection.

Hydrogen peroxide is widely used in the dye industry for bleaching. It has antibiotic properties and therefore finds some use in sterilization. The thermochemical determination proposed could have some advantages over other methods (s. 3.4) as regards the analysis of H_2O_2 in complex samples.

Materials and Methods

The type and source of catalase used was described in the preceding section. All other relevant materials and methods, including method of enzyme immobilization, have also been described elsewhere. Hydrogen peroxide (Aristar; 30% w/v) was obtained from BDH, Poole England. Samples were prepared from a 8.35M stock solution by diluting with phosphate buffer (0.2M, pH6.8; 10^{-3}M EDTA); 0.5 CM^3 samples were injected into a flow

stream of the same buffer via an Altex sample loop. EDTA was necessary to prevent metal ion catalysed disproportionation of hydrogen peroxide, (cf ascorbate determination).

Results

In the absence of EDTA, repeated injection of samples of hydrogen peroxide (10^{-3}M) resulted in successively larger peaks. The use of a marginally acid buffer containing 10^{-3}M EDTA resulted in reproducible results being obtained. The results of the transient analysis of hydrogen peroxide ($\leqslant 8.35 \times 10^{-1}$M) are listed in Table (3.5.3.1) and shown in Figure (3.5.3.1).

Table (3.5.3.1) Transient Analysis of Hydrogen Peroxide (H_2O_2) using CPG-CAT (0.2M phosphate buffer, pH 7.0; 10^{-3}M EDTA)

$[H_2O_2]$ M	Pk.Ht. (μV)
8.35×10^{-1}	4075 $\pm$ 35
4.17×10^{-1}	1975 $\pm$ 106
2.10×10^{-1}	925 $\pm$ 106
8.35×10^{-2}	378 $\pm$ 18
4.17×10^{-2}	160 $\pm$ 1
2.10×10^{-2}	81
1.67×10^{-2}	62
8.35×10^{-3}	31
4.17×10^{-3}	17.5
2.10×10^{-3}	10.0
8.35×10^{-4}	4.7
4.17×10^{-4}	2.2
2.10×10^{-4}	1.1

$2.10 \times 10^{-4}M \leqslant H_2O_2 \leqslant 8{,}35 \times 10^{-3}M$, r = 0.9960

$2.10 \times 10^{-3}M \leqslant H_2O_2 \leqslant 8.35 \times 10^{-1}M$, r = 0.9992;

FIG(3·5·3·1)- Transient analysis of hydrogen peroxide (H_2O_2)· Plot of Log [H_2O_2] against Log(Pk.ht)

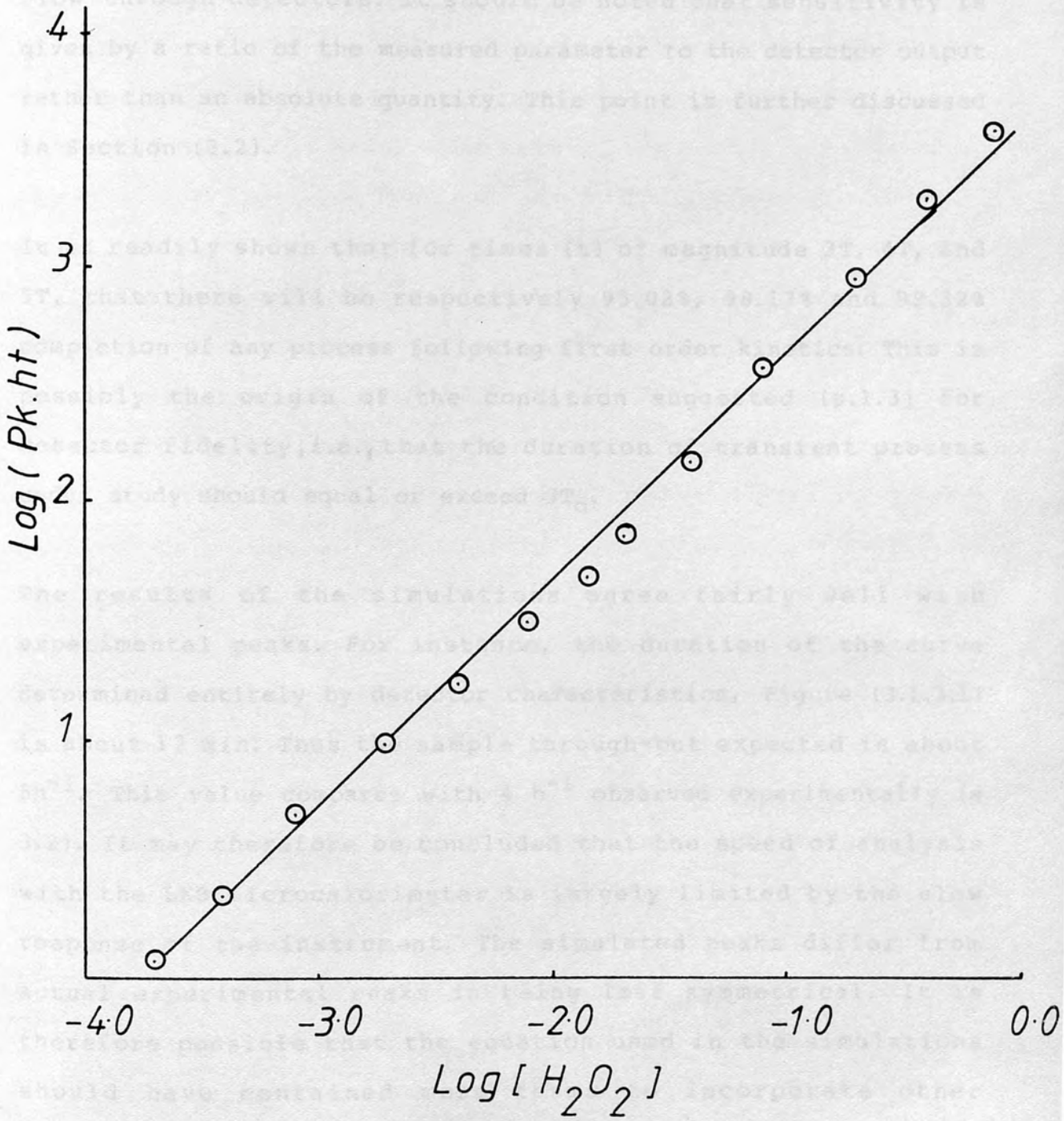

3.6 Discussion

3.6.1 Simulation Studies

The considerations in (s.3.1) are expected to apply to most flow-through detectors. It should be noted that sensitivity is given by a ratio of the measured parameter to the detector output rather than an absolute quantity. This point is further discussed in Section (3.2).

It is readily shown that for times (t) of magnitude 3T, 4T, and 5T, that there will be respectively 95.02%, 98.17% and 99.32% completion of any process following first order kinetics. This is possibly the origin of the condition suggested (s.1.3) for detector fidelity, i.e., that the duration of transient process under study should equal or exceed $3T_d$.

The results of the simulations agree fairly well with experimental peaks. For instance, the duration of the curve determined entirely by detector characteristics, Figure (3.1.3.1) is about 12 min. Thus the sample through-put expected is about $5h^{-1}$. This value compares with 4 h^{-1} observed experimentally (s 3.2). It may therefore be concluded that the speed of analysis with the LKB microcalorimeter is largely limited by the slow response of the instrument. The simulated peaks differ from actual experimental peaks in being less symmetrical. It is therefore possible that the equation used in the simulations should have contained more terms to incorporate other

determinants of the speed of analysis. However, it is hoped that the above work and the disussion in Section 1.3 together give some idea of the the type of analysis possible for most flow-through detectors and flow injection analysis systems.

3.6.2 Enthalpy Determination and Sample Analysis

The higher literature dH_R values listed in Table (3.2.3) are, within experimental error, the same as the enthalpy values for urea hydrolysis in phosphate and tris buffers determined in this work. Small (eg. $\pm$ 2 kJ) differences in the values listed can be attributed to the use of slightly different buffer concentrations and pH values in the various studies. Larger variations, however, are perhaps most readily explained with reference to the fractional conversion of sample (X) and factors affecting this. Reaction enthalpy will be underestimated in cases where insufficiently high enzyme activity and/or low volumetric flow rate are used. It would appear the the condition $k_1"t \nwarrow 5$ is a good guide in these situations; the corresponding transformation of substrate during a single pass through the immobilized enzyme reactor is then better than 99%.

Inspection of Tables (3.2.1) and (3.2.2) shows that there appears to be some discrepancy between the observed and predicted fractional conversion of substrate, particularly at low column enzyme activity. Thus low dH_R' values could not be extrapolated to give proper estimates of dH_R, eg., when X is 0.67552 or 0.3382. The Michaelis constant (Km^{app}) may then be dependent on,

e.g., flow rate, support diameter and support enzyme loading. Thus the value of the apparent Km for immobilized urease in phosphate buffer, Table (3.2.1), ranged from 66.4mM to 29.6mM. Although fractional conversion is expected to be reduced in the presence of diffusion effects, equation (3.2.5) should not fail under such circumstances. The above results might be the results of uneven flow (channelling) through the enzyme reactor. The decrease of X by channelling would be expected to be more important in a low enzyme activity column and at low sample flow rates. On the other hand, a better correspondence between actual and theoretical fractional conversion would possibly result from increased mixing of, and therefore improved contact of, substrate molecules with the immobilized enzyme support at higher flow rates.

The difference in enthalpies of urea hydrolysis in phosphate and tris buffer, of 43 kJ mol^{-1}, corresponds very closely to the 42.74 kJ mol^{-1} difference in the heats of protonation of the two buffers. The difference in heats of reaction could also arise from the different products formed in the two buffers (150). Urea hydrolysis in tris buffer produces ammonium carbonate whilst hydrolysis in phosphate buffer leads to ammonium and bicarbonate ions. It is a general principle of thermometric enzyme methods that sensitivity of analysis may often be improved by an appropriate choice of buffer; in the present example phosphate is to be preferred to tris buffer.

Finally, the optimum conditions for reaction enthalpy determination, i.e. high reactor enzyme activity and low sample

flow rate, may also lead to a more equilibrium-type analysis. The benefits of such analysis,relative to a kinetic-type analysis, include improved sensitivity and reduced susceptibility to temperature or pH fluctuations. An initially high column enzyme activity in addition often results in an increase in useful column life.

The three indices of analysis (s. 3.3) discussed previously are in order of the highest precision; peak area > peak height > peak initial slope. Another important condideration in selecting which index to use is that peak area determination by mechanical means (a planimeter was used in this work) is slow and inherently imprecise.

Some of the important contributions to peak broadening by subsystems in a F.I.A. set up have been discussed (s. 1.3). Because of these the dependance of total system output on flow rate would be expected to be complex. It is in fact difficult to resolve completely detector effects from those due to the other subsystems. For instance, the changes in peak area with flow rate, Figure (3.3.3) are consistent with the effect of flow rate on detector response (s. 3.1) or the effects of flow rate on fractional conversion (s. 3.2). That detector factors are not wholly predominant, however, can be inferred from the dependence of peak height on flow rate; peak height does not decrease with increasing flow rate (c.f. Figure (3.1) and Figure (3.3.2)).

Transient and steady state analysis represent quite different approaches to F.I.A.. Where analysis of discrete samples is

required then transient analysis may be preferred. Compared to steady state analysis it has the advantages of higher sample throughput, greater linearity range, and of requiring a lower sample volume. Continuous analysis might be more appropriate for on-line analysis e.g. of product streams. Analysis could then in principle be carried out without need for sampling.

The increase in linearity range and maximum quantity of heat evolved for transient relative to steady state analysis is undoubtedly related to sample dilution and dispersion occuring in the former case. This view is supported by the results of a preliminary study of the kinetics of glucose conversion by CPG-GLO/CAT. With $0.5cm^3$ pulsed substrate injections Km^{app} was found to be 2.6 times greater than Km^{app} derived from a study where continous injection of substrate was used, Table (3.4.3). Sample dispersion and dilution do not occur with continuous sample injection. As a consequence of dispersion, a $0.5cm^3$ pulsed sample will be expected to have a greater residence time than, (the ratio V_R/F; cf CSTR and PFR) model kinetics, s. 1.3) a $0.5cm^3$ volume element in steady state analysis. Such a difference in sample residence times is required to explain the difference in maximum heat evolved in Figure (3.3.5) and Figure (3.3.6).

On the basis of the above arguments it is proposed that the real residence time for $0.5cm^3$ pulsed samples in these studies is about 2.5 T. That is, the sample spreading/dilution characteristics of the present IMER is about half way between those of the PFR and a CSTR limits. It is possible that the ratio

of maxima, in, e.g., Figure (3.3.5), i.e., 3.6, is larger than can wholly be attributed to sample spreading. There are likely to be differences in the average product concentration in the reactor with pulsed and continuous injection modes. Hence the maxima with the latter approach could be more depressed as a result of greater product and/or substrate inhibition. Both CPG-GLO/CAT and CPG-urea systems have been shown to be susceptible to such forms of inhibition (Chapter 4).

It is a common assertion that steady state analysis results in greater sensitivity of analysis relative to transient analysis. This is correct only where peak height is the index for analysis; as discussed above, the difference in sensitivity is largely a consequence of sample dispersion which only affects the transient output. When the peak integral is used as an analytical index, there would appear to be no differences in the sensitivity of analysis between the two forms of sample injection.

In some cases the term 'sensitivity' has been used to describe the minimal detectable concentration of analyte; the latter is lower for steady state compared to transient analysis. However, because minimal detectable concentration can differ from day to day, (e.g. as a result of poor baseline quality) on the same instrument, it is perhaps not the best measure of sensitivity. The sensitivity of an analytical system has been defined as the ratio of signal change to the amount of analyte (s. 1.3). In a thermochemical system the reaction enthalpy (with the dimensions J mol^{-1}) clearly meets this definition; dH_R (ie. the slope in

Figure (3.3.5), Figure (3.3.6) at low concentrations of analyte) is independent of the mode of sample injection provided the essential condition of complete conversion is met. Reaction enthalpy also encompasses 'sensitivity' in the specific sense of minimal detectable concentration. Given that noise and other factors have determined a particular lower limit of instrument response below which precision is unacceptably poor, the minimal instrument response is readily translated into a value for the minimal detectable concentration using the enthalpy of reaction and the appropriate instrument calibration constant, (c.f. Table (3.3.5)

3.6.3 Determination of Miscellaneous Substrate

Catalase catalysis the disproportionation of hydrogen peroxide, (3.6.3.1).

$$H_2 O_2 \longrightarrow H_2O + 1/2\ O_2 \qquad (3.6.3.1)$$

hence in the presence of this enzyme the net reaction for glucose oxidation (ie. the sum of (3.4.1) and (3.6.3.1) can be written as:

$$\text{Glucose} + 1/2\ O_2 \longrightarrow \text{B - Gluconic Acid} \qquad (3.6.3.2)$$

Given this stoichiometry, and a buffer-dissolved oxygen concentration of 0.25×10^{-3}M, (Chapter 4), the expected upper limit of linearity is at 0.5×10^{-3}M glucose. This is indeed the observed value, (Table (3.4.3); steady state analysis) thus

confirming the limitation of linearity in glucose analysis by oxygen concentration. Owing to sample dilution, these stoichiometric considerations would not be expected to apply with respect to transient analysis (s.3.3).

As regards the relative effectivness of prospective oxygen substitutes, it is likely that kinetic as well as the more expected thermodynamic considerations are important. Some relevant formal redox potentials are 1,4 benzoquinone (280 mV), oxygen (263 mV), DCPIP (227 mV), Toluidine blue, (27 mV) and methylene blue, (11mV). Thus all compounds listed should reoxidize flavine adenin dinucleotide, ($-440 < E^{o'} < -19$ mV) the enzyme redox compound which initially accepts electrons from glucose. Interestingly, methylene blue appeared more effective than DCPIP or toluidine blue in this role, though on thermodynamic grounds alone it is the least suitable compound. A more complete assessment in this respect must take into full view the structural requirements of enzyme substrate interaction.

After normalizing the observed limits of linearity for the concentration of cosubstrate present, the relative values with oxygen; : 1,4- benzoquinone:methylene blue was 1:1.11:0.02. These relative values confirm again the importance of buffer-dissolved oxygen concentration. More importantly, however, they imply that 1,4 benzoquinone is ,perhaps as good as or, a better co-substrate than oxygen. There is thus some impetus for continuing the search for alternative electron acceptors.

The use of CPG-hexokinase in combination with LKB 2107-30 microcalorimeter for thermochemical analysis (s.3.5.1) resulted in a system with some unique characteristics. A comparison with immobilized glucose oxidase-catalase system is warranted.

Some important considerations include a. the requirement for cofactor, b. low susbtrate specificity and c. about a 3 - fold decrease in sensitivity with the hexokinase system; the reported enthalpy of glucose phosphorylation (71.0kJ mol^{-1}) compares with a nominal 261.0kJ mol^{-1} for the GLO/CAT reaction. Unlike the latter system, however, the hexokinase method is not susceptible to interference from reducing compounds. Also the low specificity for glucose can be considered as lending this method a certain flexibility. Most samples, depending on their origin, will only contain a limited range of hexoses.

The source of the background heat, observed with the hexokinase system, is uncertain. Type c-300 hexokinase is 'substantially' free of the ATP hydrolytic enzyme, ATPase. The possibility that hexokinase may itself be able to catalyse the hydrolysis of ATP in the absence of glucose has therefore to be considered.

The similarity between the optimum magnesium ion concentration for CPG-hexokinase and the soluble enzyme in a low ionic strength media is indication that accumulation of Mg^{2+} within the matrix phase is unlikely. This implies that the modified glassy phase is not strongly charged. Unmodified controlled porosity glass is slightly anionic (Chapter 2).

The upper limit of linearity for ascorbate detection is about the same as that for glucose determination (1mM substrate; Table 3.2.5). As discussed for IM-GLO/CAT, linearity is most likely limited by the low buffer dissolved oxygen concentration. This interpretation is further supported by the effect of buffer oxygen saturation on ascorbate oxidation. Figure (3.5.2.1).

The normal range of plasma ascorbate concentration in a fasting individual is beteen 0.28×10^{-4}M and 0.85×10^{-4} M (168). The present technique is not sensitive to ascorbate over this range. There would be some difficulty in quantifying low plasma levels. The concentration of ascorbate in non-clinical samples will vary depending on the material; concentrations in excess of 1×10^{-3}M can be accommodated after sample dilution. The sensitivity of the immobilized ascorbate/catalase system is about one half the sensitivity observed with the IMM-GLO/CAT system. The enthalpy of ascorbate oxidation was estimated as 112.0 kJ mol^{-1} (s. 4.4). It should be noted that whilst oxygen is reduced to hydrogen peroxide in the reaction catalysed by glucose oxidase, with ascorbate oxidation oxygen is reduced to water (s. 3.4; s. 4.4).

Under the usual conditions of transient analysis, the concentration of hydrogen peroxide encountered by oxidases would not exceed 1mM. The upper limit of linearity for hydrogen peroxide detection, using CPG-catalase, far exceeds this. Catalase could therefore provide quite effective protection from hydrogen peroxide when co-immobilized with oxidases. The effectiveness of such protection is however unlikely to be as

high as suggested by the linearity range observed with the CPG-catalase system. Hydrogen peroxide generated in situ initially appears at the enzyme active site of oxidases and would then probably become subject to the action of catalase only after diffusing out.

The Km value of soluble catalase for hydrogen peroxide is about 1M. The wide linearity range observed with CPG-catalase is therefore not unexpected. As discussed before (s 1.4) the upper limit of linearity in analysis with an immobilized enzyme may approach or exceed Km of the corresponding soluble enzyme.

CHAPTER 4

Application of flow microcalorimetry to the study of the kinetics of reactions catalysed by immobilized enzymes

The main considerations in the study of reactions catalysed by enzymes in free solution and immobilized on insoluble supports have been outlined (s 1.2; s 1.4). As discussed above, non-initial rate conditions become important when substrate conversion exceeds 5%. The correspondingly large build-up of product can then lead to enzyme inhibition or reaction reversal, Fig (4.1.1). Unlike non-initial rate effects, microenvironmental effects are usually confined to immobilized enzymes systems. Of these effects mass transfer limitations are perhaps the most important. As well as being of academic interest mass transfer effects present a potent obstacle to the practical study and effective use of immobilized enzymes. In the presence of such effects, e.g. data relating to the stability, Ollis 1972 (171) inhibition, Engasser and Horvarth 1974 (102) and pH-activity profile, Engasser and Horvarth 1974 (172) cannot be interpreted unambiguously. Implicit in the concept of effectiveness factor, the efficiency of immobilized enzyme systems is reduced by diffusion limitations.

In spite of the many advantages of flow microcalorimetric monitoring (Chapter 1) there do not appear to be any reports of its application to the study of immobilized enzyme kinetics. In addition, the non-requirement for artificial (e.g. colorigenic) substrates in calorimetry allows a decrease in the level of perturbation, of the system under study, in comparison with other

FIG(4·1·1)- Some considerations in the study of immobilized enzyme kinetics

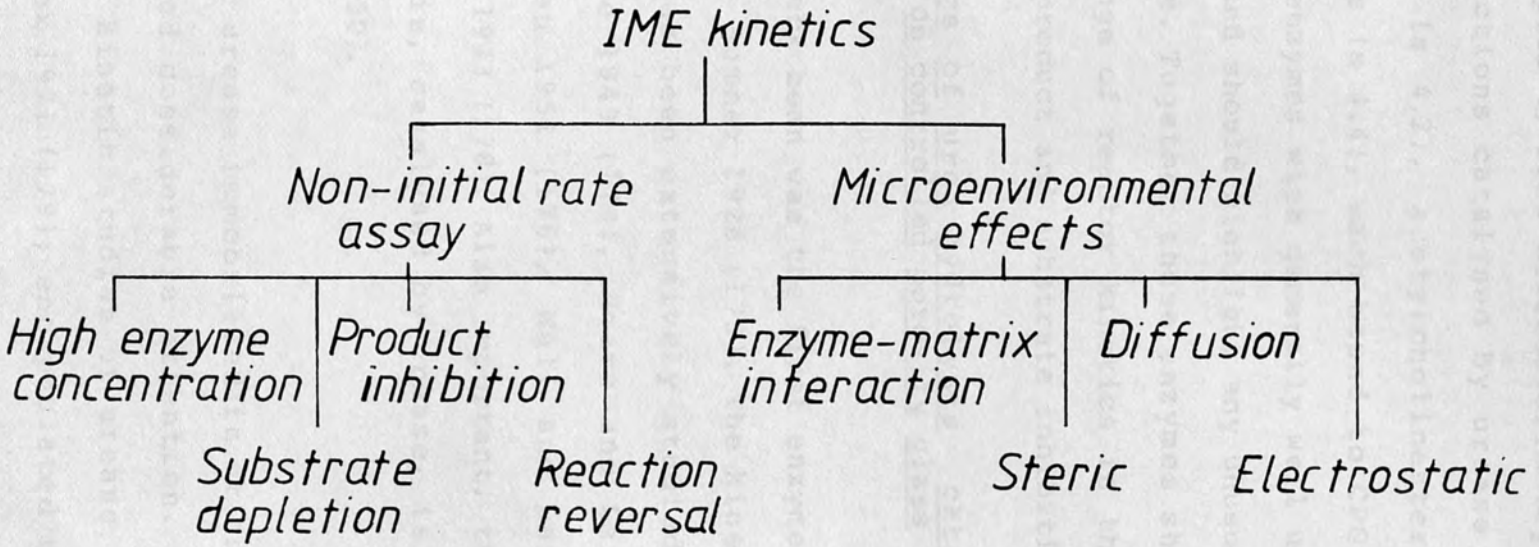

approaches. In chapter 4, flow-microcalorimetry is applied to the study of the reactions catalysed by urease (s 4.1), glucose oxidase/catalase (s 4.2), acetylcholinesterase (s 4.3), and ascorbate oxidase (s 4.4), each bound to CPG glass. The above choice comprises enzymes with generally well understood kinetics in free solution and should highlight any unusual kinetics in the immobilized state. Together these enzymes should also offer a representative range of reactor kinetics in the presence of the various forms of product and substrate inhibition.

4.1 The kinetics of urea hydrolysis catalysed by urease immobilized on controlled porosity glass

Introduction

Urease from the Jack bean was the first enzyme to be isolated in crystalline form, Sumner 1926 (173). The kinetics of the native soluble enzyme has been extensively studied, for example by Laidler and Hoare 1949 (174), Hoare and Laidler 1950 (175), Fasman and Nieman 1951 (176), Wall and Laidler 1953 (177), or Gazzola et al. 1973 (178). Also important, the thermochemistry of urea hydrolysis, catalysed by urease, is well understood, Jesperson 1975 (150).

The properties of urease immobilized in or on various supports have also received considerable attention. Examples of work reported include kinetic studies of urease adsorbed on clay, Sundaram and Crook 1971 (179); encapsulated in nylon beads and liposomes, Sundaram 1973 (180), Madiera 1977 (181), covalently bound to non-porous glass, Ramachandran and Pelmutter 1976 (182), or entrapped in polyacrylamide gel, Atkinson and Rousseau 1977

(183). More recently the characteristics of urease bound to molecular sieves and nylon have been reported by Iyengar et al. 1982 (184) and Onyezili et al. 1982 (185). Urease is currently widely used in the analysis of urea in the medical field (s 3.1); immobilized urease in particular may find future application, in blood detoxification organ supports, in cases of kidney failure.

Materials and Methods

Reagents

Urease (EC 3.5.1.5; Type VI from Jack bean), urea, APTES and glutaraldehyde (20% w/w) were supplied by Sigma (UK). controlled porosity glass (CPG; 200/400 mesh, nominal pore diameter 126Å 187.1 m^2g^{-1}, 55μ mean particle diameter and the similar support CPG; 140m^2g^{-1}, 7.5μ mean particle diameter) as well all other reagents used were purchased from BDH Ltd, Poole, England. All flow injection accessories were suplied by LKB Produkter, Bromma, Sweden.

Enzyme Immobilization

The functionalization of controlled porosity glass with APTES and activation of the resulting aminosilyl glass with glutaraldehyde followed the method described by Robinson et al 1971. (135) and is again described in detail in Chapter 2. The two different diameter supports used were prepared simultaneously using the same reagent mixtures in an attempt to reproduce similiar immobilization surfaces. Blocking of unreacted aldehyde groups was performed during the time required for instrument thermal

equilibration to reduce the time between the preparation and kinetic study of the immobilized enzyme. Urease immobilized on the 7.5μ and 55μ diameter porous glass beads are henceforth termed $CPG_{7.5}$ urease and CPG_{55} urease respectively. Between 153 mg. and 171mg. moist CPG-urease were studied.

Enzyme assay

The rates of urea hydrolysis catalysed by CPG-urease were measured thermochemically using the LKB 2017-30 flow-microcalorimeter. The detailed set-up was identical to that used for the analysis of urea (s 3.3) Steady state rate measurements were made using phosphate buffer (0.2M, pH 7.0; 10^{-3}M EDTA) as carrier or reference medium. A peristaltic pump (LKB 10,700) was used to pass substrate (5mM - 200mM urea) over the bed of CPG-urease at a flow rate of 10-13 $cm^3\ h^{-1}$. Typically, about 6 - 8 cm^3 of sample were required per single measurement of the steady-state heat effect. These power measurements (dQ/dt, J s^{-1} or watt) were transformed into more conventional rate measurements via the expression $v(\text{mol dm}^{-3}\ \text{min}^{-1}) = 60\ (\text{s min}^{-1}) \times dQ/dt/(dH \times V_p)$, where dH and V_p are the mole reaction enthalpy (J mol^{-1}) and volume of enzyme support (dm^3) respectively. The reaction enthalpy for urea hydrolysis in phospate buffer was determined previously (s 3.2) as 60 $\pm$ 3.0 kJ mol^{-1}.

Determination of apparent kinetics constants

The same kinetic plots as those frequently used in the analysis of data from soluble enzyme systems were used in addition to the integrated Michaelis-Menten plot incorporating the effects of non-competitive product inhibition (s 1.2). As described above, a plot of $P/t\,(1 + P/2\,K_p)$ against $1/t\,(1 + S/K_p)\ln(S/(S - P))$ will give a linear response provided the correct value for the inhibition constant K_p is available. When the actual value of K_p is unknown, [this may be the case for most situations dealing with immobilized enzymes owing to diffusion effects (s 1.4)] estimates are inserted and repeated plots made until the correct value is found. Two criteria were applied in the search for the apparent inhibition constant, K_p''. These are:

a. optimal linearity of the resulting plot and

b. $K_p'' < Km$, Eftink et al. 1981 (14); 'plots' were in practice carried out with a linear regression program on a programmable calculator (CASIO, FX 702-P).

The determination of a unique value of K_p" is facilitated if the results of such analysis are presented in the form of a graph of the negative logarithm of the assumed inhibition constant against the correlation coefficient, r, from each plot (Fig. 4.1.2). The CPG-urease system was also examined for the possible effects of substrate inhibition (s 4.3)

Assessment of diffusion effects

Attempts at quantitative determination of the degree of external and/or internal diffusion control in the CPG-urease systems were

FIG(4·1·2)-Dependence of the IMM PLOT linearity(r), for $CPG_{7.5}$ urease(□) and CPG_{55} urease(⊙), on the inhibition constant estimate(K_p) cf. Table(4·1·5)

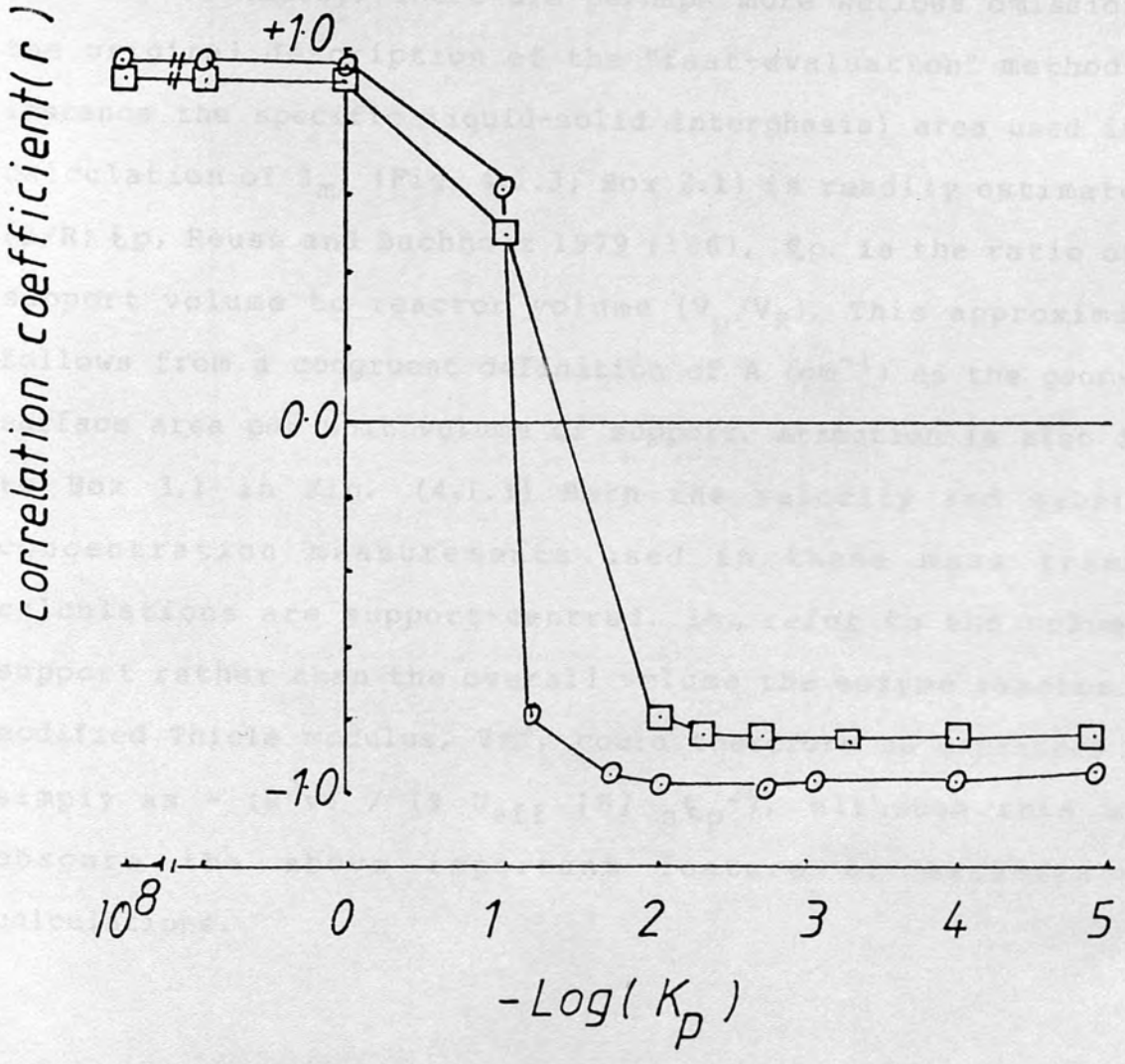

made using the following three approaches:

a. the "fast evaluation" method, Engasser 1978 (104)

b. the direct calculation of the appropriate substrate moduli

c. the comparative method, Engasser and Horvarth 1973 (92).

Summaries of approaches a. and c. are presented in a flow-chart form, Fig. (4.1.3) and Fig (4.1.4). The expression for the first order internal effectiveness factor in Box 4 of Fig. (4.1.4) has been altered from $1/\emptyset[1/\tanh(3/\emptyset)-(3/\emptyset)]$ appearing in the original source. $E_{i,1}$ values calculated using this latter expression show little sensitivity to the value of $\emptyset$, $(0.1<\emptyset<10)$, contrary to theory. There are perhaps more serious omissions in the original description of the "fast-evaluation" method. For instance the specific liquid-solid interphasial area used in the calculation of Z_m, (Fig. 4.1.3; Box 2.1) is readily estimated as $(3/R)\,\xi p$, Reuss and Buchholz 1979 (186), ξp. is the ratio of the support volume to reactor volume (V_p/V_R). This approximation follows from a congruent definition of A (cm^{-1}) as the geometric surface area per unit volume of support. Attention is also drawn to Box 3.1 in Fig. (4.1.3) Both the velocity and substrate concentration measurements used in these mass transfer calculations are support-centred, i.e., refer to the volume of support rather than the overall volume the enzyme reactor. The modified Thiele modulus, $\emptyset m^2$, could therefore be expressed more simply as $-(R^2 v) / (9\, D_{eff}\, [S]_s\, \xi_p^2)$, although this would obscure the above important feature of mass-transfer calculations.

FIG(4·1·3)- Flowchart of the" fast evaluation" method for assessing external and internal diffusion control

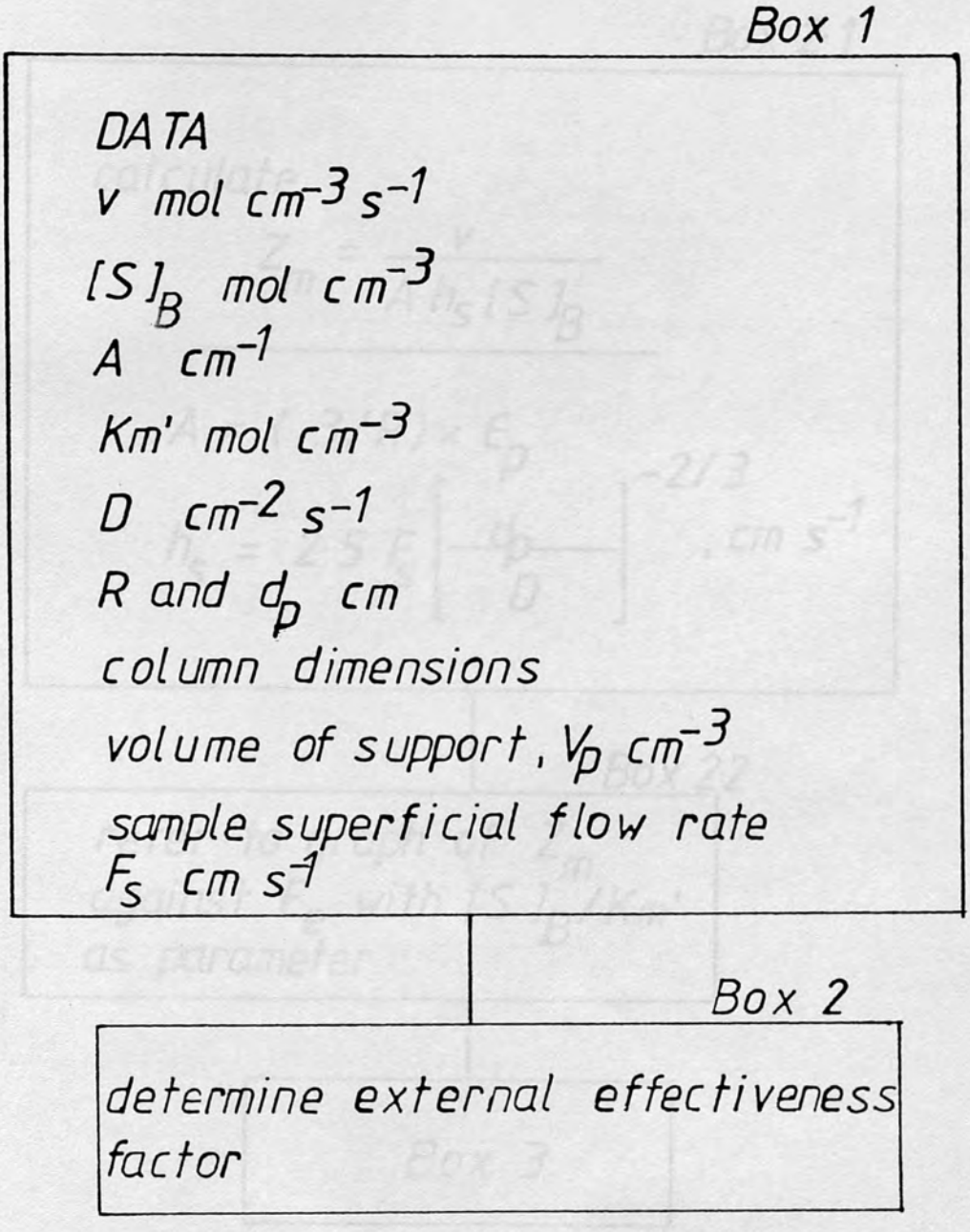

(continued)

FIG(4·1·3)continued

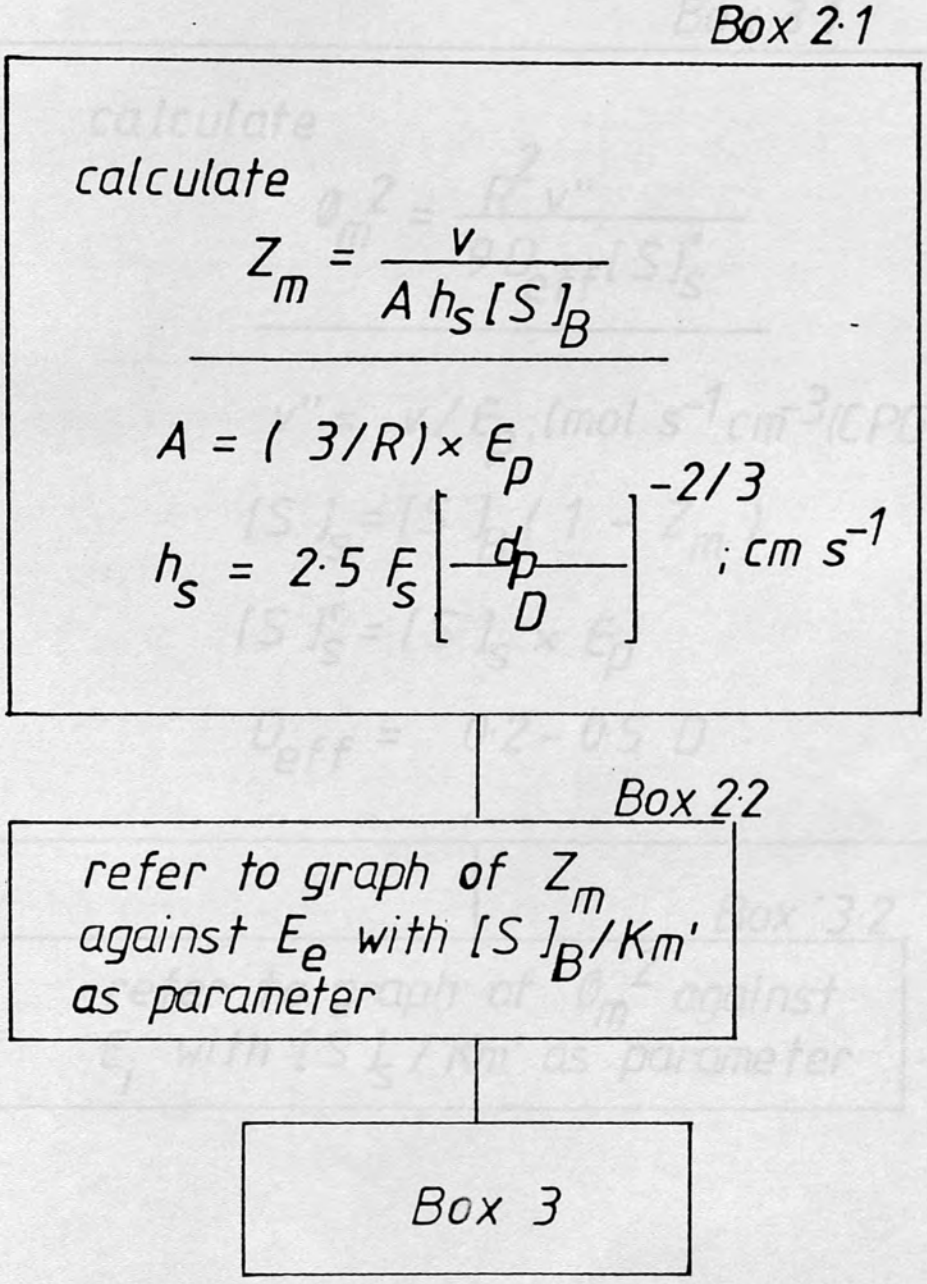

(continued)

FIG(4·1·3)continued

Box 3

Box 3·1

calculate

$$\emptyset_m^2 = \frac{R^2 v''}{9 D_{eff} [S]_s^*}$$

$$v'' = v / \epsilon_p \; ; (\text{mol } s^{-1} cm^{-3} (CPG))$$

$$[S]_s = [S]_B (1 - Z_m)$$

$$[S]_s^* = [S]_s \times \epsilon_p$$

$$D_{eff} = 0{\cdot}2 - 0{\cdot}5 \; D$$

Box 3·2

refer to graph of $\emptyset_m^2$ against E_i with $[S]_s / Km'$ as parameter

FIG(4·1·4)- Flowchart of the comparative method for assessing internal diffusion control

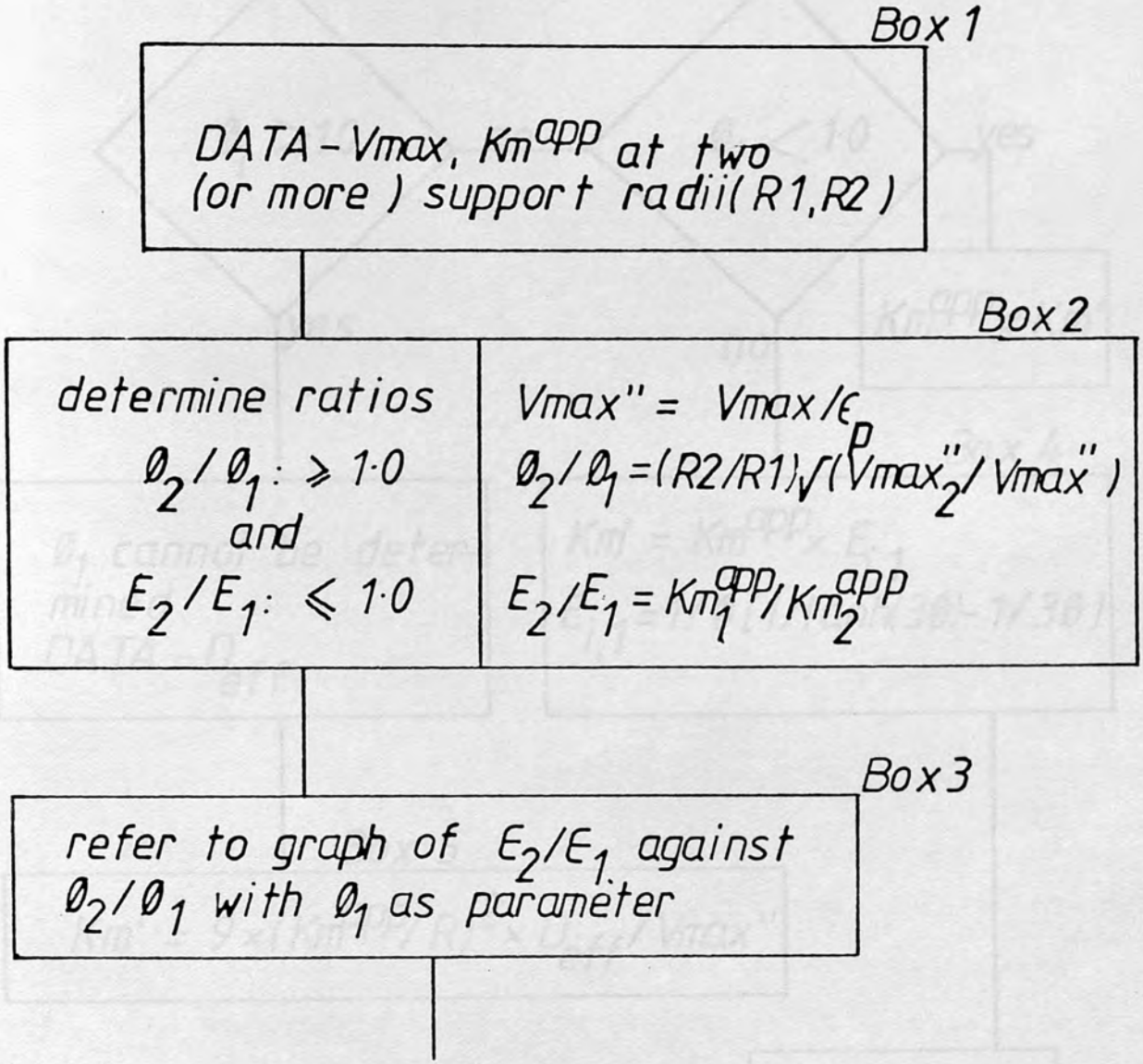

(continued)

FIG(4·1·4)continued

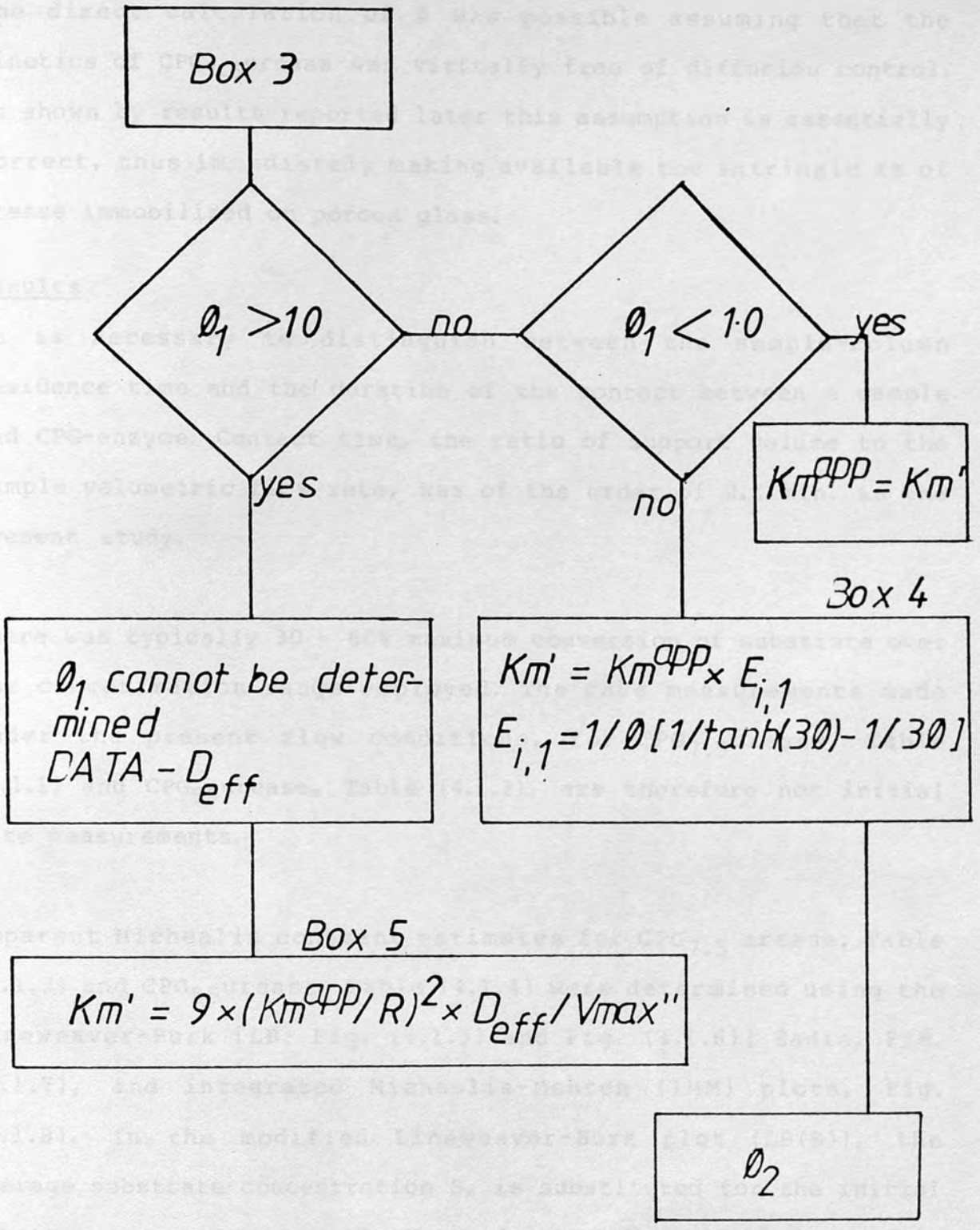

The direct calculation of $\emptyset$ was possible assuming that the kinetics of $CPG_{7.5}$urease was virtually free of diffusion control. As shown by results reported later this assumption is essentially correct, thus immediately making available the intrinsic Km of urease immobilized on porous glass.

Results

It is necessary to distinguish between the sample-column residence time and the duration of the contact between a sample and CPG-enzyme. Contact time, the ratio of support volume to the sample volumetric flow rate, was of the order of 0.1 min. in the present study.

There was typically 30 - 60% maximum conversion of substrate over the concentration range employed. The rate measurements made under the present flow conditions, for $CPG_{7.5}$urease, Table (4.1.1) and CPG_{55}urease, Table (4.1.2), are therefore not initial rate measurements.

Apparent Michealis constant estimates for $CPG_{7.5}$ urease, Table (4.1.3) and CPG_{55}urease, Table (4.1.4) were determined using the Lineweaver-Burk [LB; Fig. (4.1.5) and Fig. (4.1.6)] Eadie, Fig. (4.1.7), and integrated Michaelis-Menten (IMM) plots, Fig. (4.1.8). In the modified Lineweaver-Burk plot (LB(S)), the average substrate concentration S, is substituted for the initial substrate concentration, S. These data handling methods present various degrees of correction for the effects of non-initial rate assay, Lee and Wilson 1971 (187), Atkins and Nimmo 1978 (188) and

Table (4.1.1)

[a] S (M)	[b] SS-disp (μV)	v(M min^{-1} mg^{-1})	S (M)	v/ S_B (min^{-1})	[c] Q(mg^{-1})
20×10^{-2}	317.5	49.11×10^{-3}	15.13×10^{-2}	0.2455	0.3365
15×10^{-2}	272.5	42.15×10^{-3}	10.82×10^{-2}	0.2810	0.4110
10×10^{-2}	225.0	34.80×10^{-3}	6.55×10^{-2}	0.3480	0.5910
50×10^{-3}	145.5	22.51×10^{-3}	27.70×10^{-3}	0.4502	1.1245
20×10^{-3}	57.5	8.63×10^{-3}	11.45×10^{-3}	0.4321	0.9742
10×10^{-3}	29.5	4.56×10^{-3}	5.48×10^{-3}	0.4563	1.1845
5×10^{-3}	14.8	2.28×10^{-3}	2.74×10^{-3}	0.4564	1.1863

a Urea concentration

b Steady state instrument response

c $Q = - (1/t) \ln (S/ (S - P) * (1 + P/Kp)$ - (min^{-1} mg^{-1}); $Kp = 10^8$

Table (4.1.2)[a]

[a]S (M)	[b]SS-disp (V)	V(M min^{-1} mg^{-1})	S (M)	v/ S_B (min^{-1})	[c]Q(Mg^{-1})
20×10^{-2}	111.0	22.94×10^{-3}	18.70×10^{-2}	0.1147	0.1231
15×10^{-2}	102.8	21.25×10^{-3}	13.80×10^{-2}	0.1415	0.1542
10×10^{-2}	92.2	19.61×10^{-3}	8.90×10^{-2}	0.1910	0.2153
50×10^{-3}	60.5	12.50×10^{-3}	42.80×10^{-3}	0.2500	0.2950
20×10^{-3}	32.8	6.80×10^{-3}	16.10×10^{-3}	0.3385	0.4292
10×10^{-3}	15.5	3.21×10^{-3}	8.15×10^{-3}	0.3214	0.4060
5×10^{-3}	7.8	1.61×10^{-3}	4.10×10^{-3}	0.3214	0.4016

a see notes in Table (4.1.1)

Table (4.1.3) Apparent Kinetic Constants for $CPG_{7.5}$urease

PLOT	Vmax (M $min^{-1}mg^{-1}$)	Km*	r	Km^*/Km^{app}
LB	143.71×10^{-3}	308.90×10^{-3}	0.9998	40.81
EADIE	98.90×10^{-3}	198.00×10^{-3}	-0.9365	26.16
LB(S)	99.37×10^{-3}	116.03×10^{-3}	0.9996	15.33
[b]IMM	62.97×10^{-3}	47.66×10^{-3}	-0.9373	6.30
[c]IMM	24.83×10^{-3}	7.56×10^{-3}	-0.8402	1
[d]IMM	89.60×10^{-3}	70.98×10^{-3}	-0.9495	-

a. General estimate of Km^{app}

b. $Kp^{app} = 10^8$

c. Non-competitive inhibition Kp" = 7.08×10^{-3}M

d. Substrate inhibition Ks" = 3×10^{-1}M

Fractional conversion (X) = 60% with 5mM urea.

Table (4.1.4) Apparent Kinetic Constants for CPG_{55}urease

PLOT	Vmax (M $min^{-1}mg^{-1}$)	$^{a}Km^{*}$	r	Km^{*}/Km^{app}
LB	50.54×10^{-3}	150.8×10^{-3}	0.9988	2.8
EADIE	34.63×10^{-3}	92.42×10^{-3}	-0.9649	1.72
LB(S)	46.10×10^{-3}	111.50×10^{-3}	0.9984	2.07
^{b}IMM	31.91×10^{-3}	67.34×10^{-3}	0.9662	1.25
^{c}IMM	26.27×10^{-3}	53.82×10^{-3}	0.9224	1
^{d}IMM	48.53×10^{-3}	109.10×10^{-3}	0.9787	-

a, b. See Table (4.1.3)

c. Non competitive inhibition, Kp" = 35.7×10^{-3}M

d. Substrate inhibition, Ks = 3×10^{-1}M

Functional converstion (X) = 32% with 5mM urea

Table 4.1.5

Kp^{app} (M)	r	SLOPE	INT (M min^{-1})	$^{*}Km^{app}$ (M)	Vmax (M min^{-1})
1×10^{-4}	-0.9690	-0.0303	-0.1335	1.00×10^{-4}	4.42×10^{-3}
1×10^{-3}	-0.9695	-0.0315	-0.1472	1.03×10^{-3}	4.82×10^{-3}
5×10^{-3}	-0.9707	-0.0371	0.0441	2.13×10^{-3}	5.30×10^{-3}
1×10^{-2}	-0.9702	-0.0450	0.0345	12.86×10^{-3}	9.88×10^{-3}
3.57×10^{-2}	-0.9224	-0.0491	-0.0520	53.82×10^{-3}	26.27×10^{-3}
5×10^{-2}	-0.8046	-0.0521	-0.0684	74.48×10^{-3}	33.51×10^{-3}
1×10^{-1}	0.6411	0.1600	0.0841	61.55×10^{-3}	32.36×10^{-3}
1×10^{0}	0.9611	0.0744	0.0353	62.24×10^{-3}	32.86×10^{-3}
1×10^{1}	0.9658	0.0680	0.0321	67.55×10^{-3}	32.03×10^{-3}
1×10^{8}	0.9662	0.0673	0.0319	67.35×10^{-3}	31.94×10^{-3}

FIG(4·1·5)- LINEWEAVER-BURK PLOT for CPG$_{7.5}$ urease(○-LB(S); ⊡-LB)

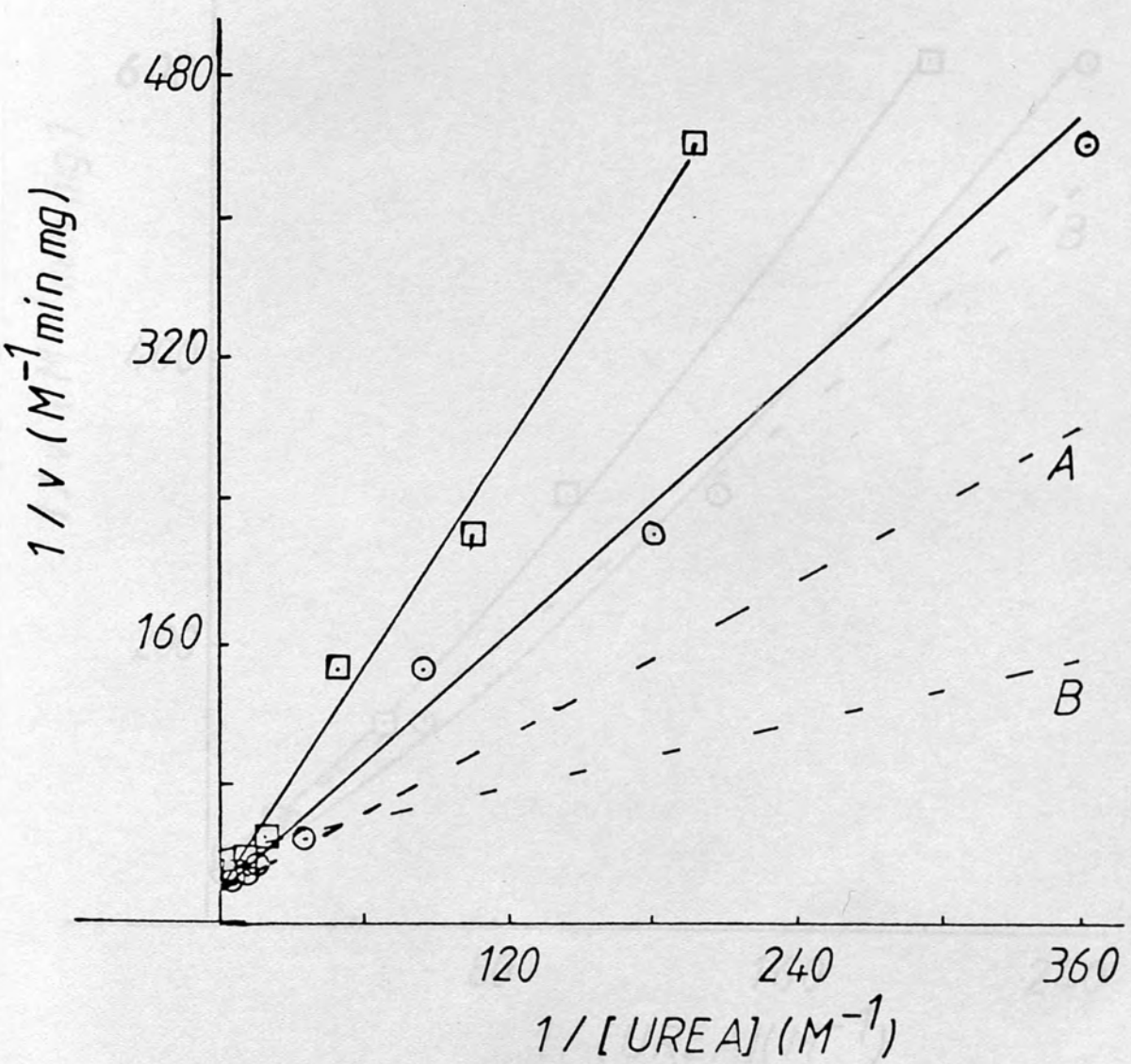

FIG(4·1·6)-LINEWEAVER-BURK PLOT for CPG_{55} urease(⊙-LB(S); ⊡-LB)

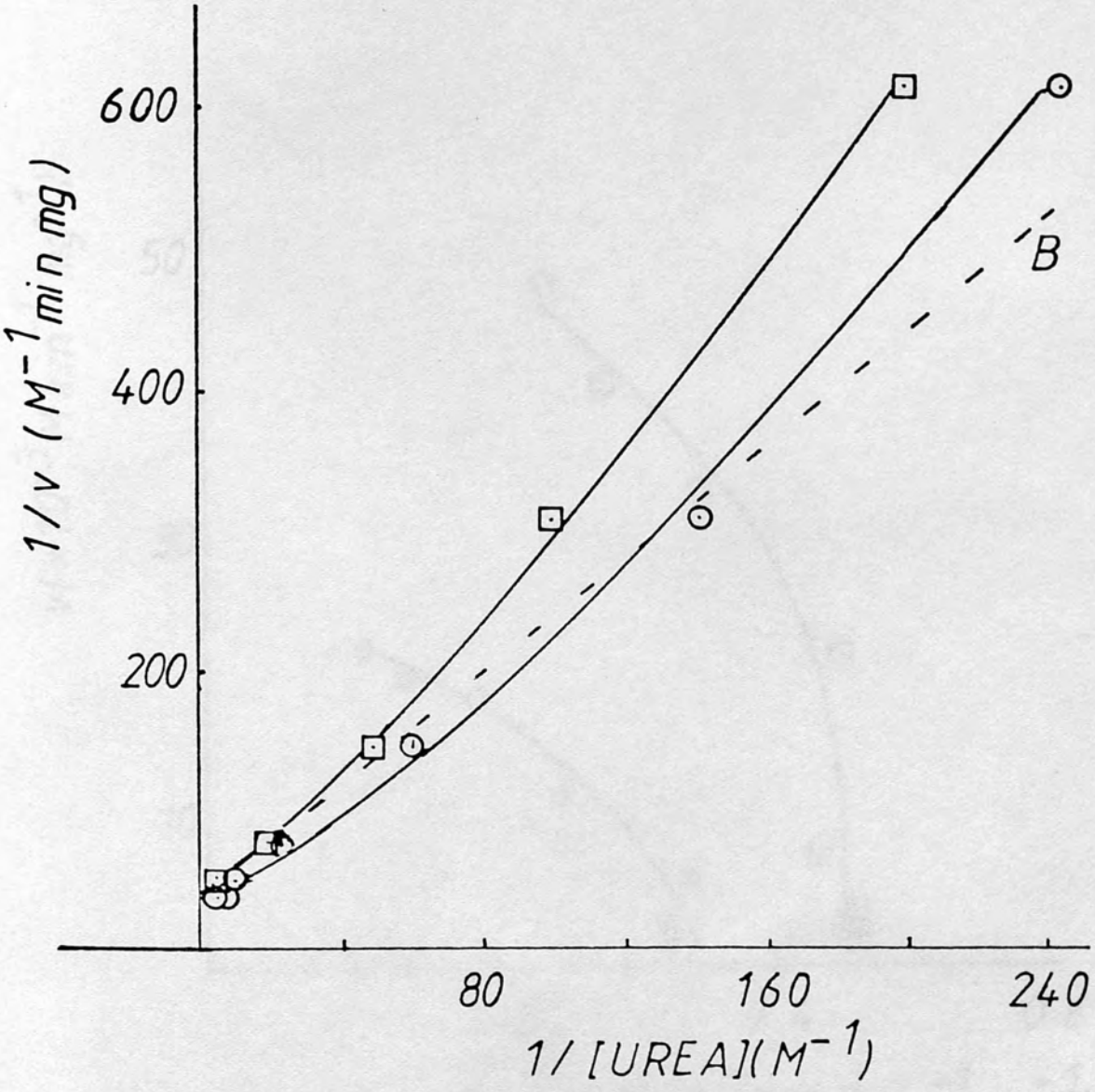

FIG(4·1·7)- EADIE PLOT for $CPG_{7.5}$ urease (□) and CPG_{55} urease (○)

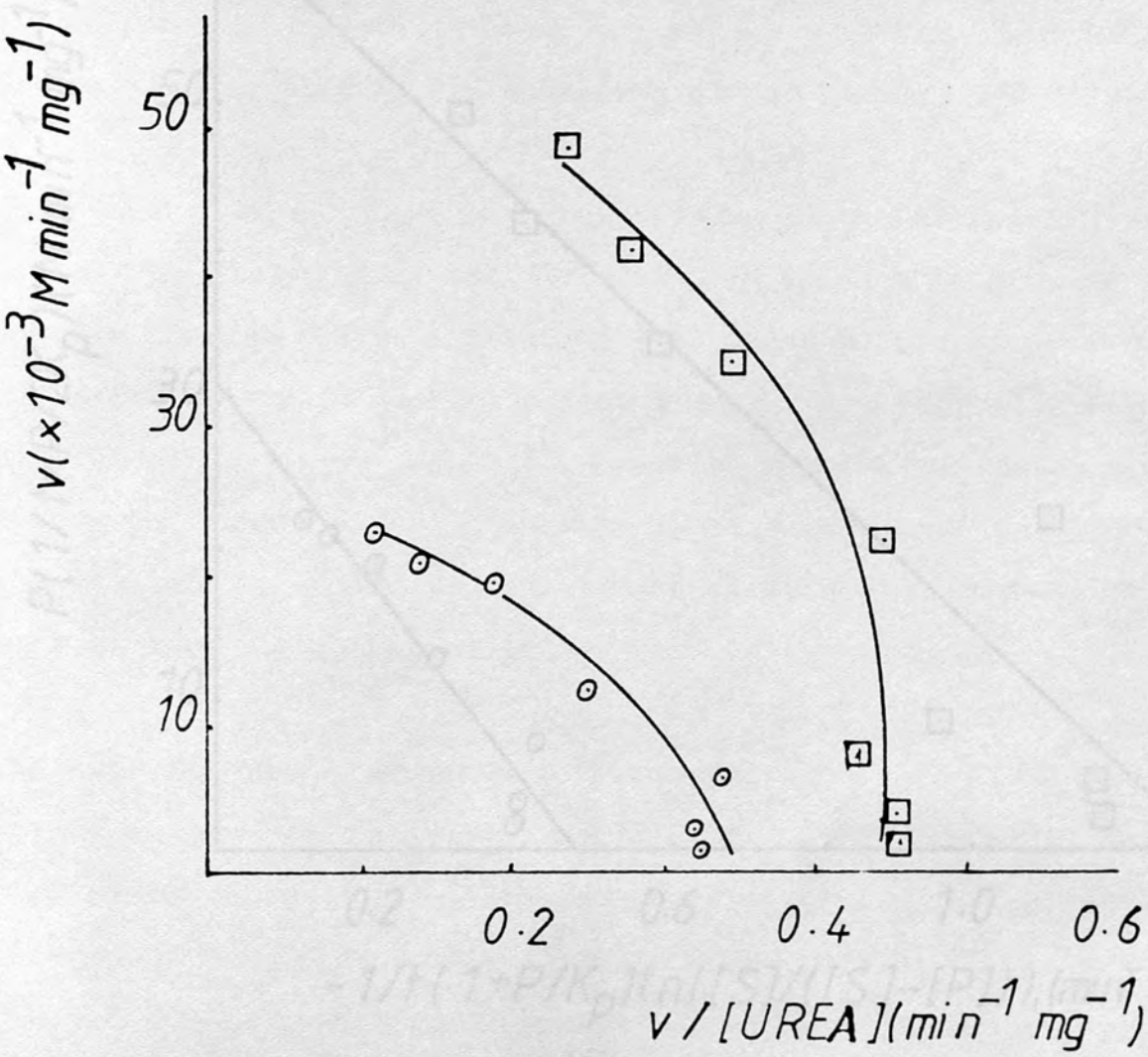

FIG(4·1·8)- INTEGRATED MICHAELIS-MENTEN PLOT for $CPG_{7.5}$ urease(⊡) and CPG_{55} urease(⊙)

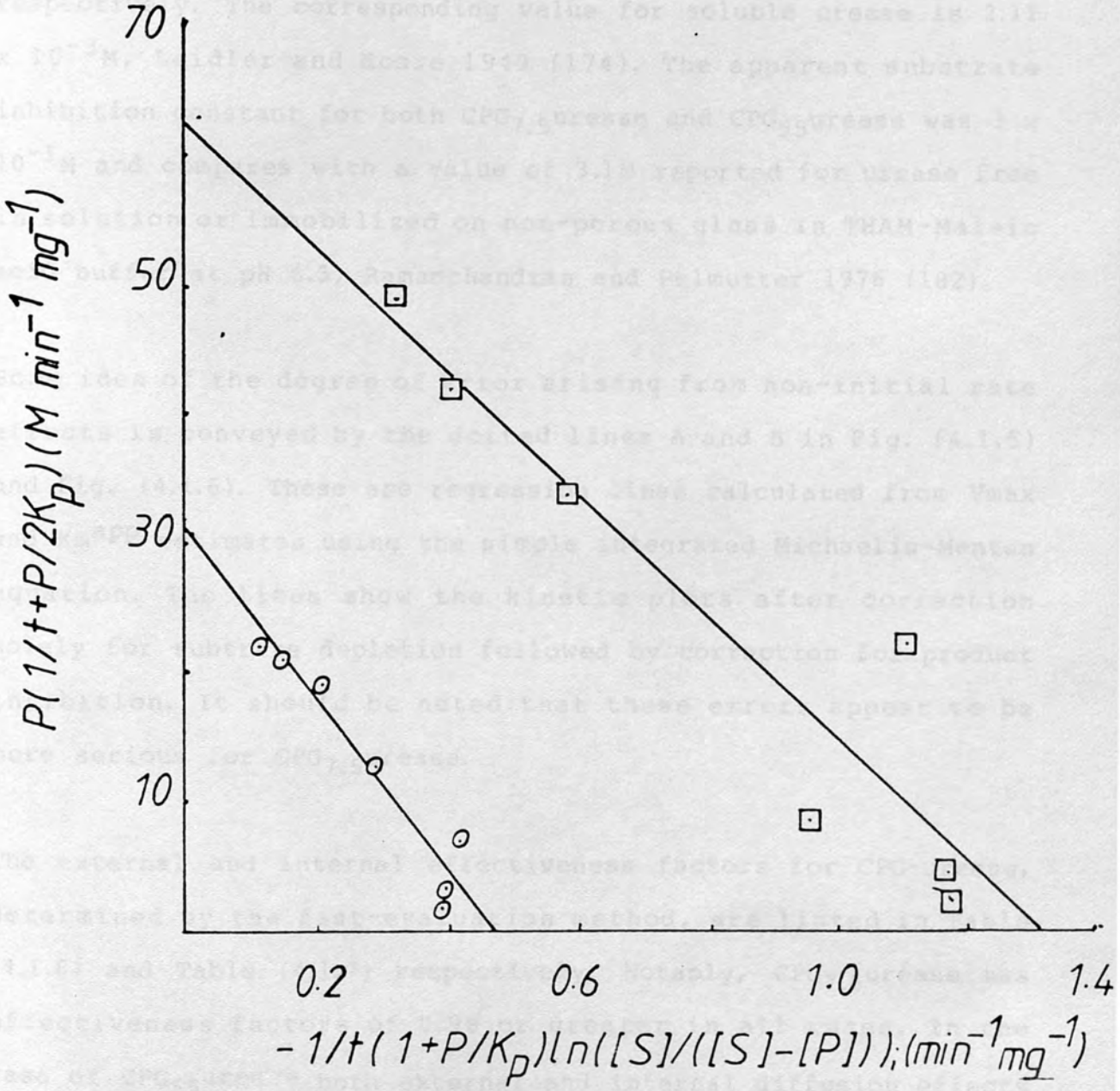

Karanth and Srivastava 1980 (189). No attempt was made to assess the extent of, or correct for the effects of, reaction reversal. Urease may be susceptible to non-competitive inhibition by the ammonium ion, a product of urea hydrolosis in buffered media. The use of the appropriate integrated Michaelis-Menten equation, as described above, resulted in inhibtion constant values of 7.10 x 10^{-3}M and 35.7 x 10^{-3}M for $CPG_{7.5}$urease and CPG_{55}urease respectively. The corresponding value for soluble urease is 2.11 x 10^{-3}M, Laidler and Hoare 1949 (174). The apparent substrate inhibition constant for both $CPG_{7.5}$urease and CPG_{55}urease was 3 x 10^{-1}M and compares with a value of 3.1M reported for urease free in solution or immobilized on non-porous glass in THAM-Maleic acid buffer at pH 6.5, Ramanchandran and Pelmutter 1976 (182).

Some idea of the degree of error arising from non-initial rate effects is conveyed by the dotted lines A and B in Fig. (4.1.5) and Fig. (4.1.6). These are regression lines calculated from Vmax and Km^{app} estimates using the simple integrated Michaelis-Menten equation. The lines show the kinetic plots after correction solely for subtrate depletion followed by correction for product inhibition. It should be noted that these errors appear to be more serious for $CPG_{7.5}$urease.

The external and internal effectiveness factors for CPG-urease, determined by the fast-evaluation method, are listed in Table (4.1.6) and Table (4.1.7) respectively. Notably, $CPG_{7.5}$urease has effectiveness factors of 0.98 or greater in all cases. In the case of CPG_{55}urease both external and internal diffusion effects

Table 4.1.6 The effect of urea external mass transfer limitation on the reaction catalysed by CPG-urease.

$[U]_B$ (mol cm^{-3})	v (mol cm^{-3} s^{-1})	Zm	E_e
[a] 20×10^{-6}	2.83×10^{-6}	0.0180	0.98
20×10^{-5}	-	-	-
[b] 20×10^{-6}	2.51×10^{-6}	0.3653	0.83
20×10^{-5}	8.52×10^{-6}	0.1200	0.98

a. $R = 3.75 \times 10^{-4}$cm; $h_s = 2.87 \times 10^{-2}$ cm s^{-1}

b. $R = 27.5 \times 10^{-4}$cm; $h_s = 8.30 \times 10^{-3}$ cm s^{-1}

$D = 10^{-5}$ cm^2 s^{-1}

Table 4.1.7 The effect of urea internal mass transfer limitation on the reaction catalysed by CPG-urease.

$[U]_S^*$ (mol cm^{-3})	v" (mol cm^{-3} s^{-1})	$\emptyset m^2$	E_i
6.84×10^{-7}	82.75×10^{-6}	0.5400	>0.09
6.84×10^{-6}	471.05×10^{-6}	0.3100	>0.09
4.87×10^{-7}	66.16×10^{-6}	32.95	0.045
6.66×10^{-6}	224.21×10^{-6}	8.33	0.22

a. $R = 3.75 \times 10^{-4}$ cm; $D_{eff} = 3.5 \times 10^{-6}$ cm^2 s^{-1}

b. $R = 27.5 \times 10^{-4}$ cm.

are present. However, the former is only important at low substrate concentration. Over the first-order phase of reaction the external effectiveness factor is 0.83 and increases to about 0.98 at higher substrate concentration. The corresponding values for the internal effectiveness factor were about 0.045 and 0.22 for low and high concentrations of urea.

Assuming that the Michaelis constant for $CPG_{7.5}$urease was the same as the intrinsic constant of CPG-urease, the Thiele modulus could be estimated for CPG_{55}urease. This enabled a second estimate of Km´ to be made from studies involving the larger diameter support, Table (4.1.8). In this latter assessment, an external effectiveness factor of 0.83 was not taken into account. An attempt at the direct calculation of the external substrate modulus (s 1.4) gave spurious results for CPG_{55}urease; this would be expected due to the presence of internal diffusion effects.

Finally, an assessment of mass transfer effects by the direct comparison of the kinetics of $CPG_{7.5}$urease and CPG_{55}urease, (Fig. 4.1.3) was relatively unsuccessful. The Thiele modulus for $CPG_{7.5}$urease was greater than 10 in contradiction to assessments by the fast evaluation method.

Table (4.1.8) Mass Transfer and kinetic parameters for CPG_{55}urease

	a	b	c
$\emptyset^a$ $\emptyset m^b$	-	5.74	14.50
E_i	-	0.045	0.07
Km´ (M)	-	2.42×10^{-3}	3.71×10^{-3}
Km´ $(M)_{7.5}$	-	7.56×10^{-3}	-

a. Comparative method

b. Fast-evaluation method; $\emptyset m = R/3\ (v"/D_{eff}\ [S]_s^*))^{1/2}$

c. Direct calculation $\emptyset = R/3\ (Vmax"/D_{eff}\ Km'_{7.5}{}^*))^{1/2}$

d. Precision of the Km´ estimate is ±10%

4.2 The kinetics of glucose oxidation catalysed by glucose oxidase/catalase co-immobilized on controlled porosity glass

Introduction

Glucose oxidase, formally notatin, appears to have been discovered by Muller 1928 (190). Its early characterization has been discussed by Keiline and Hartree 1948 (160). The enzyme has widespread use as an analytical tool for monitoring glucose in medicine, food, processing and fermentation industries, (Chapter 3). The production of gluconic acid, desugaring of eggs, deoxygenation of soft drinks, and sterilization of milk are other examples of some current applications, Beck and Scott 1974 (191).

Glucose oxidase catalyses the aerial oxidation of β-D-glucose to produce a γ-lactone and hydrogen peroxide. The former then undergoes spontaneous hydrolysis to gluconic acid. The kinetics of the reaction in free solution is well characterised. Nakamura and Ogura 1962 (192), Masey et al. 1964 (193), Bright and Gibson 1967 (194). The overall reaction can be simply represented by a two stage scheme, Fig. (4.2.1).

$$E_{ox} + G \underset{k_{-1}}{\overset{k_{+1}}{\rightleftharpoons}} E_{ox} - G \xrightarrow{k_{+2}} E_r + P(I)$$

$$E_r + O_2 \xrightarrow{k_{+4}} E_{ox} + H_2O_2$$

$$k_{cat} = k_{+2} \; ; \; k_{ox} = k_{+4} \; ; \; k_r = k_{+1}\, k_{+2}/(k_{-1} + k_{+2})$$

$$Km_G = k_{cat}/k_r \; ; \; Km_O = k_{cat}/k_{ox}$$

Figure (4.2.1) - A general scheme of the reaction catalysed by glucose oxidase. k is a microscopic rate constant for the step shown. k_{ox} and k_r are the overall rate constants for the oxidation and reduction of glucose oxidase respectively.

This depicts classical two-substrate ping-pong kinetics for which the steady state equation is:

$$v = \frac{Vmax\ [G]\ [O_2]}{[G]\ [O_2] + Km_G\ [O_2] + Km_O\ [G]} \qquad (4.2.1)$$

When either glucose or oxygen is in vast excess, the expression (4.2.1) reduces to the straightforward Michaelis-Menten equation. Under normal experimental conditions the Michaelis constant for each substrate depends on the concentration of the co-substrate. That is, glucose oxidase is not expected to have a `unique´ Km for glucose, Km_G and Km_O with saturating concentration of the corresponding co-substrate have values of 1.1×10^{-1}M and 2×10^{-4}M (phosphate buffer, pH 5.6, 25°C) respectively, Barman 1969 (195).

The kinetics and other characteristics of immobilized glucose oxidase (IMGLO) have been extensively studied by Weibel and Bright 1971 (196), Rovito and Kitrell 1973 (197), Ramachandran and Pelmutter 1976 (198), Buchholz and Jarowek 1978 (199), Reuss and Buchholz 1979 (186) Ngo et al. 1980 (200), and also by Malikkides and Weiland 1982 (201). IMGLO serves as a versatile model for the study of many characterisics of immobilized enzyme systems. It is perhaps most frequently adopted as a model for the practical study of mass transfer effects.

The reoxidation of reduced glucose oxidase (E_r) back to the oxidized form (E_{ox}) is the fastest step in the overall catalytic

cycle, Fig. (4.2.1) (k_{ox}/k_{red} = 140; k_{ox}/k_{cat} = 2000 M^{-1}) Weibel and Bright (196).

This stage can however become limiting because of the low solubility of oxygen. The concentration of oxygen in an aqueous medium is typically 2.5 x 10^{-4}M, (1 atm, 25°C) thus whenever glucose concentration is in excess, oxygen mass transfer rate becomes an important consideration.

In an open vessel oxygen for the oxidation of glucose is ultimately derived from the atmosphere. The rate of gas to liquid-phase tranfer is proportional to the oxygen partial pressure difference at the gas-liquid interphase. The proportionality constant is the gas-liquid phase mass transfer coefficient for oxygen. Quantitative treatment of mass transfer across the gas-liquid and liquid solid interphases together results in equations analogous to those described for mass transfer through the Nernst layer and a membrane, (s 1.4). The membrane permeability coefficient term is replaced by the gas-liquid mass transfer coefficient for oxygen. This latter term accounts for the dependence of system performance on variables like the rate of agitation or aeration, Lilly et al. 1978 (202), Reuss and Buchholz (186). Other important variables in relation to oxygen mass transfer limitations include glucose oxidase and catalase activities as well as the glucose concentration. As discussed in the previous section, mass transfer effects are important because the unambiguous interpretation of data first requires the removal of diffusion masking from the system under

study. From the practical standpoint, diffusion control reduces the efficiency (ie. effectiveness factor) of an immobilized enzyme.

Mass transfer limitation is also an important determinant of the operational stability of IMGLO. Glucose oxidase is inhibited by hydrogen peroxide. The exact mechanism is unclear, but inhibition requires the presence of glucose. One view is that inactivation results from the attack of hydrogen peroxide on the reduced form of the enzyme. The requirement for glucose might also mean that there exists a particularly susceptible enzyme conformation. The rate of inactivation is first order with respect to, and depends on factors which change, hydrogen peroxide concentration. The presence of catalase enhances the stability of IMGLO preparations by catalysing the disproportionation of hydrogen peroxide, Reuss and Buchholz (186), Malikkides and Weiland (201). The Michaelis constant of catalase for hydrogen peroxide is of the order of IM, making catalase well suited for this protective role, (s. 3.5). The use of catalase, however, is perhaps not the most ideal arrangement because the enzyme is itself susceptible to hydrogen peroxide inactivation. The immobilization of glucose oxidase on catalactic surfaces, eg. manganese, Lilly et al. (202) or titanium oxide Reuss and Buchholz (186), also provides protection from hydrogen peroxide.

Glucose oxidase was chosen as a model in the present study for the following reasons. As discussed above, depending on the conditions, oxygen can be made the limiting substrate. This is

useful because the diffusivity of oxygen in aqueous media is well known. Secondly, the IMGLO system has two substrates; it may therefore be possible to compare the mass transfer effects with respect to each of these under identical conditions. Thirdly, IMGLO is an example of an immobilized oxidase, therefore its behaviour as regards diffusion control will undoubtedly increase the understanding of other oxidases. Finally, past studies of IMGLO have largely involved oxygen monitoring or the spectrophotometric monitoring of the flavin group at 450 nm, Weibel and Bright (196). There does not yet appear to be any examples of kinetic studies of IMGLO, using calorimetry. In the study reported below, the apparent and intrinsic kinetics of glucose oxidase and catalase, co-immobilized on controlled porosity glass, were examined by flow microcalorimetry.

Materials and Methods

Reagents:

Glucose oxidase (β- D - Glucose: Oxygen 1-oxyreductase, EC 1.1.34; Type X from *Aspergillus niger*, 100,000 - 150,000 units per gram solid ($\sim$0.75g protein)) and catalase (H_2O_2 oxidoreductase, EC 1.11.1.6; purified powder, 2000 - 5000 units per mg protein) were purchased from Sigma UK. All other materials and sources were as described previously (s 4.1).

Methods:

Enzyme immobilization and thermochemical assay followed the

procedures described above (s 4.1). Between 146.1 and 148.6 mg of moist CPG-enzyme were studied. The methods used for data reduction are largely the same as described in previous sections: Glucose oxidase and urease may differ in the nature and degree of enzyme-product interaction. Competitive product inhibition is possible here because the product (gluconolactone) and substrate have a similar structure. Therefore, the integrated Michaelis-Menten equations incorporating the effects of competitive inhibition of substrate inhibition Table (1.2.3.1), were used. The extent of external and internal mass transfer limitations were assessed also using the methods described in previously (s 4.1).

Results

The apparent kinetic constants for $CPG_{7.5}GLO/CAT$ and $CPG_{55}GLO/CAT$, Table (4.2.1; 4.2.2), were determined using the same enzyme kinetic plots described above. Sample experimental data are presented in Tables (4.2.3) and (4.2.4). The apparent Michaelis constant values determined from the LB plot were between 75% larger and smaller than the values fully corrected for the effects of non-initial rate assay. The inhibition constant, Kp", was determined from a -Log Kp" against correlation coefficient plot. Using the criteria of optimal linearity and Kp" < Km^{app}, - Log K_p" was 4.05 and 3 for $CPG_{7.5}GLO/CAT$ and $CPG_{55}GLO/CAT$ respectively, Fig. (4.2.2). The corresponding values of Kp" are 8.91×10^{-5}M and 1×10^{-3}M respectively. The apparent

FIG(4·2·2)-Dependence of the IMM PLOT linearity(r), for $CPG_{7.5}$ GLO/CAT(⊡) and CPG_{55} GLO/CAT(⊙), on the inhibition constant estimate(K_p)

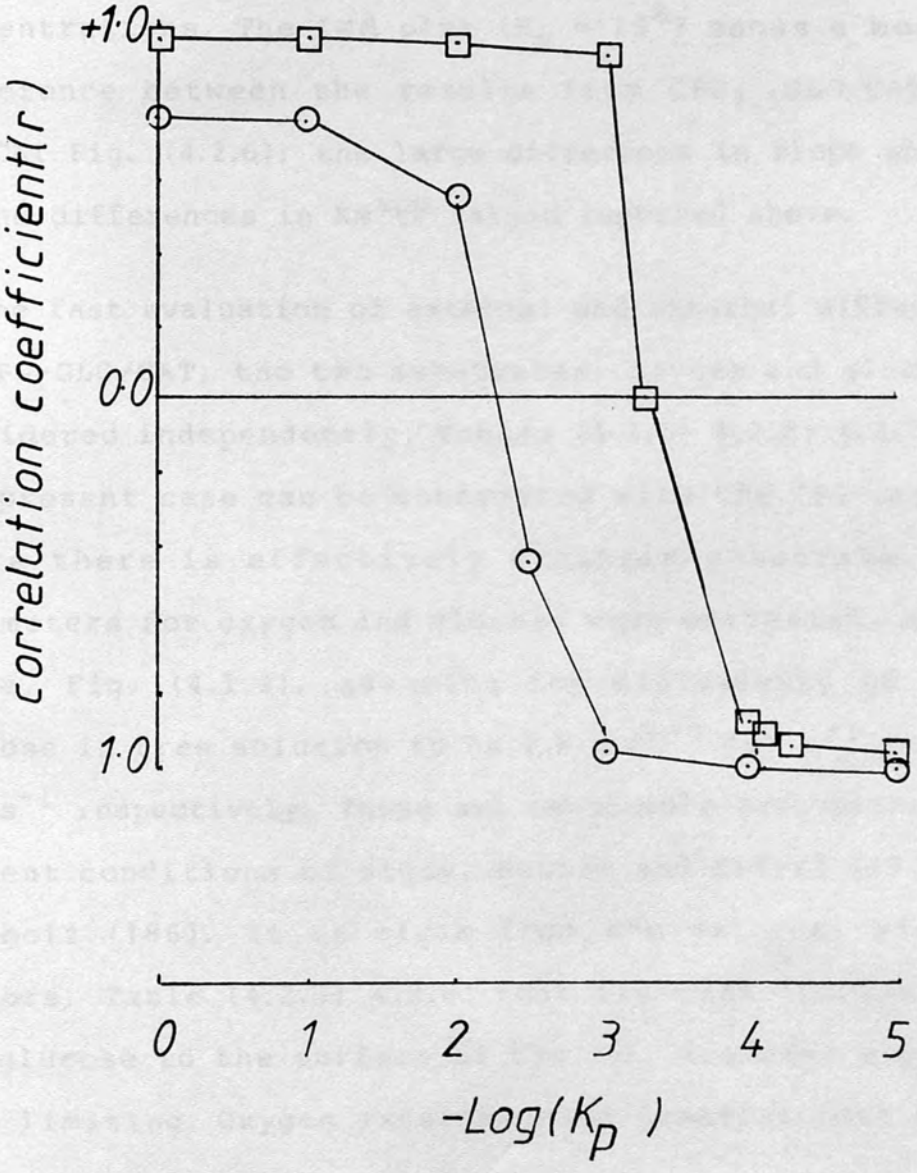

Michaelis constant values for $CPG_{7.5}$GLO/CAT and CPG_{55}GLO/CAT were 3.20×10^{-4}M and 6.78×10^{-3}M respectively. The corresponding maximum activities were 2.65×10^{-4}M min^{-1} mg^{-1} (CPG)or 2.17×10^{4}M min^{-1} mg^{-1} CPG. The ideal double reciprocal plot is compared with the observed LB and LB(S) plot for $CPG_{7.5}$GLO/CAT, Fig. (4.2.3). The Eadie plot for CPG-GLO/CAT, Fig (4.2.5), does not produce the simple linear response expected from a system following classical Michaelis-Menten kinetics. At both support diameters the slope of the Eadie plot increases towards infinity at lower substrate concentrations. The IMM plot ($K_p = 10^8$) shows a more distinct difference between the results from $CPG_{7.5}$GLO/CAT and CPG_{55} GLO/CAT Fig. (4.2.6); the large difference in slope shown relates to the differences in Km^{app} values reported above.

In the fast evaluation of external and internal diffusion effects on CPG-GLO/CAT, the two substrates, oxygen and glucose, can be considered independently, Tables (4.2.5; 4.2.6; 4.2.7 and 4.2.8). The present case can be contrasted with the CPG-urease system where there is effectively a single substrate. Transport parameters for oxygen and glucose were estimated, as described above, Fig. (4.1.3), assuming the diffusivity of oxygen and glucose in free solution to be 2.6×10^{-5} cm^2 s^{-1} and 1.0×10^{-5} cm^2 s^{-1} respectively. These are reasonable assumptions under the present conditions of study, Rovito and Kitrel (197) Reuss and Buchholz (186). It is clear from the external effectiveness factors, Table (4.2.5; 4.2.6) that the mass transfer of oxygen and glucose to the surface of the 7.5 diameter support is not rate limiting. Oxygen external mass transfer rate limitations

Table (4.2.1) Apparent kinetic constants for $CPG_{7.5}GLO/CAT$

PLOT	Vmax (M min^{-1} mg^{-1})	a_{Km}*	r	Km^*/Km^{app}
LB	4.65×10^{-4}	9.31×10^{-4}	0.9977	1.75
EADIE	3.63×10^{-4}	5.97×10^{-4}	-0.9208	1.37
LB(S)	4.01×10^{-4}	4.34×10^{-4}	0.9979	1.51
IMM^b	2.58×10^{-4}	2.24×10^{-4}	-0.9785	0.97
IMM^c	2.24×10^{-4}	3.20×10^{-4}	-0.9036	1.00
IMM_d	3.71×10^{-4}	2.86×10^{-4}	-0.9829	-

a. General estimate of Km^{app}

b. $K_p" = 10^8 M$;

c. Competitive inhibition model, $Kp" = 8.91 \times 10^{-5} M$

d. Substrate inhibition model, $Ks = 1 \times 10^{-1} M$

Fractional conversion (X) = 87.2% with $5 \times 10^{-5} M$ glucose

Table (4.2.2) Apparent kinetic constants for CPG_{55}GLO/CAT

PLOT	Vmax (M min^{-1} mg^{-1})	a_{Km}*	r	Km^*/Km^{app}
LB	6.50×10^{-4}	6.56×10^{-3}	0.9980	0.96
EADIE	3.50×10^{-4}	2.75×10^{-3}	-0.7725	0.52
LB(S)	6.32×10^{-4}	5.98×10^{-3}	0.9980	0.88
^{b}IMM	2.17×10^{-4}	2.54×10^{-3}	0.7778	0.37
^{c}IMM	2.17×10^{-4}	6.78×10^{-3}	0.9612	1.00
^{d}IMM	7.36×10^{-4}	6.34×10^{-3}	0.9331	-

a. b. See notes to Table (4.2.1)

c. Competitive inhibition model, Kp" = 1×10^{-3}M

d. Substrate inhibition model; Ks = 8×10^{-3}M

Fractional conversion (X) = 13% with 2.5×10^{-4}M glucose.

TABLE (4.2.3)

$[S]^B$ (M)[a]	ss-disp (μV)	V(M min^{-1} mg^{-1})	$[S]^B$ (M)	V/ S (min^{-1} mg^{-1})	Q(mg^{-1})
20.41×10^{-1}	7.65	3.02×10^{-4}	20.13×10^{-3}	0.0148	0.0149
10.21×10^{-3}	8.55	3.37×10^{-4}	9.90×10^{-3}	0.0330	0.0341
5.10×10^{-3}	8.55	3.37×10^{-4}	4.78×10^{-3}	0.0661	0.0706
2.04×10^{-3}	7.58	3.00×10^{-4}	1.76×10^{-3}	0.1465	0.1712
1.02×10^{-3}	6.52	2.57×10^{-4}	0.78×10^{-3}	0.2524	0.3416
5.10×10^{-4}	5.32	2.10×10^{-4}	3.13×10^{-4}	0.4112	0.7910
2.04×10^{-4}	2.17	8.58×10^{-5}	1.23×10^{-4}	0.4204	0.8304
1.02×10^{-4}	1.25	4.94×10^{-5}	0.56×10^{-4}	0.4837	1.2686
5.10×10^{-5}	0.60	2.40×10^{-5}	2.78×10^{-5}	0.4639	1.0930

a. Glucose concentration

b. $Q = 1/t\ (1 + S/Kp)\ \ln\ (\ S\ /(\ S\ /(\ S - P\ ))$; $Kp" = 10^8$

Table (4.2.4)

$[S]^B$ (M)[a]	ss-disp (μV)	V(M min^{-1} mg^{-1})	$[S]^B$ (M)	V/ S (min^{-1} mg^{-1})	Q(mg^{-1})
10.13×10^{-3}	6.22	2.47×10^{-4}	9.96×10^{-3}	0.0244	0.0248
5.07×10^{-3}	6.75	2.68×10^{-4}	4.88×10^{-3}	0.0529	0.0550
2.03×10^{-3}	4.80	1.91×10^{-4}	1.90×10^{-3}	0.0942	0.1008
1.01×10^{-3}	2.25	8.94×10^{-5}	9.53×10^{-4}	0.0882	0.0940
5.06×10^{-4}	1.20	4.77×10^{-5}	4.74×10^{-5}	0.0942	0.1007
2.53×10^{-4}	0.60	2.38×10^{-5}	2.37×10^{-4}	0.0942	0.1007

a. Glucose concentration

b. $Q = -1/t\ (1 + S/Kp)\ \ln\ (\ S\ /(\ S - P);\ Kp = 10^8$

FIG(4·2·3)-LINEWEAVER-BURK PLOT
for $CPG_{7.5}$GLO/CAT(⊙-LB(S); ⊡-LB)

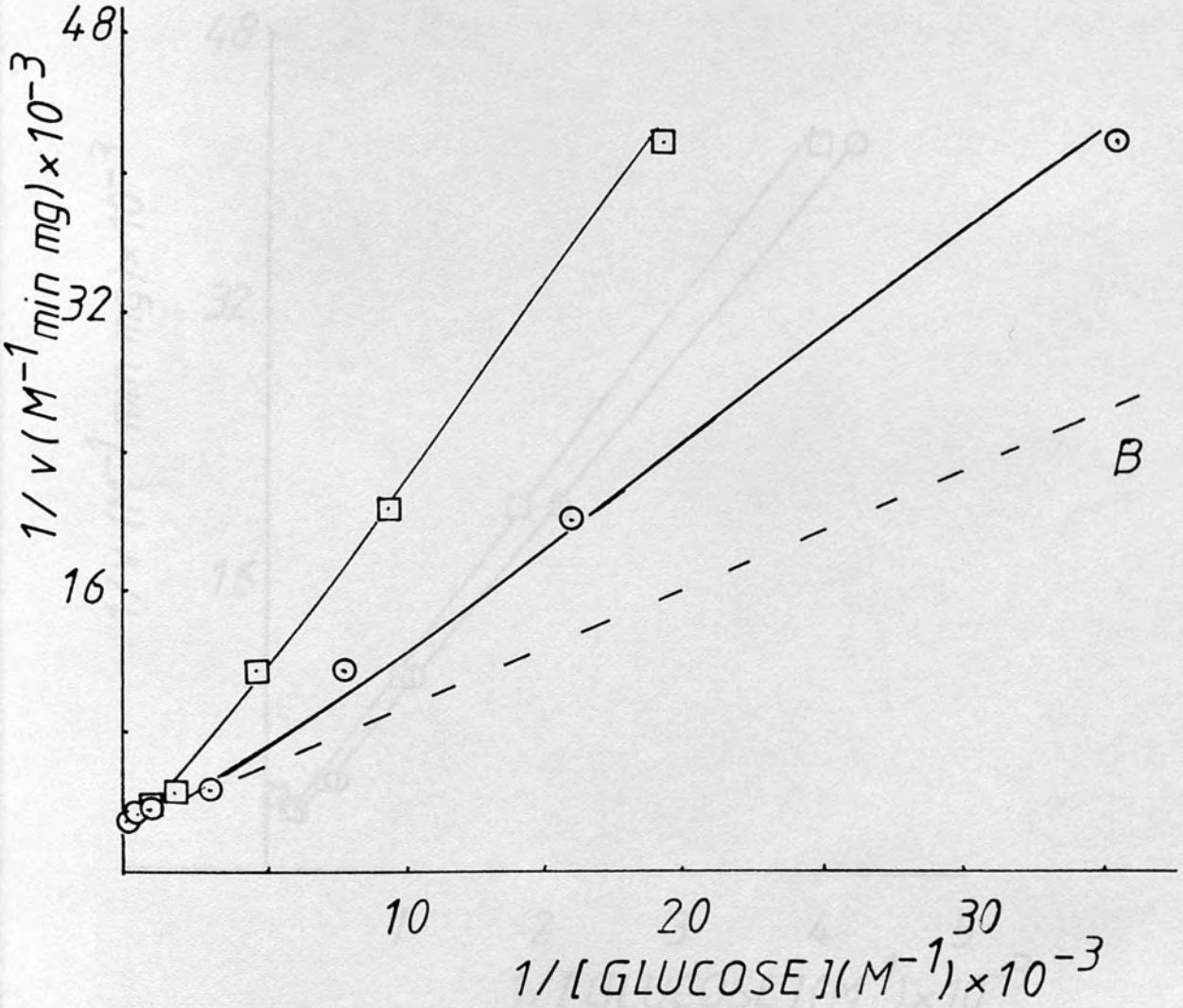

FIG(4·2·4)-LINEWEAVER-BURK PLOT
for CPG_{55}GLO/CAT(⊙-LB(S);⊡-LB)

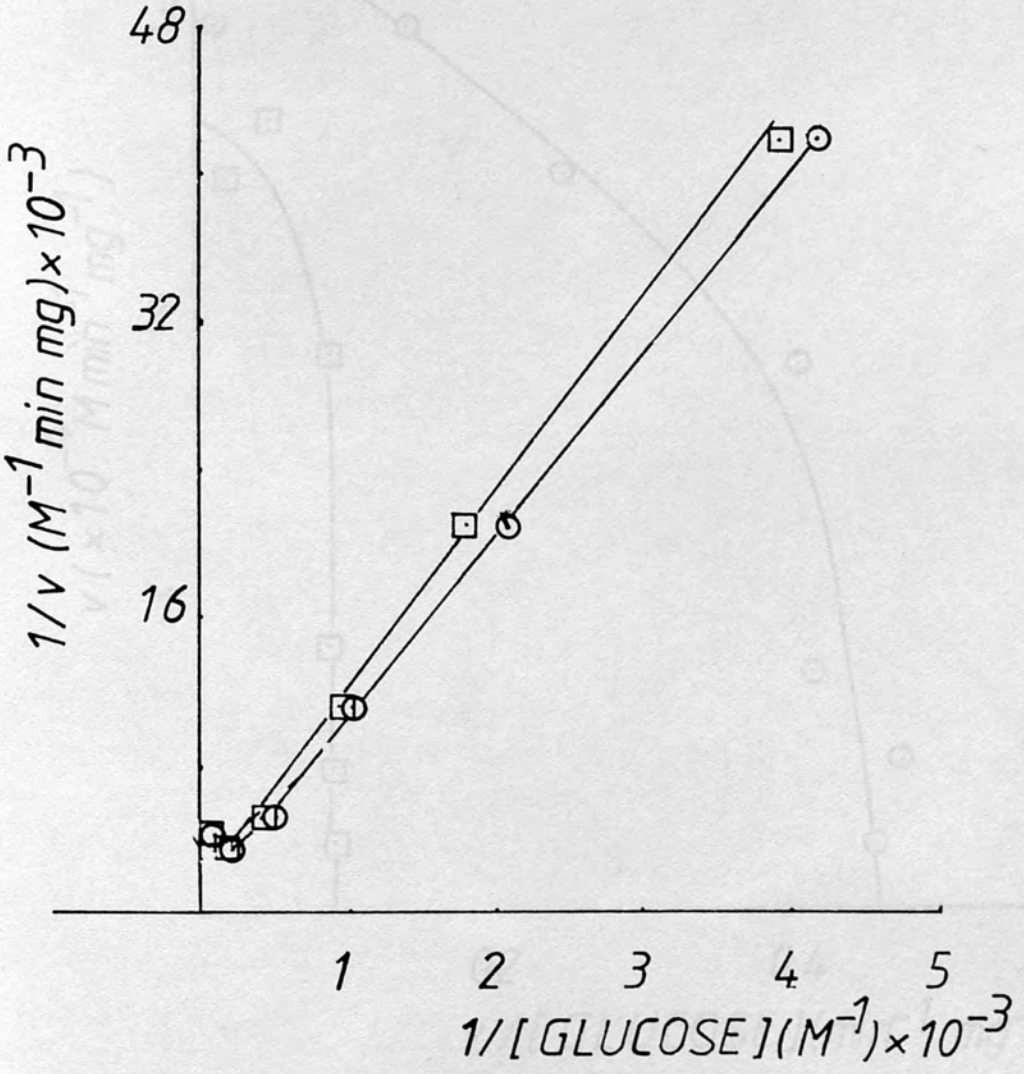

FIG(4·2·5)-EADIE PLOT for $CPG_{7.5}$GLO/CAT(⊙)and CPG_{55}GLO/CAT(⊡)

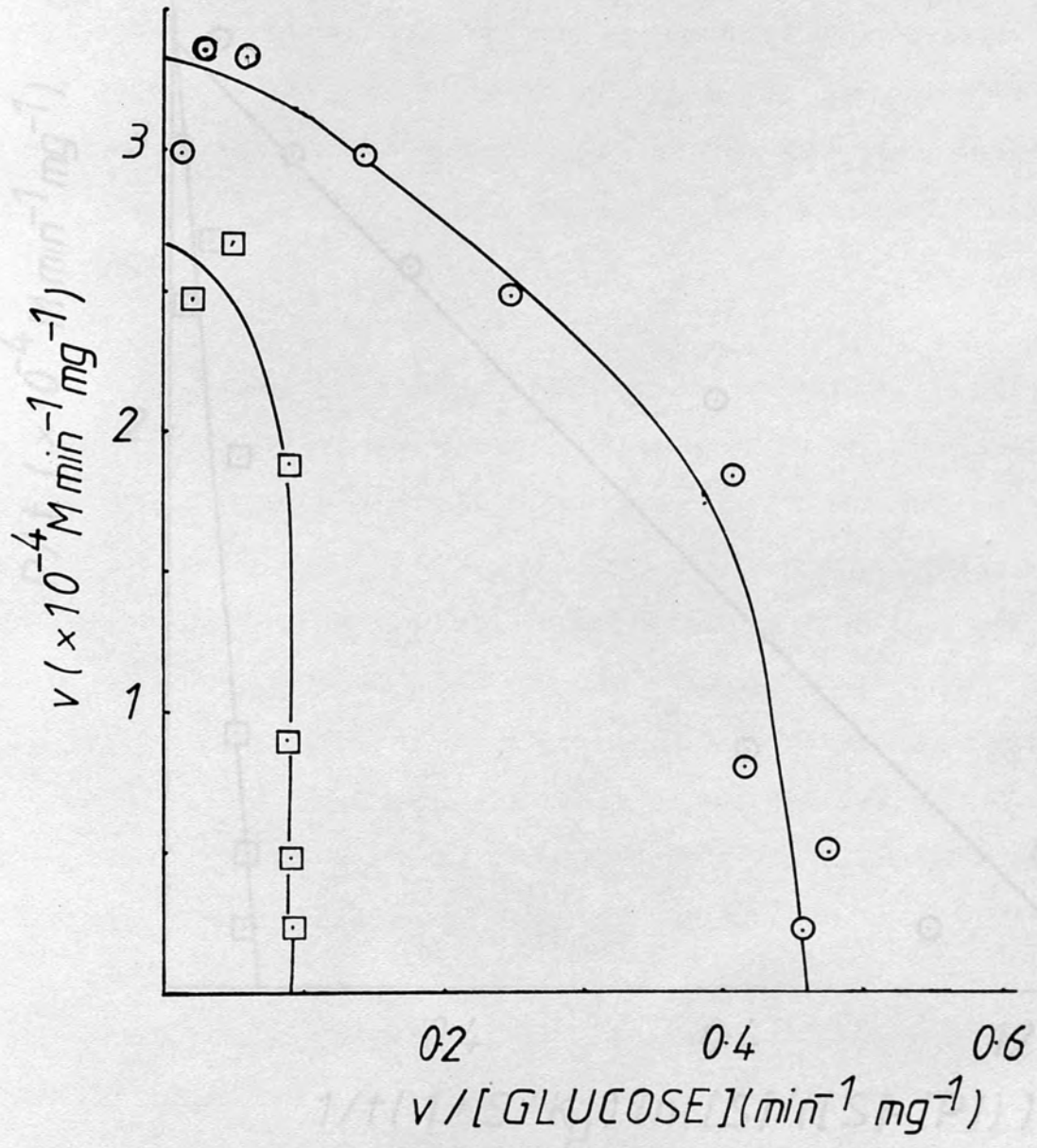

FIG(4·2·6)- INTEGRATED MICHAELIS-MENTEN PLOT for $CPG_{7.5}$ GLO/CAT(⊙) and CPG_{55} GLO/CAT(⊡)

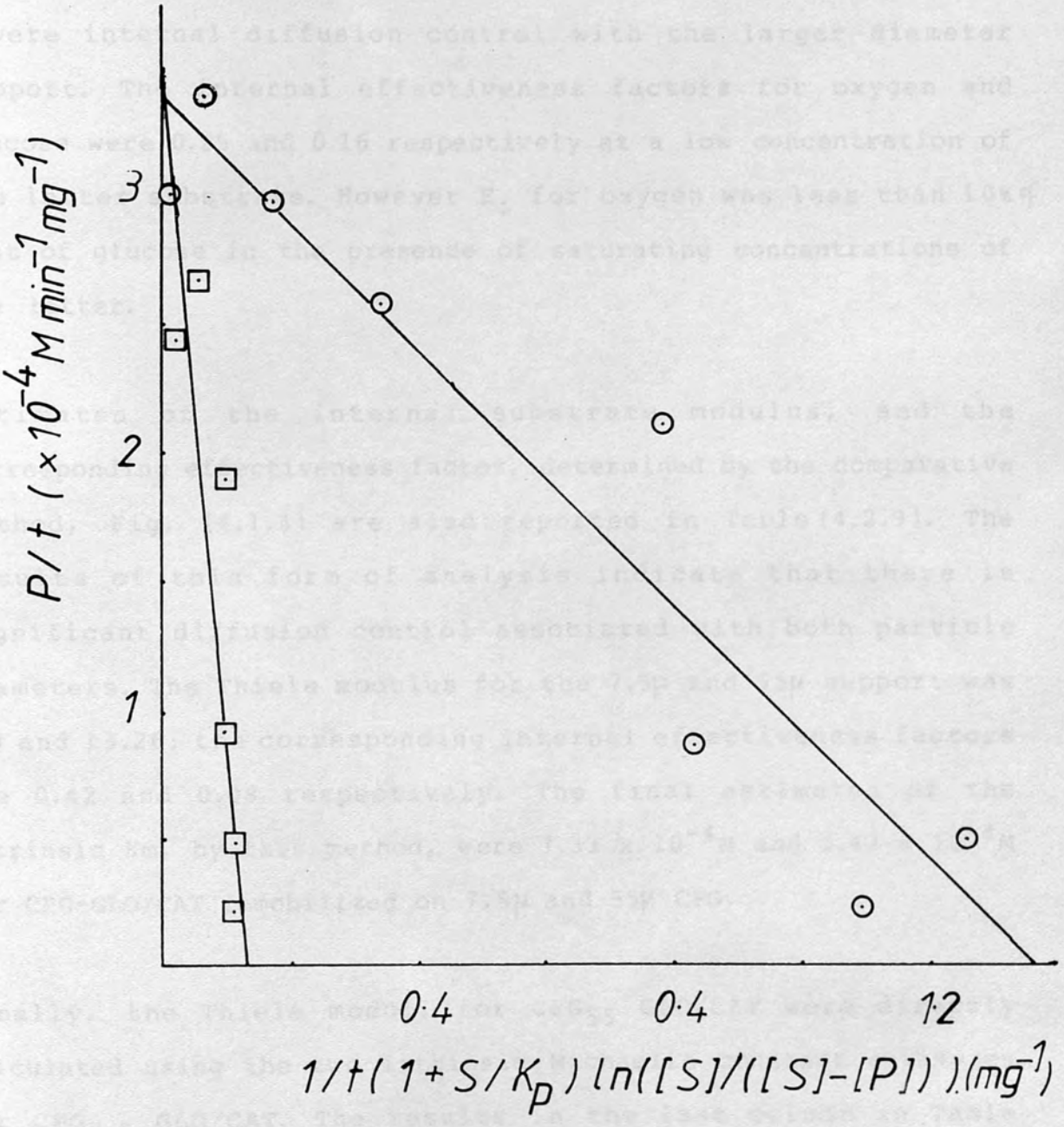

however appear to be significant, for the large diameter support, in the presence of saturating concentrations of glucose.

Examination of the data in Table (4.2.7; 4.2.8) indicates that $CPG_{7.5}$GLO/CAT is virtually free from internal diffusion effects with respect to both substrates. In contrast there appears to be severe internal diffusion control with the larger diameter support. The internal effectiveness factors for oxygen and glucose were 0.25 and 0.16 respectively at a low concentration of the latter substrate. However E_i for oxygen was less than 10% of that of glucose in the presence of saturating concentrations of the latter.

Estimates of the internal substrate modulus, and the corresponding effectiveness factor, determined by the comparative method, Fig. (4.1.4) are also reported in Table(4.2.9). The results of this form of analysis indicate that there is significant diffusion control associated with both particle diameters. The Thiele modulus for the 7.5μ and 55μ support was 2.0 and 13.26; the corresponding internal effectiveness factors are 0.42 and 0.08 respectively. The final estimates of the intrinsic Km, by this method, were 1.33×10^{-4}M and 5.42×10^{-4}M for CPG-GLO/CAT immobilized on 7.5μ and 55μ CPG.

Finally, the Thiele moduli for CPG_{55} GLO/CAT were directly calculated using the two intrinsic Michaelis constant estimates for $CPG_{7.5}$ GLO/CAT. The results in the last column in Table

Table (4.2.5) The effect of oxygen external mass transfer limitation on the reaction catalysed by CPG-GLO/CAT

$[O]_B$ (mol cm^{-3})	v (mol cm^{-3} s^{-1})	Zm	E_e
2.50×10^{-7} [a,b]	2.76×10^{-8}	0.0080	1.00
2.50×10^{-7} [c,b]	10.68×10^{-8}	0.0300	>0.95
2.50×10^{-7} [a,d]	1.51×10^{-8}	0.1110	>0.95
2.50×10^{-7} [c,d]	8.50×10^{-8}	0.6200	0.57

a. [Glucose] = 5.06×10^{-7} mol cm^{-3}

c. [Glucose] = 5.06×10^{-6} mol cm^{-3}

b. $R = 3.75 \times 10^{-4}$ cm; $h_s(0) = 5.24 \times 10^{-2}$ cm s^{-1}

d. $R = 27.5 \times 10^{-4}$ cm; $h_s(0) = 1.51 \times 10^{-2}$ cm s^{-1}

$D = 26.6 \times 10^{-6}$ cm^2 s^{-1}

Table (4.2.6) The effect of glucose external mass transfer limitation on the reaction catalysed by CPG-GLO/CAT

$[G]_B$ (mol cm^{-3})	v (mol cm^{-3} s^{-1})	Zm	E_e
5.06×10^{-7} [a,b]	1.51×10^{-8}	0.100	0.95
5.06×10^{-6} [a,b]	8.50×10^{-8}	0.0560	1.00

a. bulk oxygen concentration is 2.50×10^{-7} mol cm^{-3}

b. $R = 27.5 \times 10^{-4}$cm; $h_s(G) = 8.30 \times 10^{-3}$ cm s^{-1}

$D = 1.0 \times 10^{-5}$ cm^2 s^{-1}

TABLE (4.2.7) The effect of oxygen internal mass transfer limitation on the reaction catalysed by CPG-GLO/CAT

$[O]_s$(mol cm^{-3})	v"[a]	ϕm^2	E_i
8.65×10^{-9}[b,c]	7.98×10^{-7}	0.1500	>0.9
8.65×10^{-9}[d,c]	3.14×10^{-6}	0.6100	>0.9
8.25×10^{-9}[b,e]	4.58×10^{-7}	5.01	0.25
8.25×10^{-9}[d,e]	2.57×10^{-6}	74.90	< 0.02

a. v"(mol s^{-1} cm^{-3} (CPG))

b. [Glucose] = 2.04×10^{-7} mol cm^{-3}

d. [Glucose] = 5.06×10^{-6} mol cm^{-3}

c. R = 3.75×10^{-4} cm

e. R = 27.5×10^{-4}cm

D_{eff} = 9.3×10^{-6} cm^2 s^{-1}

Table (4.2.8) The effect of glucose internal mass transfer limitation on the reaction catalysed by CPG-GLO/CAT

$[G]_s^*$ (mol cm^{-3})	v''^a	$\emptyset m^2$	E_i
3.53×10^{-9} [b]	4.60×10^{-7}	0.08	>0.95
1.76×10^{-7}	3.15×10^{-6}	0.01	>0.95
1.67×10^{-8} [c]	4.60×10^{-7}	6.60	0.16
1.67×10^{-7}	2.57×10^{-6}	3.70	0.28

a. v(mol s^{-1} cm^{-3} (CPG))

b. $R = 3.75 \times 10^{-4}$ cm; $[O_2]^* = 8.65 \times 10^{-9}$ mol cm^{-3}

c. $R = 27.5 \times 10^{-4}$ cm; $[O_2]^* = 8.25 \times 10^{-9}$ mol cm^{-3}

$D_{eff} = 3.5 \times 10^{-6}$ cm^2 s^{-1}

Table (4.2.9) Mass transfer and kinetic parameters for CPG_{55}GLO/CAT

	a	b	c
$^{a}\emptyset$; $\emptyset m^{b}$	13.26	2.57	10.65 ; 6.88
E_i	0.08	0.16	0.09 ; 0.14
Km´ (M)	5.42×10^{-4}	10.85×10^{-4}	-
$Km_{7.5}$ (M)	1.33×10^{-4}	3.20×10^{-4}	-

a. `Comparative´ method

b. `Fast Evaluation´ method

c. Direct calculation, $\emptyset = R/3\ (Vmax"/(D_{eff}\ Km_{7.5}{}^{*}))^{1/2}$

(4.2.9) enable the direct comparison of the fast-evaluation and comparative methods. The modified Thiele modulus cannot otherwise be directly compared to the Thiele modulus. In the last column, the first and second numbers refer to estimates using the Km´ from the comparative and fast-evaluation methods respectively.

4.3 The kinetics of acetylcholine hydrolysis catalysed by acetylcholinesterase immobilized on controlled porosity glass

Introduction

The cholinesterases are perhaps one of the most widely studied hydrolytic enzymes; Karczmar et al. 1970 (203), O´Brien 1975 (204), Hallenbrand and Krupka 1970 (205). They consist of all esterases which hydrolyse choline esters at a faster rate than other esters. All cholinesterases are also inhibited by the alkaloid eserine (10^{-5}M). Two classes of enzymes are normally described by the above term. These are:

a. Acetylcholine acetylhydrolase (E C 3.1.1.7), usually designated AcChE and

b. acetylcholine acylhydrolase (E C 3.1.1.8) or ψChE.

The name acetylcholinesterase usually refers specifically to the former enzyme, whilst `cholinesterase´ is usually reserved for the latter. There does not appear to be a sharp distinction between the properties of AcChEs and ChEs; the former class will generally hydrolyse benzoyl choline whilst ChEs will not. AcChEs are also usually susceptible to substrate inhibition.

Although the function of AcChE is apparently still a subject of

some controversy, it is generally accepted that this enzyme plays an important role in nerve impulse transmission across neuromuscular junctions. The inhibition of AcChE probably underlies the action of a number of drugs, insecticides and the so-called nerve gases.

AcChE catalysis the hydrolysis of esters according to the scheme.

$E + S \rightleftharpoons ES \longrightarrow EAC + P1$

$EAC + H_2O \longrightarrow E' + P2$

S - substrate RCOOR,' e.g. $(CH_3)^+_3NCH_2CHO.OCH_3$

EAC - acylated enzyme intermediate

P1 - alcohol e.g. choline $(CH_3)N^+CH_2\ CH_2\ OH$

P2 - acid e.g. acetic acid

As described for GLO (s 4.2), this is a bisubstrate reaction; however, the kinetics are approximately Michaelis-Menten. Under the usual conditions of study, water is in a vast excess. Acetylcholine (AcCh) is not the only substrate for AcChE. The hydrolysis of propionylcholine, butyrylcholine and other homologues is also catalysed. Generally, the more closely these structurally resemble acetylcholine the better they serve as substrates. The Km of soluble AcChE for AcCh is about 1.4×10^{-4}M. Acetylcholinesterase is very likely membrane-bound in the natural state.

The characteristics of immobilized AcChE has received considerable attention Ngo and Laidler 1975 (206), 1978 (101), Ngo and Yam 1978 (207). This interest is perhaps largely owing to the attractive prospect of using the immobilized enzyme in the rapid screening for possible reversible inhibitors. Many such

compounds have some potential as drugs and as environmental pollutants, Morris 1961 (208), Sadar et al. 1970 (209). The nylon tube immobilized AcChE system often shows signs of external diffusion control. Entrapment in slices of polyacrylamide gel results in internal diffusion effects related to the support thickness. These diffusion effects are indicated by such features as a non-linear Lineweaver-Burk plot, altered pH-activity profile (compared to that of the soluble enzyme) and a non-uniform slope of the Arrhenius plot. The apparent Michealis constant is usually an order of magnitude larger than the soluble enzyme Km value although the exact increase depends on the flow rate, support enzyme loading and support thickness. For example the apparent Km, with AcCh as substrate, of AcChE immobilized on glass was 3×10^{-3}M compared to 2×10^{-4}M for the soluble enzyme, Alsen et al. 1975 (210).

The reaction catalysed by AcChE is usually followed by spectrophotometry or by measuring the amount of acid formed. At present there does not appear to be any report of a study, of the kinetics of the AcChE reaction, using calorimetry. A study of the kinetics of the reaction catalysed by AcChE immobilized on controlled porosity glass, using flow-microcalorimetric monitoring, is reported below. As discussed elsewhere (Chapter 1) a distinct advantage of the present approach is that the natural substrate acetylcholine, rather than artificial substrates, can be used. As was the case in the preceding sections (s 4.1, 4.2) the main concern in the present study was the assessment and removal of non-initial rate assay and diffusion effects.

Materials and Methods

Reagents

Acetylcholinesterase (acetylcholine acetylhydrolase, EC 3.1.1.7; Type VI-S from electric eel; 200-400 units per mg. protein) and acetylcholine chloride were purchased from Sigma UK. All other materials and sources were as described above (s 4.1).

Methods

AcChE was immobilized to alkylamine glass using glutaraldehyde as coupling agent as described previously (Chapter 2). Glass beads with an average diameter of 7.5μ and 55μ were used. The supports came from the same batches as used for immobilization of urease (s 4.1) and glucose oxidase (s 4.2). As before, the two enzyme preparations studied are distinguished by refering to the support diameter. For instance $CPG_{7.5}$ AcChE and CPG_{55}AcChE refers to AcChE immobilized on the 7.5μ and 55μ diameter support respectively. The method of exposing quantities of controlled porosity glass to excess protein, in order to achieve similar protein loading, could not be adopted in this study AcChE is more expensive than either urease or glucose oxidase.

The study of CPG-AcChE was carried out in THAM buffer (0.2M, pH 7.5, 25^{o}C). Steady state power measurements were converted to average velocity measurements as described above; the enthalpy of acetylcholine hydrolysis was estimated as 41.30 $\pm$ 1.34 kJ mol^{-1}. As discussed above AcChE may be susceptible to substrate inhibition as well as to product inhibition. These possibilities

were examined using the appropriate integrated Michaelis-Menten relationships, Table (1.2.3.1) and methods described previously (s. 4.1). The inhibition constant Ks is found by using the same criteria used for the other inhibition models (s 1.4, s 4.1). Acetylcholine (MW= 161) is similar in size to glucose (MW = 180.2) and is expected to have similar mass transfer characteristics.

Results

The apparent kinetic constants, Km^{app} and Vmax, for CPG-AcChE are listed in Tables (4.3.1) and (4.3.2) As indicated there, the LB, Eadie, LB(S) and various IMM plots were again employed to extract Km^{app} and Vmax´ estimates. The LB plot for both CPG-AcChE preparations show a slight curvature, Fig. (4.3.1) and Fig. (4.3.2). It can be seen from the LB(S) plot superimposed on the respective figures that substrate depletion is important in both cases. The maximum extent of substrate (2×10^{-3}M AcCh) conversion was 95% and 68% for $CPG_{7.5}$ AcChE and CPG_{55}AcChE systems respectively; corresponding Vmax values are 7.12×10^{-3} M min^{-1} mg^{-1} and 23.64×10^{-3}M min^{-1} mg^{-1}. The relative slopes of the IMM plot, ($Kp = 10^{8}$) Fig. (4.3.3), are again consistent with the differences in the Km^{app} values reported above.

AcChE is likely to have complex characteristics as regards possible inhibition under non-initial rate assay conditons. Both products of AcCh hydrolysis, choline and acetic acid, resemble parts of the substrate and are therefore potential competitive inhibitors. AcChE is known to be inhibited by its substrate. Based

on the criterion of optimum linearity of the resulting plot, all three inhibition models, i.e., competitive product inhibition, non-competitive product inhibition and substrate inhibition, fit reasonably well, Fig (4.3.4). The values of the various apparent inhibition constants are listed in Table (4.3.1) and Table (4.3.2). Since these values are equal or greater than Km^{app} in all cases, it may be that the actual extent of inhibition is small under present conditions of study. It is, moreover, difficult to arrive at a decision as to the predominant pattern of inhibition. Therefore, in subsequent data analysis these effects were ignored.

The results of diffusion assessment, using the methods described in section 4.1, show external mass transfer effects to be virtually negligible for both support diameters, Table (4.3.3). Internal diffusion control is also minimal in the $CPG_{7.5}$AcChE system. The reaction catalysed by CPG_{55}AcChE is however subject to considerable internal diffusion control, Table (4.3.4). The first and zero order effectiveness factors were about 0.06 and 0.24 respectively. Finally estimates of the intrinsic Km of CPG-AcChE are listed in Table (4.3.5). The Thiele modulus for The CPG_{55}AcChE reaction, determined from the comparative and fast evaluation methods, are compared in the last column of this table.

Table (4.3.1) Apparent kinetic constants for $CPG_{7.5}$AcChE

PLOT	Vmax ($Mmin^{-1}$ mg^{-1})	$^{a}Km^{*}$	r	Km/Km^{app}
LB	17.01×10^{-3}	60.00×10^{-3}	0.9988	8.00
EADIE	10.11×10^{-3}	27.94×10^{-3}	-0.8080	4.12
LB(S)	19.58×10^{-3}	37.10×10^{-3}	0.9915	5.11
IMM[b]	7.12×10^{-3}	7.26×10^{-3}	0.9120	1.00
IMM[c]	2.13×10^{-3}	1.51×10^{-3}	0.8699	-
IMM[d]	3.00×10^{-3}	1.20×10^{-3}	0.7566	-
IMM[e]	15.70×10^{-3}	18.75×10^{-3}	0.9685	-

a., b. see notes to Table (4.2.1)

c. Competitive inhibition model, Kp" = 10^{-3}M

d. Non-competitive inhibition model, Kp" = 10^{-3}M

e. Substrate inhibition model, Ks = 2×10^{-2}M

Fractional conversion (X) = 95% with 2×10^{-3}M AcCh.

Table (4.3.2) Apparent kinetic constants for CPG_{55}AcChE

PLOT	Vmax ($Mmin^{-1}$ mg^{-1})	a_{Km}*	r	Km^*/Km^{app}
LB	64.36×10^{-3}	188.34×10^{-3}	0.9997	5.50
EADIE	28.00×10^{-3}	68.58×10^{-3}	-0.8134	2.00
LB(S)	52.15×10^{-3}	100.10×10^{-3}	0.9993	2.94
IMM[b]	23.64×10^{-3}	34.05×10^{-3}	0.8676	1.00
IMM[c]	32.30×10^{-3}	51.04×10^{-3}	0.9444	1.5
IMM[d]	267.10×10^{-3}	465.30×10^{-3}	0.9950	-

a.,b. See notes to Table (4.2.1)

c. Competitive inhibition model, Kp" = 10^{-2}M

d. Substrate inhibition model, Ks = 7×10^{-3}M

Fractional conversion (X) was 68% with 2×10^{-3}M AcCh.

FIG(4·3·1)-LINEWEAVER-BURK PLOT
for $CPG_{7.5}$ AcChE(○-LB(S);□-LB)

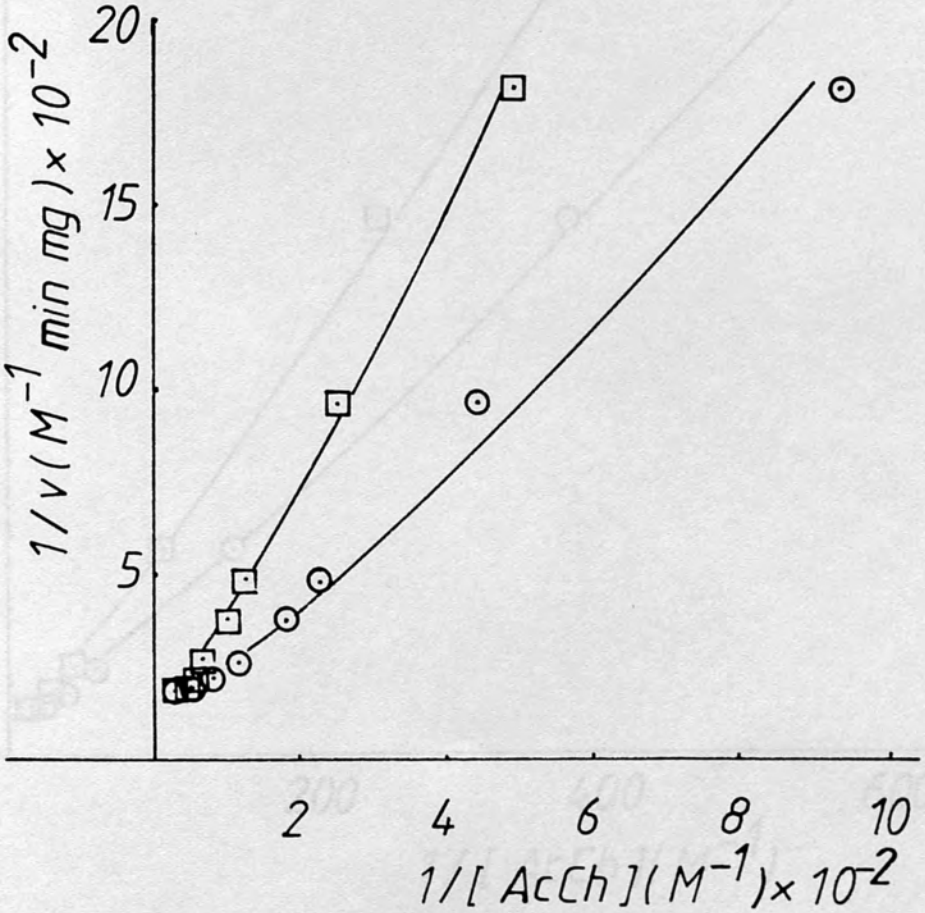

FIG(4·3·2)-LINEWEAVER-BURK PLOT
for CPG_{55} AcChE(○-LB(S); ⊡-LB)

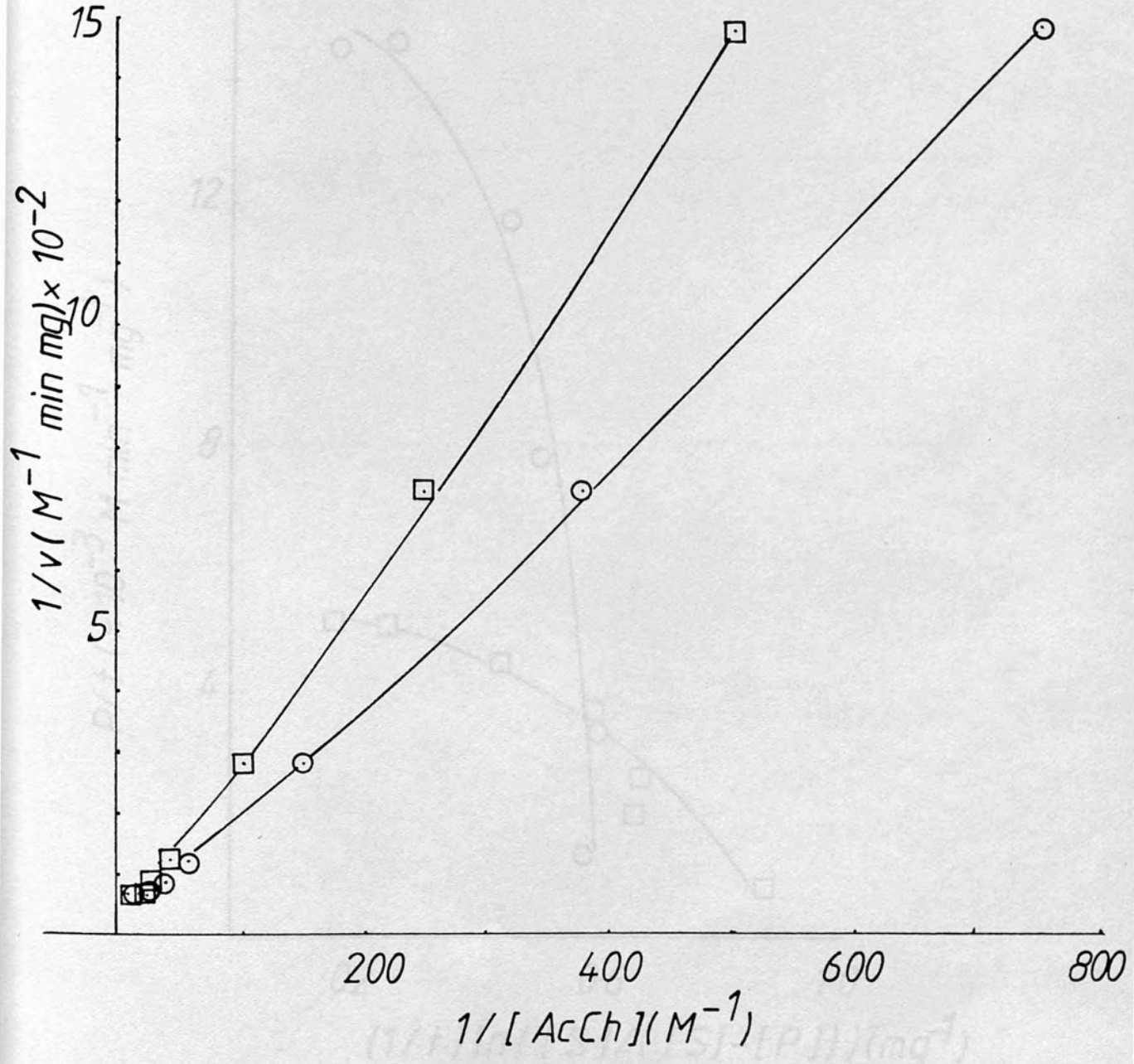

FIG(4·3·3)- INTEGRATED MICHAELIS-MENTEN PLOT for CPG_{75} AcChE(□) and CPG_{55} AcChE(○)

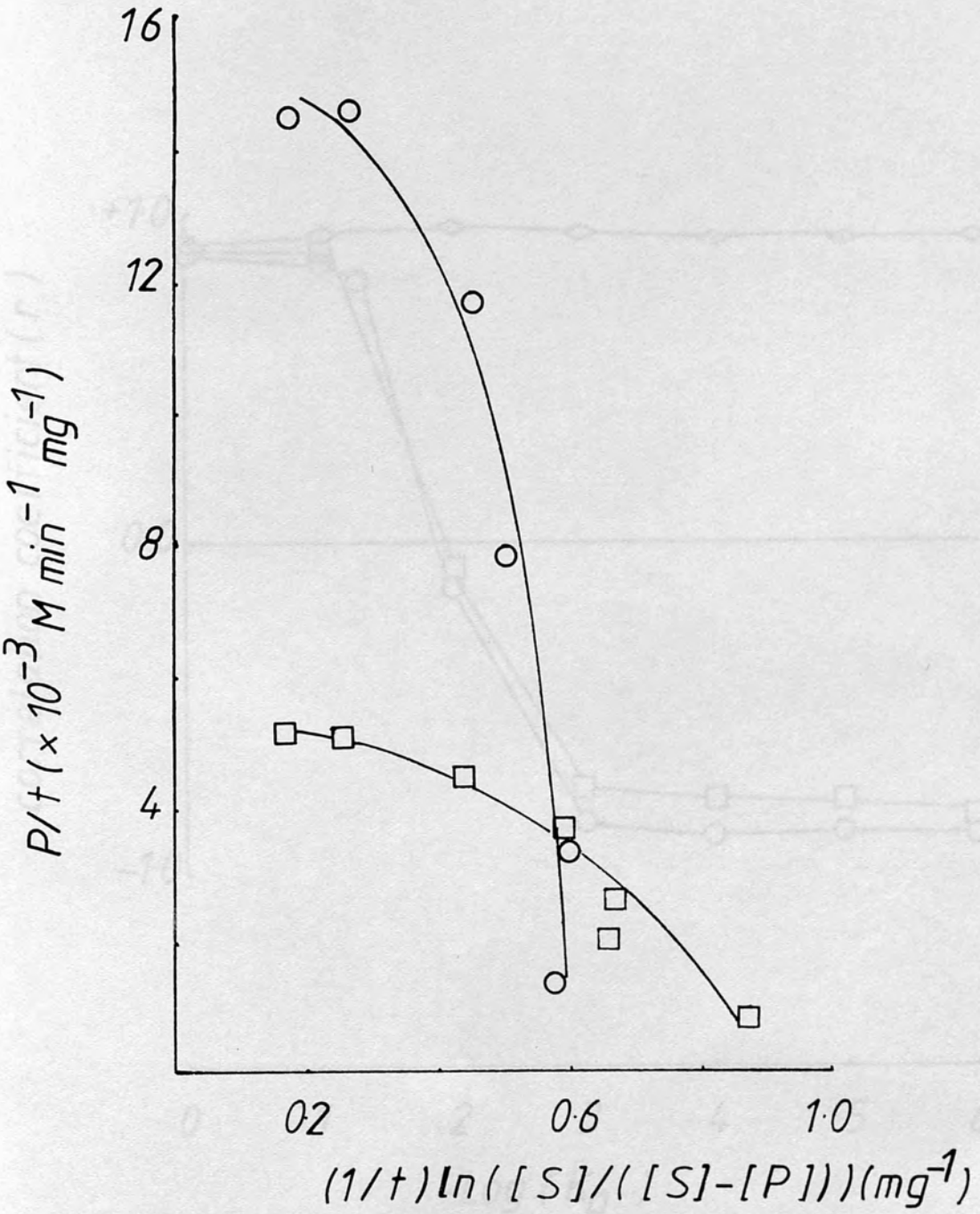

FIG(4·3·4)- Comparison of the competitive product inhibition(⊙), non-competitive product inhibition(⊡) and substrate inhibition(◇)models for $CPG_{7.5}$ AcChE

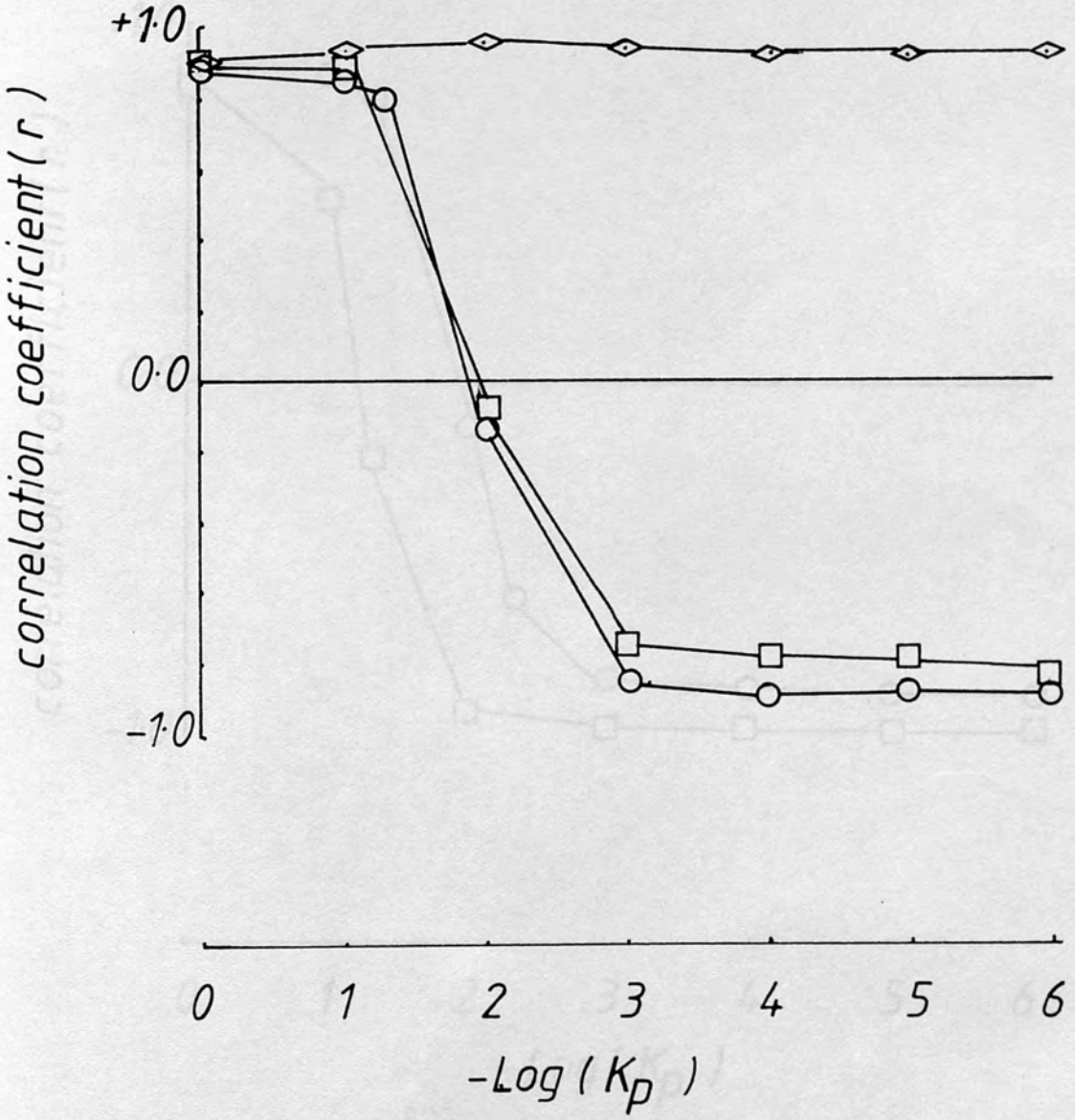

FIG(4·3·5)-Dependence of the IMM PLOT linearity(r), for $CPG_{7.5}$ AcChE(o) and CPG_{55} AcChE(□) on the inhibition constant estimate(K_p)

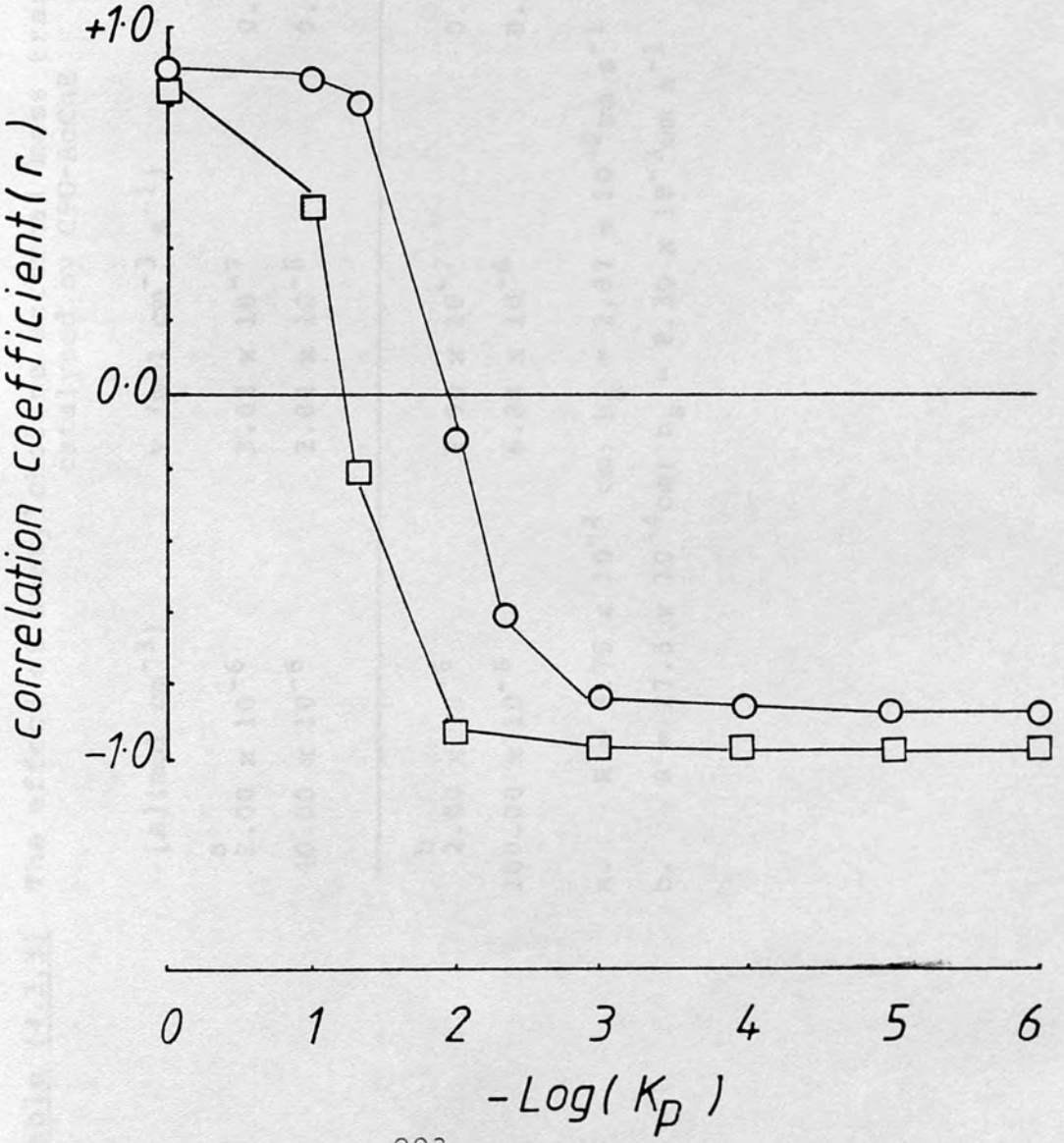

Table (4.3.3) The effect of acetylcholine external mass transfer limitation on the reaction catalysed by CPG-AcChE

[A](mol cm^{-3})	v (mol cm^{-3} s^{-1})	Zm	E_e
a			
2.00×10^{-6}	3.02×10^{-7}	0.0114	1.0
40.00×10^{-6}	2.84×10^{-6}	0.0054	1.0
b			
2.00×10^{-6}	2.90×10^{-7}	0.3546	0.95
100.00×10^{-6}	6.28×10^{-6}	0.1540	>0.98

a. $R = 3.75 \times 10^{-4}$ cm; $h_s = 2.87 \times 10^{-2}$cm s^{-1}

b. $R = 27.5 \times 10^{-4}$cm; $h_s = 8.30 \times 10^{-3}$cm s^{-1}

Table (4.3.4) The effect of acetylcholine internal mass transfer limitation on the reaction catalysed by CPG-AcChE

$[A]^*$ (mol cm^{-3})	v"[a]	$\emptyset m^2$	E_i
[b] 1.14×10^{-7}	5.28×10^{-6}	0.2064	>0.9
2.30×10^{-6}	4.96×10^{-5}	0.0967	>0.9
9.02×10^{-8}	6.44×10^{-6}	17.13	0.06
4.51×10^{-6}	13.97×10^{-5}	7.44	0.24

a. v" (mol s^{-1} cm^{-3} (CPG))

b. $R = 3.75 \times 10^{-4}$ cm

c. $R = 27.5 \times 10^{-4}$ cm

$D_{eff} = 3.5 \times 10^{-6}$ cm^2 s^{-1}

Table (4.3.5) Mass transfer and kinetic parameters for CPG_{55}AcChE

	a	b	c
$^{a}\emptyset$; $\emptyset m^{b}$	40.20	17.13	37.87; 24.29
E_i	0.03	0.06	0.026; 0.04
Km´ (M)	8.4×10^{-4}	2.04×10^{-3}	-
$Km_{7.5}$ (M)	2.15×10^{-3}	6.17×10^{-3}	-

a. `Comparative method´

b. `Fast Evaluation method´

c. Direct calculation, (See notes to Table (4.2.9))

4.4 The kinetics of ascorbate oxidation catalysed by ascorbate oxidase immobilized on controlled porosity glass

Ascorbate oxidase catalyses the oxidation of L-ascorbate to L-dehydroascorbate (4.4.1).The aerial oxidation of various hydroquinones, aminophenols and ascorbic acid derivatives is also catalysed.

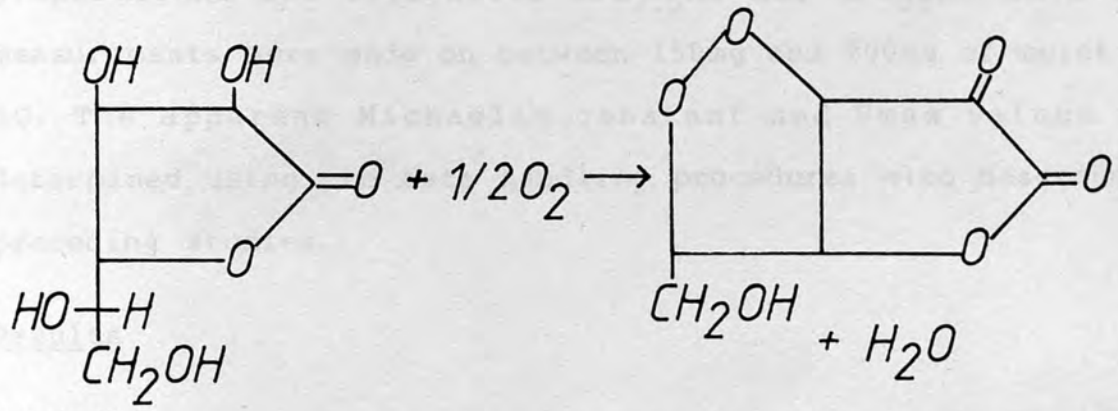

(4.4.1)

Ascorbate oxidase differs from glucose oxidase (s 4.2) in being a cupraprotein and not a flavoprotein; it can be seen from the above reaction (4.4.1) that oxygen is reduced to water and not hydrogen peroxide as in the glucose oxidase reaction . Thus the stoichiometry of ascorbate oxidation is similar to that of glucose oxidation by glucose oxidase in the presence of catalase.

Materials and Method

Ascorbate oxidase or L-Ascorbate:O_2 oxidoreductase (E.C. 1.10.3.3; Type A2769 from Curcubita species, 121 units per mg protein), and L-ascorbic acid were commercial samples, Sigma UK.

All other materials and suppliers were as described in previous sub-sections.

Ascorbate oxidase (AO) was immobilized on 7.5μ and 55μ diameter porous glass supports as described elsewhere (Chapter 2; s 4.1). As in the preceding examples the two immobilized enzyme preparations are designated $CPG_{7.5}AO$ and $CPG_{55}AO$ as before; measurements were made on between 150mg and 200mg of moist CPG-AO. The apparent Michaelis constant and Vmax values were determined using the data handling procedures also described in preceding studies.

Results

The enthalpy of ascorbate oxidation in phosphate buffer (0.2M, pH 7.0; with 10^{-3}M EDTA) was estimated as 111.7 kJ mol^{-1}.

The apparent kinetic constants for $CPG_{7.5}AO$ and $CPG_{55}AO$ are listed in Table (4.4.1) and Table (4.4.2); the final estimates for Km^{app} are 9.6×10^{-5}M and 1.4×10^{-4}M for the small and large diameter support respectively. It should be noted that the linearity of the simple IMM plot is low for both support diameters. The kinetic data from CPG-AO were subsequently fitted to the non-competitive/competitive product inhibition and substrate inhibition models. For $CPG_{7.5}AO$ the substrate inhibition model ($Ks = 1.8 \times 10^{-2}$M) appears to provide the best fit to the data whilst for $CPG_{55}AO$ the best fit is obtained from the competitive product inhibition pattern ($Kp'' = 2.5 \times 10^{-5}$ M)

Table (4.4.1) Apparent kinetic constants for $CPG_{7.5}A0$

PLOT	Vmax ($Mmin^{-1}$ mg^{-1})	a_{Km}*	r	Km/Km^{app}
LB	4.42×10^{-4}	7.81×10^{-4}	0.9401	8.16
EADIE	3.20×10^{-4}	3.00×10^{-4}	-0.5848	3.12
LB(S)	4.10×10^{-4}	4.11×10^{-4}	0.9203	4.29
IMM [b]	2.94×10^{-4}	9.57×10^{-5}	0.5300	1.0
IMM [c]	1.97×10^{-4}	2.30×10^{-6}	0.4330	-
IMM [d]	3.80×10^{-4}	1.74×10^{-4}	0.7085	-

a. General estimate of Km^{app}

b. $Kp = 10^{8}$

c. Competitive product inhibition, $Kp'' = 2.5 \times 10^{-5}M$

d. Substrate inhibition, $Ks'' = 1.8 \times 10^{-2}M$

Table (4.4.2) Apparent kinetic constants for CPG_{55} AO

PLOT	Vmax ($Mmin^{-1}$ mg^{-1})	a_{Km}*	r	Km/Km^{app}
LB	2.33×10^{-4}	1.35×10^{-3}	0.9285	9.40
EADIE	1.25×10^{-4}	2.56×10^{-4}	-0.4852	1.78
LB(S)	2.28×10^{-4}	8.18×10^{-4}	0.8950	5.70
IMM	1.10×10^{-4}	1.44×10^{-4}	0.4770	1.0
IMM[c]	1.13×10^{-4}	5.16×10^{-5}	0.8100	-
IMM[d]	1.70×10^{-4}	3.34×10^{-4}	0.6400	-

a.,b. see notes to Table (4.4.2)

c. Competitive product inhibition, Kp" = 2.5×10^{-5}M

d. Substrate inhibition Ks = 10^{-2}M

Because of some uncertainty in assigning a particular inhibition pattern for both enzymes, subsequent accessment of diffusion effects employed data from the sample IMM plot.

The results of the fast evaluation of external and internal mass transfer are presented in Table (4.4.3) and Table (4.4.4) for $CPG_{55}AO$ only. $CPG_{7.5}AO$ exhibited no external or internal diffusion control according to the assessment by the above method. According to the comparative approach the internal effectiveness factor for $CPG_{7.5}AO$ was only 0.35. Other mass transfer and kinetic data are listed in Table (4.4.5). From these the final intrinsic Km estimate is $(2 \pm 0.8) \times 10^{-5}$M for $CPG_{55}AO$ and $(6 \pm 4) \times 10^{-5}$M for $CPG_{7.5}AO$

Table (4.4.3) The effect of oxygen mass transfer on the reaction catalysed by $CPG_{55}AO$

v(mol cm^{-3} s^{-1})	Zm	ϕm^2	E_e	E_i
a,b 2.38×10^{-8}	0.0920	-	0.9	-
a,c 7.90×10^{-8}	0.3042	-	0.70	-
v"(mol s^{-1} cm^3 (CPG))				
b,d 3.78×10^{-7}	-	2.15	-	0.45
c,e 1.25×10^{-6}	-	10.30	-	0.12

a. $[O_2] = 2.5 \times 10^{-7}$ mol cm^{-3}

b. $[A] = 2.1 \times 10^{-7}$ mol cm^{-3}

c. $[A] = 2.1 \times 10^{-6}$ mol cm^{-3}

d. $[O_2]^*_s = 1.58 \times 10^{-8}$ mol cm^{-3} (CPG)

e. $[O_2]^*_s = 1.10 \times 10^{-8}$ mol cm^{-3} (CPG)

Table (4.4.4) The effect of ascorbate mass transfer on the reaction catalysed by $CPG_{55}AO$

v(mol cm^{-3} s^{-1})	Zm	$\emptyset m^2$	E_e	E_i
a,b 2.38×10^{-8}	0.2029	-	0.9	-
a,c 7.90×10^{-8}	0.0270	-	1.0	-
v"(mol s^{-1} cm^3 (CPG))				
b,d 3.78×10^{-7}	-	0.81	-	0.14
c,e 1.25×10^{-6}	-	9.55	-	0.18

a. $[A] = 2.10 \times 10^{-7}$ mol cm^{-3}

b. $[A] = 5.14 \times 10^{-6}$ mol cm^{-3}

c. $[A]^*_s = 1.03 \times 10^{-8}$ mol cm^{-3} (CPG)

d. $[A]^*_s = 3.15 \times 10^{-7}$ mol cm^{-3} (CPG)

Table (4.4.5) Mass transfer and kinetic parameters for $CPG_{55}A0$

	a	b	c
0, Om	10.38	8.81	10.74; 6.31
E_i	0.964	0.2	0.093; 0.13
Km (M)	1.40×10^{-5}	2.53×10^{-5}	-
$Km_{7.5}$ (M)	3.32×10^{-5}	9.57×10^{-5}	-

a. Comparative method

b. Fast evaluation method

c. Direct calculation

4.5 Discussion

4.5.1 Non-initial rate effects

Although the LB, Eadie, and Hanes plots, Table (1.2.2.1), are all variants of the Michaelis-Menten equation they do not give equally accurate estimates of kinetic constants. The LB plot is currently the most frequently used method for data reduction in enzyme kinetics. It is however also the least accurate plot for determining Km and Vmax values from unweighted data. This is owing to the undue weight given to initial rate measurements from the lower end of the substrate concentration range. The LB plot is the least sensitive to deviations from Michaelis-Menten behaviour and gives the best closeness of fit to data at any level of imprecision. By comparsion, the Eadie and Hanes plots are both equally superior with respect to the above considerations, Dowd and Riggs 1965 (211).

It would appear that these remarks apply equally well in the presence of non-initial rate effects. According to Lee and Wilson (187), the use of the modified double reciprocal, LB(S), plot instead of the LB plot, will result in acceptable estimates (i.e., with <5% precision) of Km at as high as 50% substrate conversion. This view has however been questioned by Karanth and Srivastara (189); they showed that the level of precision involved under the above circumstances to be an order of magnitude greater. It is their recommendation that the IMM plot should be adopted whenever X exceeds 10%.

The ratio Km^*/Km^{app} may give some indication of the level of non-initial rate effects and the inherent shortcomings of the LB plot. That is, a large ratio might be expected when deviation from Michealis-Menten behaviour is greatest as a result of substrate depletion and inhibition by product(s) or substrate(s). However, overall it is difficult to see a clear pattern, for instance between X and Km^*/Km^{app}, Table (4.5.1.1). The ratio is is largest for the $CPG_{7.5}$urease system although X is not. A pattern which does emerge, however, is that the errors in the Km^{app} estimate are with the exception of CPG-AO, greater for enzymes on the 7.5μ diameter support. Product inhibition interestingly follows this same pattern. With the exception of the CPG-AO system, the apparent strength of product inhibition (this is related to 1/Kp") is about on order of magnitude greater for enzymes immobilized on the 7.5μ as compared to the 55μ support. As discussed elsewhere, (s 1.4) and in more detail below, diffusion effects too can contribute to errors in the estimation of Km^{app}. An interesting possibility is that particular deviations from Michaelis-Menten behaviour arising from diffusion effects can cancel out the effects of e.g., competitive product inhibition so as to give seemingly normal behaviour. In accord with the earlier suggestion that the Eadie plot is superior to the LB plot, the former gave smaller errors in the estimation of Km^{app} for all eight examples studied. In the evaluation of Km^*/Km^{app} it was assumed that the simple IMM plot gave the most accurate estimates of Km^{app}; it is certainly true that the IMM plot often gave the smallest estimates. Non-initial rate effects result in a positive error in, or inflation of, the

Table (4.5.1.1) Non-Initial rate effects for selected CPG-immobilized enzymes

System	X	S/Km´	Km^*/Km^{app}
$CPG_{7.5}$urease	0.60	0.64	40.8
CPG_{55}urease	0.32	2.0	2.8
$CPG_{7.5}$GLO/CAT	0.87	2.2	1.7
CPG_{55}GLO/CAT	0.13	0.62	1.0
$CPG_{7.5}$AcChE	0.95	0.50	8.0
CPG_{55}AcChE	0.68	0.4	5.5
$CPG_{7.5}$AO	0.78	1.0	8.2
CPG_{55}AO	0.62	1.0	9.4

general estimate of Km^{app}, Km^{*}.

4.5.2 Non-linear kinetic plots

Various non-linearities in the LB and Eadie plots have been widely discussed in connection with immobilized enzyme kinetics. As mentioned above (s 1.4) the slope of the LB plot is increased in the presence of mass transfer limitation. There is also an upward curvature in the region of low substrate concentration where diffusion effects are greatest. In the presence of competitive product inhibition a pattern of deviation similar to that caused by diffusion control can arise.

The Eadie plot is more useful than the LB plot in that more distinctive irregularities are expected to result from non-Michaelis-Menten behaviour. As shown by Engasser and Hovarth (99) this plot is linear in the absence of diffusion control. A convex plot, however, may arise either from the effects of external diffusion control or non-competitive product inhibition. Competitive inhibition on the other hand produces a concave plot. Since the effects of external diffusion (convex plot) and competitive product inhibition (concave plot) are opposite, their combination can produce a linear, seemingly Michaelis-Menten, response. Finally, internal diffusion control results in a sigmoidal Eadie plot. This shape can, however, be obscured if a study is carried out over an insufficiently wide range of substrate concentration. A deficit of high substrate

deficit of high substrate concentration points) it is readily shown, by comparing the relative positions of the co-ordinates v,v/s andv, v/(S) in an Eadie plot that this pattern can also be caused by substrate depletion. The convexity of the Eadie plot for enzymes immobilized on the 7.5μ support may thus be due to substrate depletion. It is true that a greater non-linearity is seen for 55μ supports, in most cases, as would be expected if diffusion effects were also important.

In view of the above results the diagnostic significance of particular non-linearities in the classical kinetic plots, as suggested by theoretical studies, must now be in some doubt. Under non-ideal, experimental conditions when there may be significant non-initial rate effects, particular diagnostic features appear to be less specifically due to single mechanisms. Greater care is recommended therefore in deriving conclusions from such irregularities in the absence of other supporting evidence.

4.5.3 Analysis of inhibition effects

Inhibition by substrates and products is an important means of control of enzyme activity in nature. The extent of such inhibition is also an important determinant of the apparent kinetics. Inhibition may for example reduce the efficiency of an immobilized enzyme column (in the absence of diffusion effects) and must therefore be considered a potential problem. The approach used in obtaining a three-parameter fit to kinetic data

was based on a suggestion by Eftink et al.(35); only the case for competitive product inhibition was examined by these workers. In addition non-competitive product inhibition and substrate inhibition have been shown to be amenable to similar analysis in s. 4.1 to 4.4. In fitting the raw data to particular inhibition models it was found useful to present first the results in a pictorial -log Kp against $t_{(\frac{1}{2})}$ plot. A general feature of such plots is that maximal linearity (large correlation coefficient) is observed at very large or very small assumed values of the inhibition constant, Kp. The apparent inhibition constant was determined as the lowest assumed value consistent with 95% maximum linearity. The location of Kp" by such means was completly empirical; the condition for significant product inhibition (Kp" < Km) however was only even occasionally met when the above approach was adopted for finding Kp".

In the analysis for non-competitive product inhibition, it is necessary to assume that Km << Kp in order to remove an unknown term Km from the right-hand side of the appropriate IMM equation. This changes the expression P/t [1 - P/(2Km - 2Kp)] to P/t (1 + P/2Kp). There would appear to be no clear reason for supposing that enzyme affinity for the substrate will be greater than the affinity for the product, especially since binding occurs at different sites, in non-competitive inhibition.

The shape of the - log K_s against r plots differs from the product inhibition curves in two respects. First, the former only

have positive slopes. Secondly, there is single maximum and a relatively weak dependence of linearity, r, on the assumed value of K_S.

The results of the above analyses are summarized in Table (4.5.3.1) together with other kinetic parameters. Inspection of, e.g., Table (4.1.3), (4.2.1), (4.3.1), (4.4.1) and (4.4.2) will reveal that in all cases more than a single inhibition pattern fits. This may be because most of the enzymes studied are susceptible to inhibition by more than a single species. Urease, for instance, is inhibited by the substrate and product, urea and the ammonium ion respectively, Wall and Laidler (177)), Hoare and Laidler (175). This enzyme is also inhibited by potassium and sodium ions, and activated by phosphate, Fasman and Nieman (176). Acetylcholinesterase is known to be inhibited by acetylcholine and choline, (substrate and product respectively). Various ammonium ion analogue are also good inhibitors Krupka and Hallenbrand 1974 (212). This is important because it means that protonated THAM buffer $(CH_3OH)_3\ N^+H$ may also inhibit AcChE. Acetate too is a structural analogue of part of the substrate and may also be capable of inhibition. The present method for studying inhibition therefore does not allow clear identification of the inhibiting species. The correct fit of data to a particular inhibition model is however useful; it could perhaps form the basis of a decison to carry out more detailed study along the lines suggested by Dixon 1953 (213).

The product inhibition constants for CPG-urease, CPG-GLO/CAT and

Table (4.5.3.1) Summary of kinetic parameters for selected CPG immobilized enzymes

System	Km^{app}(M)	Km´(M)	Vmax	E_i	Ki (M)
$CPG_{7.5}$urease	7.56×10^{-3}	7.56×10^{-3}	24.83×10^{-3}	-	Kp - 7.1×10^{-3} Ks - 3×10^{-1}
CPG_{55}urease	53.82×10^{-3}	2.42×10^{-3}	26.27×10^{-3}	0.07	Kp- 35.0×10^{-3} Ks - 3×10^{-1}
$CPG_{7.5}$GLO/CAT	3.20×10^{-4}	$2 \pm 1.3 \times 10^{-4}$	3.20×10^{-4}	-	Kp - 8.91×10^{-5} Ks - 1×10^{-1}
CPG_{55}GLO/CAT	6.78×10^{-3}	$8 \pm 3.4 \times 10^{-4}$	2.17×10^{-4}	0.09; 0.14	Kp - 1.0×10^{-3} Ks - 8×10^{-3}
$CPG_{7.5}$AcChE	7.26×10^{-3}	$4 \pm 2.8 \times 10^{-3}$	7.12×10^{-3}	-	Kp - 1.0×10^{-3} Ks - 2×10^{-2}
CPG_{55}AcChE	34.10×10^{-3}	$1.4 \pm 0.8 \times 10^{-3}$	23.64×10^{-3}	0.03; 0.04	Kp - 1.0×10^{-2} Ks - 7×10^{-3}
$CPG_{7.5}$AO	9.57×10^{-5}	$6 \pm 4.5 \times 10^{-5}$	2.94×10^{-4}	-	Kp - 2.5×10^{-5} Ks - 1.8×10^{-2}
CPG_{55}AO	1.44×10^{-4}	$2 \pm 0.8 \times 10^{-5}$	1.10×10^{-4}	0.09; 0.13	Kp - 2.5×10^{-5} Ks - 1×10^{-2}

CPG-AcChE are between 5-11X larger for the 55μ diameter supports compared to the 7.5μ support. Under such circumstances Kp must be considered an apparent product inhibition constant, Kp". The strength of product inhibition is reduced by a factor of 5 to 11 for the larger diameter supports. This may be practical evidence for the antienergistic interaction between mass transfer limitations and enzyme inhibition proposed by Engasser (s 1.3). Other factors, such as a possible difference in the microenvironment of associated with the 7.5μ and 55μ supports, may also be important regarding the above difference in Kp".

Substrate inhibition will appear to be quite unique regarding possible interaction with mass transfer effects. It can be seen from Table (4.5.2) that Ks is either insensitive to support diameter (CPG-urease) or decrease in value with the larger diameter support.

4.5.4 Intrinsic kinetics of CPG bound enzymes

It is of interest to consider the Km estimates for CPG-urease, CPG-GLO/CAT, CPG-AcChE and CPG-AO with regard to:

a. the corresponding Km^{app} values

b. the methodology for their evaluation

c. the congruency of the Km estimates from pairs of supports and

d. the relation to the Km of the same enzyme in free solution.

External and internal mass transfer effects are expected to result in an increase in the intrinsic Km. With either form of diffusion control the increase in Km is related to the respective

substrate moduli. These are in turn a function of enzyme activity, the intrinsic Km, support dimensions and substrate (effective) diffusivitiy. As these variables mostly differ from one enzyme system to another the same ratio of Km^{app}/Km' would not be expected in the four pairs of immobilized enzymes.

The two methods for the indirect assessment of diffusion effects give surprisingly similar results in view of the considerable differences in approach involved. Internal diffusion control, is consistently assessed as 33 - 35% less by the comparative method than by the fast evaluation approach. Some merits of the fast evaluation method are as follows:

a. only a single immobilized enzyme preparation is required
b. diffusion assessment is possible from a minimum of data, ie. one rate measurement at any substrate concentration of choice,
c. external and internal diffusion effects can be measured separately, and
d. mass transfer effects expressed towards individual species (e.g. for enzymes, with multiple substrate, like glucose and ascorbate oxidase) can be analysed separately.

The main disadvantages of the fast evaluation method is the need to know substrate mass transfer rate parameters like the diffusivity, effective diffusivity and external mass transfer coefficient; the latter can be estimated (s 4.1).

The comparative approach depends on the direct comparison of two

or more immobilized enzyme preparations differing only with respect of support dimensions (and hence the extent of diffusion limitations). It has the virtue that the only additional information required are the two support radii. On the other hand the application of the comparative method initially requires steady state kinetic analysis to determine a minimum of two Vmax" and Km^{app} measurements. The above method is also only applicable to the analysis of internal mass transfer effects. It is required that external diffusion limitations are rendered insignificant by the use of high sample flow rates during a study.

The requirement for two or more similar immobilized enzyme preparations, on closer examination, is not so easily satisfied. Diffusion control also acts upon the mass transfer of products from a support surface. Thus there may be greater accumulation of product within the microenvironment of an enzyme immobilized on a larger rather than a smaller diameter, support. In the case of an enzyme like urease, a large difference in product accumulation between two immobilized enzyme preparations, differing only in terms of support diameter, would be translated into a greater microenvironmental pH increase in the case of the larger diameter support. The Km of urease decreases with increasing pH, Howell and Sumner 1934 (215), therefore two such immobilized urease preparations might be expected to show differences in intrinsic kinetics.

A similar diffusion related micro-environmental difference in oxygen concentration could result in different intrinsic kinetics

expressed by oxidases immobilized on supports of widely differing diameters. The Km of glucose and ascorbate oxidase for their respective reducing substrates decreases with decreasing oxygen concentration. The mass transfer of oxygen would appear to be limiting for both oxidases immobilized on the 55μ, but not the 7.5μ support; Table (4.2.5), Table (4.2.7), and Table (4.4.3). Thus the intrinsic Km of these immobilized enzymes would be expected to be lower on the larger diameter support. Evidence is presented below in support of this view. It can be seen therefore that the requirement for two or more similar immobilized enzyme preparations may be difficult to meet even after standardising such variables as the choice of support, immobilization chemistry and the conditions of study.

The Km of soluble urease in phosphate buffer is sensitive to the buffer capacity. For instance the Km at neutrality is 27×10^{-3}M, 26×10^{-3} M, 50×10^{-3} M, and 60×10^{-3} M with 0.067M, 0.158M, 0.267 M, and 0.75M phosphate buffer respectively, Beezer (149). With a buffer concentration of IM the Km is 126.4×10^{-3} M, Laidler and Hoare (174). The Km of urease in THAM-H_2SO_4 buffer (4.0×10^{-3}M) is however independent of buffer concentration, Wall and Laidler (177). When urease is studied in the absence of buffer, using a "pH-stat" method (pH 7.0), the Km is typically $2.5 - 3.0 \times 10^{-3}$ M Sundaram (180). As stated earlier urease is activated by the phosphate anion; it may be that a Km increase under such circumstances is an integral part of this effect. There may also be some relation between the increased Km and high

ammonium ion concentration. Given the above background it is clearly difficult to compare the apparent Michaelis constant estimates for $CPG_{7.5}$ urease (7.56×10^{-3}M) and CPG_{55} urease (53.83×10^{-3} M) with the Km of the soluble enzyme (n 20 - 30 $\times 10^{-3}$ M). As discussed above, the immobilized urease system is often characterised by a drop in the microenvironmental pH and hence reduced buffer capacity within the support matrix. Under these circumstances a Km of 7.56×10^{-3}M might be expected. This would mean that the immobilization of urease on CPG does not affect the Km of urease under the present conditions of study. Apart from the special case of oxidases (see below) there is little or no precedence for a large decrease in Km as a result of glutaraldehyde coupled enzyme immobilization to alkylamine glass. On the other hand Ramachandran and Pelmutter (182) have determined the Km of soluble and non-porous glass (NPG) bound urease as 3.9×10^{-3} M and 5.4×10^{-3} M, (THAM - Maleic acid buffer, pH 6.5) respectively.

There have been surprisingly few reports during dealing with the steady state kinetics of oxidases under ordinary laboratory conditions i.e., at ambient oxygen partial pressure. Most investigators have instead preferred to determine the ratios of microscopic rate constants, $[K_{ox}/K_{cat}]$ and $[K_{ox}/K_r]$, Fig. (4.2.1). As discussed above these ratios relate to the Michaelis constant for oxygen and glucose at a saturating concentration of the other co-substrate.

Table (4.5.4.1) Kinetic parameters for soluble and immobilized glucose oxidase and ascorbate oxidase

System	$k_{ox}/k_{cat}(M^{-1})$	Km_0 (M)	k_{ox}/k_r	Km_s (M)
a,b,c GLO	2000	5×10^{-4}	140	70×10^{-3}
a,b NPG-GLO	1650	6.1×10^{-4}	139	84×10^{-3}
c CPG-GLO	2000	5×10^{-4}	10	5×10^{-3}
d CPG-GLO/CAT*	-	-	1.6	8.1×10^{-4}
e CPG-GLO/CAT*	-	-	0.46	2.3×10^{-4}
f AO	4166	2.4×10^{-4}	2.20	5.3×10^{-4}
f AO*	-	-	0.87	2.1×10^{-4}
d CPG-AO*	-	-	0.08	1.96×10^{-5}
e CPG-AO*	-	-	0.27	6.44×10^{-5}

a Malikkides and Weiland 1972; dp = 841-1000

b Ramachandran and Pelmutter 1976, dp = 200

c Weibel and Bright 1971; dp = 200, E = 0.06

d This work, dp = 55μ ; E = 0.09 - 0.14

e This work, dp = 7.5μ

f Burstein et al. 1976

* ambient oxygen partial presssure

The above data mostly relates to saturated concentration of co-substrate; studies at ambient partial pressures of oxygen are indicated with an asterisk.

Firstly it is apparent from Table (4.5.4.1) that the intrinsic Km of glucose oxidase is unaffected by immobilization on NPG. Binding to CPG however resulted in a 14 times decrease in the Km for glucose in a saturating concentration of oxygen; the Km of CPG-GLO for oxygen; however, remained unchanged. The decrease in Km for glucose was thought to be a reflection of a true change in intrinsic kinetics or else be the result of a microenvironmental accumulation of glucose by an electrostatic mechanism, Weibel and Bright (196). A more plausible explanation given by Ramachandran and Pelmutter (182) is based on external and internal diffusion control of oxygen mass transfer and the dependence of Km_G on a reduced microenvironmental oxygen concentration, very much as outlined above. To reiterate this point, the Km of an immobilized enzyme is usually expected to be larger than the Km of the corresponding soluble enzyme. Oxidases would appear to be a special case since diffusion limitation here appears to result in a decrease in the Km for glucose. This may be a consequence of the dependence of Km_G on oxygen concentration and diffusion control expressed towards oxygen mass transfer rate. That is, mass transfer limitation expressed towards oxygen and glucose transport may be opposite on their effect on Km_G.In support of this view the Km for the reducing substrate was decreased at ambient partial pressures of oxygen for both CPG-GLO/CAT and CPG-AO. The above idea predicts that Km_G' should be smaller for GLO/CAT immobilized on the 55μ relative to the 7.5μ support. However, from examination of the estimates in Table (4.5.4.1)using the Student's t-test (α = 0.05), it was found that Km' for enzymes immobilized on the 7.5μ and 55μ supports were not

significantly different. (The above analysis could not be carried out for CPG-urease as an insufficient number of Km estimates were available).

A general appraisal of some of the key ideas above seems necessary. First, the dependence of Km_s on co-substrate (e.g. oxygen) concentration is a general fact applicable to all bi-substrate enzyme systems. Mass transfer control with respect to oxygen for the CPG_{55}GLO/CAT would also appear to be quite certain. In that case the expected difference in Km´ for $CPG_{7.5}$ GLO/CAT and CPG_{55}GLO/CAT might not have materialized for several possible reasons. Firstly, the possibility that there may not have been a sufficiently large number of estimates for effective statistical analysis must be considered; and yet the two pairs of estimates used technically comprise an adequate sample size. Secondly, the glucose oxidase reaction results in the production of acid. Greater acid accumulation in the larger diameter support (cf. urease system) would obscure the expected Km´ difference, provided that the Michaelis constant of glucose oxidase increased with incresing acidity. This question does not appear to have received attention in the literature. The above discussion also applies in general to the ascorbate oxidase system.

The second thing which is clear from Table (4.5.4.1) is that the effectiveness factor for oxidases is reduced by an order of magnitude or slightly more as a result of immobilization on porous support. The theoretical effectiveness factor for CPG-

GLO/CAT (200μ diameter support) has been estimated by Reus and Buchholz (186) as between 0.1 and 0.25 for a system with saturating concentration of oxygen. The range of 0.09 - 0.14 for experimental values (55μ diameter support), in this work at ambient oxygen pressures therefore agrees well with theoretical expectation. The conclusions of Rivito and Kitrel (197) are also interesting. For enzymes with a similar substrate and turnover number as oxygen and glucose oxidase respectively, diffusion free kinetics are expected only when $dp < 26\mu$. For larger molecular weight substrates, (like succinate, MW = 118, D 7.5×10^{-6} cm^2 s^{-1}), the critical particle diameter is 16μ. Such theoretical prediction again seem to be borne out by the experimental results presented in sections 4.1 - 4.4.

It is likely that the activity observed for the 55μ enzyme preparations was derived from enzyme molecules immobilized nearmost to the support surface. Assuming an even distribution of enzyme throughout the support, and from the value of the effectiveness factor, it follows that such enzymes were predominantly located in the 9 -14% outermost layer of support. This conclusion is in accord with the findings of Weibel and Bright (196) and those of Reuss and Buchholz (186).

Finally, all the Km´ estimates for CPG-AcChE combine to give a single estimate with a value of 28×10^{-4}M $\pm$ 23×10^{-4} M. This estimate is not significantly different from the Km of soluble AcChE (1.4×10^{-4} M) assuming the latter to have been determined with 50% precision.

4.5.5 Flow microcalorimetric monitoring of immobilized enzyme systems.

The number of practical, as compared with the number of theoretical, studies of immobilized enzymes is still small. This is in part owing to the physical difficulties involved with the assay of immobilized enzymes outside of flow systems. Flow microcalorimetry, as indicated in Chapter 4, can be applied in a relatively straightforward manner to the study of immobilized enzymes. In fact the practical aspects of the study are little different from those adopted in the steady state analysis of substrate, (Chapter 3). As shown above, the differences between steady state substrate analysis and steady state kinetic analysis lies largely in the methods of data reduction and analysis. Perhaps one of the most cumbersome steps in the kinetic study is the correction of rate measurements for non-initial rate effects. However, although of interest, it is not certain that such correction is in fact necessary for the assessment of diffusion effects. With the fast evaluation method no thought was given to the effects of non-initial rate assay.

Most of the advantages of calorimetric monitoring, over the spectrophotometric or electrochemical methods, discussed in Section 1 apply to the use of calorimetry to the kinetic study of immobilized enzyme systems. The non requirement of artificial (colorigenic) susbtrate with calorimetry is particularly important. An artificial substrate may have a different molecular weight, shape, and electrical properties from the real substrate;

such molecular properties are important determinants of immobilized enzyme characeristics. It is therefore possible for the use of artificial substrates to result in different kinetics being manifest.

The graphical estimation of the apparent inhibition constants and internal and external effectiveness factors represent potential sources of error in the work reported; so do the estimates of the substrate mass transfer parameters (D, D_{eff} and h_s) used. The magnitude of such error in unknown. But the final results will obviously reflect the accuracy of the various parameters used. There are, at this time, insufficient numbers of practical assessment of the fast evaluation and comparative methods in the literature, and thus no current views on these methods. However, it is hoped that the findings reported in Section 4.1 - 4.4, and the discussions above, inspires some degree of confidence in the two approaches.

Chapter 5

The use of viable yeast, Saccharomyces cerevisiae cells immobilized by entrapment in calcium alginate gel in flow microcalorimetric analysis

5.1 General overview of immobilized cell technology

5.1.1 Immobilized cells

Cell immobilization is a natural phenomenon. Thus a large number of cell types have a tendency to form aggregates or become attached to solid surfaces. Stones in a pool or a river may, for example, carry a natural layer of photosynthetic or non-photosynthetic organisms depending on the depth of covering water. The term immobilized cell is however usually applied to artificially contrived examples of bound cell systems. An immobilized cell is any cell, dead or alive, fixed to a carrier or another cell by chemical or physical forces so as to enable re-use, Messing 1980 (216). The terms `structured bed fermentation´ and `controlled catalytic biomass´ have been applied more specifically to immobilized cells involved in complex biocatalysts by Vierth and Venkatsubramanian 1979 (217). The above terms have connotations of the complex subcellular structuring or organisation of enzymes, flow reactor design and control, as well as of the possibility of control of cell activity e.g. by nutrient activation (s 5.3.1). The cells may be viable or non-viable. A distinction is also necessary between immobilized cell systems employing single or multiple enzyme reactions.

Fig. (5.1.1.1)

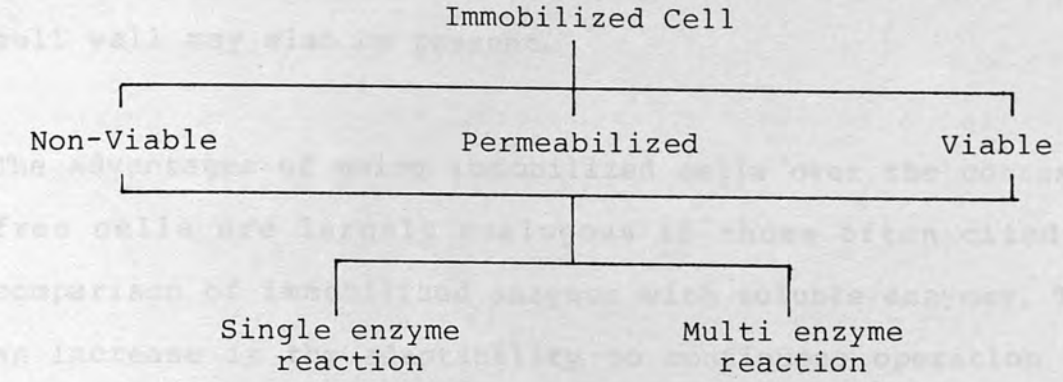

Some of the reasons commonly given for chosing an immobilized cell over the equivalent co-immobilized enzyme system are listed in Table (5.1.1.1).

Table 5.1.1.1) Some reasons for cell immobilization

1. Enzyme extraction and purification unnecessary;
2. Generally increased operational stability;
3. Lower effective catalyst cost;
4. High yield of enzyme activity on immobilization;
5. Cofactor regeneration more easily achieved;
6. Greater likelihood of the retention of native enzyme structure;
7. Greater resistance to environmental perturbation.

It can be seen that these factors combine to make the use of immobilized cells, rather than the corresponding co-immobilized enzyme system, economically more attractive. Against these positive considerations must be balanced a lower specificity due

to the presence of other enzymes, a decreased enzyme concentration per unit volume of reactor, and an extra mass transfer barrier in the form of a plasma membrane; sometimes a cell wall may also be present.

The advantages of using immobilized cells over the corresponding free cells are largely analogous to those often cited in the comparison of immobilized enzymes with soluble enzymes. There is an increase in the adaptability to continuous operation or flow analysis. Free cell cultures can be operated under flow conditions, e.g., in chemostats, James et al. 1976 (218). Such chemostat cultures are however only compatible with relatively low nutrient flow rates in order to avoid the washout of cells. Immobilization enables the use of high dilution or nutrient flow rates without loss of cells from the culture vessel. There is often actual as well as effective increase in the stability of cells as a result of immobilization. The effective or operational stability of immobilized cells may be enhanced by nutrient activation, i.e., periodic exposure to growth media, Foerberg 1983 (219). It seems that entrapment of cells inside the pores within a gel matrix may eventually impose a physical constraint on the increase in cell numbers or biomass. As a result, a greater proportion of substrate is channelled into the formation of product, rather than biomass increase, i.e., there is increased product yield. Finally, owing to the greater concentration of cells per unit reactor volume (compared to the situation with free cells), greater rates of conversion are possible. Alternatively similar rates conversion can be achieved with

smaller reactors.

The four main classes of methods for the immobilization of cells are listed in Table (5.1.1.2) together with a representative selection of supports. Both are virtually the same as those commonly used for enzyme immobilization.

Table (5.1.1.2) Methods and supports for cell immobilization

Adsorbtion	Cross-linking
anion exchange resins	glutaraldehyde
DEAE-cellulose	albumin
metal oxides	gelatin
porous bricks	
glass	
concanavalin-A	
polyvinyl chloride	

Covalent binding	Entrapment
hydroxyaklmethacrylate	polyacrylamide
carboxymethylcellulose	agarose
alkylamine glass	alginate
	collagen
	k-carrageenan
	agar

There is however a difference in emphasis; entrapment rather than covalent binding is the most frequently used method for the

immobilization of cells. The generally mild conditions involved with entrapment results in, on average, the highest (80 - 90%) recovery of cell activity. The problem of leaching of biocatalyst from the gel matrix is less serious with entrapped cells relative to entrapped enzymes owing to the (ca 10^3) greater diameter of cells. Mass transfer effects are,however, on the whole most serious with entrapment.

5.1.2 Co-immobilized multistep enzyme-coenzyme systems and permeabilized cells

Co-immobilized enzyme-coenzyme systems have generated sustained interest over the years as a possible alternative to the use of immobilized cells. The approach may be illustrated by considering the conversion of glucose to alcohol by yeast cells according to the net reaction below, Lehninger 1975 (220).

$$\text{Glucose} + 2\,\text{Pi} + 2\text{ADP} + 2\text{NAD} \longrightarrow 2\,\text{Ethanol} + 2\,CO_2 + 2\,\text{ATP} + 2\,\text{NAD} + 2H_2O$$

The above reaction, alcoholic fermentation, takes place via 12 enzyme catalysed stages. Half the stages involve coenzyme-requiring enzymes. Thus the artificial structuring of alcoholic fermentation would require the co-immobilization of the 12 enzymes together with the coenzymes nicotinamide adenine dinucleotide (NAD), adeninosine-triphosphate (ATP) and a facility for coenzyme regeneration. Such a complex system has not yet been realized. Mosbach and coworkers have however studied two, three and four co-immobilized enzyme systems, Mattiasson and Mosbach 1971 (221). Others have also expended considerable effort in the

study of coenzyme regeneration, LeGoffic and Vincent 1980 (222), Lowe 1981 (223). Some central themes of this work are as follows:

a. regeneration requires the immobilization of the coenzyme in order to allow retention in a reactor for re-use;

b. active coenzyme analogues with long side chains (e.g., available from Sigma UK), rather than the native molecules, are immobilized;

c. the support used can be the same as that used for enzyme immobilization. Binding of both molecules to an insoluble support tends to reduce the frequency of interaction between the immobilized enzyme and immobilized coenzyme. A useful alternative is to immobilize enzyme or coenzyme on a high molecular weight but soluble support eg. dextran, polyethelene glycol or polyacrylamide gel;

d. the actual regeneration may be carried out by electrochemical, photochemical or enzymic means.

The second alternative to the use of immobilized intact cells in complex biocatalysis is the use of immobilized permeabilized cells. The cell envelope, i.e., plasma membrane (and cell wall in plants) is an important means of homeostasis (i.e., for maintaining constancy in the intracellular environment) due to its selective permeability. Generally only small molecular weight or neutrally charged molecules can enter or leave the cell freely. Other species enter after extracellular hydrolysis and/or interaction with carrier proteins in the cell membrane.

The term permeabilization is applied to a series of unrelated

techniques for the partial or complete removal of the permeability barrier to the passage of substrate and solute. Permeabilization may result from physical damage to the cell membrane. Examples of treatments resulting in cell permeabilization include exposure to electric current, Knight 1982 (224), organic solvents, antibiotics, detergents and chelating agents. Permeabilization may also be achieved by physical methods, e.g. temperature or osmotic shock. The subject of permeabilized cells has recently been reviewed by Felix 1982 (225).

The use of permabilized cells would appear to be essential where there is emphasis on:

a. the transformation of large molecular weight substrates e.g. steroids, Larsson et al., 1979 (226) and alkaloids, Brodelius and Nilsson 1983 (227);
b. the assay of complex processes e.g. protein and deoxyribonucleic acid (DNA) synthesis, and their interaction with xenobiotics, in situ,
c. coenzyme regeneration by immobilized cell systems.

In each of the cases cited , permeabilization allows the exchange of added reagent across the cell envelope.

5.1.3 General and analytical application of immobilized cells

Some current and foreseeable areas for the application of immobilized cells are in:

a. syntheses or transformations;

b. analyses (cf Table (5.1.3.1);

c. waste water treatment;

d. biological fuel cells;

e. affinity chromatography;

f. medicine,

g. the recovery of metals from effluents.

The area of production has received much attention. The commercial production of, e.g., aspartic acid, malic acid and ethanol using immobilized cells has been established. There is also active interest in immobilized cell based production of antibiotics, hormones, Mosbach et al 1983 (228) immunoglobulins, Nilsson et al 1983 (229), viruses, coenzymes, and various organic acids (249).

Bioassay, the use of living systems for assay purposes, has a long history, Bush 1982 (229). The basic principle is the measurement of growth of an organism in response to amounts of analyte. Significant progress in this area has been made in the past 10 years (as can be seen in the development of microbial electrodes for a large number of organic species, Table (5.1.3.1) A major factor was the realization that the index in classical bioassay, i.e. cell growth, is always preceded by relatively rapid changes in metabolism. Thus the exposure of cells to substrate may result in a change in the steady state uptake of oxygen and excretion of, e.g., NH_4^+ or CO_2. So, the presence of an inhibitor (e.g., a drug or environmental pollutant) may produce a concentration-related change in some aspect of metabolism.

Table (5.1.3.1)

Substrate	Organism	Sensor	Reference
ethanol, acetic acid ammonia	Trichosporan brassiae	oxygen electrode	231
glucose	saccharomyces cerevisiae	thermistor	232
chloresterol		oxygen electrode	234
biodegradeable organic matter	mixed culture clostridium butyricum	oxygen electrode	235 238
nitrate	nitrobacter spc	oxygen electrode	235
phenol		oxygen electrode	237
tyrosine	citrobacter freundii sugar beet (slice)	NH_3 (gas) electrode oxygen electrode	238 239
L-histidine	pseudomonus spc		240
L-serine	clostridium acidiurici	NH_3(gas) electode	241
L-glutamine	Sacina flava	NH_4^+ (ISE*)	242
purvrate			243
cephalosporins	citrobacter freundii	glass (pH) electrode	244
glucose	pseudomonas flourescens	oxygen electrode	244
5´-AMP	rabbit muscle slice	NH_3 (gas) electrode	245
hydrogen peroxide	liver slice		246

(*ISE -ion electrode)

An important difference between immobilized cell and immobilized enzyme based analysis relates to specificity. Owing to the presence of a large number of enzymes, cell-based analytical systems are generally less descriminating between related compounds. The general nonspecificity of immobilized cells compared to immobilized enzymes leads to the possibility of developing broad spectrum sensors, i.e. sensors sensitive to a complex mixture of ill-defined (but biodegradable) organic compounds in a sample. Table (5.1.3.1) lists some of the species so far determined using immobilized cells (or tissue slices) in combination with various sensors.

There is now an extensive literature on immobilized cells. The reviews by Messing 1980 (216) Bucke and Wiseman 1981 (230), Bucke 1982 (247) and Chibata 1983 (248) are useful sources dealing with general aspects of immobilized cell technology; the recent monograph, `Immobilized cells and organelles´ Volume I and Volume II, edited by Mattiasson 1983 (249) deals with all major aspects of this rapidly developing area. Analytical applications have recently been reviewed by Mattiasson 1979 (250).

5.1.4 Yeast structure and characteristics

The yeast are single-celled rather than coencytic (i.e., a multinucleate mass of protoplasm without dividing cell membrane) like the majority of organisms belonging to the group fungi. Beyond that the term `yeast´ appears to have little taxonomic significance and applies to organisms with diverse characteristics.

Saccharomyces cerevisiae, perhaps the most familiar yeasts (cf baker's years, brewer's yeast) are spheroid, ovoid or elongated cells with overall dimensions of 3 - 10μ by 4 - 20μ, Singleton and Sainsbury 1978 (251). A cell envelope comprising a plasma membrane and a cell wall surrounds each cell. The structure of the former would appear to conform to the fluid mosaic model of membrane structure proposed by Singer and Nicholson 1972 (252). The cell wall consists of a two-layer glucan layer and an external mannan layer. The cell envelope as a whole contains about 51% lipid (i.e.,compounds soluble in organic solvents eg. fats and nonsaponifiable classes like steroids and squalene.)

The plasma membrane functions as a general barrier to the entry of polar compounds into yeast cells. Hexoses, eg., glucose, fructose, and mannose, gain entry only after binding with specific membrane carriers or transport proteins. The cell wall appears to serve in a mechanical role. It maintains cell shape and prevents osmotic disruption. The mannan layer contains hydrolytic enzymes,eg. invertase and β - glucoamylase, which enable yeast to utilize oligo-and polysaccharide substrates like sucrose and starch, Suomalamen and Nurminen 1973 (253). The above enzymes are considered to be extracellular.

The two reviews dealing with the thermochemical aspects of growth and metabolism in bacteria, Belaich 1980 (254) and yeast cells, Lamprecht 1980 (255) were important sources for the work discussed below.

5.2 Estimation of the enthalpy of substrate conversion by S. Cerevisiae entrapped in calcium alginate gel

The important variables in the accurate estimation of dH_R for enzyme catalysed reaction under flow conditions were discussed in Chapter 3. Thus the use of small diameter immobilization support, high reactor enzyme activity and a low sample flow rate will facilitate the determination of dH_R. Such considerations are also important in the determination of dH_R for more complex reactions, e.g., alcoholic fermentation. Additional considerations can be expected owing to the greatly more complex catalyst involved. For instance, more than a single reaction pathway is available in an intact yeast cell. The heat output rate may also be affected by the nutritional state of cells and by oxygen concentration. Since immobilized cells are frequently stored and used for long periods there is some interest in any time dependent changes in their characteristics. In this section the effect of storing immobilized yeast at 0 - 4°C, with or without substrate (for 10 - 13 days) on the reaction enthalpy for sucrose conversion was studied.

Materials and Methods

Saccharomyces cerevisiae, Type 1 (baker's yeast) fast-dried to yield 90% active viable cells; yeast extract, sodium alginate and substrates were supplied by Sigma UK. All other reagents were of laboratory grade and supplied by BDH Ltd. The entrapment of the yeast cells in calcium alginate has been described in Chapter 2. The strings of alginate obtained (0.5 - 1.5 mm diameter) were cut

into 2mm lengths for study. Portions (<200mg) were retained inside the calorietric flow vessel using teflon filters as described for immobilized enzymes (Chapter 3 and Chapter 4). Other portions from the same batch of alginate entrapped yeast (IMYSC) were suspended in (5g dm^{-3} sucrose, 5 g dm^{-3} yeast extract), or kept without nutrient. These IMYSC preparations were stored in a cold room (0 - 4°C) for 10 - 13 days. The dH_R for the reaction catalysed by each batch of differently treated IMYSC was then determined.

Results

The dH_R estimates for the transformation of sucrose and several hexoses by freshly prepared IMYSC are listed below, Table (5.2.1).

Table (5.2.1) dH_R estimates for the transformation of sucrose and selected hexoses by IMYSC

Substrate	[a,c] H_R (kJ mol^{-1})
Sucrose	65 ± 1.0
Glucose	38 ± 1.1
	*240 ± 15
Fructose	25 ± 2.2
Mannose	31 ± 1.3
[b]Glucose/Fructose	68 ± 5.0

a. $\bar{x} \pm SD_{n-1}$, n = 4

b. equimolor mixture, dH_R (kJ mol^{-1} "disaccharide")

c. studies were conducted in 0.03M calcium chloride (pH 6.0 - 6.5, T = 30°C)

* - dH_R determined with a new batch of cells from the supplier.

The enthalpy of sucrose conversion using stored IMYSC was in all cases greater than the value observed with freshly prepared cells. The dH_R values for sucrose conversion by starved IMYSC and IMYSC exposed to sucrose or growth media for the preceding 10 days was 90 $\pm$ 5.1, 48 $\pm$ 1.4 and 74 $\pm$ 4.1 kJ mol^{-1} respectively.

5.3 Analysis of substrate using S. cerevisiae entrapped in calcium alginate gel and thermochemical monitoring

There are few examples of the use of thermochemical monitoring with immobilized cells in flow analysis. Table (5.1.3.1). Also there is increasing interest in the characterisation of immobilized cells as their potential as biocatalysts becomes more nearly realised. Calorimetry has already proved particularly useful for the study of free cells and microbiological calorimetry is a rapidly growing area (s. 1.1). In this section the use of S. cerevisiae entrapped in calcium alginate gel for the analysis of glucose, fructose, mannose and sucrose is examined. The Km^{app} and maximal rates of heat output with these substrates could in addition be determined from the steady state analysis data. IMYSC was also monitored thermochemically during exposure to growth media and after treatment with several organic solvents. The yeast Saccharomyces cerevisiae was chosen for study because the free cells have been widely studied by calorimetry. This is important as any extraordinary characteristics of the immobilized cell should then stand out.

Method

Between 150 mg - 200 mg of IMYSC was loaded into the flow calorimetric vessel as described before. For analytical studies fully mutarotated D-hexoses samples were injected continuously. All studies were carried out in calcium chloride solution (0.03M, pH 6.0 - 6.5) at a temperature of 30°C. To examine the possibility of growth of the yeast within the calcium alignate gel matrix, growth media (5 g dm^{-3} glucose, 5 g dm^{-3} yeast extract in 0.03M calcium chloride) was passed continuously through the bed of IMYSC and the heat ouput rate monitored for between 4 -6 h. A recorder sensitivity of 300 μV FSD and a chart speed of 0.5mm min^{-1} were used to enable uninterrupted thermal monitoring. Finally, the effects of pretreatment of IMYSC with acetone, butan-1-ol or toluene was studied. The level of exposure could be varied according to the concentration of organic solvent or duration of contact with the immobilized cells.

Results

The concentration-response curves from the steady state and transient analysis of glucose are compared over the concentration range of 0 - 10mM glucose, Fig (5.3.1). The apparent Michaelis constant and maximal heat output rate, (dQ/dt) max for glucose and other substrates, Table (5.3.1) were determined using the LB and Eadie plots as described before. However owing to some uncertainty regarding dH_R values with IMYSC (s 5.2) power output measurements were plotted directly rather than being initially transformed into rates of product formation (i.e. V, mol dm^{-3} min^{-1})

FIG(5·3· 1)- Steady state(⊡) and transient(⊙) analysis of glucose using alginate entraped yeast.

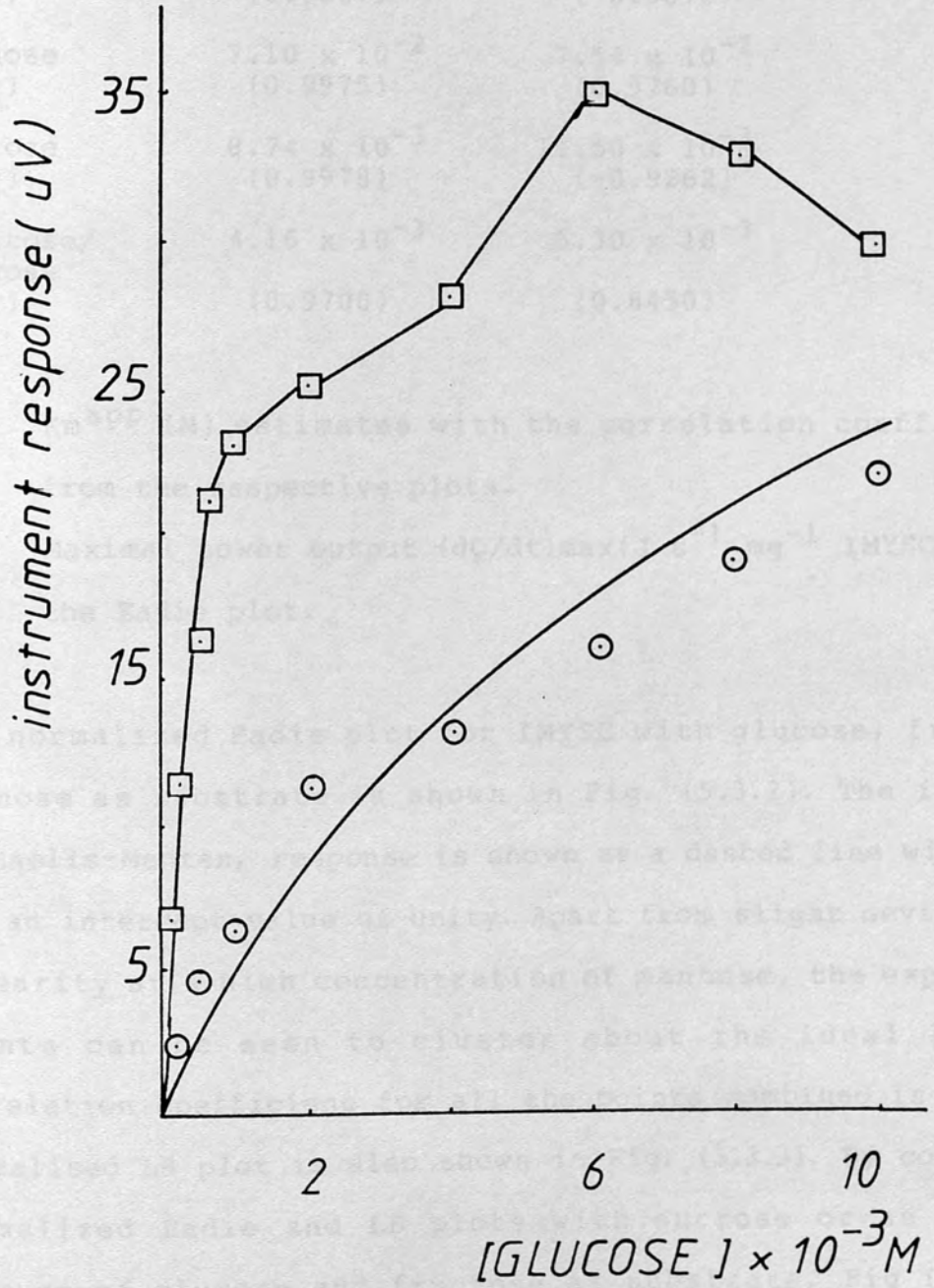

(Table 5.3.1) Kinetic parameters for IMYSC with selected substrates

Substrate	[a]LB plot	[a]Eadie plot	[b](dQ/dt)max
Glucose (r)	3.70×10^{-4} (0.9660)	3.92×10^{-4} (0.9641)	3.91
Fructose (r)	3.25×10^{-3} (0.9827)	3.66×10^{-3} (-0.9676)	3.23
Mannose (r)	7.10×10^{-2} (0.9975)	7.54×10^{-2} (0.9760)	18.20
Sucrose (r)	8.74×10^{-3} (0.9978)	11.50×10^{-3} (-0.9262)	7.60
Fructose/ Glucose (r)	4.16×10^{-3} (0.9700)	6.30×10^{-3} (0.8450)	4.40

a. Km^{app} (M) estimates with the correlation coefficient (r) from the respective plots.

b. Maximal power output (dQ/dt)max(J s^{-1} mg^{-1} IMYSC) from the Eadie plot.

The normalized Eadie plot for IMYSC with glucose, fructose or mannose as substrate is shown in Fig. (5.3.2). The ideal, i.e. Michaelis-Menten, response is shown as a dashed line with a slope and an intercept value of unity. Apart from slight deviation from linearity at a high concentration of mannose, the experimental points can be seen to cluster about the ideal line; the correlation coefficient for all the points combined is -0.9816. A normalised LB plot is also shown in Fig. (5.3.3). By contrast the normalized Eadie and LB plots with sucrose or an equimolar mixture of glucose and fructose as substrate, Fig (5.3.4) and

FIG(5·3·2)-Normalized EADIE PLOT for alginate entraped yeast with glucose(⊙), fructose(⊡) or mannose(*) as substrate.

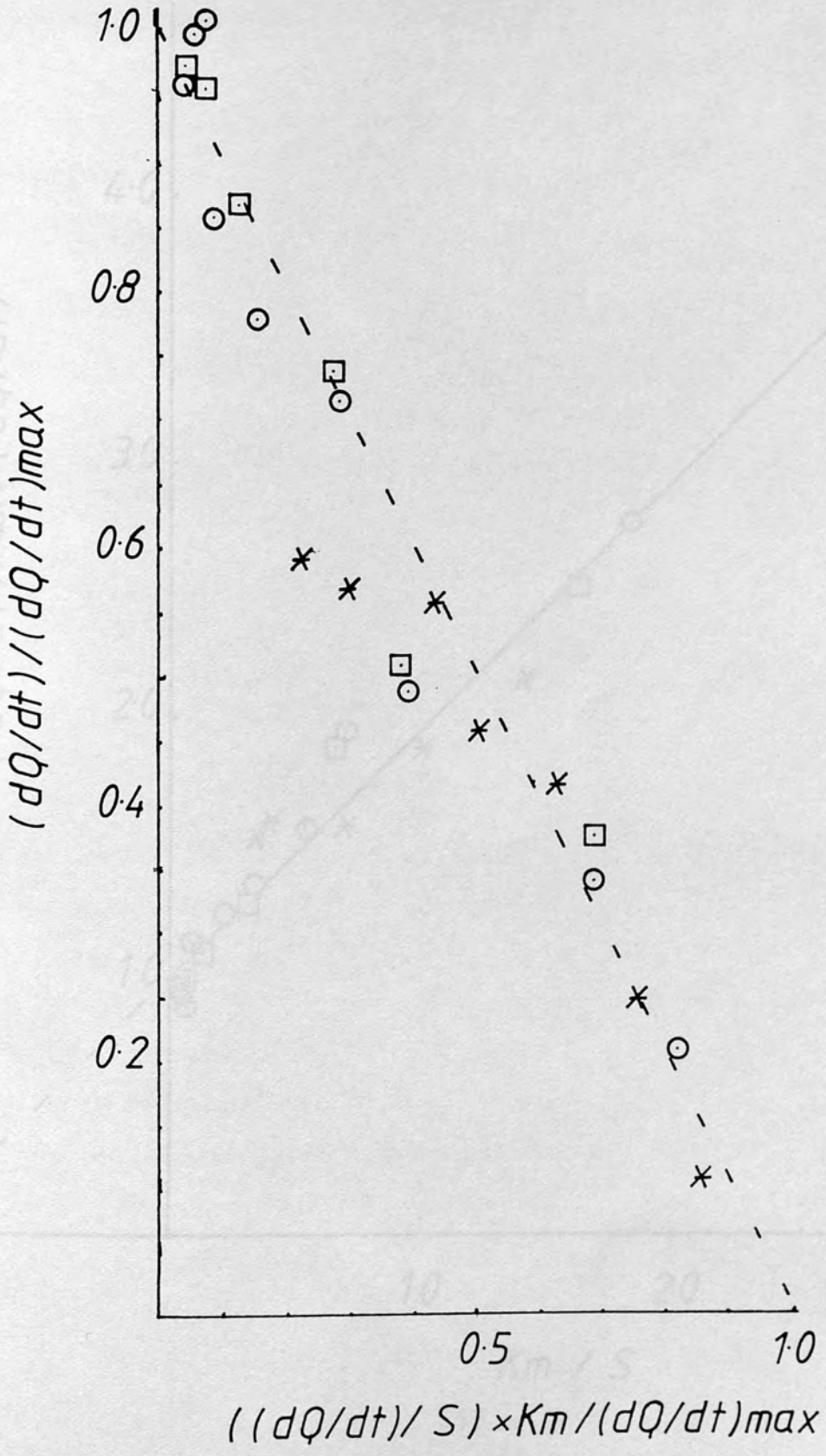

FIG(5·3·3)- Normalized LINEWEAVER-BURK PLOT for alginate entraped yeast with glucose(⊙) fructose(⊡) or mannose(*) as subtrate

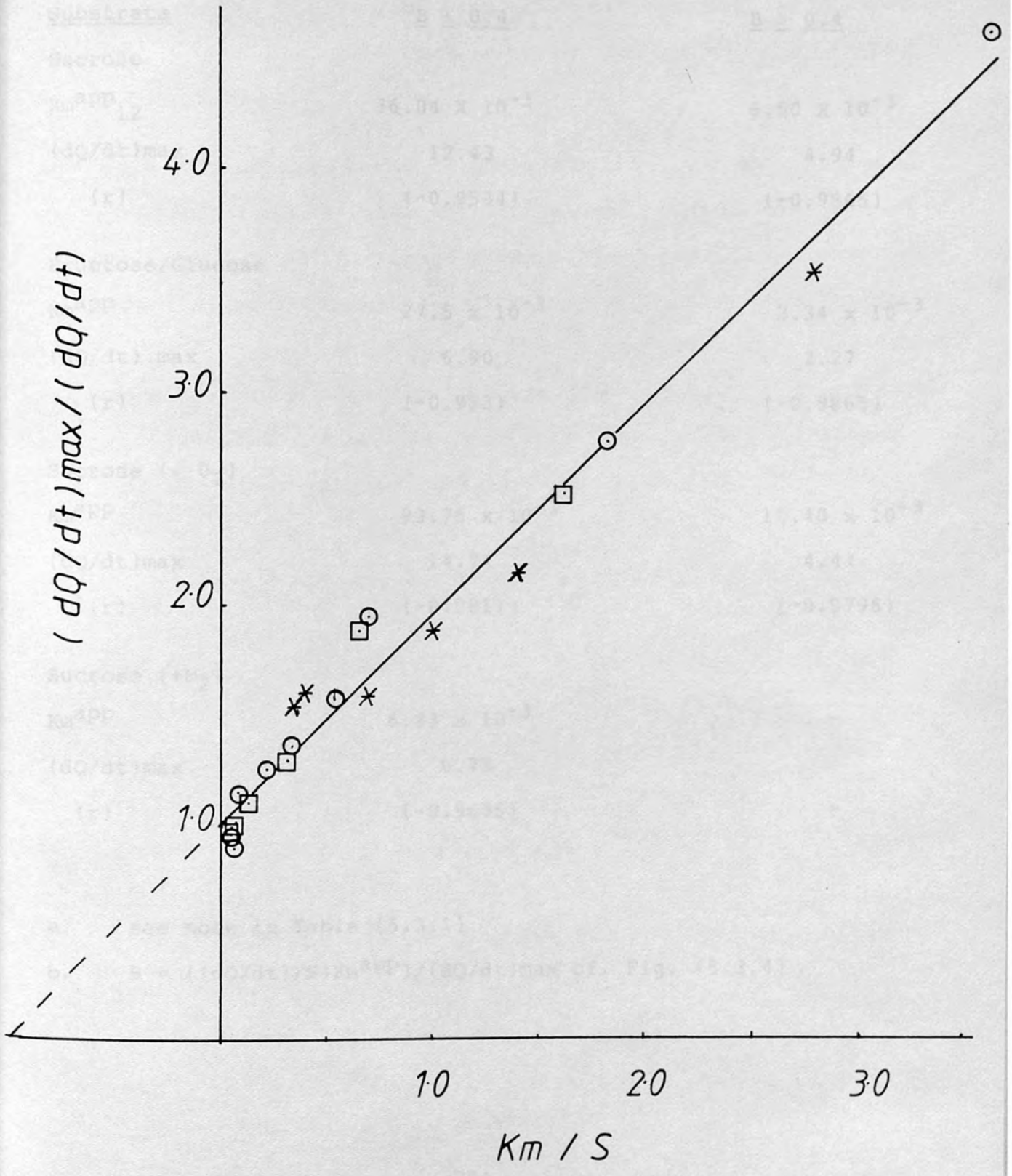

Table (5.3.2) Dual Km^{app} and (dQ/dt)max estimates for IMYSC[a]

Substrate	[b] $B \leq 0.4$	$B \geq 0.4$
Sucrose		
Km^{app}_{12}	36.04×10^{-3}	6.50×10^{-3}
(dQ/dt)max	12.43	4.94
(r)	(-0.9534)	(-0.9865)
Fructose/Glucose		
Km^{app}	27.5×10^{-3}	2.34×10^{-3}
(dQ/dt) max	6.90	2.27
(r)	(-0.953)	(-0.9865)
Sucrose (+ O_2)		
Km^{app}	93.75×10^{-3}	10.40×10^{-3}
(dQ/dt)max	14.74	4.47
(r)	(-0.9811)	(-0.9796)
Sucrose (+N_2)		
Km^{app}	6.83×10^{-3}	-
(dQ/dt)max	0.75	
(r)	(-0.9696)	-

a. see note in Table (5.3.1)

b. $B = ((dQ/dt)/S)Km^{app})/(dQ/dt)max$ cf. Fig. (5.3.4)

Fig. (5.3.5) are less ideal. It can be seen that the experimental points have two linear sections. It was possible to fit two straight lines and therefore obtain two Km^{app}, (dQ/dt)max estimates, Table (5.3.2).

The extent of mass transfer rate limitations on susbtrate conversion by IMYSC is of interest. However, a full analysis of internal and external diffusion effects along the lines described in Chapter 4 was not possible. With unavailability of clear dH_R values, power measurements could not be transformed into reaction rate measurements with the appropriate dimensions for mass transfer assessment. The effects of flow rate on Km^{app} estimates could on the other hand be examined, Table (5.3.3).

Table (5.3.3) The effect of sample flow rate on the kinetic constants for IMYSC with sucrose as substrate

F ($cm^3\ h^{-1}$)	Km^{app}(M)	[b](dQ/dt)max	t(h)[a]
22.9	24.30×10^{-3}	3753.85	0
36.6	21.4×10^{-3}	3113.17	24
46.4	12.71×10^{-3}	2286.65	48
22.8	19.64×10^{-3}	2148.2	72

a. time interval between successive studies on a single IMYSC preparation.

b. $\ln (dQ/dt)max = -0.00826\ (t) + 8.2177$

$r = 0.9740$

$$t_{1/2} = \frac{-\ln 2}{-0.00826\ (h^{-1})} \quad 83.90h.$$

FIG(5.3.4)- Normalized EADIE PLOT for alginate entrapped yeast with sucrose(○;*) or a mixture of glucose and fructose(□)as substrate.

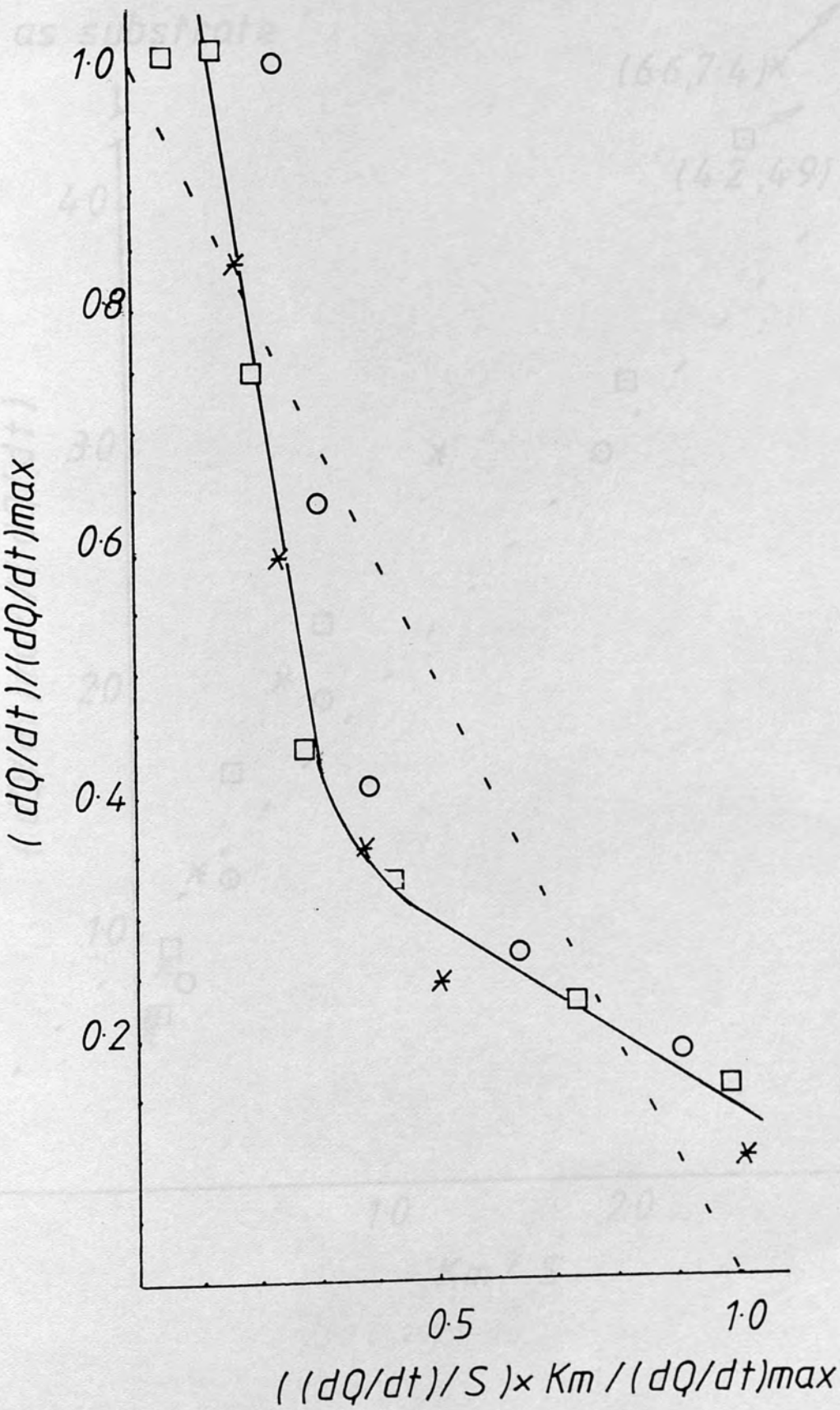

FIG(5·3·5)-Normalized LINEWEAVER-BURK PLOT for alginate entraped yeast with sucrose(⊙) or a mixture of glucose and fructose(⊡) as substrate

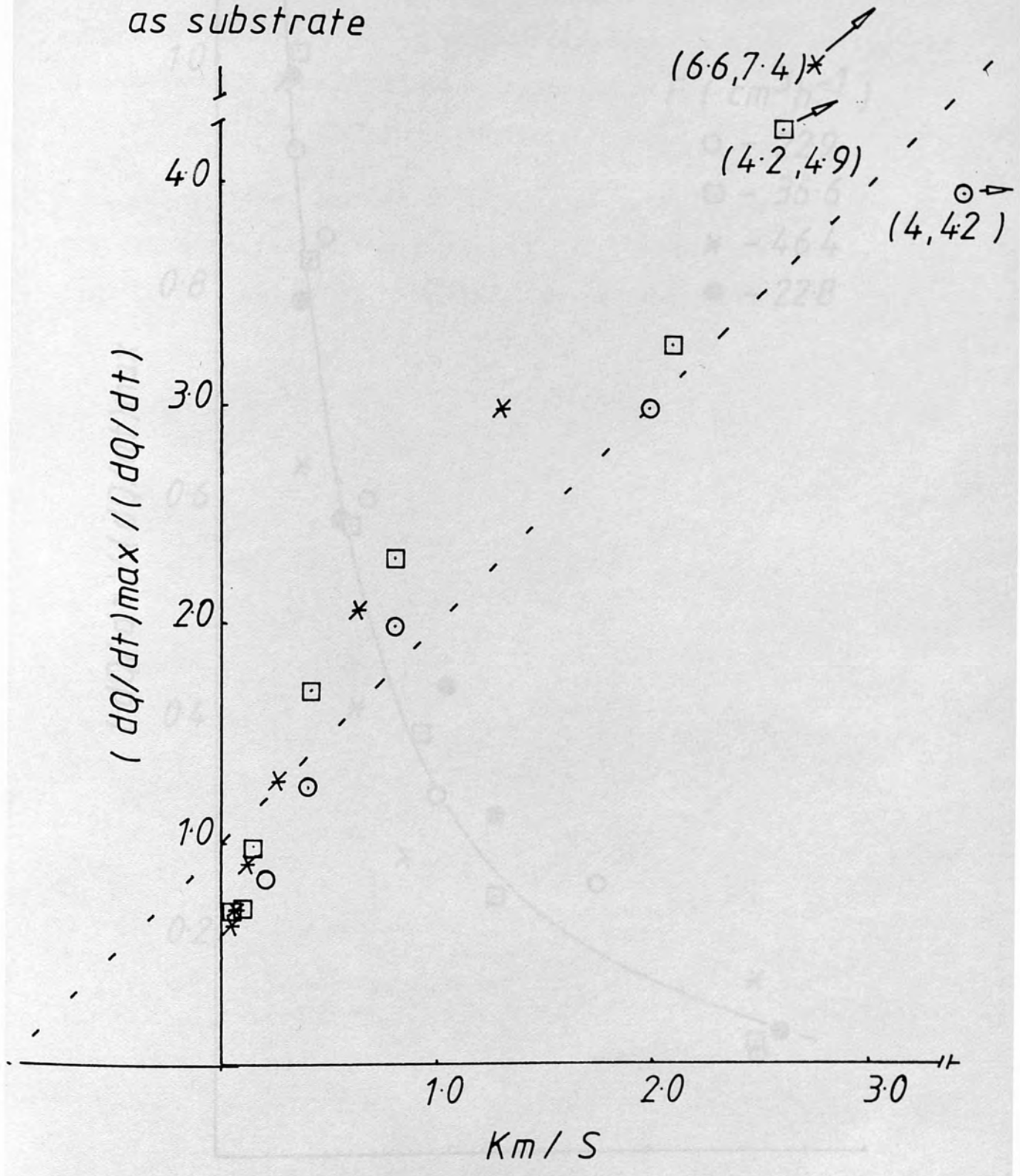

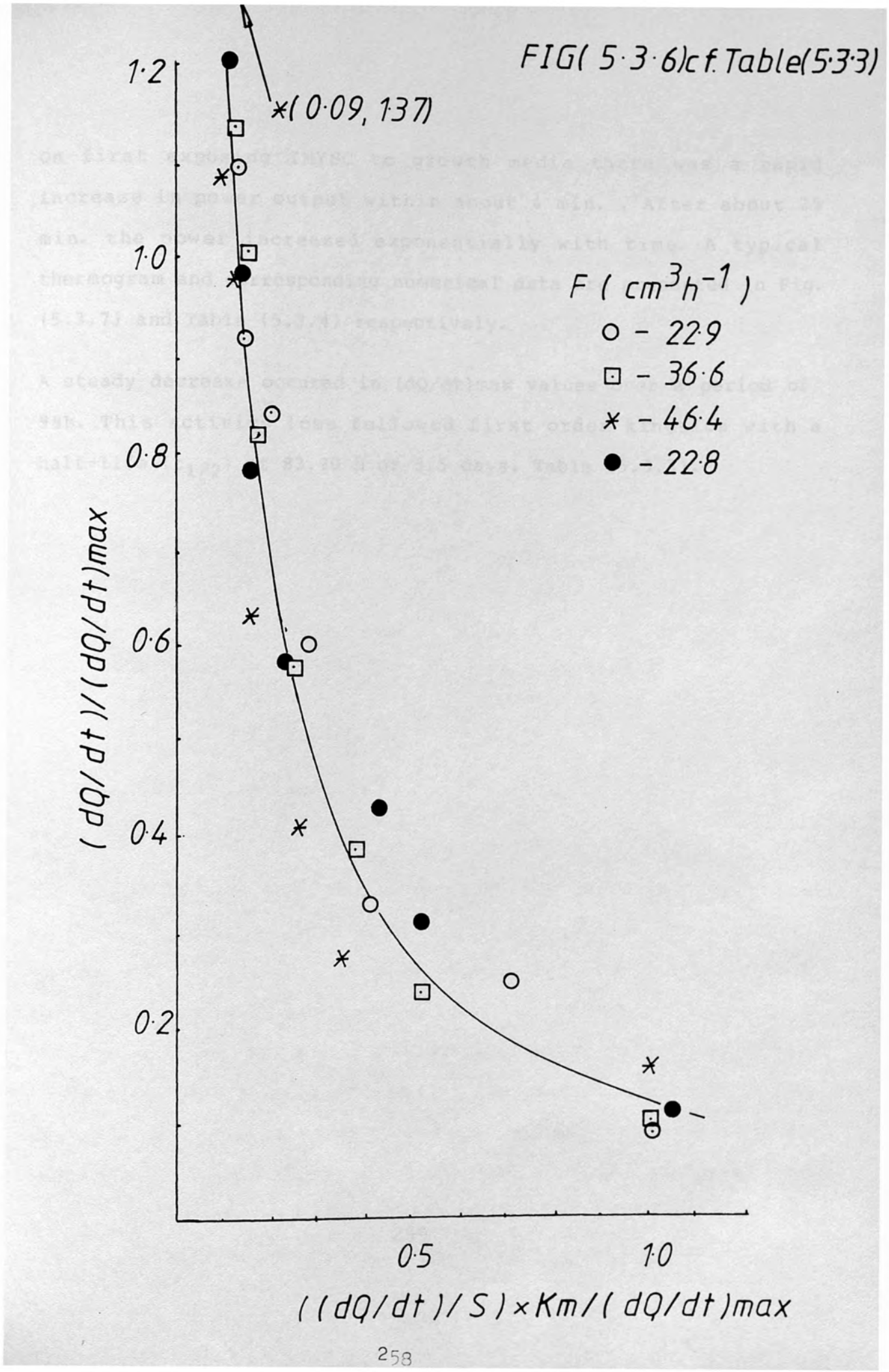
FIG(5·3·6)cf. Table(5·3·3)
*(0·09, 1·37)
F (cm3h-1)
○ - 22·9
⊡ - 36·6
* - 46·4
● - 22·8
1·2
1·0
0·8
0·6
0·4
0·2
(dQ/dt)/(dQ/dt)max
0·5
1·0
((dQ/dt)/ S) × Km/(dQ/dt)max

On first exposing IMYSC to growth media there was a rapid increase in power output within about 4 min. . After about 25 min. the power increased exponentially with time. A typical thermogram and corresponding numerical data are presented in Fig. (5.3.7) and Table (5.3.4) respectively.

A steady decrease occured in (dQ/dt)max values over a period of 98h. This activity loss followed first order kinetics with a half-life ($t_{1/2}$) of 83.90 h or 3.5 days, Table (5.3.3).

Table (5.3.4) Power output from IMYSC with continuous injection of growth media

t (min)	ss - disp (μV)[b]	ln (ss - disp)[a]
20	19.5	2.97
60	28.5	2.35
100	37.5	3.62
140	46.5	3.84
180	60.0	4.10
240	84.0	4.43
300	84.0	4.43
300	114.0	4.74
360	150.0	5.01

a. $\ln(\text{ss-disp}) = 0.00586\ (t) + 2.981$; Fig. (5.3.8)

$r = 0.9951$

$$t_2 = \frac{0.6931}{k_1 \times 60}$$

$$= 1.97\text{h}$$

b. E_{ss} was 17.95 ($J\ s^{-1}\ V^{-1}$)

The doubling time (t_2) was estimated as 2.2 $\pm$ 0.3h from three different batches of IMYSC differing in the initial power output. The exponential increase in power output from IMYSC exposed to a continual supply of nutrient did not continue indefinitely. A plateau was reached after a time which was longer for those immobilized cell preparations with a low initial power output. In the results reported above, there was an approximately 7-fold increase in steady state power output over the 6h period of study. At the maxima of the thermogram from IMYSC undulations with a period of about 10 min. were on occasion observed.

FIG(5·3·7)

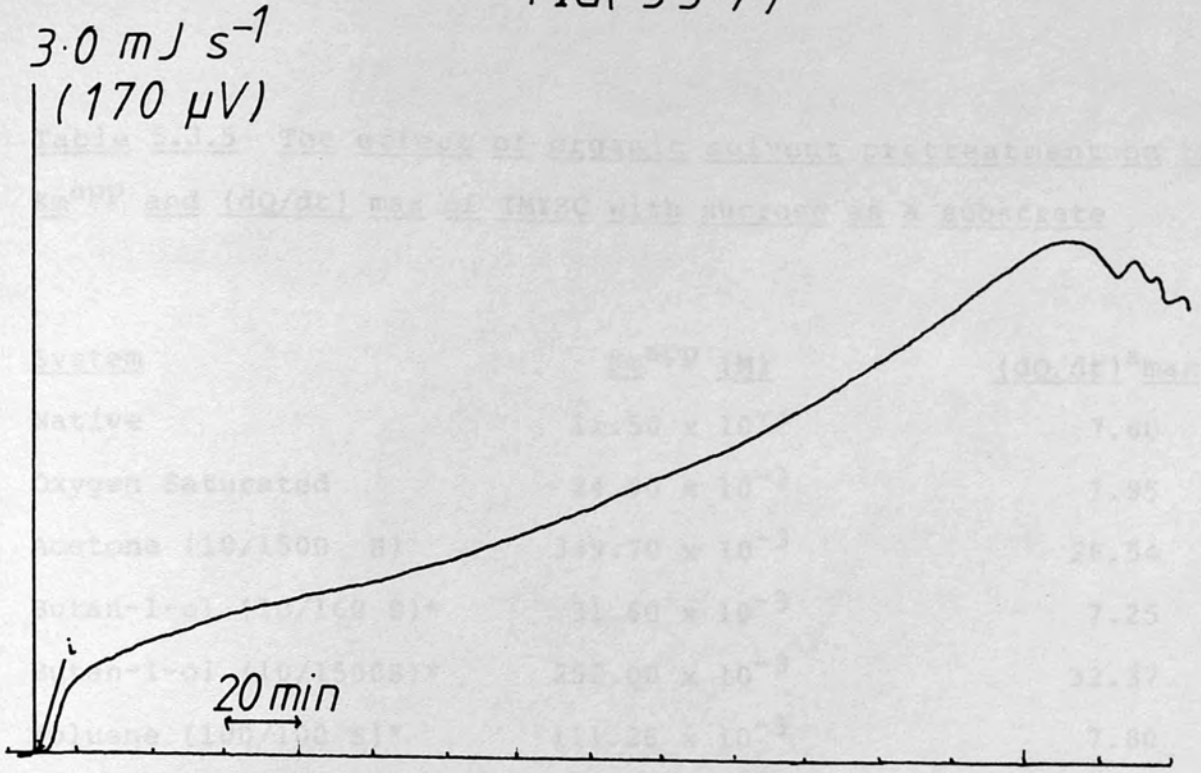

FIG(5·3·8)

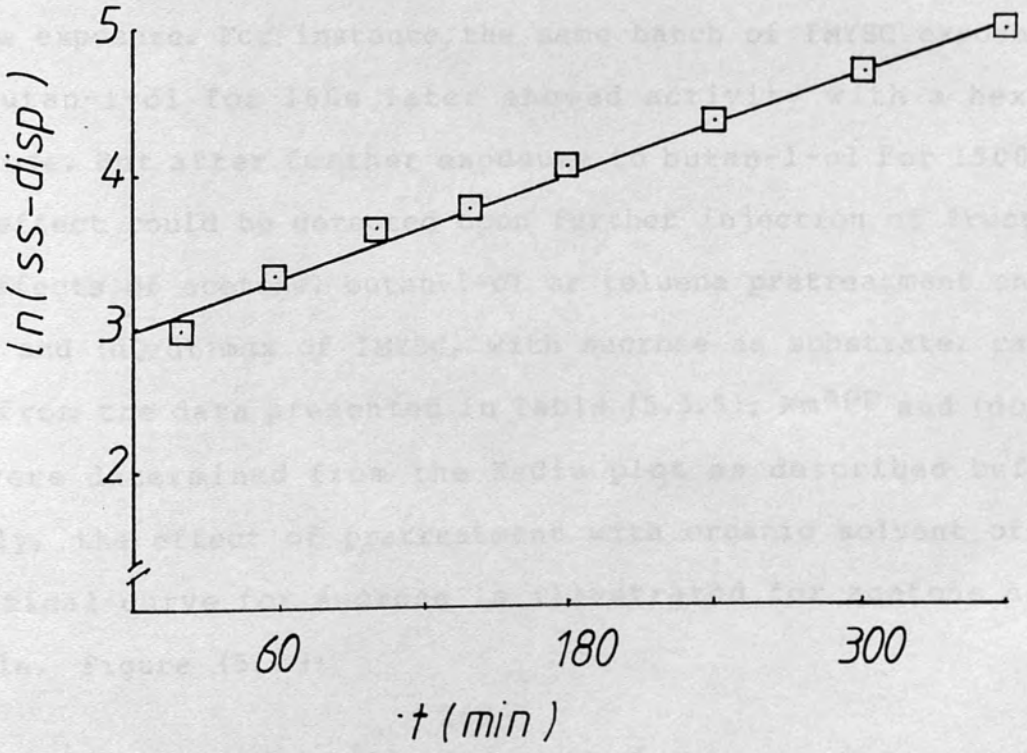

Table 5.3.5 The effect of organic solvent pretreatment on the Km^{app} and (dQ/dt) max of IMYSC with sucrose as a substrate

System	Km^{app} (M)	$(dQ/dt)^{a}max$
Native	11.50×10^{-3}	7.60
Oxygen Saturated	24.90×10^{-3}	7.95
Acetone (10/1500 S)	349.70×10^{-3}	26.54
Butan-1-ol (10/160 S)*	31.60×10^{-3}	7.25
Butan-1-ol (10/1500S)*	252.00×10^{-3}	32.37
Toluene (100/100 S)*	111.26×10^{-3}	7.80
Toluene with oxygen saturation	440.19×10^{-3}	26.96

* concentration (v/v) and length of pretreatment time, t(s).

a. $J\ s^{-1}$ mg IMYSC

The effects of pretreating IMYSC with organic solvents would appear to be dependent on the concentration used and the duration of the exposure. For instance, the same batch of IMYSC exposed to 10% butan-1-ol for 160s later showed activity with a hexose, fructose. But after further exposure to butan-1-ol for 1500s no heat effect could be detected upon further injection of fructose. The effects of acetone, butan-1-ol or toluene pretreatment on the Km^{app} and (dQ/dt)max of IMYSC, with sucrose as substrate, can be seen from the data presented in Table (5.3.5); Km^{app} and (dQ/dt) max were determined from the Eadie plot as described before. Finally, the effect of pretreatment with organic solvent of the analytical curve for sucrose is illustrated for acetone as an example, Figure (5.3.9)

FIG(5·3·9)-Concentration-response curve for sucrose(IMYSC -⊙, acetone pretreated IMYSC-⊡)

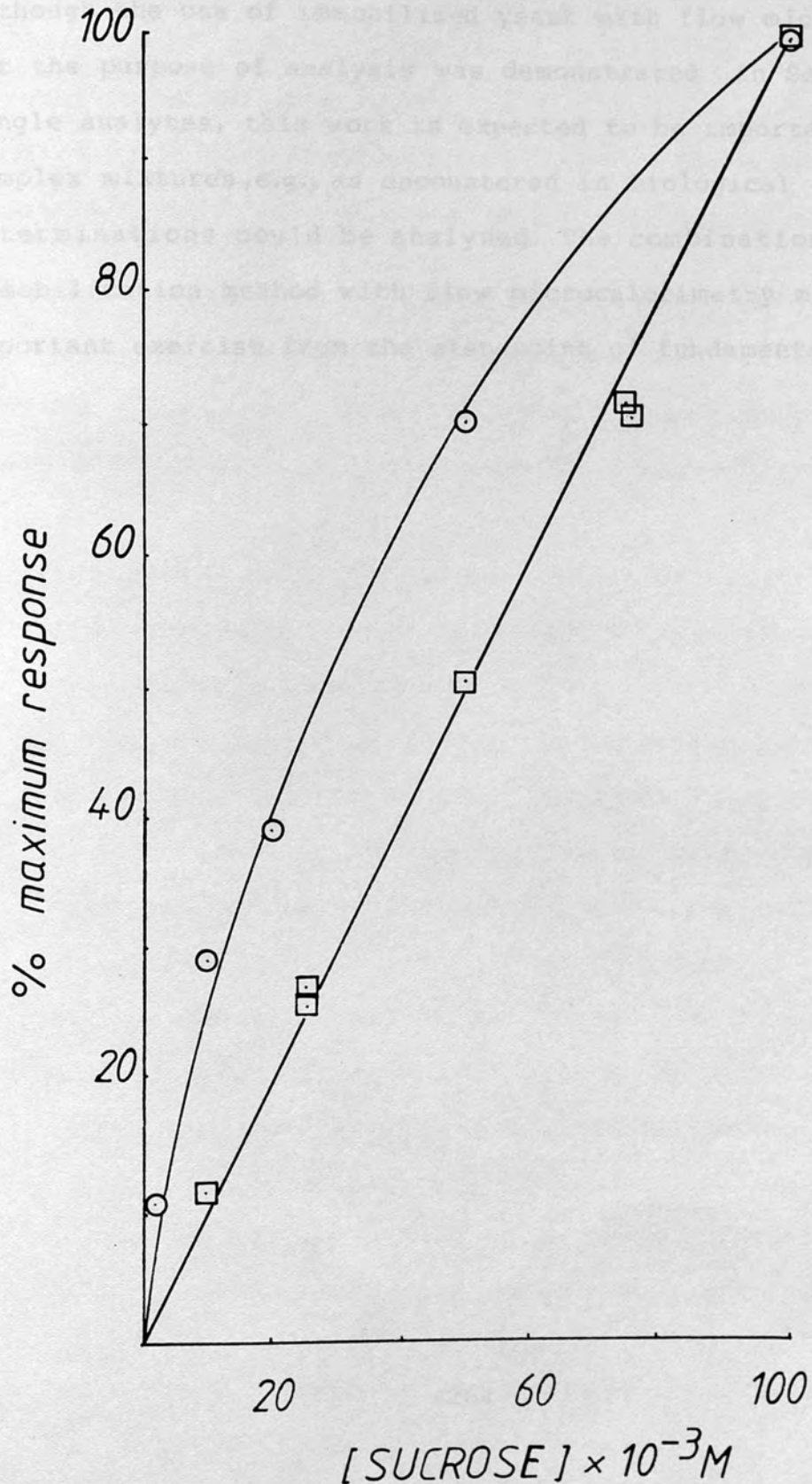

5.4 Flow microcalorimetric characterization of yeast entrapped in calcium alginate gel

Although the use of immobilized yeast with flow microcalorimetry for the purpose of analysis was demonstrated in Section 5.3 for single analytes, this work is expected to be important generally; complex mixtures, e.g., as encountered in biological oxygen demand determinations could be analysed. The combination of the cell immobilization method with flow microcalorimetry may also be an important exercise from the standpoint of fundamental research.

Cell types may differ, e.g., according to the range of substrate converted. Such differences will in part determine the suitability of particular cell types for specific bioconversions. The differentiation of cells in this regard would therefore be expected to be valuable in the field of applied microbiology. The combination of cell immobilization and flow microcalorimetry may result in a relatively straightforward approach to this problem.

A study directed at differentiating between three strains of Saccharomyces cerevisiae using the immobilization technique together with flow microcalorimetric monitoring is reported below. Some important features of this general approach are as follows:

a. there is a reduction in the amount of cells required for study because of the capacity for re-use. This may be particularly important where cells may have been newly developed (e.g., by enrichment or genetic engineering techniques) and therefore are not available in large quantities;

b. immobilization by calcium alginate entrapment is reversible thus enabling the recovery of cells from the support matrix;

c. after immobilization, cells may be protected from contamination by the support matrix. There may therefore be little need to work under sterile conditions;

d. the generality of heat effects means that the calorimetric monitoring of immobilized cells is in principle applicable to most cell types; both oxygen requiring (aerobic) and oxygen non-requiring (anearobic) cells may be studied.

Materials and Methods

Glass vials containing 0.5mg of dried *S. cerevisiae* cells were obtained (courtesy of the Laboratory of the Government Chemist , LGC). The cells, dated 7/JUN/1982, were the strains NCYC 587, NCYC 762 and NCYC 1380. At the time of study, the glass vials had been stored at 0 - 5^{o}C for 1.5 years. The vials were opened in the shadow of a bunsen flame and the contents suspended in 2 - 3 cm^3 of previously boiled deionized water at room temperature (20^{o}C). The suspension of yeast cells was then added to an equal volume of 4% sodium alginate gel and the resulting mixture extruded into a solution of 0.03M calcium chloride as described before. The alginate entrapped yeast preparations, IMNCYC 587, IMNYC 762 or IMNCYC 1380) was then cut into rod-shaped pieces (1 x 2 - 3 mm.) and exposed to growth media for three to five days before study. Calorimetric monitoring was essentially as described in previous sections; 150 - 200 mg of alginate entrapped yeast was retained within the calorimetric flow vessel and the steady state power output in response to continuous substrate injection monitored. Studies were conducted in 0.03M calcium chloride (pH 6.5, T = 30^{o}C, F = 13.6 - 14.2 $cm^3\ h^{-1}$).

Results

The concentration - power output data from NCYC 587 Table (5.4.1) is characteristic of the results obtained from the other immobilized yeast strains. The corresponding concentration - response curve, with glucose as substrate, is shown in Fig. (5.4.1).

Table (5.4.1) Steady state analysis of glucose or sucrose using IMNCYC 587

[Glucose] x 10^{-3} M	ss - disp(μV)[a]	[Sucrose] x 10^{-3} M	ss-disp (μV)[a]
50.0	13.45	200.0	71.50
40.0	14.55	100.0	53.25
30.0	15.30	50.0	35.00
20.0	14.30	20.0	25.50
10.0	13.75	10.0	19.00
5.0	10.80	5.0	15.00
2.0	8.85	2.0	11.25
1.0	7.60	1.0	8.65
0.5	5.4	0.5	6.50
0.2	2.92	0.2	3.90
0.1	1.30	0.1	2.35

a. E_{ss} = 42.9 (J s^{-1} V^{-1}); F = 13.9 (cm^3 h^{-1})

FIG(5·4·1)-Concentration-response curve for glucose conversion catalysed by IMNCYC 587

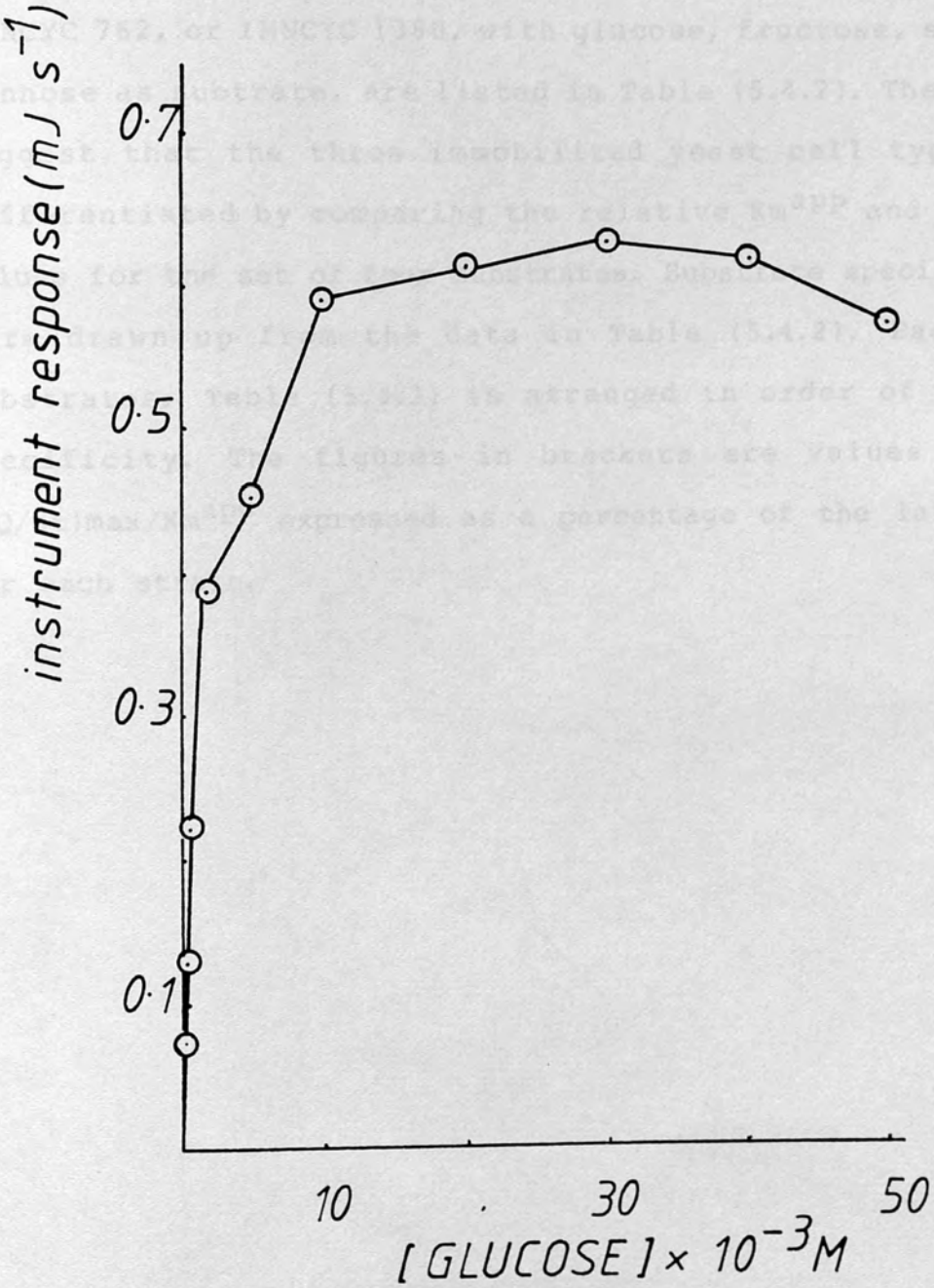

The kinetic parameters Km^{app} and (dQ/dt)max were determined using the Eadie plot. The normalized plot with e.g. glucose as substrate, Fig. (5.4.2) is very much as observed for IMYSC (s 5.3). It can be seen that the Eadie plot shows either one or two linear sections with glucose or sucrose as substrate respectively. The Km^{app} and (dQ/dt)max estimates for IMNCYC 587, IMNCYC 762, or IMNCYC 1380, with glucose, fructose, sucrose and mannose as subtrate, are listed in Table (5.4.2). These results suggest that the three immobilized yeast cell types may be differentiated by comparing the relative Km^{app} and (dQ/dt)max values for the set of four substrates. Substrate specificity list were drawn up from the data in Table (5.4.2). Each list of substrates, Table (5.4.3) is arranged in order of descending specificity. The figures in brackets are values for ratio $(dQ/dt)max/Km^{app}$ expressed as a percentage of the largest value for each strain.

FIG(5·4·2)-Normalized EADIE PLOT for IMNCYC 587 with glucose(⊙) or sucrose(⊡) as substrate.

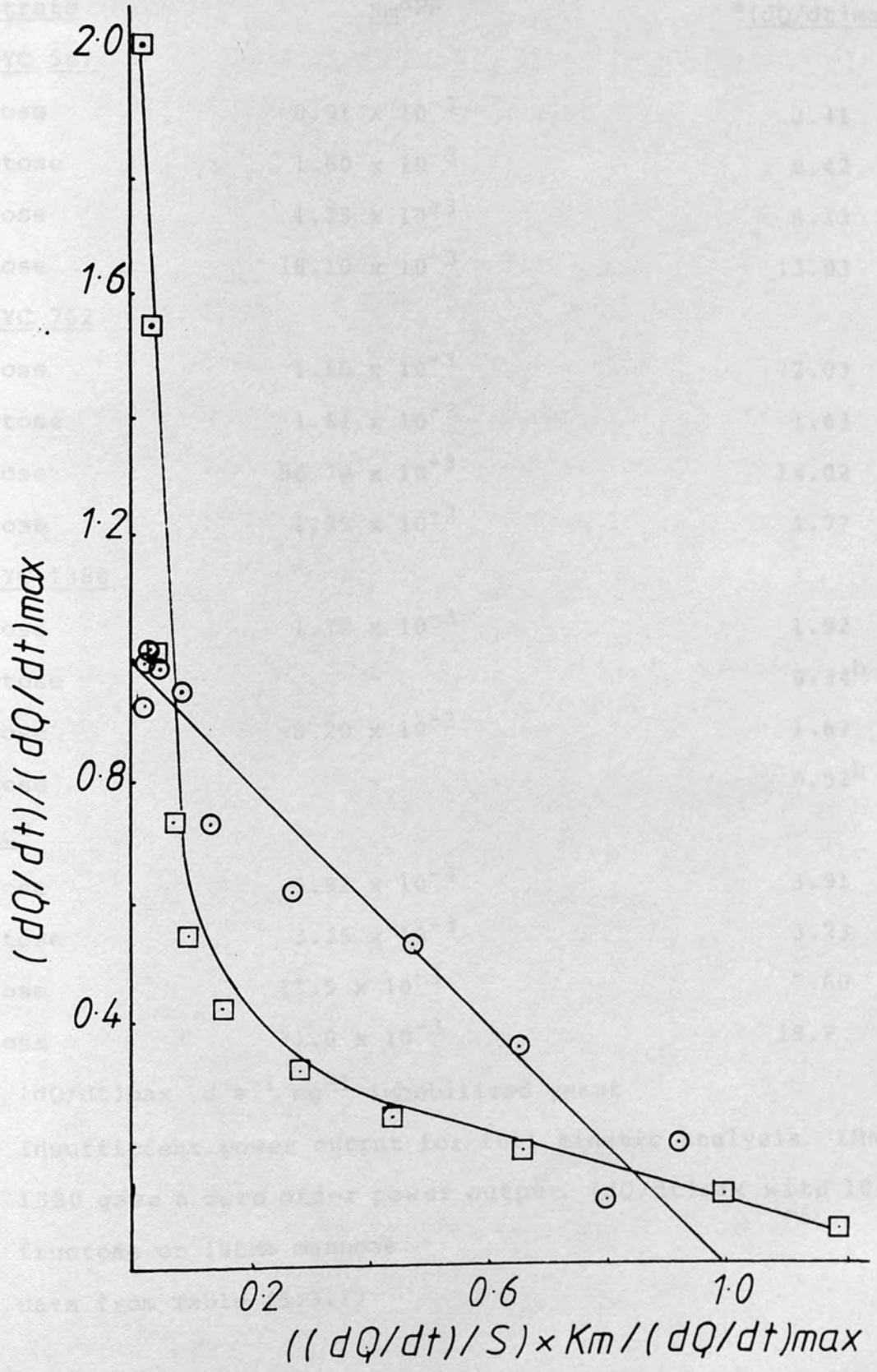

Table (5.4.2) Kinetic parameters for different strains of yeast cells entrapped in calcium alginate gel.

Substrate	Km^{app}	[a](dQ/dt)max
IMNCYC 587		
Glucose	0.91×10^{-3}	3.41
Fructose	1.60×10^{-3}	8.42
Sucrose	1.73×10^{-3}	8.13
Mannose	18.10×10^{-3}	13.03
IMNCYC 762		
Glucose	1.10×10^{-3}	2.03
Fructose	1.61×10^{-3}	1.63
Sucrose	56.70×10^{-3}	14.02
Mannose	1.35×10^{-3}	1.77
IMNCYC 1380		
Glucose	1.72×10^{-3}	1.92
Fructose	-	0.34[b]
Sucrose	3.20×10^{-3}	1.87
Mannose	-	0.52[b]
IMYSC[c]		
Glucose	3.92×10^{-4}	3.91
Fructose	3.25×10^{-3}	3.23
Sucrose	11.5×10^{-3}	7.60
Mannose	71.0×10^{-3}	18.2

a. (dQ/dt)max J s^{-1} mg^{-1} immobilized yeast

b. Insufficient power output for full kinetic analysis. IMNCYC 1380 gave a zero order power output, (dQ/dt)max with 10mM fructose or 100Mm mannose.

c. data from Table (5.3.1)

Table (5.4.3) Substrate specificity lists for different strains of yeast cells entrapped in calcium alginate gel

NCYC 587	NCYC 762	NCYC 1380	YSC
Fructose (100)	Glucose (100)	Glucose (100)	Glucose (100)
Sucrose (90)	Mannose (90)	Sucrose (52)	Fructose (10)
Glucose (72)	Fructose (55)	Mannose (-)	Sucrose (7)
Mannose (14)	Sucrose (15)	Fructose (-)	Mannose (2.5)

A notable feature of Table (5.4.3) is that the sequence of substrate in each column is different.

5.5 Discussion

The value of dH_R for substrate conversion by S. cerevisiae depends on the end products. When oxygen concentration is high glucose may be completely degraded to carbon dioxide and water. From heats of formation data dH_R for this reaction is readily estimated as 2,834 kJ mol^{-1}. If either oxygen is absent or glucose is in excess of 2.5×10^{-4}M, (the solubility of oxygen in water) then it is converted predominantly to ethanol and carbon dioxide (dH_R c.a. 98 kJ mol^{-1}) (43,44). Not all the energy from glucose oxidation is released as heat. Starved cells compared to non-starved cells use a greater proportion of the free energy of the substrate to replenish their energy reserves. Consequently dH_R for glucose oxidation is decreased in starved cells. The results from Section 5.1 are not consistant with the above view. (but c.f Table 5.2.1). dH_R for the conversion of sucrose was found to be greater using starved cells. Thus within the microenvironment of the alginate gel it is uncertain if the relative heat release from freely suspended starved and non-starved yeast cells remains unchanged. The time-related changes in the characteristics of yeasts would appear to be a general problem in analytical applications where a large initial concentration of cells are employed. Beezer et al., 1976 (256) tackled this problem during the use of S. cerevisiae in the calorimetric assay of the antibiotic nystatin. When stored in liquid nitrogen, cells retained a constant reactivity with nystatin for well over 500 days.

The differences between transient and steady state analysis discussed previously (Section 3.2) also apply to analysis using IMYSC. Thus there were the expected differences sample throughput, linearity range, and sensitivity (with peak height data).

The Km of intact cells for a specific substrate is characteristic of the membrane-bound carrier protein involved in its uptake (259). For freely membrane permeable substrate Km the property of a limiting enzyme in the sequence of enzymes involved in its metabolism. The Km^{app} of values IMYSC determined in Section 5.3, are compared with published values in Table (5.5.1).

Table (5.5.1) Reported values for the Km[a] of free and immobilized yeast

Reference	Glucose	Fructose	Mannose	Sucrose
This work*	0.38	3.46	73.00	10.11
257	1.9	4	-	-
258[b]	1.51 ± 0.25	6 ± 2	-	-
	20 ± 8	40		
259	5	17	27	-

a. Km x 10^{-3}M

b. Two transporters are proposed

It may be seen that comparisons between values obtained in different studies does not appear to be very useful. This may be due to the use of different strains of cells in various studies. The nomenclature employed in describing different strains of cells does not appear to be standardized; it is therefore difficult to assess this source of variability in values within Table (5.5.1).

The ratio $(dQ/dt)max/Km^{app}$ (J s^{-1} mg^{-1} M^{-1}) by analogy to Vmax/Km may give some idea of the relative specifity of IMYSC for the range of substrate studied. Using the above ratio as an index, it may be concluded that the order of specificity is glucose (100), fructose (10), fructose/glucose (7), sucrose (6.5) and mannose (2.5) for IMYSC (S 5.3).

The normalized Eadie plot is arrived at by dividing the appropriate expression in Table (1.2.2.1) by Vmax to give v/Vmax = (v/S) Km/Vmax + 1. Thus a plot of v/Vmax against (v/S) Km/Vmax, for a system showing Michaelis-Menten kinetics, has a slope and intercept value of unity. IMYSC showed essentially Michaelis-Menten kinetics with hexoses as susbtrate. Some deviation is however suggested at a high concentration of glucose and mannose. The former susbtrate is reported to inhibit S. cerevisiae at high concentration (257). With either sucrose on fructose/glucose as substrate the normalized Eadie plot for IMYSC was concave with two linear sections. As discussed above (Chapter 4) this pattern is consistant with:

a. competitive inhibition in the absence or presence of external diffusion effects;
b. internal diffusion effects when there is a deficit of experimental points at sufficiently high substrate concentration,
c. the presence of two distinct enzymes or carriers for a specific substrate.

Glucose and fructose are similar enough in structure such that each could act as a competitive inhibitor to the uptake of the other. The current view of glucose and fructose uptake by S. cerevisiae supports this interpretation of the concave Eadie plot. Glucose and fructose uptake occur by way of the same carrier protein, Cooper 1982 (260). With glucose/fructose as substrate two Km^{app} values, 2.34×10^{-3} and 27.5×10^{-3}M, were determined, Table (5.3.2). These values compare with the values

of 3.7×10^{-4}M and 3.4×10^{-3} M estimated as the Km^{app} for glucose and fructose separately. The Km^{app} of S. cerevisiae for a substrate would be expected to increase in the presence of a competitive inhibitor. The above results are therefore consistant with the view that the uptake of glucose or fructose is subject to competitive inhibition by the other hexose.

Two aspects of the present results do not appear to fit in with the accepted view of the glucose/fructose transport in yeast. First, the effects of buffer oxygen saturation and de-aeration with nitrogen gas on the two Km^{app} values determined with sucrose as substrate suggests that the uptake of glucose and fructose is somehow linked to the metabolism of yeast. The current view of sucrose uptake is that the disaccharide is hydrolysed by extracellular invertase. Glucose and fructose are produced, which then enter the cell via an energy-independent carrier mediated, diffusing mechanism. This non-requirement of energy is not readily rationalized with the apparent sensitivity of the uptake to factors affecting cell metabolism. Secondly, Bisson and Froenkel, (258) have recently presented evidence for the presence of two distinct glucose or fructose carriers in S. cerevisiae, Table (5.5.1). The evidence comprised of concave Eadie plots very similar in appearance to those in this work. Unlike the results presented above, however, the concave Eadie plot was obtained in the presence of glucose or fructose alone.

Finally, the explanation of the concave Eadie plot based on

internal diffusion limitations and an insufficient number of experimental points at high substrate concentration seems least plausible. Although immobilization by entrapment is generally associated with poor mass transfer characteristics, alginate gel is particularly noted for its open structure, Chapter 2. Oxygen mass transfer limitations are probable, however, it is uncertain how yeasts capable of anearobic metabolism will be affected. In the studies above substrate concentration were sufficiently high to result in zero order kinetics.

The changes in the Km^{app} value of S. cerevisiae in Table (5.3.3) occur as a function of:

a. increasing sample flow rate

b. decrease in (dQ/dt)max,

c. time.

It is not clear which of these variables is most important. The half-life of the (dQ/dt)max decrease reflects a corresponding change in the number of immobilized yeast cells, Volesky et al. 1982 (261). The half-life of the IMYSC preparation under operational condition (30°C, pH 6.5; intermittent injection of sucrose) was thus 3.5 days. This value might be increased almost indefinitely by the periodic exposure to growth medium. The doubling time for alginate entrapped S. cerevisiae of 2.2 ± 0.2 h, Table (5.3.4) compares with 6.03 h for the S. cerevisiae in free suspension (261). An increase in the growth rate of s. cerevisiae as a result of immobilization has also been reported by Navaro, 1980 (262). The doubling times for S. cerevisiae in suspension, adsorbed on, or covalently bound to, APTES- modified

glass were reported as 8 h, 4h and 1.75 h respectively.

Growth medium was continuously injected during the growth study above (s 5.3). The plateau in the thermogram of IMYSC, Fig. (5.3.7) is therefore unlikely to be the result of the limiting effect of a depleted nutrient component. Increase in cell numbers within calcium alginate gel might, however, be limited by the available pore space. Another possibility is that cell mass increase may be limited predominately to those regions of a support where the oxygen concentration is high, ie. the outermost layers (s. 4.5). These possible limits to the growth of entrapped cells may be different but their effects are expected to be the same. Even when all nutritional requirements for growth are met, immobilized cells would not be expected to divide indefinitely.

Exposure to organic solvents produced changes in some characteristics of IMYSC. Perhaps the most significant from the standpoint of analysis was the increase in Km^{app} value for sucrose. Also importantly permeabilized IMYSC did not appear to transform the hexose fructose. The Eadie plot for sucrose was also linear with one section. Such changes perhaps suggest damage of the glucose and fructose transporters, but no definite conclusions can be drawn. A more thorough calorimetric study of the effects of milder permeabilization treatment is required. The imiscibility of organic solvents with water buffer posed a problem related to the study of the effects of exposure to intermediate concentrations on IMYSC. Detergents, chelators and other water soluble permeabilizing agents might be used to

greater effect.

The identification of microorganisms by microcalorimetric study of the growing cells has been attempted, Boiling et al 1973 (263). Distinct thermograms were obtained from which it was possible to distinguish between different species of cells. The approach proposed above (s 5.4) depends on establishing the order of specificity for a range of substrates. The present method is expected to be particularly suitable for differentiating between closely related cell types.

Chapter 6

Application of immobilized enzymes in electrochemical analyses

6.1 Introduction

Electrochemical analysis or electroanalytical chemistry is the generic term applied to methods of chemical analyses based on the phenomena associated with reactions of metal electrodes in contact with electolyte solutions, Lingane 1958 (146). Some idea of the range of techniques implied by this definition is given by Figure (6.1.1).

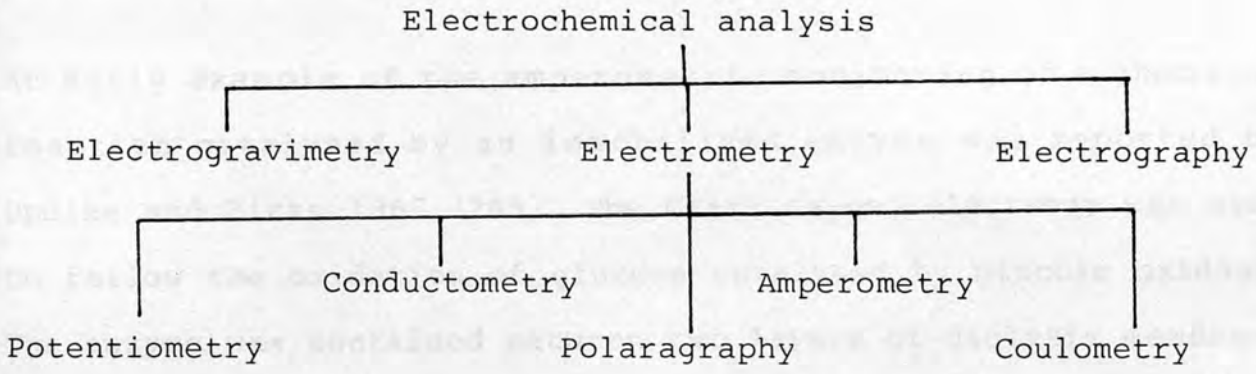

Figure (6.1.1)

The following discussion will be limited to amperometric and potentiometric monitoring as these are the most frequently applied in analyses employing immobilized enzymes.

6.1.1 Amperometric monitoring and immobilized enzyme based analyses

Amperometry belongs to a class of analytical methods characterised by an electrochemical circuit functioning in an electrolytic rather than a galvanic mode. Usually a small fixed potential is applied between two micro-electrodes, and the

resulting current, which is proportional to the concentration of the electroactive species, is measured. A series of related terms also require examination. The term voltametry is applied to the general area of electrochemistry dealing with the determination and interpretation of current - voltage (CV) curves, Laitinen and Kolthoff 1941 (264). The synonymous terms polargraphy and polarometry are specifically applied when a dropping mercury electrode (as opposed to solid metal electrode), with a facility for automatic or manual current measurement respectively, is used.

An early example of the amperometric monitoring of a chemical reaction catalysed by an immobilized enzyme was reported by Updike and Hicks 1967 (265). The Clark oxygen electrode was used to follow the oxidation of glucose catalysed by glucose oxidase. The enzyme was contained between two layers of dialysis membrane held in close association with an amperometric sensor. Although this was probably the first reported example of an `enzyme electrode´, both the concept and the term originated five years earlier, Clark and Lyons 1962 (266). Subsequent developments in the area of amperometric monitoring of immobilized enzyme reactions is reasonably well charted by the papers from the following workers, Williams et al. 1970 (164), Guilbault and Lubrano 1973 (144), Weibel et al. 1973 (267), Nango and Guilbault 1974 (268), Nango and Guilbault 1975 (269), Wolff and Mottola 1977 (270) and lastly Updike et al. 1979 (271).

Recent developments along several fronts are now briefly

outlined. First, there has been an increase in the range of substrates, determined, from glucose, L-amino acids and ethanol, Table (6.1.1.1). Second, this area has recently expanded to include the amperometric assay of enzyme immunoasay determinations, Eggers 1982 (283). Third, commercial amperometric substrate analyzers are marketed e.g. by Beckman and Yellow Springs Instrument Company. Fourth, considerable effort continues to be directed at minuturization and implantation of a glucose sensor as part of the development of a regulated insulin infusion device (the artificial pancrease) for diabetes management, Clark and Duggan 1982 and other articles in the same journal (284). The fifth and final area of active research is in the area of chemically modified electrodes and direct electron transfer electrodes. Amperometric, chemically modified electrodes for xanthine and glucose have been described by Ianniello et al. 1982 (285) and Yao 1983 (286) respectively. The work of Higgin and Hill 1983 (287), well illustrates the second approach.

6.1.2 Potentiometric monitoring and immobilized enzyme based analysis

Potentiometry is based on the concentration (or activity) dependence of potential differences developed at liquid-liquid or liquid-solid interphases. The exact relationship between the concentration of a chemical species and the potential, E is summarized by the Nernst equation.

$$E = E_o + \frac{RT}{nF} \log \frac{(C)_1}{(C)_2}$$

Table (6.1.1-1) Some determinations with immobilized enzymes and amperometric monitoring

Analyte	Imm-enzyme	Reference
L-ascorbic acid	ascorbic acid oxidase	(272, 278)
analine	cyt - P450	(273)
alcohol	alcohol oxidase	(274)
galactose	galactose oxidase	(275)
o-dianizidine	peroxidase	(276)
benzidine	"	"
3,4 diaminobenzene sulphonic acid	"	"
1,2 - diamino-benzene	"	"
cholesterol	cholesterol oxidase	(277)
phenol	phenol oxidase	(278)
cholinesterase	choline oxidase	(279)
dextran	dextranase/glucose oxidase	(280)
NADH	diaphorase	(281)
triglycerides	glycerol dehydrogenase/ diaphorase	(282)

where $(C)_1$ and $(C)_2$ are the concentrations in phase 1 and 2 respectively. Potentiometric electrodes have been classified as metallic or membrane electrodes. The latter class is further subdivided according to the nature of the membrane. Thus there are glass membrane electrodes, liquid membrane electrodes (where a potential is developed across a liquid ion exchange resin held on a porous hydrophobic layer), solid-state or precipitate electrodes and gas-sensing or air-gap electrodes, Skoog and West 1975 (289). The glass membrane electrodes (eg. for H^+, NH_4^+) and gas sensing electrodes (eg. for NH_3, (CO_2) have found widespread use in immoblized enzyme based analysis, Table (6.1.2.1).

Table (6.1.2.1) Some determinations with immobilized enzymes and potentiometric monitoring

Analyte	Imm. enzyme	Sensor	Reference
urea	urease	1	(289)
arginine	arginase/urease	2	(290)
oxaloacetate	oxaloacetate decarboxylase	3	(291)
penicillin, glucose, urea	penicillinase, glucose oxidase, urease	4	(145)
amygdalin	β- glucosidase	5	(292)

Sensor - 1. NH_4^+ glass electrode,

2. NH_3 air-gap electrode,

3. CO_2 air-gap electrode

4. glass membrane pH electrode

5. solid state CN^- sensitive electrode.

Some recent developments are now considered. The possiblity of potentiometric monitoring of enzyme-linked immunoassay determinations has been considered by Gebauer and Rechnitz 1982 (293). The galvanic response underlying potentiometry is, at least in one instance, being considered as a possible basis of a bioelectrochemical fuel cell, Lahoda et al. 1975 (294). Recent progress in semiconductor technology has led to, amongst other things, chemically sensitive field effect transistors (CHEMFET) as an extension to ion selective electrodes, Janata and Huber 1980 (295). CHEMFET devices have been used as the basis of urea analysis e.g. by Danielsson et al. 1979 (296) and Miyahara et al. 1983 (297).

The above represents a brief sketch of the current status of electrometric analysis using immobilized enzymes. The literature preceding 1979 - 80 has been extensively reviewed by Carr and Bowers 1980 (68). Reference might be made to the recent reviews by Wingard 1979 (298), Guilbault 1980 (299), Janata and Huber 1980 (295), Kobos 1980 (300), Rechnitz 1982 (301), Lessler 1982 (302), Karube 1983 (303) or Motolla et al. 1984 (304) for further discussions. Electrometric analyses using immobilized whole cells were reviewed in Chapter 5.

6.2 Characteristics of a Type 3 potentiometric enzyme electrode for glucose

Potentiometric monitoring represents one of the two main electrochemical principles for immobilized enzyme analysis (s 6.1). The enzyme electrode chosen for study employs a glass membrane H^+ sensitive electrode as a base sensor. This is the most inexpensive, commercially available, potentiometric electrode. The principle behind glucose analysis is as follows. Glucose diffusing through a glucose oxidase-BSA layer is oxidised by dissolved oxygen to gluconic acid and hydrogen peroxide, and the resulting change in pH is then measured, (s. 3.4).

As the signal being measured is an acidity change (dpH) analytical sensitivity is expected be affected by the buffer concentration, pH and pka. These factors approximately determine the buffer capacity as described in the Henderson-Hasselbach equation. The effects of buffer concentration and pH on the characteristics of the potentiometric glucose electrode were therefore studied.

Materials and Methods

Details of the materials used and procedure for fabricating a Type-3 electrode were described in Chapter 2. Potentiometric recordings were made by connecting the enzyme electrode and a double junction silver/silver chloride reference electrode to a digital pH/mV meter, (Orion Res. Inc. USA) with a recorder output.

Samples were analysed by dipping both electrodes in 9 cm^3 of phosphate buffer (10^{-3}M, pH 7.0) and then adding 1 cm^3 of glucose standard solution. After brief stirring, potentiometric readings were made under quiescent conditions. In between determinations the electrode was quickly rinsed with distilled water and then dipped into a 200cm^3 stirred (0.1M) buffer reservoir until the return of the potentiometric response to a steady baseline value. It was then equilibrated with 10^{-3}M buffer.

Results

The effects of buffer concentration (at a constant initial pH) and acidity (at a constant concentration of buffer) on the glucose electrode response are shown in Fig. (6.2.1) and Fig. (6.2.2) respectively.

The steady state glucose electrode reponse to saturating concentrations of glucose (0.5M) decreased with increasing concentration of phosphate buffer (10^{-1} - 10^{-3}M). The electrode recovery characteristics were also affected, Fig. (6.2.1). The speed of recovery from glucose determinations over the same range of buffer concentration were measured as the residual dpH after washing for 15 min. It can be seen that the wash characteristics of the potentiometric glucose electrode become increasingly poorer with lower concentrations of buffer.

The buffer pH-dependence of the glucose electrode response over the range of pH 5 - 7 can be seen in Fig. (6.2.2). There is a

maximum in the pH-response profile of about pH 6.0. To allow resolution of the effects of buffer pH, on glucose oxidase activity from the effects on the analytical signal strength (ie. dpH) the pH - response profile for a Type - 1 amperometric glucose electrode (s 6.3) is superimposed for comparison. As will be discussed in detail shortly the amperometric signal is less affected by acidity.

The effect of glucose concentration on the electrode response is reported in Table (6.2.1).

Table (6.2.1) Determination of glucose uisng a Type-3 potentiometric enzyme electrode

[Glucose] M	Electrode response dpH x 10^2
0.8	20.7 $\pm$ 0.2
0.5	21.0 $\pm$ 0.3
0.4	17.5 $\pm$ 0.4
0.25	12.0 $\pm$ 0.6
0.05	7.0 $\pm$ 0.7
0.125	6.0 $\pm$ 1.4

$1.25 \times 10^{-2} \leqslant$ Glucose $\leqslant 5 \times 10^{-1}$ M

$r = 0.9948$; slope = 0.3035 dpH M^{-1}

FIG(6·2·1·)-Effect of buffer concentration on the sensitivity(⊙) and recovery(⊡) of a potentiometric glucose electrode

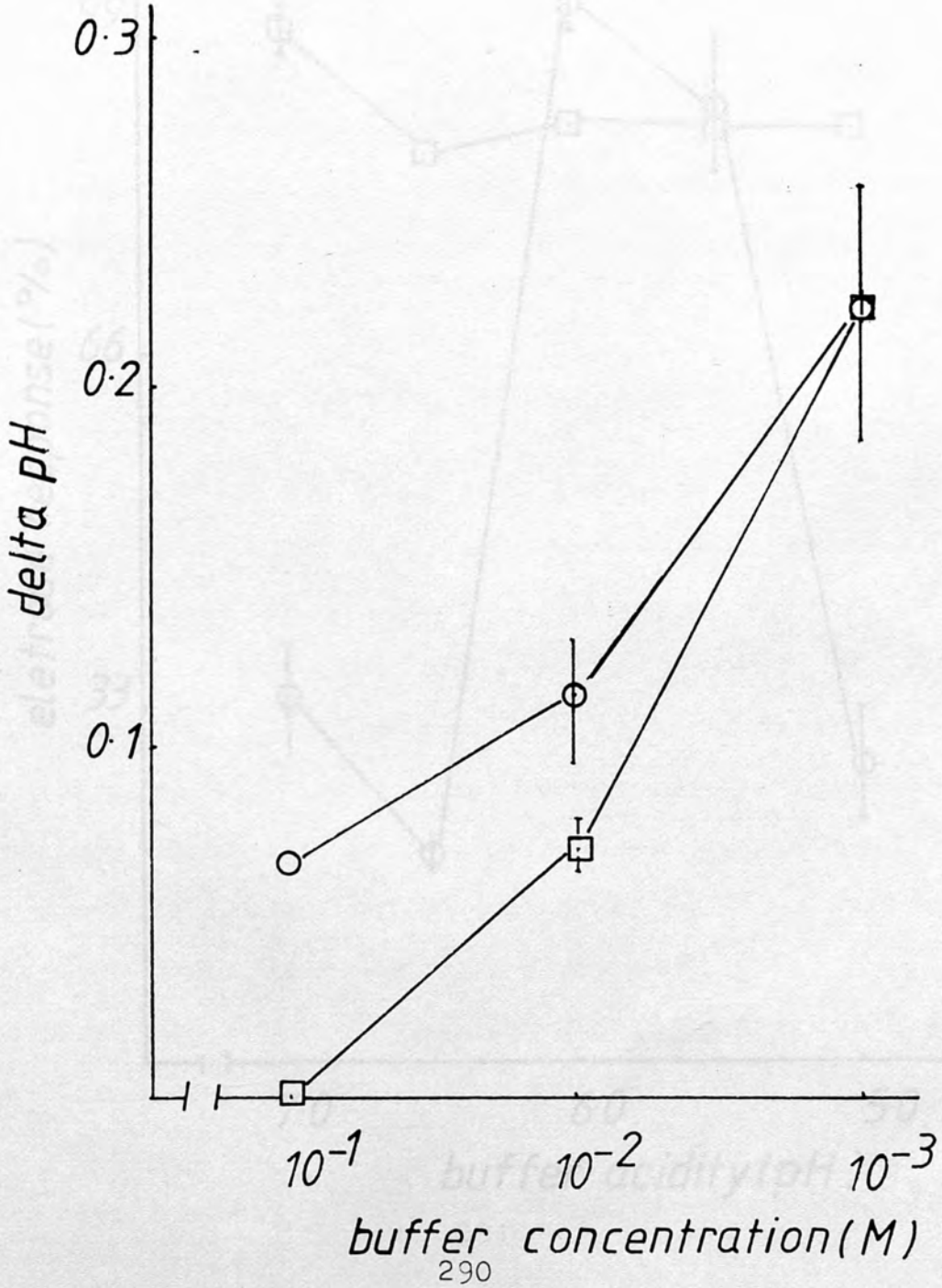

FIG(6·2·2)-Effect of buffer acidity on the response of a potentiometric(⊙) or amperometric(□)glucose electrode

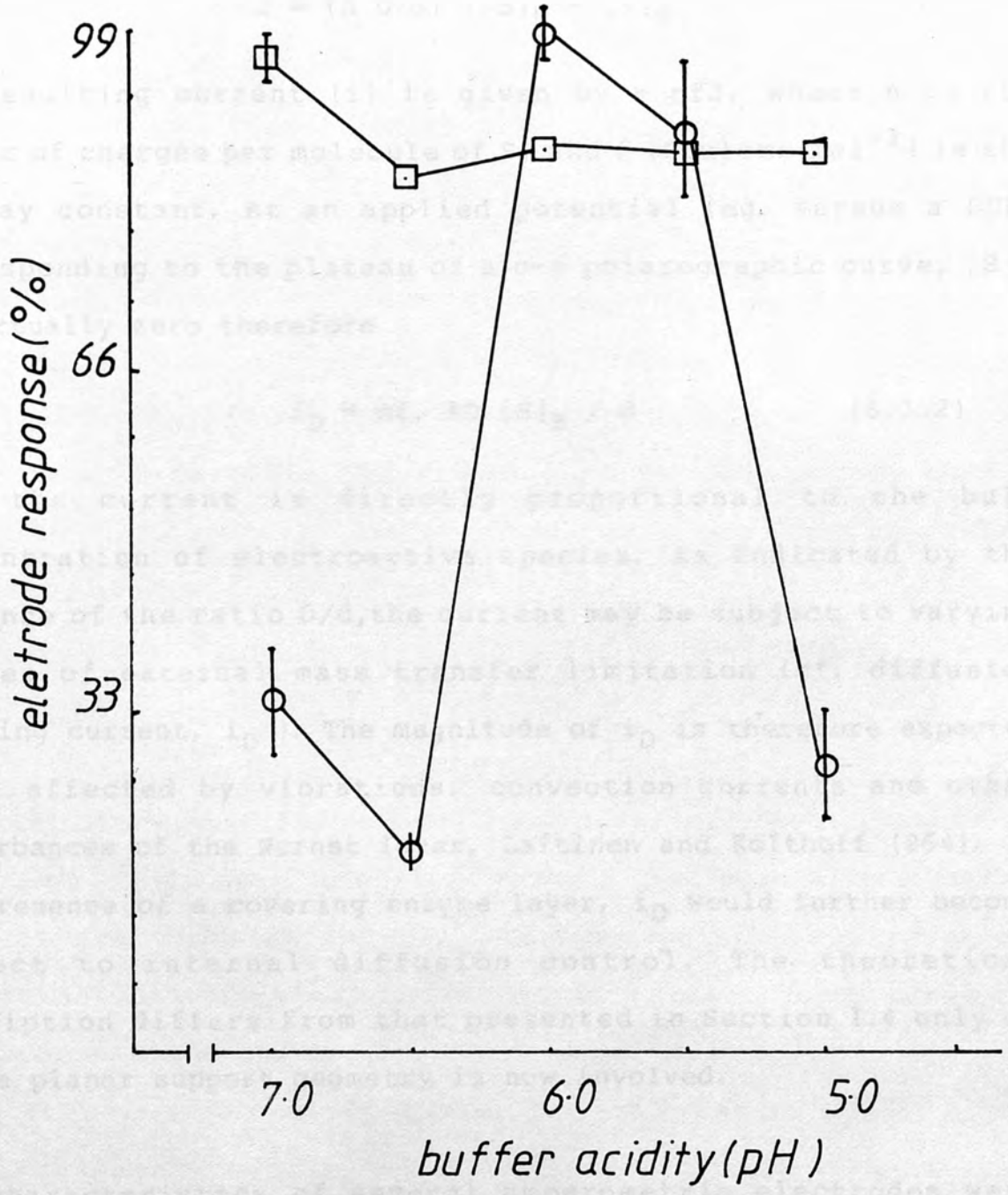

6.3 Determination of substrates using a Type-1 amperometric enzyme electrode

From Fick's law, the flux (J, mol s^{-1}) of electroactive species (S) across a diffusion layer (d,cm) to an electrode, (surface area, A cm^2) is given by (6.3.1), (s 1.4).

$$J = (A\ D/d)\ ([S]_B - [S]_S) \qquad (6.3.1)$$

The resulting current (i) is given by - nfJ, where n is the number of charges per molecule of S, and f (Coulomb mol^{-1}) is the Faraday constant. At an applied potential (eg. versus a SCE) corresponding to the plateau of a c-v polarographic curve, $[S]_S$ is virtually zero therefore

$$i_D = nf.\ AD\ [S]_B\ /\ d \qquad (6.3.2)$$

i.e. the current is directly proportional to the bulk concentration of electroactive species. As indicated by the presence of the ratio D/d,the current may be subject to varying degrees of external mass transfer limitation (cf. diffusion limiting current, i_D). The magnitude of i_D is therefore expected to be affected by vibrations, convection currents and other disturbances of the Nernst layer, Laitinen and Kolthoff (264). In the presence of a covering enzyme layer, i_D would further become subject to internal diffusion control. The theoretical description differs from that presented in Section 1.4 only in that a planar support geometry is now involved.

The characteristics of several amperometric electrodes were

studied. Analysis of substrate depended on the oxidation of hydrogen peroxide formed within the enzyme layer at a platinum electrode at + 0.5 Volt versus a standard mercuric sulphate electrode (SMSE).

Materials and Methods

All enzymes and substrates were commercial, Sigma UK. The construction of a Type-1 enzyme electrode and a current measuring apparatus were described in Sections 2.2.1 and 2.2.2 respectively. The arrangement for substrate analysis under stationary conditions was essentially as depicted in Fig. (2.2.4.2) for flow analysis. The difference is that the enzyme electrode and SMSE are first immersed in reference buffer and sample standards added. The direct current power source ("dc" in Fig. (2.2.4.2) is the Millivolt 404S model from Time Electronics Ltd. Kent, England.

Results

In preliminary studies, the c-v curves for hydrogen peroxide and dissolved oxygen were determined using a platinum solid electrode against the SMSE ($\pm$ 2V) and a manual polarograph (Southern Analytical Ltd. England). From the polarometric c-v curve for hydrogen peroxide and oxygen, i_D occurred at + 0.5 Volt and - 1.0 Volt Pt vs. SMSE respectively. Further there was a linear relationship between i_D and hydrogen peroxide concentration (1.66×10^{-4} M - 8.33×10^{-2}M; r = 0.9974).

The results of glucose or sucrose analysis using a Type-1 enzyme electrode constructed with a glucose oxidase or glucose oxidase/invertase bi-enzyme layer are presented below, Table (6.3.1).

Table (6.3.1) Determination of glucose or sucrose using a Type-1 amperometric enzyme electrode

[Glucose/Sucrose] M	Electrode response (mv)	
	a	b
10×10^{-3}	56 ± 0.8	52
5×10^{-3}	56 ± 0.8	52
2×10^{-3}	29 ± 2.6	40
1×10^{-3}	14 ± 1.2	30 ± 1.8
5×10^{-4}	6.2	16 ± 1.4
2.5×10^{-4}	3.6	-
2.0×10^{-4}	-	6 ± 0.2

* electrode response $x \pm SD_{n-1}$ (+ 0.5 Volt Pt. vs. SMSE)

a. glucose electrode $2.5 \times 10^{-4} \leqslant G \leqslant 2 \times 10^{-3}$; $r = 0.9989$

b. sucrose electrode $2 \times 10^{-4} \leqslant Su \leqslant 2 \times 10^{-3}$; $r = 0.9687$

The corresponding concentration response curves are shown in Fig. (6.3.1). Analyses were carried out in phosphate buffer (0.2M, pH7.0; 10^{-3}M EDTA) at room temperature (24 - 26.5°C) in an unthermostated vessel. The overall precision of analysis was 5.5%.

FIG(6·3·1)-Determination of glucose(⊙) and sucrose(⊡) using an amperometric enzyme electrode

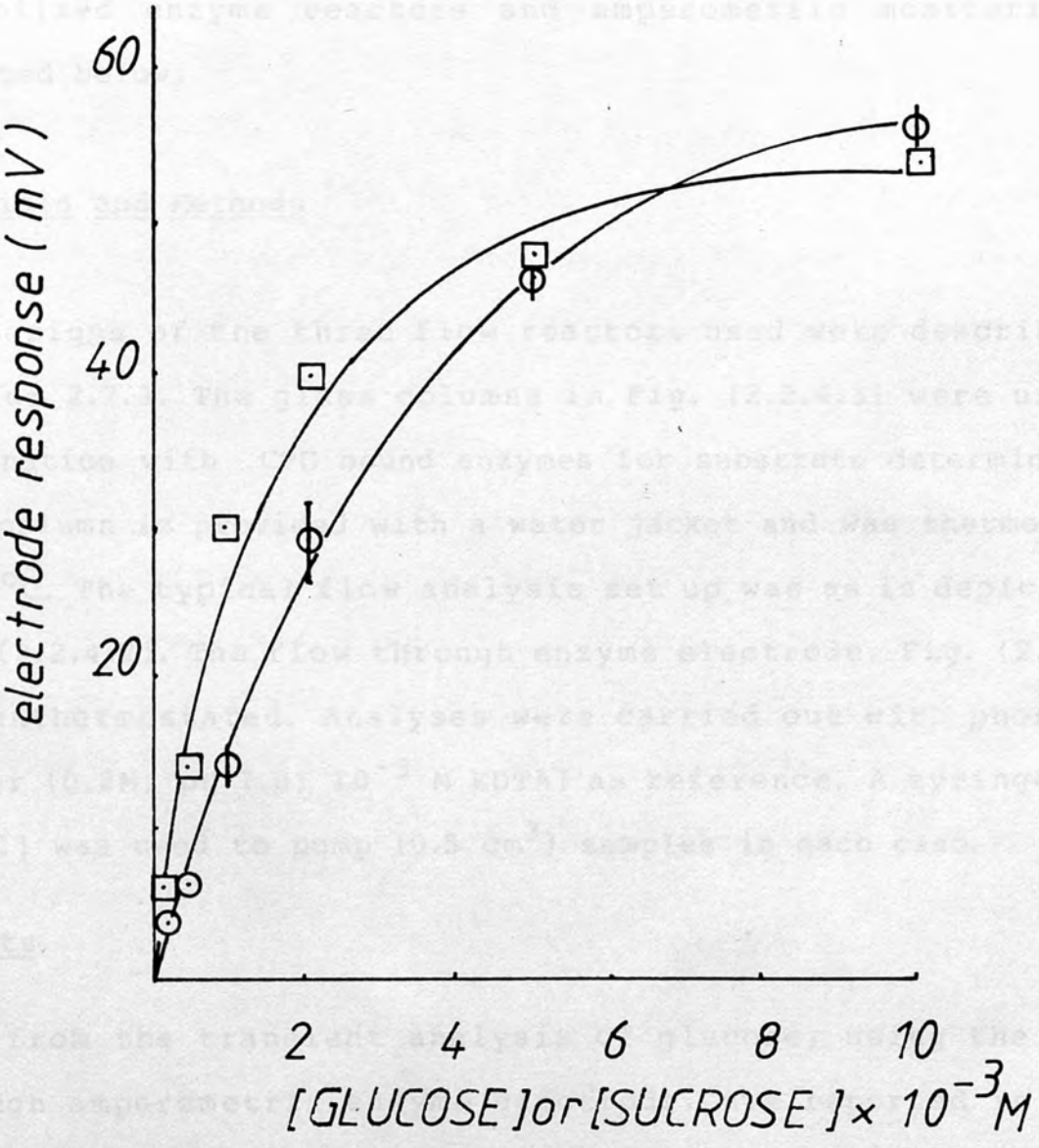

6.4 Flow amperometric analyses using immobilized enzymes

Some reasons for carrying out determination under flow, rather than stationary, conditions include:

a. easier and more rapid sampling;

b. improved precision of analysis;

c. increased sample throughput,

d. increased potential for automation.

The study of the flow analysis of substrates using several immobilzed enzyme reactors and amperometric monitoring is reported below.

Materials and Methods

The designs of the three flow reactors used were described in Section 2.2.3. The glass columns in Fig. (2.2.4.3) were used in combination with CPG bound enzymes for substrate determination. Each column is provided with a water jacket and was thermostated at 25^{o}C. The typical flow analysis set up was as is depicted in Fig. (2.2.4.2). The flow through enzyme electrode, Fig. (2.2.4.1) was unthermostated. Analyses were carried out with phosphate buffer (0.2M, pH 7.0; 10^{-3} M EDTA) as reference. A syringe pump (Razel) was used to pump (0.5 cm^3) samples in each case.

Results

Data from the transient analysis of glucose, using the flow-through amperometric enzyme electrode, are reported in Table (6.4.1). For a sample volumetric flow rate of 9 cm^3 h^{-1},

18 $cm^3\ h^{-1}$ or 66 $cm^3\ h^{-1}$ the mean peak base width over the linear response range (i.e. $G \leqslant 0.5 \times 10^{-3}M$) were 5.22 $\pm$ 0.43, 3.17 $\pm$ 0.20 and 1.18 $\pm$ 0.15 min. respectively. The corresponding values for the sample throughput (s 1.2) are 11.5 $\pm$ 0.95, 19 $\pm$ 1.2 and 51 $\pm$ 6.5 h^{-1}.

The concentration-response curves for these sample flow rates are shown, with peak area as the analytical index, in Fig. (6.4.1). It can be seen that analytical sensitivity decreases with increasing flow rate. The ratios of sensitivity for the curves shown (for $G \leqslant 4 \times 10^{-4}$ M) are in order of increasing flow rate 4.6 : 3.5 : 1. On the other hand the ratio of the slopes for the corresponding peak height data was 1.1 : 1 : 1 at a flow rate 9, 18 and 66 $cm^3\ h^{-1}$. However, when the peak heights are normalized for the extent of conversion, a clear dependence of peak height on flow rate emerges, Fig. (6.4.2).

The present enzyme electrode was examined for a possible galvanic response to glucose. The enzyme electrode and SMSE were connected (without an external power source) to a pH/mV meter with a recorder output and standard glucose samples determined. The results from the analysis under stationary or flow conditions are presented in Table (6.4.2), Fig. (6.4.3) and Table (6.4.3), Fig. (6.4.4) respectively.

The correlation between peak area and peak height is good (0.9946) therefore only the latter are presented in Fig (6.4.4). The LOG plot was fitted with a straight line (r = 0.9881).

Table 6.4.1

[Glucose] x 10^{-4} M	Pk. area (mm^2)			Pk. height (mv)		
	(a)*	(b)	(c)	(a)*	(b)	(c)
10	3048	2472	696	46	52	44
8	2723	1926	590	44	48	41
5	2305	1485	423	40	43	32
4	1881	1284	339	36	38	27
3	1300	972	213	26	31	18
2	-	551	145	-	18	14
1	744	255	52	16	15	9
Precision %	-	2.5	8.3	-	3.8	6.2

Flow rate ($cm^3\ h^{-1}$) (a) = 9, (b) = 18 and (c) = 66

* Single determinations

FIG(6·4·1)-Determination of glucose using an amperometric enzyme electrode; effect of flow rate (F is (○) 66, (□) 18, and (*) 9 $cm^3 h^{-1}$) on peak area

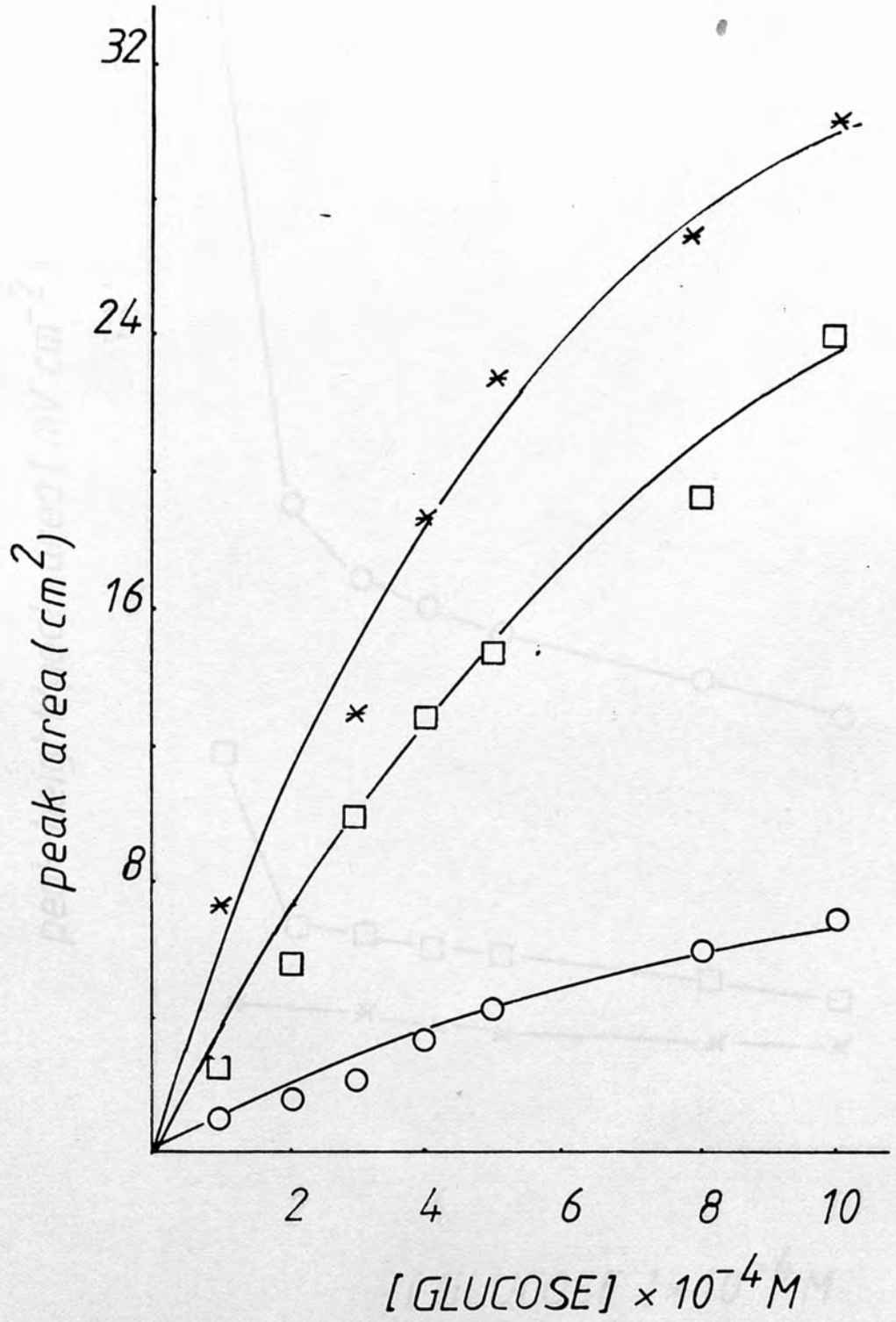

FIG(6·4·2)-Determination of glucose using an amperometric enzyme electrode; effect of flow rate (F is (○)66, (□)18, and (*) 9 $cm^3 h^{-1}$) on the peak height/peak area ratio

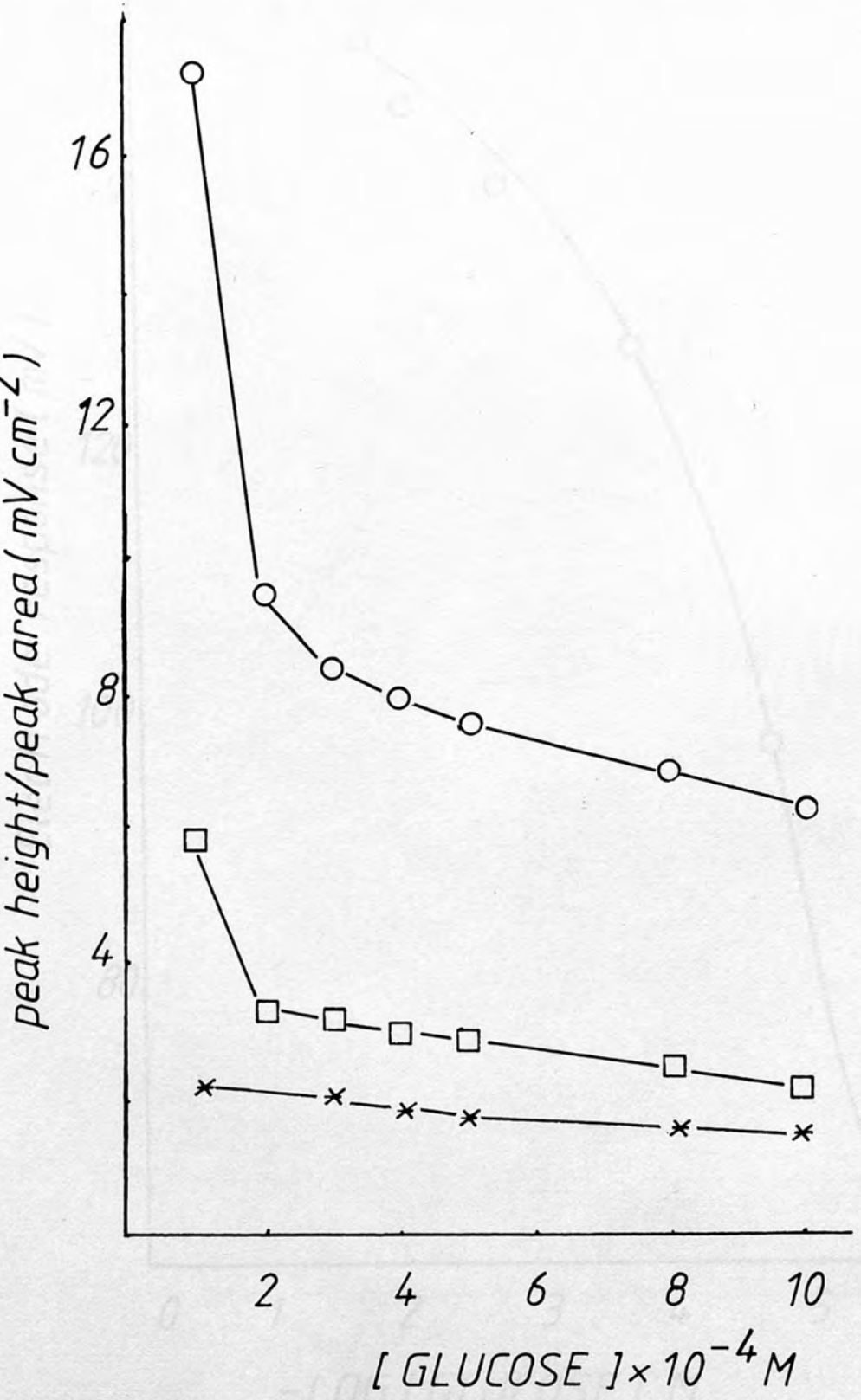

FIG(6·4·3)-Determination of glucose using a galvanic cell arrangement under stationary conditions

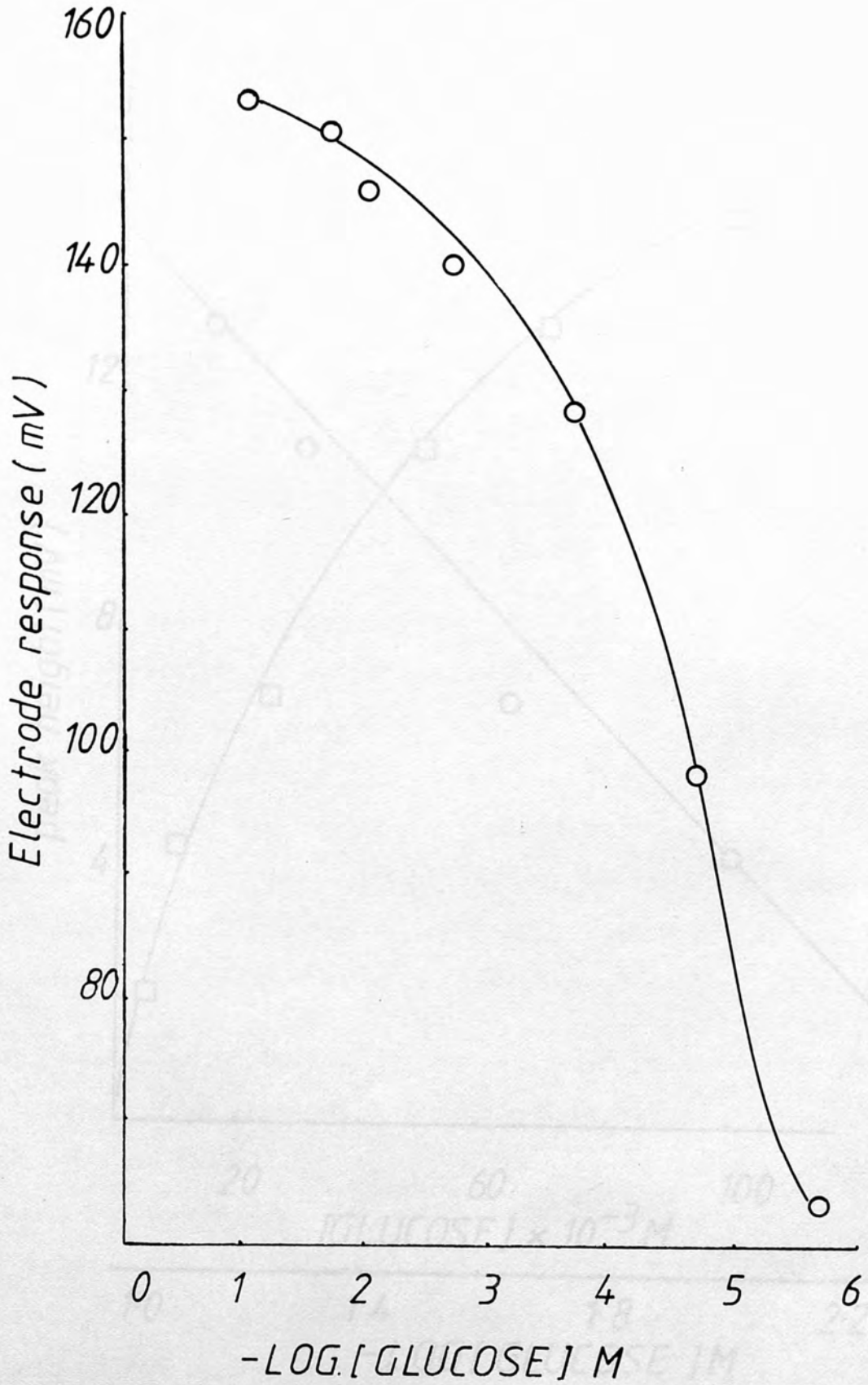

FIG(6·4·4)-Determination of glucose using a galvanic cell arrangement under flow conditions(o - LOG scale)

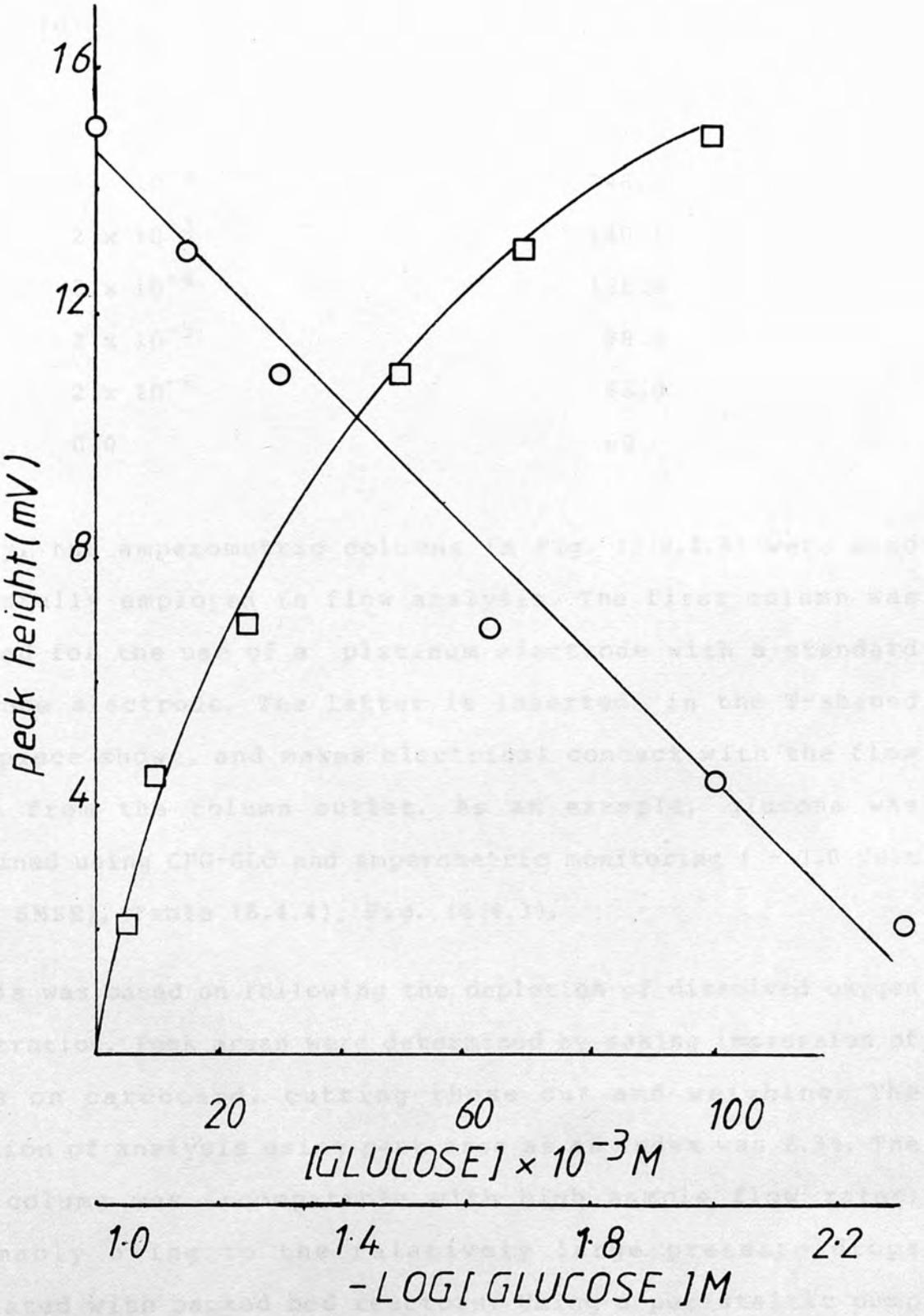

Table (6.4.2) Determination of glucose using a galvanic cell arrangement under stationary conditions

[Glucose] M	Response (mV)
100×10^{-3}	153.0
20×10^{-3}	151.2
10×10^{-3}	146.3
2×10^{-3}	140.1
2×10^{-4}	128.6
2×10^{-5}	98.5
2×10^{-6}	63.0
0.0	60

Finally, the amperometric columns in Fig. (2.2.4.3) were also successfully employed in flow analysis. The first column was designed for the use of a platinum electrode with a standard reference electrode. The latter is inserted in the T-shaped glass piece shown, and makes electrical contact with the flow stream from the column outlet. As an example, glucose was determined using CPG-GLO and amperometric monitoring (- 1.0 Volt pt vs. SMSE), Table (6.4.4); Fig. (6.4.3).

Analysis was based on following the depletion of dissolved oxygen concentration. Peak areas were determined by making impression of traces on cardboard, cutting these out and weighing. The precision of analysis using peak area as an index was 2.3%. The above column was incompatible with high sample flow rates, presumably owing to the relatively large pressure drops associated with packed bed reactors. Using a peristaltic pump

Table (6.4.3) Determination of glucose using a galvanic cell arrangement under flow conditions

Glucose M	Pk.ht(mV)	Pk.area (cm^2)
100×10^{-3}	15.5	45.2
70×10^{-3}	13.1	42.4
50×10^{-3}	11.1	31.2
25×10^{-3}	7.0	19.1
10×10^{-3}	4.5	11.0
5×10^{-3}	2.1	2.8

with a pumping rate of 13 cm^3 h^{-1} resulted in a sample throughput of 10 h^{-1}. Attempts at using higher flow rates resulted in leakages in the flow line, particularly at the flow connection to the column inlet.

The above column when filled with Tyrosinase (EC 1.14.18.1; Sigma UK) bound to CPG was used to determine phenol. All other conditions for this determination were as described before. The linearity range was between 5 x 10^{-5}M and 1 x 10^{-3} M (r = 0.9942). The present application highlights a significant difference between oxygen and hydrogen peroxide monitoring. Phenol is electroactive at a positive applied potential (Pt vs. SMSE). Hydrogen peroxide could therefore not be monitored as a basis of the specific analysis of phenol. This last point also pin-points the only real difference found between the performance of the glass column with the platinum/SMSE (used above) or twin-platinum electrode arrangement. The former represents a more selective arrangement for amperometric determinations.

Table (6.4.4) Determination of glucose using an IMER and amperometric monitoring (-1.0 volt pt vs. SMSE)

[Glucose] M	Pk. ht (mV)[a]	Pk. area (cm^2)[b]
10×10^{-3}	25.0 ± 0.2	22.91 ± 0.48
8×10^{-3}	23.1 ± 0.2	21.07 ± 0.34
6×10^{-3}	22.0	18.44 ± 0.34
4×10^{-3}	20.0	12.03 ± 1.5
2×10^{-3}	9.5	5.76 ± 0.35
1×10^{-3}	6.3	2.93 ± 0.30
8×10^{-4}	5.1 ± 0.2	1.64 ± 0.08
4×10^{-4}	2.5 ± 0.1	0.88 ± 0.11

a. $4 \times 10^{-4} \leqslant G \leqslant 4 \times 10^{-3}$M; r = 0.9960

b. $4 \times 10^{-4} \leqslant G \leqslant 6 \times 10^{-3}$ M; r = 0.9900

correlation between pk.ht and pk.area = 0.9677

FIG(6·4·5)-Determination of glucose using an IMER and amperometric monitoring(- 1·0 Volt Pt. vs. SMSE ;(○)peak height (□)peak area)

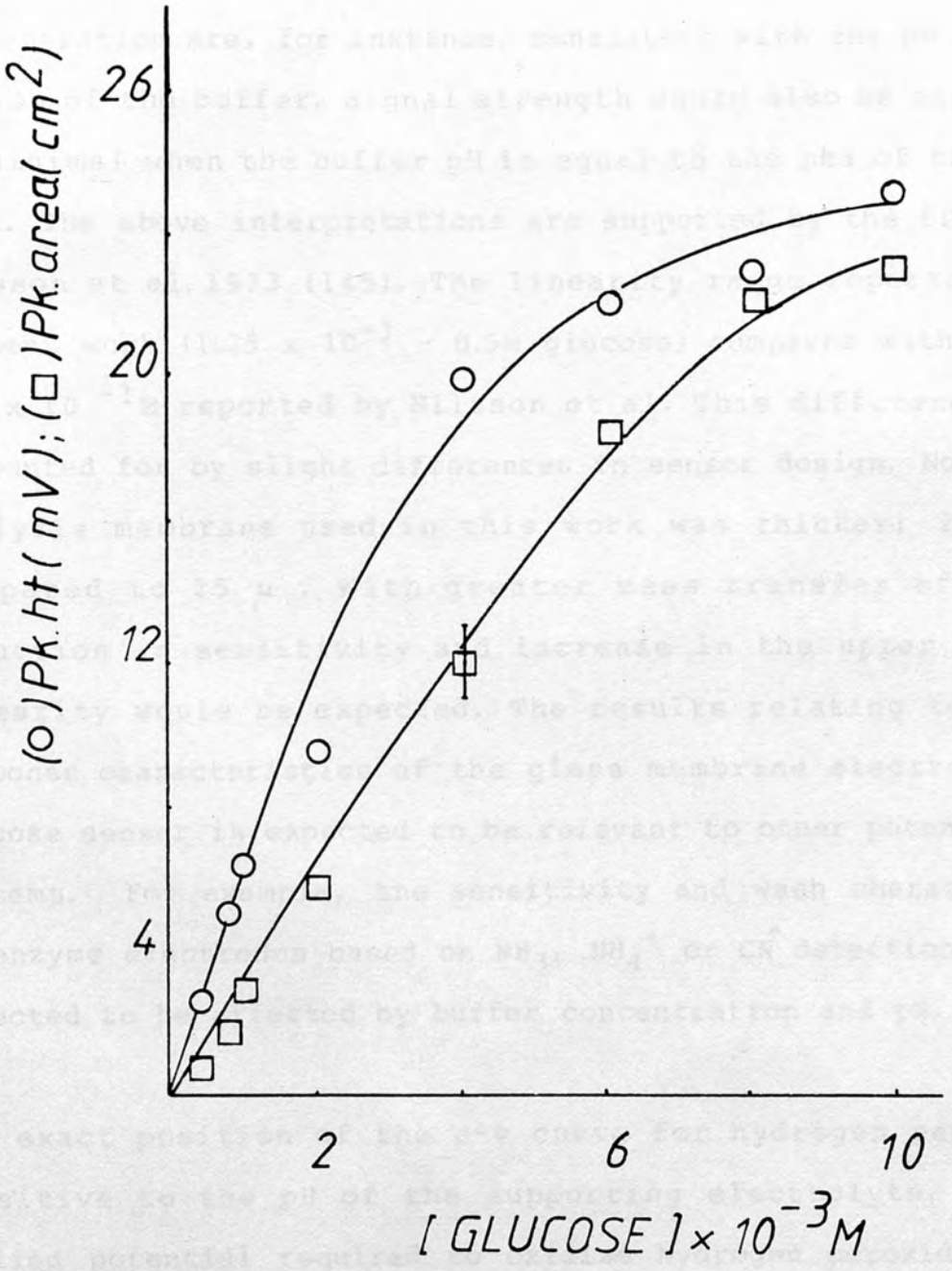

6.5 Discussion

The behaviour of the potentiometric enzyme electrode for glucose (s 6.2) reflects the effect of reaction conditions on the signal strength (d-pH) as well as on the enzyme activity. The decrease in the electrode response to a saturating concentration of glucose and improved recovery with increasing buffer concentration are, for instance, consistent with the pH quenching action of the buffer. Signal strength would also be expected to be minimal when the buffer pH is equal to the pka of the buffer ions. The above interpretations are supported by the findings of Nilsson et al. 1973 (145). The linearity range reported in the present work (1.25×10^{-3} - 0.5M glucose) compares with 1×10^{-3} - 1×10^{-1}M reported by Nilsson et al. This difference may be accounted for by slight differences in sensor design. Notably the dialysis membrane used in this work was thicker; 250 μ as compared to 25 μ . With greater mass transfer effects, a reduction in sensitivity and increase in the upper limit of linearity would be expected. The results relating to the pH-response characteristics of the glass membrane electrode-based glucose sensor is expected to be relevant to other potentiometric systems. For example, the sensitivity and wash characteristics of enzyme electrodes based on NH_3, NH_4^+ or CN^- detection would be expected to be affected by buffer concentration and pH.

The exact position of the c-v curve for hydrogen peroxide is sensitive to the pH of the supporting electrolyte. Thus the applied potential required to oxidize hydrogen peroxide becomes

more positive with increasing acidity, Guilbault and Lubrano 1973 (144). However, since the i_D occurs at a plateau in the c-v curve the former is largely still insensitive to pH. This may explain the insensitivity of the amperometric glucose electrode to acidity (pH 5 - 7). A sharp fall in electrode response occurred at pH > 8; this was probably due to enzyme inactivation. Exposure to media of pH 8.5 resulted in a decrease in the electrode zero-order response. Subsequently, placement in a buffer at pH 7.0 lead to a slow recovery of activity. Finally overnight storage in the thiol reagent, dithiothreitol, resulted in 100% recovery of activity. From these observations, the effect of highly alkaline media may be attributed to the oxidation of thiol groups essential for glucose oxidase activity.

The upper limit of linearity of the amperometric glucose electrode (+ 0.5 Volt vs. SMSE) is not expected to be determined by the dissolved oxygen concentration. This is because oxygen is regenerated from hydrogen peroxide by the electrode reaction, Guilbault and Lubrano 1973 (144). The determinants of linearity in endpoint analysis is a topic which appears to have attracted little attention. The value of the equilibrium constant for the enzyme reaction is certainly one important parameter. The linearity range for glucose or sucrose determination reported for this work (2×10^{-4} - 2×10^{-3} M) compares with 2×10^{-3} - 20×10^{-3} M reported by Guilbault and Lubrano.

A bi-enzyme electrode design may be adopted where, as with the hydrolysis of sucrose to fructose and glucose, the reactant or

products of an enzyme-catalysed reaction are not immediately electroactive. On the other hand, the presence of more than one enzyme usually results in a degree of nonspecifity. For instance the sucrose electrode described above is also sensitive to glucose. A solution to this problem has been proposed by Scheller and Renneberg 1983 (305). It involves placing a primary enzyme layer before the bi-enzyme layer to remove the interfering compound. For instance a glucose oxidase layer placed before a glucose oxidase/invertase bi-enzyme layer enabled the analysis of sucrose samples containing glucose.

Another aspect of enzyme electrode specificity relates to the susceptibility to interference by indigenous electroactive species often present in samples,eg.,of biological origin. The placement of a cellulose acetate membrane over a bare platinum electrode can render it insensitive to uric acid, ascorbic acid and other reluctants, Wingard 1983 (306). As a corollary, such compounds may also decrease electrode sensitivity, as a result of reaction with hydrogen peroxide. For the same reason, catalase impurity in glucose oxidase samples used for fabricating enzyme electrodes, should be as low as possible when hydrogen peroxide concentration is being monitored. Many of the above problems appear to be avoided by monitoring oxygen depletion.

The effect of sample flow rate on the sensitivity of analyses with the flow through amperometric enzyme electrode is consistent with the relations between residence time, fractional conversion

and sample throughput discussed in Section 3.2. From similar arguments to those presented earlier, it follows that a sensitivity parameter, analogous to dH_R in calorimetry, may be defined for amperometric analysis. The appropriate dimensions are Coulombs mol^{-1} which is the dimensions of the Faraday constant (f). By analogy to flow calorimetry the two relations below may be written.

$$d(q)/dt = n\, k_1\, S\, V_R\, f \qquad (6.5.1)$$

and

$$d(q)/dt = S \,.\, F \,.\, nf' \qquad (6.5.2)$$

where d(q)/dt is the current ($C\ s^{-1}$). All the other symbols are as defined previously. As before (s 3.2) a plot of d(q)/dt against S.F ($mol\ s^{-1}$) should be linear with a slope of nf provided that X is 98 - 100%

For an amperometric enzyme electrode it seems that 1.5 d^2/D_{eff} is the time taken for substrate, diffusing through the enzyme layer towards the electrode surface, to reach a steady state concentration. This ratio is also the enzyme electrode response time, Mell and Maloy 1975 (307). It may also be taken as "sample residence" time in that increasing the enzyme layer thickness results in increased sensitivity owing an increase the length of time required for the substrate to tranverse the enzyme layer, (cf.$X = 1 - \exp(k_1 t)$). It may considered that once a substrate molecule enters the enzyme layer, it becomes essentially subject to the rules outlined above. Thus the increase in the sensitivity of analysis with an enzyme electrode resulting from the use of

low sample flow rate may be explained as due to the greater length of time allowed for substrate molecules to enter the enzyme layer. When sample flow rate is virutally zero, the resulting condition will be similar to analyses under stationary conditions.

The origin of the enzyme electrode response to glucose, with a galvanic arrangement is uncertain. The potential difference observed could be in response to changes in pH, oxygen tension or hydrogen peroxide concentration which accompany the glucose oxidase reaction.

CHAPTER 7

Concluding remarks

7.1 Achievements of the work described in this thesis

This thesis is concerned with the application of immobilized enzymes (and cells) in analytical chemistry primarily using flow microcalorimetric monitoring (electrochemical methods were considered relatively briefly in Chapter 6).

The application of calorimetry in related areas was reviewed in Section 1.1 . Otherwise it can be seen from Chapter 1 and 2 that the present work has theoretical anticedence largely in the fields of chemical engineering and (affinity) chromatography. The descriptions of sample dispersion, reactor kinetics, diffusion control of reactions in heterogenous systems and also of matters relating to immobilization supports and chemistry are derived from these fields of study.

There is a paucity of quantitative descriptions of flow microcalorimetric monitoring of immobilized enzyme reactions. Notably, Beezer 1972 (147), 1973 (152), 1974 (12) and more recently Eftink et al. 1981 (14) have dealt with the kinetics reactions catalysed by soluble enzymes. The basic precept of the work described in Chapter 3 is that the IMER/flow microcalorimeter combination can be considered as a FIA system with a thermochemical detector. Some conclusions following from this assumption , are as follows:

1. The sample throughput consistent with a full detector fidelity/sensitivity in transient analysis is limited by the detector response speed, to about 5 h^{-1}.
2. The sensitivity of analysis is a function of X (s 1.4; s 3.2). The degree of conversion of substrate was shown experimentally to be dependent on the column enzyme activity, Km^{app} and sample residence time. (The effect of a plethora of other factors on analytical sensitivity can be understood through the expression X = 1 - exp(-kt); (s 1.4)).
3. The linearity range and sample throughput are greater with pulsed relative to continuous sample injection though the latter gives a lower minimum detectable concentration. These differences are largely due to sample dispersion/dilution which occurs with pulsed but not continuous sample injection.

In Chapter 4 it was shown that flow microcalorimetry could be applied to the study of the kinetics of reactions catalysed by immobilized enzymes, though traditional initial rate enzyme kinetics methodology was inapplicable. The reactions catalysed by urease, glucose oxidase, actylcholinesterase and ascorbate oxidase immobilized on CPG were all shown to be diffusion controlled. The ratio of observed to the actual enzyme zero-order activity present was usually less than 0.25 for enzymes immobilized on a 55μ support.

Microcalorimetry may be combined with immobilized cells for analysis. In Chapter 5 emphasis was, however, drawn to the potential value of this approach for fundamental study since it appears that cells maybe immobilized without altering their native characteristics. Substrate specificity lists were, e.g., determined and the order of 'preference' shown to be distinctive for particular strains of yeast. The hypothesis was presented that such an approach may provide a means of distinguishing between closely related strains of cells.

Electrochemical monitoring was studied as an example of a non-thermal analytical principle in Chapter 6. This approach could be almost as widely applicable as the thermal approach. Most enzyme catalysed reactions result in changes of concentration of species detectable by electrochemical means. The bulk of the work involved amperometric systems. With a flow-through enzyme electrode format a high sample throughput ($51 \pm 6\ h^{-1}$) was possible. As no attempts at optimization were attempted there may be some scope for improving such performance.

7.2 Suggestions for further work

The present stage in the development of biological calorimetry may perhaps be compared to spectrophotometry some 30 years ago. Thus although the advantages and scope for application are widely recognised calorimetry is not yet a common technique in clinical and industrial laboratories. This maybe due to the unavailability of easily operated, sensitive commercial

instruments. Apart from the efforts of Mosbach and others, at the Lund university, Sweden few serious attempts appear to have been made to meet this need (s. 1.1).

There are a number of substrates for which analysis using the combinaton of immobilized enzymes and calorimetry seems imminent. Examples include creatinine, creatine, diamines, ethanol, a large number of organic acids and starch. The respective enzymes are readily available. Flow microcalorimetric analyses using immobilized cells represents another area requiring yet further attention. The work described in Chapter 6 might be extended to other types of native or permeabilized cells; the use of more complex substrates in establishing differences between strains of cells may also be examined.

Electrochemical analyses using immobilized enzymes

The foremost areas of research in this field were outlined in Chapter 6. These include CHEMFET based biosensors, CME, miniturization, biofuel cells, and the use of electrochemical monitoring for solid phase immunoassay.

Other Areas

Chemiluminescence and bioluminescence analysis, the use of immobilized lectins in analysis and enzyme linked immunoassay (ELISA), are areas which continue to command considerable interest. So too does the use of computer aided data acquisition

in analysis and control.

Analytical chemistry is characterised by the identification and quantification of particular chemical components in often complex mixtures. Such enumeration forms the basis of large parts of research in, e.g., microbiology and bio/chemistry. It seems then that there may be scope for relevant work in any field employing enzymes and similarly active or specific molecules.

References

1. Lavoisier, A.L., de Laplace, P.S., (1780). Sur la Chleur, Paris
2. McGlothlin, C.D., Jordan, J., (1975). Anal. Chem. 47 1479 - 81
3. Mosbach, K., (1977). U.S. US 4,021,307
4. Christensen, J.J., Johnston, H.D., Izatt, R.M., (1968). Rev. Sci. Intrum. 39, 1546 - 9
5. Prosen, E.J., (1973). NBS Interim Report, Washington D.C., 73 - 179
6. Wadso, I., (1968) Acta. Chem. Scand. 22, 925 - 937
7. Schachinger, L., Hochhauser, E., Ohiaeri, J., (9183). Thermochim. Acta 69, 269 - 271
8. Poore, V.M., Beezer, A.E., (1983). Thermochim. Acta. 63, 133 - 144
9. Poe, M., (1970). 25th Annu. Calorim. Conf. Gothesburg, 19 - 22
10. Rehak, N.N., Jones, G., Young, D.S., (1977). Clin Chem. 23 195 - 199
11. Monk, P., Wadso I., (1969). Acta. Chem. Scand. 23 29-36
12. Beezer, A.E., Steenson, T.J., Tyrell, J.V., (1974). Talanta 21, 467 - 474
13. Tribout, M., Parades, S., Leonis, J., (1976) Biochem. J. 153, 89 - 91
14. Eftink, M.R., Johnson, R.E., Biltonen, R.L., (1981). Anal. Biochem. 111, 305 - 320

15. Konickova, J., Wadso, I., (1971). Acta. Chem. Scand. 25, 2360 - 2

16. Beezer, A.E., Stubbs, C.D., (1973). Talanta 20, 27-31

17. Goldberg, R.N., Prosen, E.J. Staples, B.R., Boyd, R.N. Armstrong, G.T., (1975). Anal. Biochem. 64, 68 - 74

18. McGlothlin, C.D., Jordan J., (1975. Anal. Chem. 47, 786 - 789

19. Johanson, A., Lundberg, J., Mattiasson, B., Mosbach, K., (1973). Biochim. Biophys. Acta. 304, 217 - 221

20. Schmidt, H.L., Krisam, G., Grenner, G., (1976). Biochim. Biophys. Acta. 429, 283 - 290

21. Danielsson, B., Gadd, K., Mattiasson, B., Mosbach, K., (1976) Anal. Letts. 9, 987 - 1001

22. Beezer, A.E., Chowdhry, B.Z., Newell, R.D., Tyrrell, H.J.V. (1977) Anal. Chem. 49, 1781 - 4

23. Mattiasson, B., Larsson, B., Mosbach, K., (1977). Nature, 268, 519 - 520

24. Beezer, A.E., (1980) (Ed) Biological Microcalorimetry Academic Press

25. Cerny, L.C., Cook, F.B., and Stasiw, D.M. (1974). Biorheology 11, 235

26. Spink, C., Wadso, I., (1976) Methods. Biochem. Anal. 23, 1 - 159

27. Martin, J.P., Marini, M.H., (1979). CRC. Crit. Rev. Anal. Chem. 8, 221 - 286

28. Spink, C.H., (1980). CRC. Crit. Rev. Anal. Chem. 9, 1 - 54

29. Sturtevant, J.M., (1974). Ann. Rev. Biophys. Bioeng. 3, 35 - 51

30. Brown, A.J., (1902). J. Chem. Soc. 81, 373 - 388

31. Michaelis, L., Menten, M.L., (1913) Biochem. Zeitschr. 49, 333 - 369

32. Shaw, D.J., (1979) "Introduction to colloid and surface chemistry". Butterworths

33. Vieth, W.R., Venkatsubramanian, K., Constantinides, A., Davidson, B., (1976) Appl. Biochem. Eng. 1, 221 - 327

34. Wharton, C.R., (1983). Biochem. Soc. Trans. 11, 817-825

35. Eftink, M.R., Johnson, R.E., Biltonen, R.L., (1981) Anal. Biochem. 111, 291 - 304

36. Cha, S., (1970) J. Biol. Chem. 245, 4814 - 8

37. Engasser, J., Horvarth, C., (1973) J. Theor. Biol. 42, 137 - 157

38. Skeggs Jr., L.T., (1957) Am. J. Pathol. 28, 311 - 322

39. Ruzicka, J., Hansen, E. H., (1975) Anal. Chim. Acta. 78, 145 - 157

40. Salpeter, J., Leperch, J., (1981) Am. Lab. 13, 78, 80 - 81, 83 - 85

41. Ruzicka, J., Hansen, E.H., (1978) Anal. Chim. Acta. 99, 37 - 76

42. Ruzicka, J., Hansen E., (1980) Anal. Chim. Acta. 114, 19 - 44

43. Ruzicka, J., (1981) Anal. Proc. (London) 18, 267 - 269

44. Snyder, L.R., (1980) Anal. Chim. Acta. 114, 3 - 18

45. Ruzicka, J., Hansen, E.H., (1981). "Flow Injection Analysis", J. Wiley and Sons

46. Sokal, R.R., Rohlf, F.J., (1973) "Introduction to Biostatistics". Kennedy, D., Park, R.R., (Eds). W.H. Freeman and Comapany. San Francisco.

47. Snyder, L.R., (1972) J. Chr. Sci. 10, 369 - 378

48. Taylor, G.,I., (1953) Proc. Roy. Soc. Lond. A235, 67

49. Schifreen, R.S., Hanna, D.A. Bower, L.D., Carr, P.W., (1977) Anal, Chem. 49, 1929 - 39

50. Martin, J.P.A., Synge, R.L.M., (1941) J. Biol. Chem. 35, 1358 - 68

51. Giddings, J.C., (1970) "Dynamics of Chromatography" 2nd edn. Academic Press. N.Y.

52. Snyder, L.R., (1969) J. Chr. Sci. 7, 352 - 360

53. Gruska, E., Snyder, L.R., Knox, J.H., (1975) J. Chr. Sci. 13, 25 - 37

54. Poppe, H., (1980) Anal. Chim. Acta. 114, 59 - 70

55. Reisel, E., Katchalski, E. (1964) J. Biol. Chem. 239, 1521

56. Ikeda, S., Sumi, Y., Fukui, S., (1974) Febs. Letts. 47, 295

57. Hicks, G.P., Updike, S.J., (1966) Anal. Chem. 38, 726 - 730

58. Johansson, G., Edstrom, K., Ogren, L., (1976) Anal. Chim. Acta. 85, 55 - 60

59. Updike, S.J., Hicks, G.P., (1967) Science, 158, 270

60. Auses, J.P., Cook. S.L. Maloy, J.T., (1975) Anal. Chem. 47, 244 - 249

61. Cambell, J., Hornby, W.E., Morris, D.L., (1975) Biochim. Biophys. Acta, 384, 304 - 316

62. Iob, A., Mottola, A., (1981) Clin. Chem. 27, 195 - 196

63. Horvarth, C., Solomon, B.A., (1972) Biotechnol. Bioeng. 14, 885 - 914

64. Ramaswamy, M., Mottola, H., (1982) Anal. Chem. 54, 283 - 286

65. Wolff, C., M., Mottola, H.A., (1978) Anal. Chem. 50, 94 - 98

66. Johansson, G., (1982) Appl Biochem. Biotehcnol. 7, 96 - 106

67. Johansson, G., Ogren, L., Olsson, B., (1983) Anal. Chim. Acta. 145, 71 - 85

68. Carr, P.W., Bowers, L.D., (1980) "Immobilized enzymes in analytical and clinical chemistry. Fundamentals and applications". J. Wiley and Sons, Chichester

69. Johansson, G., Olsson, B., Ogren, L., (1984) Anal. Chem. Symp. Ser. 18, 99 - 120

70. Mottola, H.A., (1983) Anal. Chim. Acta. 145, 27 - 39

71. Lilly, M.D., Hornby, W.E., Crook, E.M., (1966) Biochem. J. 100, 718 - 723

72. Nernst, W., (1904) Z. Phys. Chem. 47, 52

73. Lee, S.B., Ryu, D.D., (1979) Biotechnol. Bioeng. 21, 1499 - 505

74. Goldman, R., Kadem, O., Katchalski, E., (1971) Biochem. 10, 165 - 172

75. Onyezili, F.N., Onitiri, A.C., (1981). Biochim. Biophys. Acta. 659, 244 - 248

76. Dugas, M.C., Ramaswamy, K., Crane, R.K., (1975). Biochim. Biophys. Acta. 382, 576 - 589

77. Bunting, P.S., Laidler, K.J., (1972). Biochem. 11, 4477 - 83

78. Muller, J., Zwing, T., (1982) Biochim. Biophys. Acta. 705, 117 - 123

79. Goldstein, L., Levin, Y., Katchalski, E., (1964) Biochem. 3, 1913 - 19

80. Levin, Y., Pecht, M., Goldstein, L., Katchalski, E., (1964) Biochem. 3, 1905 - 13

81. Hornby, W.E., Lilly, M.D., Crook, E.M., (1966) Biochem. 98, 420 - 425

82. Remy, M.H., David, A., Thomas, D., (1978) Febs. Letts. 82, 332 - 336

83. Duggal, S.K., Buchholtz, K., (1982) Eur. J. Appl. Microb. Biotechnol. 16, 81 - 87

84. Koch - Schmidt, A.C., Mosbach, K., (1977) Biochem. 16, 2101 - 4

85. Koch - Schmidt, A.C., Mosbach, K., (1977) Biochem. 16, 2105 - 9

86. Warburg, O., (1923) Biochem. Z. 142, 317 - 335

87. Blum, J.J., (1956) Biochim. Biophys. Acta 21, 155 - 166

88. Winne, D., (1973) Biochim. Biophys. Acta 298, 27 - 31

89. Kasche, V. (1983) Enzyme Microb. Technol. 5, 2 - 13

90. Thiele, E.W., (1939) Ind. Eng. Chem. 31, 916 - 920

91. Moo-Young, M., Kabayashi, T., (1972) Can. J. Chem. Eng. 50, 162 - 157

92. Engasser, J.M., Horvarth, C., (1973) J. Theor. Biol. 42, 137 - 157

93. Engasser, J.M., Horvarth, C., (1976) Appl. Biochem. Eng. I, 127 - 220

94. Hamilton, B.K., Gardner C.R., Colton, C.K., (1974) Imm. Enzymes Food Microb. Process Symp., 205 - 224

95. Lee, Y.Y., Tsae, G.T., (1974) J. Food Sci. 39, 667-672

96. Pitcher, Jr., W.H., (1978). Adv. Biochem. Eng. 10, Ghose, T.K., Fietcher, A., Blakebrough, N. (Eds) Springer-Verlag. N.Y., 1 - 26

97. Vincent, J.C., Thellier, M., (1983) Biophys. J. 41, 23 - 28

98. Hamilton, B.K., Gardner, C.R., Colton, C.K., (1974) Amer. Inst. Chem. Eng. J. 20, 503 - 510

99. Engasser, J. M., Horvarth, C., (1974) Biochem. 13, 3849 - 54

100. Preston, R.L., (1982) Biochim. Biophys. Acta. 688, 422 - 428

101. Ngo, T.T., Laidler, K.J., (1978) Biochim. Biophys. Acta 525, 93 - 102

102. Engasser, J.M., Horvarth, C, (1974) Biochem. 13, 3845 - 9

103. Kobayashi, T., and Laidler, K., (1973), Biochim. Biophysc. Acta. 302, 1 -12

104. Engasser, J.M., (1978) Biochim. Biophys. Acta 526, 301 - 310

105. Nelson, J.M., Griffin, E.G., (1916) J. Am. Chem. Soc. 38, 1109 - 15

106. Nelson, J.M., Hitchcocks, D.I., (1921) J. Am. Chem. Soc. 43, 1956 - 61

107. Langmuir, I., Schaefer, V.J., (1938) J. Am. Chem. Soc. 60, 1351 - 60

108. Grubhofer, N., Schleith, L. (1953) Naturwissenschaften 40, 508

109. Manecke, g., Gilbert, K.E., (1955) Naturwissenschaften 42, 212

110. Brandenberger, H., (1956) J. Plym. Sci. 20, 215

111. Manecke, G., Singer, S., (1960) Makromol. Chem. 37, 119

112. Mitz, M.A., summaria, L.J., (1961) Nature 189, 576-577

113. Levin, Y., Pecht, M., Goldstein, L., Katchalski, E., (1964) Biochem. 3, 1905 - 13

114. Weetall, H.H., Weliky, N., (1964) Nature 204, 896 - 897

115. Mosbach, K., Mosbach, R., (1966) Acta. Chem. Scand. 20, 2807 - 10

116. Axen, R., Porath, J., (1966) Nature 210, 367 - 369

117. Weetall, H.H., (1969) Nature 223, 959 - 960

118. Hornby, W.E., and Filippusson, H., (1970) Biochim. Biophys. Acta. 220, 343

119. Cornet, J.L., (1979) Polym. Prepr. Am. Chem. soc. Div. Polym. Chem. 20, 878 - 879

120. Mattiasson, B. (1983) Trends. Biotehcnol. I, 16 - 20

121. Mattiasson, B. (1982) Appl. Biochem. Biotechnol. 7, 121-125

122. Messing, R.A., (1975) in "Immobilized Enzymes for industrial reactors" Messing, R.A., (Ed). Academic Press, London. 63 - 78

123. Haller, W., (1965) Nature 206, 693 - 696

124. Pierce: Handbook and General Catalog. (1982 - 1983)

125. Pharmacia Catalogue 1983. AB Pharmacia, Upsala, Sweden

126. Weetall, H.H., (1973) Food. Prod. Dev. 7, 46 - 52

127. Filbert, A.M., (1975) in "Immobilized enzymes for industrial reactors." Messing, R.A., (Ed) Academic Press. London. 36 - 60

128. Goldstein, L., Manecke, G., (1976). Appl Biochem. Bioeng. I, 23 - 127

129. Kilara, A., Shahini, K.M., (1979), Crit. Rev. Food Sci. Nutr. 12, 161 - 198

130. Haller, W., (1983) Chem. Anal. 66, 535 - 597

131. Messing, R.A., (1975) in "Immobilized enzymes for industrial reactors", Messing, R.A., (Ed). Academic Press, London. 63 - 78

132. Weetall, H.H., Ed. (1975) "Immobilized enzymes antigens, antibodies and peptides". Marcel Decker, N.Y.

133. Mosbach, K., Ed. (1976) Methods Enzymol. 44 (Immobilized enzymes). Springer-Verlag N.Y.

134. Ghose, T.K., Fietcher, A., Blakebrough, N., Eds. (1978) Adv. Biochem. Eng. 10 Springer-Verlag. N.Y.

135. Robinson, P.J., Dunnill, P., Lilly, M.D., (1971) Biochim, Biophys. Acta 242, 659 - 661

136. Messing, R.A., Weisz, P.F., Baum, G., (1969) J. Biomed. Matter Res. 3, 425 - 430

137. Ford, D.J., Pesce, A.J., (1981) in "Enzyme Immunoassay". Shikawa, E., Kawai, T., Miyai, K., (Eds) Igaku-Shoin, N.Y., 54 - 66

138. Kierstan, M., Darcy, G., Reilly, J., (1982) Biotechnol. Bioeng. 24, 1507 - 17

139. Kierstan, M., Bucke, C., (1977) Biotechnol. Bioeng. 19, 387 - 397

140. Larsson, P. O., Mosbach, K., (1979) Biotechnol. Letts. 1, 501 - 506

141. Krouwell, P.C., (1979). Antonie van. Leeuwenhoek 45, 646

142. Svensson, B., Ottesen, M., (1981) Calsberg. Res. Commun. 46, 13 - 24

143. Tran-Minh, C., Broun, C., (1975) Anal. Chem. 47, 1359 - 64

144. Guilbault, G.G., Lubrano, G.J., (1973) Anal. Chim. Acta. 64, 439 - 455

145. Nilsson, H., Akerland, A.C., Mosbach, K., (1973) Biochim. Biophys. Acta. 320, 529 - 534

146. Lingane, J.J., (1958) "Electroanalytical chemistry" 2nd edn. Intersci., London.

147. Beezer, A.E., Tyrrell, H.V., (1972) Sci. Tools, 19, 13 - 16

148. Randzio, S.L., Suurkuusk, J., (1980) in "Biological Microcalorimetry" Beezer A.E. (Ed) Academic Press, London. 311 - 342

149. Beezer, A.E., (1973) Thermochim. Acta. 7, 241 - 246

150. Jespersen, N.D., (1975) J. Am. Chem. Soc. 97, 1662 - 7

151. Trewhella, M.J. (1981) Ph.D Thesis. London

152. Beezer, A.E., Steenson, T.I., Tyrrell, H.J.V., (1973) Protides. Biol. Fluids. Proc. Colloq. 1972. 20, Peters, H.D., (Ed) Pergamon, Oxford. 563 - 566

153. Brown, H.D., Chattopudhyay, S.K., Patel. A.D., Shannon, G.R. Penington, S., (1968) I.E.E.E. Record Inst. Elec. Electron. Engr. 68 (17 - Reg - 13) 19.4.5

154. Bauer, C.R., Gemmill, C.L., (1952). Arch. Biochem Biophys. 35, 110 - 120

155. Johannsson, A., (1973) Protides. Biol. Fluids. Proc. Colloq. 1972. 20, Peters, H.D., (Ed) Pergamon, Oxford. 567 - 570

156. Carraway, W.T., (1976) in "Fundamentals of Clinical Chemistry" Tietz, W. (Ed) Saunders, London. 234 - 259

157. Guilbault, G.G., Brignac, P, Zimmer, M., (1968) Anal. Chem. 40, 190 - 196

158. Auses, J.P., Cook, S.L., Maloy, J.T., (1975) Anal. Chem. 47, 244 - 249

159. Bandi, Z.L., Myers, J.L., Bee B.E., Gordon, P., (1982) Clin. Chem. 28, 2110 - 5

160. Keilin, D., Hartree, E.F., (1948) J. Biol. Chem. 28, 578 - 588

161. White-Stevens, R.H., (1982) Clin. Chem. 28, 578 - 588

162. Roddis, M.H., (1981) Lancet 2 (8247), 634 - 635

163. Franke, W., Lorenz, F., (1939) Ann. 541, 117 - 150

164. Williams, D.L., Doig, A.R., Korosi, A., (1970) Anal. Chem. 42, 118 - 121

165. Goldberg, R.N. (1975) Biophys. Chem. 3, 192 - 205

166. Peterson, J.F., Young, D.S., (1968) Anal. Biochem. 23, 301 - 316

167. Goldberg, R.N., (1976) Biophys. Chem. 4, 215 - 221

168. Zilva, J.F., Pannal, P.R., (1981) "Clinical Chemistry in Diagnosis and Treatment". 3rd edn. Lloyd-Luke (Medical books) Ltd

169. Counsell, J.N. Hornig, D.H., Eds. (1981) "Vitamin C (Ascorbic acid)". Applied Science

170. Omaye, S.T., Turnbull, J.D., Sauberlich (1979) Methods Enzymol. 62, 3 - 11

171. Ollis, D.F., (1972) Biotechnol. Bioeng. 14, 871 - 884

172. Engasser, J.M., Horvarth, C., (1974) Biochim. Biophys. Acta. 358, 178 - 192

173. Sumner, J.B., (1926) J. Biol. Chem. 69, 435 - 441

174. Laidler, K.J., Hoare, J.P. (1949) J. Am. Chem. Soc. 71, 2699 - 702

175. Hoare, J.P., Laidler K.J., (1950) J. Am. Chem. Soc. 72, 2487 - 94

176. Fasman, G.D. Nieman, C., (1951) J. Am. Chem. Soc. 73, 1646 - 50

177. Wall, M.C., Laidler, K.J., (1953) Arch. Biochem. Biophys. 43, 299 - 306

178. Gazzola, C., Blakeley, R.L., Zerner, B., (1973) Can. J. Biochem. 51, 1325 - 30

179. Sundaram, P.V., Crook, E.M. (1971) Can. J. Biochem. 49, 1388 - 94

180. Sundaram, P.V., (1973) Biochim. Biophys. Acta 321, 319 - 328

181. Madiera, V.M.C., (1977) Biochim. Biophys. Acta. 499, 202 - 211

182. Ramachandran, K.B., Pelmutter, D.D., (1976) Biotechol. Bioeng. 18, 685 - 699

183. Atkinson, B., Rousseau, I., (1977) Biotechnol Bioeng. 19, 1065 - 86

184. Iyengar, L., Bajpai, P, Rao, A.V., (1982) Indian J. Biochem. Biophys. 19, 130 - 134

185. Onyezili, F.N., Onitiri, A.C., (1981) Biochim Biophys. Acta. 659, 244 - 248

186. Reuss, M., Buchholz, K., (1979) Biotechnol. Biogen. 21, 2061 - 81

187. Lee, H.J., Wilson, I.B., (1971) Biochim. Biophys. Acta. 242, 519 - 522

188. Atkins, G.L., Nimmo, I.A., (1978) Biochem. Soc. Trans. 6, 545 - 548

189. Karanth, N.G., Srivastava, A.K., (1980) Biochim. Biophys Acta 619, 279 - 282

190. Muller, D., (1928) Biochem. Z 199, 136

191. Beck, C.I., Scott, D., (1974) in "Food related enzymes" Whitaker, J.R., (Ed) Adv. Chem. Ser. 136, ACS Washington D.C. 1 - 30

192. Nakamura, S., Ogura Y., (1962) J. Biochem. 52, 214

193. Gibson, Q.H., Swoboda, B.E.P., Massey, V., (1964) J. Biol. Chem. 239, 3927 - 34

194. Bright, H.J., Gibson, Q.H., (1967) J. Biol. Chem. 242, 994 - 1003

195. Barman, T.E., (1969) Enzyme Handbook 1 Springer-Verlag N.Y., 112 - 112

196. Weibel, M.K., Bright, H.J., (1971) Biochem. J., 124, 801 - 807

197. Rovito, B.J., Kittrel. J.R., (1973) Biotech. Bioeng. 15, 143 - 161

198. Ramachandran, K.B., Pelmutter, D.D., (1976) Biotechnol Bioeng. 18, 669 - 684

199. Buchholz, K., Jarowek, D., (1978) Enzyme Eng. 3, 139 - 144.

200. Ngo, T.T., Ivy, J., Lenhoff, H.M., (1980) Biotechnol Lett. 2, 429 - 434

201. Malikkides, C.D., Weiland, R.H., (1982) Biotechnol. Bioeng. 24, 2419 - 39

202. Lilly, M.D., Cheetham, P.S.J., Dunnill, P., (1978) Enzyme Eng. 3, 73 - 78

203. Karczmar, A.G., Usdin, E., Wills, J.H., (1970) Int. Encycl. Pharmacol. Ther. 13, Vol. 1

204. O´Brien, R.D., (1975) Pure Appl. Chem. 42, 1- 16

205. Hallenbrand, K., Krupka, R.M., (1970) Biochem 9, 4665 - 72

206. Ngo, T.T., Laidler, K.J., (1975) Biochim. Biophys. Acta 377, 303 - 319

207. Ngo, T.T., Yam, C.F., (1978) Int. J. Biochem. 9, 685 - 689

208. Morris, R.W., (1961) Pharmindex 3, 5 - 8

209. Sadar, M.H., Kuan, S.S., Guilbault, G.G., (1970) Anal. Chem. 42, 1770 - 4

210. Alsen, C., Bertram, U., Gersteur, T., Ohnesorge, F.K., (1975) Biochim. Biophys. Acta. 377, 297 - 302

211. Dowd, J.E., Riggs, D.S., (1965) J. Biol. Chem. 240, 863 - 869

212. Krupka, R.M., Hallenbrand, K., (1974) Biochim. Biophys. Acta 370, 208 - 215

213. Dixon, M., (1953) Biochem.J. 170 - 171

214. William, J.E., Pazaine, K.K., Geankoplis, C.J., (1963) Ind. Eng. Chem. Fundam. 2, 126 - 135

215. Howell, S.F., and Sumner, J.B., (1934) J. Biol. Chem. 104, 619 - 626

216. Messing, R.A., (1980) Annu. Rep. Ferment. Process 4, 105 - 121

217. Vierth, W.R., Venkatsubramanian, K., (1979) ACS Symp. Ser. 106, Venkatsubramanian, K. (Ed) ACS. Washington D.C., 1 - 12

218. James, A.M., Nichols, S.C., (1981) Biotechnol. Lett. 3 (3), 119 - 124

219. Foerberg, C., Enfors, S.O. Haeggstroem, C., (1983) Eur. J. Appl. Microbiol. Biotechnol. 17, 143 - 147

220. Lehninger A.L., (1975) "Biochemistry: The molecular basis of cell structure and function" 2nd edn. Worth. 419

221. Mattiasson, B., Mosbach, K., (1971) Biochim. Biophys. Acta 235, 253 - 257

222. Le Goffic, F., Vincent, C., (1980) Enzyme Eng. 5, 127 - 131

223. Lowe, C.R., (1981) Top. Enz. Ferm. Biotechnol 5, 13-146

224. Knight, D.E., (1982) Tech. Life Sci. Physiol. P1/1 20pp.

225. Felix, H., (1982) Anal. Biochem. 120, 211 - 234

226. Larsson, P.O., Ohlson, S., Mosbach, K., (1979) Appl. Biochem. Biogeng. 2, 291 - 301

227. Brodelius, P., Nilsson, K., (1983) Eur. J. Appl. Microbiol. Biotechnol. 77, 275 - 280

228. Mosbach, K., Birnbaum, s., Hardy, K., Davies, J., Beulow, L., (1983) Nature 302, 543 - 545

229. Busch, A.W., (1982) J. Water Pollut. Control Fed. 54, 1152 - 4

230. Bucke, C., Wiseman, A., (1981) Chem. Ind. 4,234 - 240

231. Karube, I., Suzuki, S., (1980) Enzyme. Eng. 5, 263-265

232. Mattiasson, B., Larsson, B., Mosbach, K., (1978) Nature 268, 519 - 520

233. Wollenberger, U., Scheller, F., Atrat, P., (1980) Anal. Lett. 13 (B10), 825 - 836

234. Mattiasson, B., Larsson, P.O., Lindahl, L., Sahlin, P., (1982) Enzyme Microb. Technol. 4, 153 - 157

235. Karube, I., Mitsuda, S., Matsunaga, T., Suzuki, S., (1977) J. Ferment Technol. 53, 243 - 248

236. Karube, I., Okada, T., Suzuki, S., Suzuki, H., Hikuma, M., Yasuda, T., (1982) Eur. J. Appl. Microb. Biotechnol. 15, 127 - 132

237. Neujahr, J.V., (1982) Appl. Biochem. Biotechnol. 7, 107 - 111

238. Paolantonio, C.L., Rechnitz, G., (1982) Anal. Chim. Acta. 141, 1 - 13

239. Schubert, I., Wollenberger, U., Scheller, F., (1983) Biotechnol. Lett. 5, 239 - 242

240. Walters, R.R., Buck, P.P., (1981). Prog. Enzyme Ion. Sel. Electrodes 56 - 60

241. Di Paolantonio, C.L. Arnold, M.A., Rechnitz, G.A., (1981) Anal. Chim. Acta 128, 121 - 127

242. Rechnitz, G.A., Riechel, T. L., Kobos, R.K., Meyerhoff, M.E., (1978) Science 119, 440 - 441

243. Di Paolantonio, C.L., Rechnitz, G.A., (1983) Anal. Chim. Acta. 148, 1 - 12

244. Suzuki, S., Karube, I., (1979) ACS Symp. Ser. 106, Venkatsubramanian, K., (Ed) ACS. Washington D.C., 221 - 236

245. Arnold, M.A., Rechnitz, G.A., (1981) Anal. Chem. 53, 1837 - 42

246. Mascini, M., Iannello, M., Palleschi, G., (1982) Anal. Chim. Acta 138, 65 - 69

247. Bucke, C., (1982) Philos. Trans. R. Soc. Lond. Ser. B. 300, 369 - 389

248. Chibata, I. (1983) Ann. Rep. Ferment. Process. 6, 1-22

249. Mattiasson, B., Ed. (1983) "Immobilized Cells and Organelles" Vol. I and II, CRC Press Inc. Boca. Ranton Florida, USA

250. Mattiasson, B., (1979) in "Immobilized Whole Cells" ACS Symp., Ser. 106, 203 - 220

251. Singleton, P., Sainsbury, D., (1978) "Dictionary of Microbiology" J. Wiley and Sons Chichester

252. Singer, S.J., Nicholson, G.L., (1972) Science 175, 720 - 731

253. Suomalainen, H., Nurminen, J., (1973) in "Yeast, Mould and Plant protoplast". Vallaneuva, J.R., (Ed) Academic Press 167 - 187

254. Belaich, J.P., (1980) in "Biochemical Microcalorimetry" Beezer, A.E., (Ed) 1 - 41

255. Lamprecht, J., (1980) ibid. 42 - 112

256. Beezer, A.E., (1977) Anal. Chem. 49, 34 - 37

257. Murgier, M., Belaich, J.P., (1971) J. Bact. 105, 573 - 579

258. Bisson, F., Froenkel, D.C., (1983) Proc. Natl. Acad. Aci. USA 80, 1730 - 34

259. Kotyk, A., Janacek, K., (1975) "Cell Membrane Transport" Plenum Press. N.Y. 341

260. Cooper, T.G., (1982) in "The Molecular biology of the yeast saccharomyces: Metabolism and Gene expression" Strother, J.N., Jones, E.W., Broach, J.R., (Eds) Cold Springs Harbour. 399 - 461

261. Volesky, B., Verushalmi, K., Luong, J.H.T., (1982) J. Chem. Technol. Biotechnol 32, 650 - 659

262. Navaro, J.M., Durand, G., (1980) C.R. Acad. Sci. Paris 290 Ser D., 453

263. Boiling, E.A., Blanchard, G.C., Russel, W.J., (1973) Nature 241, 472 - 473

264. Laitinen, H.A., Kolthoff, I.M., (1941) J. Phys. Chem. 45, 1061 - 79

265. Updike, S.H., Hicks, J.P., (1967) Nature 214 986 - 988

266. Clark, L.C., Lyons, C., (1962) Ann. N.Y. Acad. Sci. 102, 29

267. Weibel, M.K., Dritschilo, W., Bright, H.J., Humphrey, A.E., (1973) Anal. Biochem. 52, 402 - 414

268. Nango, M., Guilbault, G.G. (1974) Anal. Chim. Acta. 73, 367 - 373

269. Nango, M., Guilbault, G.G. (1975) Anal. Chim. Acta. 75, 169 - 180

270. Wolff, C.M., Mottolla, H.A., (1977) Anal. Chem. 49, 2118 - 20

271. Updike, S.J., Schultz, M.C., Busby, M., (1979) J. Lab. Clin. Med. 93, 518 - 527

272. Matsumo, K., Yamada, K., Osagima, Y., (1981) Anal. Chem. 53, 1974 - 9

273. Schubert, F., Kirstein, D., Scheller, F., Mohr, P., (1980) Anals. Letts. 13 (B17), 1167 - 78

274. Gulberg, L., Christian, G.D., (1981) Anal. Chim. Acta 123, 125 - 133

275. Johnson, J.M., Halsall, H.B., Heineman, W.R., (1982) Anal. Chem. 54, 1394 - 9

276. Kulys, J.J., Vidziunaite, R.N., (1983) Anal. Letts. 16 (B3), 197 - 207

277. Mascini, M., (1983) Clin. Chem. Acta 132, 7 -1 5

278. Neujahr, H.Y., (1982) Appl. Biochem. Biotechnol 7, 107 - 111

279. Mizutuni, F., Tsuda, K., (1982) Anal. Chim. Acta. 139, 359 - 362

280. Rilfer, R., (1983) Int. Sugar J. 85, 131 - 136

281. Cheng, F.S., Christian, G.D., (1977) Anal. Chem. 49, 1785 - 88

282. Winartasaputra, H., Kuan, S.S., Guilbault, G.G. (1982) Anal. Chem. 54, 1987 - 90

283. Eggers, H.M., (1982) Clin. Chem. 28, 1848 - 51

284. Clark Jr., L.C., Duggan, C.A., (1982) Diabetes Care 5(3), 174 - 180

285. Ianniello, R.M., LIndsay, T.J., Yacynych, A.M., (1982) Anal. Chem. 54, 1980 - 4

286. Yao, T., (1983) Anal. Chim. Acta 153, 175 - 180

287. Higgin, J.J. Hill, H.A.O., (1983) Eur. Pat. Appl. EP 78, 636

288. Skoag, D.A., West, D.M., (1976) "Fundamentals of Analytical Chemistry" 3rd edn. Holt-Saunders

289. Guilbault, G.G., Montalvo, J.G., (1970) J. Am. Chem. Soc. 92, 2533 - 38

290. Valle-vega., P., Young, C., Swaisgood, H.E., (1979) J. Food Sci. 45, 1026 - 30

291. Kobos, R.K., (1980) Anal. Chim. Acta 121, 111 - 118

292. Llenado, R.A., Rechnitz, G.A., (1971) Anal. Chem. 43, 1457 - 61

293. Gebauer, C.R., Rechnitz, G.A., (1982) Anal. Biochem. 124, 338 - 348

294. Lahoda, E.J., Lui, c.C., Wingard, L.B., (1975) Biotechnol. Biogeng. 17, 413 - 422

295. Janata, J., Huber, R.J., (1980) Ion Sel. Elect. Anal. Chem. 2, 107 - 174

296. Danielsson, B., Lundstrom, I., Mosbach, K., Stilbert, L., (1979) Anal. Letts. 12, 89 - 99

297. Miyahara, Y., Mariizumi, T., Shiokawa, S., Matsuoka, H., Karube, I., (1983) Nippon Kagaku kaishi 6, 823-830

298. Wingard, L.B., (1979) Process. Biochem. 14, 6 - 9, 16

299. Guilbault, G.G., (1980) Enzyme Microb. Technol. 2, 258 - 264

300. Kobos, R., (1980) ion. Sel. Elect. Anal. Chem. 2, 1-84

301. Rechnitz, G.A., (1982) Anal. Chem. 54, 1194A - 200A

302. Lessler, M.A., (1982) Methods Biochem. Anal. 28, 175 - 199

303. Karube, I., (1983) Annu. Rep. Ferment. Process. 6, 203 - 236

304. Mottola, H.A., Wolf, C-M., Iob, A., Gnanasekaran, R., (1984) Anal. Chem. Symp. Ser. 18, 49 - 75

305. Scheller, F., Keneberg, R., (1983) Anal. Chim. Acta. 152, 265 - 269

306. Wingard, L.B. Jr., (1983). Proc. Fed. Am. Soc. Exp. Biol. 288 - 291

307. Mell, L.D., Maloy, J.T., (1975) Anal. Chem. 47, 299-307